



City Research Online

City, University of London Institutional Repository

Citation: Hennelly, M. L. (2000). The Light Scattering Characteristics of the Normal and Contact Lens-Wearing Eye. (Unpublished Doctoral thesis, City, University of London)

This is the accepted version of the paper.

This version of the publication may differ from the final published version.

Permanent repository link: <https://openaccess.city.ac.uk/id/eprint/30793/>

Link to published version:

Copyright: City Research Online aims to make research outputs of City, University of London available to a wider audience. Copyright and Moral Rights remain with the author(s) and/or copyright holders. URLs from City Research Online may be freely distributed and linked to.

Reuse: Copies of full items can be used for personal research or study, educational, or not-for-profit purposes without prior permission or charge. Provided that the authors, title and full bibliographic details are credited, a hyperlink and/or URL is given for the original metadata page and the content is not changed in any way.

**THE LIGHT SCATTERING
CHARACTERISTICS OF THE NORMAL AND
CONTACT LENS-WEARING EYE**

Volume I

Michelle Louise Hennelly

**Submitted in fulfilment of the requirements for the degree of
Doctor of Philosophy**

**Applied Vision Research Centre,
Department of Optometry and Visual Science,
City University, London
October 2000**

Table of Contents

Title page	1
Table of Contents	2
List of Tables	15
List of Figures	17
Acknowledgements	23
Declaration	24
Abstract	25
Key to Abbreviations	27

VOLUME I

CHAPTER 1	28
Introduction to light scatter in the eye	
1.1 Introduction	28
1.2 The effect of light scatter on visual performance	29
1.3 Methods of assessing scattered light	29
1.3.1 Backscattered light	29
1.3.2 Forward scattered light	30
1.3.2.1 The point spread function	31
1.3.2.1.1 The functional point spread function	32
1.3.2.2 Indirect measurements of intraocular straylight	34
1.3.2.2.1 The equivalent veil technique	34
1.3.2.2.1.2 Angular dependence of scattered light	36
1.3.2.2.1.3 Wavelength dependence of scattered light	37
1.3.2.2.2 Contrast sensitivity and glare testing (The Light Scattering Factor)	39
1.3.2.2.3 The Miller-Nadler glare tester	39
1.3.2.2.4 The Brightness acuity tester	40
1.3.2.2.5 The Berkeley glare test	41
1.3.2.2.6 The Vistech MCT8000	41

1.3.2.2.7 The Baylor visual function tester	41
1.3.2.2.8 The Stereo Optical glare tester	41
1.3.2.2.9 The EyeCon 5	42
1.3.2.2.10 The Penlight test	42
1.3.2.3 Direct measurements of intraocular straylight	42
1.3.2.3.1 The direct compensation technique	43
1.3.2.3.1.1 The straylightmeter	44
1.3.2.3.1.1.1 Accuracy of the straylightmeter	45
1.3.2.4 Comparison of glare tests	46
1.3.2.5 P_SCAN 100 Light Scatter Instrumentation	48
1.4 Summary	56
CHAPTER 2	58
Sources of intraocular light scatter	
2.1 Introduction	58
2.2 The cornea	59
2.2.1 The epithelium	60
2.2.2 Bowman's layer	61
2.2.3 The stroma	61
2.2.4 Descemet's layer	62
2.2.5 The endothelium	62
2.2.6 Corneal transparency	63
2.2.7 The origin of corneal light scatter and its angular dependence	65
2.2.8 The corneal contribution to light scatter in the eye	66
2.3 The crystalline lens	68
2.3.1 The lens capsule	69
2.3.2 The lens epithelium	70
2.3.3 The lens cortical fibres	70
2.3.4 Lens fluorescence	71
2.3.5 Lenticular transparency	72
2.3.6 Lenticular wavelength dependence	74
2.4 Effect of iris and ocular wall pigmentation	75
2.5 Retinal contribution to scattered light	76
2.6 Summary	77

CHAPTER 3	79
The contrast sensitivity function	
3.1 Introduction	79
3.2 Psychophysical basis for measuring contrast sensitivity	80
3.3 The contrast sensitivity function	80
3.4 Interpretation of the contrast sensitivity function	82
3.5 Factors affecting the measurement of spatial contrast sensitivity	83
3.5.1 Stimulus variables	84
3.5.1.1 Stimulus size	84
3.5.1.2 Mean luminance of sinusoidal gratings	85
3.5.1.3 Effect of background luminance level	85
3.5.1.4 Temporal characteristics of the contrast sensitivity function	85
3.5.1.5 Effect of observation distance	87
3.5.1.6 Effect of accommodation	87
3.5.1.7 Effect of pupil diameter	88
3.5.1.8 Effect of refractive error	88
3.6 Methods of testing contrast sensitivity	89
3.6.1 Grating charts	90
3.6.1.1 Vistech and functional acuity contrast charts	90
3.6.1.2 Cambridge low contrast gratings	90
3.6.2 Letter charts	91
3.6.2.1 Pelli-Robson chart	91
3.6.3 Research-based methods of measuring contrast sensitivity	91
3.6.3.1 'Method of adjustment'	91
3.6.3.2 'Method of limits'	92
3.6.3.3 Constant stimuli	92
3.6.3.4 Adaptive procedures	93
3.6.3.5 von Bekesy procedure	93
3.6.4 Repeatability of the methods used to test contrast sensitivity	93
3.7 Summary and aims	94
3.8 The City University contrast sensitivity test	94
CHAPTER 4	96
Rationale for the research	

4.1 Introduction	96
4.2 Aims and plan for experimental work	98
CHAPTER 5	100
The light scattering characteristics of the normal eye and how these are affected by ageing	
5.1 Introduction	100
5.2 Ocular changes with age	101
5.2.1 Corneal changes with age	102
5.2.2 Crystalline lens changes with age	102
5.2.3 Pupil diameter changes with age	105
5.2.4 Retinal and neural changes with age	107
5.2.5 Temporal processing with age	108
5.3 Age and its effect on visual function	108
5.3.1 Effect of age on visual acuity	109
5.3.2 Effect of age on luminance levels	109
5.3.3 Effect of age on measurements of light scatter	109
5.3.4 Effect of age on contrast sensitivity measurements	110
5.4 Summary	113
5.5 Aim	114
5.6 Subjects	115
5.7 Methods	116
5.7.1 Scatter apparatus	116
5.7.1.1 Experimental procedure	117
5.7.1.2 Experimental set-up	117
5.7.1.3 Calibration of luminance	119
5.7.2 Contrast sensitivity apparatus	119
5.8 Results	120
5.9 Discussion of Chapter 5	122
5.9.1 Changes in light scatter with age	122
5.9.1.1 Age at which visual performance declines	123
5.9.1.2 The origins of light scatter in the ageing eye	124
5.9.1.2.1 Corneal light scatter and age	124
5.9.1.2.2 Lenticular light scatter and age	126

5.9.2 Changes in contrast sensitivity with age	127
5.9.2.1 Factors involved in reducing the contrast sensitivity function with age	128
5.10 Conclusions	136
CHAPTER 6	138
Factors causing a variation in light scatter in normal subjects	
6.1 Introduction	138
6.2 Corneal physiology	138
6.2.1 Maintenance of corneal transparency	139
6.3 Corneal oedema	141
6.3.1 Effect of anoxia on corneal integrity	141
6.3.2 Effect of hypoxia on corneal integrity	142
6.3.3 Effect of osmotic imbalance on corneal integrity	143
6.4 Histopathological changes in response to corneal oedema	143
6.4.1 Oedema of the epithelium	144
6.4.2 Oedema of the stroma	144
6.4.3 The endothelial response to oedema	145
6.5 Summary of the effects of oedema on the cornea	146
6.6 The effect of oedema on measurements of visual function	146
6.6.1 Visual acuity	146
6.6.2 Contrast sensitivity	147
6.6.3 Effect of oedema on other measures of visual performance	147
6.7 Optical Pachometry	149
6.7.1 Alignment techniques	150
6.7.2 Angle kappa	159
6.7.3 Accuracy of optical pachometry	160
6.8 Corneal topography	161
6.8.1 Corneal apex	161
6.8.2 Corneal thickness profile	161
6.9 Factors affecting corneal thickness	164
6.9.1 Corneal thickness changes with age	165
6.9.2 Genetic and environmental effects on corneal thickness	166
6.9.3 Effect of gender on corneal thickness	167

6.9.4 Correlation of weight and height with corneal thickness	168
6.9.5 Diurnal variations in corneal thickness	168
6.9.6 Overnight corneal swelling	175
6.9.6.1 Causes of observed variation in corneal thickness	178
6.9.7 Intra-individual day-to-day variation	179
6.10 Summary	180
6.11 Aims	180
6.12 Methods	181
6.12.1 Pachometrical method	181
6.12.1.2 Calibration of the pachometer	183
6.12.2 Light scatter method	186
6.13 Study 1 - Variation in light scatter during one day	186
6.13.1 Aim	186
6.13.2 Method	186
6.13.3 Results	187
6.13.4 Discussion	187
6.14 Study 2 - Repeatability of Study 1	187
6.14.1 Aim	187
6.14.2 Method	188
6.14.3 Results	188
6.14.4 Discussion	188
6.15 Study 3 - Changes in light scatter and corneal thickness following eye patching	189
6.15.1 Aim	189
6.15.2 Method	189
6.15.3 Results	190
6.15.4 Discussion	191
6.16 Study 4 - The influence of patching time on light scatter and corneal thickness	191
6.16.1 Aim	191
6.16.2 Method	191
6.16.3 Results	192
6.16.4 Discussion	192
6.17 Study 5 - The variation in scatter when longitudinal measurements are taken at the same time of day	193

6.17.1 Aim	193
6.17.2 Method	193
6.17.3 Results	193
6.17.4 Discussion	195
6.18 Discussion of Chapter 6	196
6.19 Conclusions	201
CHAPTER 7	203
The effect of the menstrual cycle on the light scattering characteristics of the eye	
7.1 Introduction	203
7.2 The female reproductive cycle	203
7.3 Ocular physiological changes	206
7.3.1 Corneal parameters	206
7.3.1.1 Corneal thickness	206
7.3.1.1.1 The effect of the contraceptive Pill on corneal thickness	210
7.3.1.2 Corneal curvature	212
7.3.1.3 Corneal sensitivity	212
7.3.2 Intraocular pressure, aqueous output facility and glaucoma	213
7.3.3 Tear production and consistency	213
7.3.4 Conjunctiva	215
7.3.5 Pupil diameter	216
7.3.6 Other ocular changes	216
7.4 The effect of the menstrual cycle on visual performance	216
7.5 Aims	219
7.6 Menstrual study design	219
7.6.1 Cycle phase designation	219
7.7 Subjects	220
7.7.1 Questionnaire	220
7.8 Procedure	221
7.8.1 Female subjects	221
7.8.2 Male subjects	222
7.9 Results	222
7.9.1 Female subjects	222
7.9.1.1 Subject MD	222

7.9.1.1.1 Scatter	222
7.9.1.1.2 Pachometry	223
7.9.1.1.3 Pupil diameter	223
7.9.1.1.4 Correlation analysis	223
7.9.1.2 Subject RS	223
7.9.1.2.1 Scatter	223
7.9.1.2.2 Pachometry	224
7.9.1.2.3 Pupil diameter	224
7.9.1.2.4 Correlation analysis	224
7.9.1.3 Subject FS	224
7.9.1.3.1 Scatter	224
7.9.1.3.2 Pachometry	224
7.9.1.3.3 Pupil diameter	225
7.9.1.3.4 Correlation analysis	225
7.9.1.4 Time series analysis	225
7.9.2 Male Subjects	226
7.9.2.1 Subject KJ	226
7.9.2.2 Subject DE	227
7.9.2.3 Subject AS	227
7.10 Discussion of male and female results	228
7.11 Pilot study to investigate the effect of acetylcysteine on light scattering measurements	
in one female subject	231
7.11.1 Baseline measurements	232
7.11.1.1 Subject	232
7.11.1.2 Method	233
7.11.1.3 Results	233
7.11.2 Effect of acetylcysteine 5% on measurements of light scatter	233
7.11.2.1 Aim	233
7.11.2.2 Method	233
7.11.2.3 Results	234
7.11.2.4 Discussion	234
7.11.3 The effect of acetylcysteine 5% and hypromellose 0.3% on light scattering measurements in female subjects	235

7.11.3.1 Aim	235
7.11.3.2 Method	235
7.11.3.3 Results	235
7.11.3.4 Discussion	235
7.12 Discussion of Chapter 7	236
7.13 Conclusions	238

VOLUME II

CHAPTER 8	7
The light scattering characteristic of abnormalities affecting the cornea	
8.1 Introduction	7
8.2 Keratoconus	8
8.2.1 Effect of keratoconus on visual performance	10
8.2.1.1 Effect of keratoconus on glare measurements	11
8.2.1.2 Effect of keratoconus on the contrast sensitivity function	11
8.3 Surgical management of keratoconus	12
8.3.1 Effect of surgical intervention on visual performance	13
8.3.1.1 Effect of surgical intervention on glare measurements	13
8.3.1.2 Effect of surgical intervention on the contrast sensitivity function	14
8.4 Other corneal abnormalities	15
8.4.1 Corneal dystrophies	15
8.4.2 Corneal guttatae	15
8.4.3 Effect of corneal abnormalities on visual performance	16
8.4.4 Effect of corneal abnormalities on measures of forward light scatter	16
8.4.5 Effect of corneal abnormalities on the contrast sensitivity function	17
8.5 Summary of introduction	18
8.6 Aims	19
8.7 Subjects	19
8.8 Methods	20
8.9 Results	21
8.9.1 Results for keratoconic subjects	21
8.9.2 Results for subjects having received penetrating keratoplasties following keratoconus	24

8.9.3 Results for a subject receiving Excimer laser treatment and a superficial keratectomy following keratoconus	25
8.9.4 Results for a subject with blue dot cataract having received an epikeratophakia following keratoconus	25
8.9.5 Results for subjects with other corneal abnormalities	26
8.10 Discussion of Chapter 8	27
8.10.1 Discussion of subjects with keratoconus	27
8.10.1.1 Measurements of forward light scatter	27
8.10.1.2 Measurements of contrast sensitivity	28
8.10.2 Discussion of subjects receiving penetrating keratoplasties following keratoconus	28
8.10.2.1 Measurements of forward light scatter	28
8.10.2.2 Measurements of contrast sensitivity	29
8.10.3 Discussion of a subject receiving Excimer laser and a superficial keratectomy following keratoconus	30
8.10.3.1 Measurements of forward light scatter	30
8.10.3.2 Measurements of contrast sensitivity	30
8.10.4 Discussion of one subject with blue dot cataract who had received an epikeratophakia following keratoconus	30
8.10.4.1 Measurements of forward light scatter	30
8.10.4.2 Measurements of contrast sensitivity	31
8.10.5 Discussion of subjects with other corneal abnormalities	31
8.10.5.1 Measurements of forward light scatter	31
8.10.5.2 Measurements of contrast sensitivity	32
8.11 Conclusions	32
CHAPTER 9	34
The light scattering characteristics of the contact lens-wearing eye	
9.1 Introduction	34
9.2 Physiological changes in response to contact lens wear	35
9.3 Short-term corneal changes in response to hypoxia caused by contact lens wear	36
9.3.1 Epithelial oedema	36
9.3.2 Stromal oedema in contact lens wear	37
9.3.3 Endothelial blebs and corneal pH	38

9.4 Long-term corneal changes in response to hypoxia caused by contact lens wear	38
9.4.1 The effect of long-term hard contact lens wear	40
9.4.1.1 Endothelial response to long-term hard lens wear	40
9.4.1.2 The effect of hard lens wear on corneal sensitivity	42
9.4.1.3 Summary	44
9.4.2 Effect of long-term hydrogel contact lens wear	44
9.4.2.1 The effect of hydrogel lens wear on corneal thickness	44
9.4.2.2 Endothelial response to long-term hydrogel lens wear	46
9.4.2.3 Corneal sensitivity in long-term hydrogel lens wear	46
9.4.2.4 Summary	46
9.4.3 Effect of long-term RGP lens wear	47
9.4.3.1 Endothelial response to RGP lens wear	47
9.4.3.2 The effect of RGP lens wear on corneal sensitivity	47
9.4.3.3 Summary	48
9.5 Effect of contact lens wear on visual performance	48
9.5.1 Effect of contact lens wear on measures of visual acuity	48
9.5.1.1 Effect of deposits on measures of visual acuity	50
9.5.2 Effect of contact lens wear on Variable Contrast Acuity	51
9.5.3 Effect of contact lens wear on the contrast sensitivity function	51
9.5.3.1 Hydrogel lenses	51
9.5.3.1.1 Studies investigating newly dispensed hydrogel lenses	51
9.5.3.1.2 Studies investigating 'used' hydrogel lenses	54
9.5.3.1.3 Summary	54
9.5.3.2 Rigid lenses	55
9.5.3.2.1 Studies investigating newly dispensed rigid lenses	55
9.5.3.2.2 Studies investigating 'used' rigid lenses	57
9.5.3.2.3 Summary	57
9.5.4 The effect of contact lens wear on glare contrast sensitivity	58
9.5.5 The effect of contact lens wear on other glare measurements	59

9.6 Effect of contact lens wear on measures of forward light scatter	60
9.7 Summary	63
9.8 Study 1 - The effect of long-term contact lens wear on the light scattering characteristics of the eye	64
9.8.1 Aims	64
9.8.2 Subject selection	65
9.8.3 Results of long-term contact lens wear	67
9.8.3.1 Results of subjects wearing hydrogel lenses for a maximum of 5 years	69
9.8.3.2 Results of subjects wearing hydrogel lenses for a maximum of 10 years	69
9.8.3.3 Results of subjects wearing hydrogel lenses for a maximum of 15 years	70
9.8.3.4 Results of subjects wearing RGP lenses for a maximum of 5 years	71
9.8.3.5 Results of subjects wearing RGP lenses for a maximum of 10 years	71
9.8.3.6 Results of subjects wearing RGP lenses for a maximum of 15 years	72
9.8.3.7 Results of subjects wearing PMMA lenses for a maximum of 15 years	73
9.8.3.8 Results of subjects wearing PMMA lenses for a maximum of 25 years	73
9.8.3.9 Results of subjects wearing a mixture of lens types for a maximum of 15 years	74
9.8.3.10 Results of subjects wearing a mixture of lens types for a maximum of 20 years	75
9.8.3.11 Results of subjects wearing a mixture of lens types for a maximum of 25 years	75
9.8.3.12 Results of subjects wearing hydrogel lenses for a maximum of 30 years	76
9.8.4 Discussion	76

9.9 Study 2 - The effect of contact lens wear on the light scattering characteristics of non-lens wearing subjects	79
9.9.1 Aims	79
9.9.2 Methods	80
9.9.3 Results of fitting contact lenses in a non-lens wearing population	80
9.9.3.1 Hydrogel lens insertion	81
9.9.3.1.1 Results	81
9.9.3.1.2 Discussion	81
9.9.3.2 RGP lens insertion	83
9.9.3.2.1 Results	83
9.9.3.2.2 Discussion	83
9.10 Discussion of Chapter 9	84
9.11 Conclusions	88
CHAPTER 10	90
Conclusions and future work	
10.1 Conclusions	90
10.2 Future work	93
References	95
Publications	132

List of Tables

Table 1.1	Repeatability results for pupil diameter comparing two sessions
Table 1.2	Table to show the range of n and k values obtained by different researchers at various glare angles
Table 1.3	n , k and k' values obtained from three subjects
Table 3.1	The parameters used to conduct the City University CS test
Table 3.2	Mean and standard deviation of six CS measurements at spatial frequencies of 1.5, 3, 5, 7, 10, 16 and 22 cpd for two observers
Table 5.1	Variations in the integrated straylight parameter k' and n for subjects grouped according to age
Table 5.2	Variations in CS thresholds for 3 cpd, 10 cpd and pupil diameter for subjects grouped according to age
Table 6.1	Review of the literature pertaining to corneal thickness measurements
Table 6.2	Peripheral and CCT in different age groups (Martola and Baum 1968)
Table 6.3	CT measurements in male (M) and female (F) Caucasian subjects (Martola and Baum 1968)
Table 6.4	Results of previous measurements of diurnal variation
Table 6.5	Results of previous measurements of overnight swelling
Table 6.6	Measured thickness (mm) of four afocal contact lenses
Table 6.7	Mean pachometry readings and equivalent CT following use of the conversion factor to transpose actual contact lens thicknesses
Table 6.8	Timing of minimum and maximum k' values following two hourly measurements for ten hours
Table 6.9	Timing of minimum and maximum k' values following hourly measurements for two hours
Table 6.10	Scatter and CT results from three subjects following patching
Table 6.11	Percentage increase in k' and CT for Subject 1 following (i) overnight eye patching, (ii) eye patching for two hours and (iii) eye patching for four hours
Table 7.1	Summary of the events of the hormonal human menstrual cycle
Table 7.2	Summary of the visual changes across the menstrual cycle
Table 7.3	The composition of acetylcysteine 5% drops
Table 7.4	Results of studies reporting an objective improvement in a range of ocular conditions following the use of acetylcysteine drops
Table 7.5	The composition of hypromellose drops
Table 8.1	Signs of keratoconus (Rabinowitz 1998)
Table 8.2	Table to show the grading scheme employed to classify subjects with keratoconus

Table 8.3	Scatter results from 11 keratoconics [Grade 2 (moderate), and 3 (advanced)]
Table 8.4	Scatter results obtained from three subjects having received penetrating keratoplasties following keratoconus
Table 8.5	Scatter results obtained from one subject who had received Excimer laser and a superficial keratectomy following keratoconus
Table 8.6	Scatter results obtained from one subject with blue dot cataract having received an epikeratophakia following keratoconus
Table 8.7	Scatter results obtained from three subjects with corneal abnormalities
Table 9.1	The corneal sequelae of contact lens-induced relative anoxia (Tomlinson 1992)
Table 9.2	The duration of lens wear of subjects included in Study 1
Table 9.3	Mean $k'-(k' \text{ age})$ and s.d. obtained from contact lens-wearing subjects grouped according to age
Table 9.4	Scatter results from four subjects wearing hydrogel lenses for a maximum of 5 years
Table 9.5	Scatter results from two subjects wearing hydrogel lenses for a maximum of 10 years
Table 9.6	Scatter results from two subjects wearing hydrogel lenses for a maximum of 10 years
Table 9.7	Scatter results from three subjects wearing hydrogel lenses for a maximum of 5 years
Table 9.8	Scatter results from three subjects wearing RGP lenses for a maximum of 10 years
Table 9.9	Scatter results from two subjects wearing RGP lenses for a maximum of 15 years
Table 9.10	Scatter results from two subjects wearing RGP lenses for a maximum of 15 years
Table 9.11	Scatter results from three subjects wearing PMMA lenses for a maximum of 25 years
Table 9.12	Scatter results from two subjects wearing a mixture of lens types for a maximum of 15 years
Table 9.13	Scatter results from two subjects wearing a mixture of lens types for a maximum of 20 years
Table 9.14	Scatter results from two subjects wearing a mixture of lens types for a maximum of 25 years
Table 9.15	Scatter results from two subjects wearing a mixture of lens types for a maximum of 30 years
Table 9.16	Scatter results from seven non-adapted subjects before and after fitting with a hydrogel lens
Table 9.17	Scatter results from seven non-adapted subjects before and after fitting with a RGP lens

List of Figures

- Figure 1.1** An eye forming a retinal image of a source through different pupils where (a) represents a natural pupil, (b) shows a small artificial pupil centered on the natural pupil and (c) shows the same artificial pupil displaced to one side so that light enters the eye near the edge of the natural pupil. As the artificial pupil is moved from position (b) to (c), the retinal image is stationary with respect to the retina (providing the eye is correctly focused for distance) (Cornsweet 1970)
- Figure 1.2** The straylight source (van den Berg 1986)
- Figure 1.3** Schematic drawing of the P_SCAN 100 scatter apparatus
- Figure 1.4** Sinusoidal modulation of the scatter source
- Figure 1.5** Computation of k and n
- Figure 1.6** Relationship between n , k and k' (Barbur et al 1995)
- Figure 1.7** Straylight parameters plotted against n for three subjects
- Figure 1.8** Diagrams showing the schematic representation of the stimulus configuration used for the measurement of scattered light on a visual display unit (A), and the geometry of the display required for the computation of annulus size as a function of eccentricity (B) (Barbur et al 1993)
- Figure 2.1** Schematic diagram showing sources of forward light scatter in the human eye
- Figure 2.2** The luminance distribution in the entoptic veil round the glare source (a). The jump at the border is either compensated by the pattern (b), or imitated by the pattern (c) (Vos and Boogard 1963)
- Figure 2.3** Three-dimensional representation of the human lens (Stafford 1990)
- Figure 3.1** Graph to show that visibility depends on both the size (spatial frequency) and the contrast of the stimulus (Wolfe 1990)
- Figure 3.2** Effect of a 1 second flash presentation on the grating sensitivity at low spatial frequencies (\square) compared to the steady state (o). The crossed-hatch area shows stimuli that are visible when a transient stimulus is switched on, but disappear after a few seconds of steady fixation (Kelly 1972)
- Figure 5.1** Pupil diameter as a function of age for each luminance condition. Data are fitted by linear regression with the 95% confidence limits indicated by the dotted line. There is a reduction in slope with increasing luminance (Winn et al 1994)
- Figure 5.2** The integrated straylight parameter (k') as a function of age
- Figure 5.3** Parameter n , (describing the angular distribution of scattered light) as a function of age
- Figure 5.4** The mean contrast sensitivity function for subjects aged less than 45 years and above 45 years
- Figure 5.5** Changes in pupil diameter with age
- Figure 5.6** The results from light scatter measurements on 124 corneas plotted against age (Allen and Vos 1967)
- Figure 5.7** Corneal scatter versus age in 93 normal subjects. Spearman's rank coefficient $r = 0.55$ ($p < 0.001$) (Olsen 1982)

- Figure 5.8** Based on Hemenger's Fig. 1 (1984). The three curves were digitised from Hemenger's graph and re-plotted. The curves represent the ratio between the modulation transfer function (MTF) of the older eye (age 65) and the MTF of the younger eye (age 30), where a term for intraocular light scatter is contained in the calculation of the MTF. Each function represents a different width of the light scatter function. \bullet = Derefeldt et al's (1979) CS data, plotted as the ratio of older adults' sensitivity (age 60-70) to the younger adults' sensitivity (age 20-40), \circ = Owsley et al's CS data (1983) (Sloane et al 1988a)
- Figure 5.9** Hypothetical function illustrating how CS and luminance are related for younger adults (-) and older adults (--). Graph A represents the effect of light absorption, Graph B represents the effect of light scatter, and Graph C represents the effect of changes in neural mechanisms (Sloane et al 1988b)
- Figure 5.10** Mean CS as a function of spatial frequency, displayed for each group (Owsley et al 1985)
- Figure 6.1** The average corneal swelling for a group of eight subjects exposed for different time intervals to various oxygen concentrations within a gas goggle (Holden et al 1984)
- Figure 6.2** Schematic showing A: overlap (alignment) of CT profile, B: touch (juxtaposition) of CT profile
- Figure 6.3** Mean thickness (mm) at five different positions as measured in the right and left corneas of 50 subjects. T = temporal, N = nasal, I = inferior, S = superior (Soni and Borish 1979)
- Figure 6.4** The geometric CT is plotted as a function of the angle between the visual and the axis-measuring direction. The solid line represents the parabolic fit to the measured points (Hitzenberger 1992)
- Figure 6.5** Relation between CT and the IOP in a subject. Data points (open circles; right eye; closed circles; left eye) represent two variables at a given time of the day (Fujita 1980)
- Figure 6.6** The diurnal variation in CCT of eight subjects ranging from 10 to 63 years of age. Measurements were taken at different time intervals over a 48 hour period. Vertical bars = sd (Harper et al 1996)
- Figure 6.7** Serum cortisol measured at several times of the day in ten young adult subjects. Open circles: mean of five males; closed circles; mean of five females. The serum cortisol is highest in the early morning, followed by a gradual decrease during the daytime (Fujita 1980)
- Figure 6.8** Optical principle of pachometry (Phillips and Stone 1989)
- Figure 6.9** Optical path of slit beam and reflected light (Mandell and Polse 1969)
- Figure 6.10** Mean pachometry reading from contact lenses plotted against equivalent corneal thickness
- Figure 6.11** Results for subject DE following scatter measurements taken over a ten hour period
- Figure 6.12** Results for subject DE following scatter measurements taken over a two hour period
- Figure 6.13** (a) scatter results and (b) central corneal thickness following eye patching for Subject 1
- Figure 6.14** (a) scatter results and (b) central corneal thickness following eye patching for Subject 2
- Figure 6.15** Scatter results following eye patching for Subject 3

- Figure 6.16** Variation in k' over 72 days for Subject MH
- Figure 6.17** Variation in k' over 31 days (month 1) for Subject MH
- Figure 6.18** Variation in k' over 41 days (month 2) for Subject MH
- Figure 6.19** Variation in k' over 41 days (month 2) for Subject MH
- Figure 6.20** Variation in k' over 34 days (month 4) for Subject MH
- Figure 6.21** Schematic drawing of the cornea showing the location and progress of lactate and H^+ produced by the epithelium. Lactate and H^+ leave the epithelium via lactate- H^+ cotransporters and diffuse toward the stroma and the aqueous. Accumulation of lactate between the epithelial cells and the stroma osmotically draws fluid into these spaces. In the epithelium, this leads to increased light scatter, and in the stroma, it causes swelling. The pump function of the stroma may also be affected as the metabolic H^+ ions lead to a drop in stromal pH levels (Tomlinson 1992)
- Figure 7.1** Schematic summary of hormone fluctuations throughout the normal menstrual cycle (Guttridge 1994)
- Figure 7.2** Changes in CCT in the female group during a complete menstrual cycle (Soni 1980)
- Figure 7.3** Changes in CCT seen in a male group over a period of 28 days (Soni 1980)
- Figure 7.4** A representative figure of the corneal trends seen in females on low dosage pills (Soni 1980)
- Figure 7.5** A representative figure of the corneal trends seen in females on high dosage pills (Soni 1980)
- Figure 7.6** (a) scatter results with s.e.s (3 'runs') and (b) central corneal thickness, as measured during a standardised menstrual cycle for Subject MD
- Figure 7.7** (a) scatter results with s.e.s (3 'runs') and (b) pupil diameter with s.e.s (15 readings), as measured during a standardised menstrual cycle for Subject MD
- Figure 7.8** k' values plotted against central corneal thickness for Subject MD
- Figure 7.9** k' values plotted against pupil diameter for Subject MD
- Figure 7.10** (a) scatter results with s.e.s (3 'runs') and (b) central corneal thickness, as measured during a standardised menstrual cycle for Subject RS
- Figure 7.11** (a) scatter results with s.e.s (3 'runs') and (b) pupil diameter with s.e.s (15 readings), as measured during a standardised menstrual cycle for Subject RS
- Figure 7.12** k' values plotted against central corneal thickness for Subject RS
- Figure 7.13** k' values plotted against pupil diameter for Subject RS
- Figure 7.14** (a) scatter results with s.e.s (3 'runs') and (b) central corneal thickness, as measured during a standardised menstrual cycle for Subject FS
- Figure 7.15** (a) scatter results with s.e.s (3 'runs') and (b) pupil diameter with s.e.s (15 readings), as measured during a standardised menstrual cycle for Subject FS
- Figure 7.16** k' values plotted against central corneal thickness for Subject FS
- Figure 7.17** k' values plotted against pupil diameter for Subject FS
- Figure 7.18** Variation in k' over a standardised 28 days for Subject MH (cycle 1)
- Figure 7.19** Variation in k' over a standardised 28 days for Subject MH (cycle 2)
- Figure 7.20** k' daily means against cycle day for Subject MH (cycles 1 and 2) and Subject MD

- Figure 7.21** Scatter results from female Subjects MD, RS, FS and MH (cycles 1 and 2)
- Figure 7.22** Correlogram for Subject MD
- Figure 7.23** Correlogram for Subject MH (cycles 1 and 2 combined)
- Figure 7.24** (a) scatter results with s.e.s (3 'runs') and (b) central corneal thickness, as measured over 35 days for Subject KJ
- Figure 7.25** (a) scatter results with s.e.s (3 'runs') and (b) central corneal thickness, as measured over 35 days for Subject KJ (outlying data points excluded)
- Figure 7.26** Scatter results for Subject DFE as measured over 36 days
- Figure 7.27** Scatter results for Subject AS as measured over 35 days
- Figure 7.28** Correlogram for Subject KJ
- Figure 7.29** Within day variance for male subjects
- Figure 7.30** Within day variance for female subjects
- Figure 7.31** Baseline scatter results as measured over five days for Subject MH
- Figure 7.32** Scatter results following installation of acetylcysteine 5% as measured over five days for Subject MH
- Figure 7.33** Scatter results following installation of acetylcysteine 5% and hypromellose 0.3% as measured over five days for Subject MH
- Figure 8.1** Relation between decimal acuity (horizontally) and strength of the light scatter (vertically) over 3.75 and 30 degrees. Data are plotted for 10 corneal dystrophic eyes. Not all eyes were measured at 3.75 degrees scatter distance (van den Berg 1986)
- Figure 8.2** Scatter profile and contrast sensitivity results for Subject NT
- Figure 8.3** Scatter profile and contrast sensitivity results for Subject SH
- Figure 8.4** Scatter profile and contrast sensitivity results for Subject DA
- Figure 8.5** Scatter profile and contrast sensitivity results for Subject GE
- Figure 8.6** Scatter profile and contrast sensitivity results for Subject AF
- Figure 8.7** Scatter profile and contrast sensitivity results for Subject BB
- Figure 8.8** Scatter profile and contrast sensitivity results for Subject ML
- Figure 8.9** Scatter profile and contrast sensitivity results for Subject GO
- Figure 8.10** Scatter profile and contrast sensitivity results for Subject MP
- Figure 8.11** Scatter profile and contrast sensitivity results for Subject MR
- Figure 8.12** Scatter profile and contrast sensitivity results for Subject AD
- Figure 8.13** Scatter profile and contrast sensitivity results for Subject CC
- Figure 8.14** Scatter profile and contrast sensitivity results for Subject MP
- Figure 8.15** Scatter profile and contrast sensitivity results for Subject JP
- Figure 8.16** Scatter profile and contrast sensitivity results for Subject AV
- Figure 8.17** Scatter profile and contrast sensitivity results for Subject JR
- Figure 8.18** Scatter profile and contrast sensitivity results for Subject ED
- Figure 9.1** CCT as a function of length of wear of hard contact lenses. Controls indicate non-contact lens wearers (Millodot 1978)

contact lens wearers (Millodot 1978)

- Figure 9.2** The relationship between forward-scatter and backscattered light. Each data point indicates one Subject. EX3m indicates excimer subjects at 3 months postoperatively; SCL indicates hydrogel contact lenses (Lohmann et al 1993)
- Figure 9.3** Change in modified k' for contact lens-wearing subjects over time in years
- Figure 9.4** Scatter profile and contrast sensitivity results for Subject EP
- Figure 9.5** Scatter profile and contrast sensitivity results for Subject PG
- Figure 9.6** Scatter profile and contrast sensitivity results for Subject BH
- Figure 9.7** Scatter profile and contrast sensitivity results for Subject WR
- Figure 9.8** Scatter profile and contrast sensitivity results for Subject AH
- Figure 9.9** Scatter profile and contrast sensitivity results for Subject PB
- Figure 9.10** Scatter profile and contrast sensitivity results for Subject IW
- Figure 9.11** Scatter profile and contrast sensitivity results for Subject PM
- Figure 9.12** Scatter profile and contrast sensitivity results for Subject PC
- Figure 9.13** Scatter profile and contrast sensitivity results for Subject AB
- Figure 9.14** Scatter profile and contrast sensitivity results for Subject AR
- Figure 9.15** Scatter profile and contrast sensitivity results for Subject SH
- Figure 9.16** Scatter profile and contrast sensitivity results for Subject TT
- Figure 9.17** Scatter profile and contrast sensitivity results for Subject MK
- Figure 9.18** Scatter profile and contrast sensitivity results for Subject EL
- Figure 9.19** Scatter profile and contrast sensitivity results for Subject MH
- Figure 9.20** Scatter profile and contrast sensitivity results for Subject MD
- Figure 9.21** Scatter profile and contrast sensitivity results for Subject JS
- Figure 9.22** Scatter profile and contrast sensitivity results for Subject DK
- Figure 9.23** Scatter profile and contrast sensitivity results for Subject JR
- Figure 9.24** Scatter profile and contrast sensitivity results for Subject CG
- Figure 9.25** Scatter profile and contrast sensitivity results for Subject GR
- Figure 9.26** Scatter profile and contrast sensitivity results for Subject SL
- Figure 9.27** Scatter profile and contrast sensitivity results for Subject RF
- Figure 9.28** Scatter profile and contrast sensitivity results for Subject ED
- Figure 9.29** Scatter profile and contrast sensitivity results for Subject TJ
- Figure 9.30** Scatter profile and contrast sensitivity results for Subject DE
- Figure 9.31** Scatter profile and contrast sensitivity results for Subject CM
- Figure 9.32** Scatter profile and contrast sensitivity results for Subject DL
- Figure 9.33** Change in (a) light scatter and (b) contrast sensitivity following insertion of a hydrogel contact lens for Subject SW
- Figure 9.34** Change in (a) light scatter and (b) contrast sensitivity following insertion of a hydrogel contact lens for Subject MB

- Figure 9.35** Change in (a) light scatter and (b) contrast sensitivity following insertion of a hydrogel contact lens for Subject RT
- Figure 9.36** Change in (a) light scatter and (b) contrast sensitivity following insertion of a hydrogel contact lens for Subject AH
- Figure 9.37** Change in (a) light scatter and (b) contrast sensitivity following insertion of a hydrogel contact lens for Subject PT
- Figure 9.38** Change in (a) light scatter and (b) contrast sensitivity following insertion of a hydrogel contact lens for Subject KJ
- Figure 9.39** Change in (a) light scatter and (b) contrast sensitivity following insertion of a hydrogel contact lens for Subject TJ
- Figure 9.40** Change in (a) light scatter and (b) contrast sensitivity following insertion of a RGP contact lens for Subject MN
- Figure 9.41** Change in (a) light scatter and (b) contrast sensitivity following insertion of a RGP contact lens for Subject RU
- Figure 9.42** Change in (a) light scatter and (b) contrast sensitivity following insertion of a RGP contact lens for Subject KJ
- Figure 9.43** Change in (a) light scatter and (b) contrast sensitivity following insertion of a RGP contact lens for Subject JH
- Figure 9.44** Change in (a) light scatter and (b) contrast sensitivity following insertion of a RGP contact lens for Subject KH
- Figure 9.45** Change in (a) light scatter and (b) contrast sensitivity following insertion of a RGP contact lens for Subject PH
- Figure 9.46** Change in (a) light scatter and (b) contrast sensitivity following insertion of a RGP contact lens for Subject PT

Acknowledgements

I gratefully acknowledge my supervisors in this project John Barbur, David Edgar and Geoffrey Woodward. My special thanks must go to David for his guidance and encouragement throughout. Furthermore, grateful thanks to all those who gave so much of their valuable time to participate in this study. I also gratefully acknowledge the financial support of the College of Optometrists.

Many people have endured the highs and lows I experienced during this thesis. I am indebted to my family and friends who have been a constant source of support and encouragement. In particular, I am indebted to my Mother and Father who have helped me in so many different ways. They are an inspiration to me. Without the support and encouragement from those close to me, this thesis would never have been completed.

Last but not least, Paul, who knows more than anybody what it has taken to come this far. His patience and understanding has never failed (well, almost) and his good humour has carried me through. I know that he is as relieved as I am to see this project completed and it is to him I dedicate this thesis.

Declaration

I grant the powers of discretion to the University Librarian to allow this thesis to be copied in whole or part without further reference to me. This permission covers only single copies made for study purposes, subject to normal conditions of acknowledgement.

Abstract

The light scattering characteristics of the eye were determined for contact lens wearers, normals, and patients with keratoconus and corneal dystrophies, using a computerised straylight program - the P_SCAN 100 scatter apparatus. This system utilises extended annular sources to assess the full scatter function, permitting the calculation of k' from the integral function of the scatter function. This parameter shows reduced subject variability compared to n (the scatter index) and k (the straylight parameter) and is proportional to the total amount of light scattered. Contrast sensitivity was assessed at seven spatial frequencies.

A normative database was created using 31 subjects (16 to 60 years) with little refractive error. k' showed no significant change up to age 45, but increased rapidly above age 45. There was no significant change in n up to 45 years of age, however, n was significantly lower in subjects over 45.

Diurnal and longitudinal variations were investigated. One subject had a highest k' value (7.60) at 08:00 hrs, falling to a steady (minimum) value of approximately 6.10. Similar results were found on retesting. Results on three eyes following patching suggested that the immediate post-patching peak in k' , and its subsequent reduction, were related to changes in corneal thickness.

Longitudinal variations in light scatter with a possible cyclical pattern were noted in one female across four menstrual cycles. Light scatter changes in the menstrual cycle were tested in a double-blind masked study. The average between-day variability for three females was 2.97 (s.d.) compared to 0.39 (s.d.) for three males. Precise cyclical trends were unclear, beyond a fall in scatter levels during menses. Variations in corneal thickness and pupil diameter appeared unrelated to changes in light scatter. Changes in mucus levels in the tear film may be a contributory factor, because administration of acetylcysteine 5% reduced light scatter during menses. Pre-menopausal females were excluded from subsequent studies.

Quantification of the effects of a range of corneal abnormalities on light scatter and the CSF allowed later comparisons with the magnitude of the effects of contact lens wear. A database of values of k' and CS was established for 11 subjects with keratoconus (18 eyes) and eight subjects (11 eyes) with a range of anterior segment abnormalities.

Long-term contact lens wearers (29 subjects, 54 eyes) had significantly greater light scatter than non-lens wearing subjects of the same age. Eight eyes had values of k' within the keratoconic range. CSF was reduced in most adapted contact lens wearers, compared to age-matched controls. Thirteen eyes revealed no CS loss, whilst 19 eyes showed loss at all spatial frequencies.

When 14 non-lens wearing subjects were fitted with either a hydrogel or RGP contact lens, neither lens type caused a statistically significant change in intraocular light scatter. Hydrogel contact lenses did not, in general, adversely affect CS. For RGP lenses, results were more variable, both within and between subjects, than for hydrogel lenses. However, no definite trends in CS emerged. Therefore, the increase in light scatter in the long-term

contact lens-wearing population is unlikely to be due to the physical presence of the contact lens. Instead, it is probably the result of a number of physiological changes that are known to occur in response to contact lens wear.

Key to Abbreviations

BAT	Brightness acuity tester
BBT	Basal body temperature
CCD	Charged couple device
CCT	Central corneal thickness
CL	Contact lens
cpd	Cycles per degree
CRT	Cathode ray tube
CS	Contrast sensitivity
CSF	Contrast sensitivity function
CT	Corneal thickness
CTT	Corneal touch threshold
CV	Coefficient of variation
FACT	Functional acuity contrast test
GAGs	Glycosaminoglycans
Hz	Hertz
IR	Infra-red
LEDs	Light emitting diodes
LSF	Light scattering factor
mm	Millimetres
ms	Milliseconds
KCS	Keratoconjunctivitis sicca
MTF	Modulation transfer function
PMMA	Polymethylmethacrylate
PSF	Point spread function
RGP	Rigid gas permeable lenses
RI	Refractive index
SD	Standard deviation
SPK	Superficial punctate keratitis
TA	Triamcinolone acetonide
VA	Visual acuity
VCAC	Variable contrast acuity chart
UV	Ultra-violet

CHAPTER 1

Introduction to light scatter in the eye

1.1 Introduction

A convergence of findings on light scatter has emerged from theoretical (Hart and Farrell 1969), psychophysical (Vos 1962; Ben-sira et al 1980) and invasive research, the latter making use of excised eyes (De Mott and Boynton 1958; Boynton and Clark 1964). It is now accepted that glare is caused by light scatter and that such scattering is present in the normal eye (Stiles and Crawford 1937; Fry and Alpern 1953; Boynton et al 1954; Trokel 1962; Vos and Bouman 1964; Olsen 1982; Vos 1984; van den Berg 1986; Wooten and Geri 1987; Ijspeert et al 1990; Smith et al 1990; Barbur et al 1993). Light scatter degrades image contrast and is equivalent to low-pass spatial filtering of the retinal image. The amount of straylight decreases with angular separation from the glare source and its angular distribution depends on the size of the particles that cause scatter in the eye (Stiles 1929).

Scattered light is a term commonly used to describe the more random change of direction of incident light, due to the irregular distribution of the small particles involved. The type of scattering is determined by size and irregularity of the scattering particles, and the separation of their centres. Two types of light scattering exist, namely elastic and non-elastic. Rayleigh scattering and Mie scattering are both elastic. Rayleigh scattering is such that the direction of the scattered photon is independent of the direction of propagation and light is scattered in all directions. It tends to be wavelength-dependent, with greater scatter occurring at the short end of the spectrum. Light is scattered in proportion to the reciprocal of the fourth power of wavelength (Stiles 1929; Wooten and Geri 1987). Rayleigh scatter is produced by inhomogeneities in the media that are small with respect to wavelength, and tend to be randomly spaced.

In the case of Mie scattering, the distribution of scattered light follows a power law relationship of θ^{-n} , where n is the scatter index and determines how rapidly the scattered light falls off with eccentricity away from the source. The scatter has little wavelength dependency, and the scattering is caused by the presence of particles which extend over large distances with respect to the light wavelength. As a consequence, the angular

distribution approximately imitates the incident beam. That is, it is localised in the forwards direction.

1.2 The effect of scattered light on visual performance

Light in the eye is scattered in both forward and backward directions. Back scattered light is not necessarily related to forward scattered light and visual performance (Allen and Vos 1967). The size and distribution of the scattering elements determine in which direction the light is scattered. The fact that the eye is transparent is attributable to the histological make-up of the ocular structures (section 2.1). Ageing or pathology may alter the characteristics of the scatter sources, or the number of scatter sources may increase. As a consequence, the amount of straylight reaching the retina increases.

Normal levels of scattered light do not significantly influence the level of functional vision that can be achieved. However, scattered light is increased in the presence of an intense glare source, and this may lead to significant loss of visual performance, which is termed 'disability glare'. As a result, increased scattered light can cause significant loss of contrast in the image of an object on the retina, the severity of which depends on the strength and position of the scattering sources and scattering properties of the eye. Increased scatter may lead to reduced VA, poor chromatic threshold sensitivity (Barbur et al 1997) and significant reduction in contrast sensitivity (CS), particularly at high spatial frequencies (Holladay 1926; Stiles 1929; Stiles and Crawford 1937; Barbur et al 1993).

1.3 Methods of assessing scattered light

1.3.1 Backscattered light

Light reflected towards the observer comprises of not only backscattered light but also reflected light. By use of a Polaroid filter, backward scatter and reflected light can be separated. This methodology has been employed by numerous investigators (e.g. Olsen 1982; Weale 1986; Smith et al 1990). Weale (1986) compared the luminance of slit lamp images through two microscope oculars. The first ocular was covered by a Polaroid analyser, the second with a variable neutral density filter. Reflected light was removed by viewing the image through a crossed polariser, leaving only backscattered light. In addition, a detector was also used to investigate wavelength dependency. The study demonstrated that the amount of light scattered in the backwards direction increased with

age (Allen and Vos 1967; Sigelman et al 1972), and that it was wavelength dependent, with greater levels of scatter being produced by short wavelengths. This study suggested that back scatter in the eye may include a strong Rayleigh scatter component.

1.3.2 Forward scattered light

Forward scattered light is of greatest clinical interest as it degrades image contrast and is equivalent to low-pass spatial filtering of the retinal image. Several different methodologies (including glare tests) are claimed to assess intraocular scattered light or straylight indirectly. Such tests assume that increases in glare are directly related to increases in intraocular light scatter. The impairment of visual function caused by the presence of a bright source at a distance is defined as disability glare. It is used to describe the contrast lowering effect of intraocular scattered light on the visual scene. Disability glare plays an ill-defined role in the measurement of straylight because measures of light scatter also depend on the peripheral part of the point spread function (PSF) (section 1.3.2.1). However, neural factors may affect the accuracy of glare measurements (Vos 1984; van den Berg 1991, 1994).

It is often assumed that the outcome of glare tests depends on the degree of straylight only. However, the assumed relationship is not always correct. Indeed, a glare source may improve sensitivity in certain subjects and under certain conditions e.g. a subject with peripheral lens opacities may show improved glare sensitivity as a result of pupil constriction. Furthermore, de Waard et al (1992) using the Vistech glare tester (Ginsburg et al 1987), reported that measures of CS were enhanced in the presence of a veiling luminance. It was suggested that the phenomenon was related to the documented observation that CS improves when the test field is not surrounded by darkness. Despite these disadvantages, glare testing is thought to be an indirect method of assessing the amount of intraocular straylight (van den Berg 1991). There is a weak relationship between the two phenomena, and Weber's Law has been postulated as a principal connecting factor (van den Berg 1995b) in that when using either glare testing or measurements of scattered light, the threshold is influenced by the luminance of the glare source and the background.

According to Weber (1834), the smallest perceptible difference of apparent brightness or luminosity is a constant fraction of the luminosity. This fraction is known as Fechner's fraction (1858). The eye can distinguish between two adjacent surfaces that differ in luminance by about 1% over a large range of retinal illuminances (Fincham and Freeman 1990; Tunncliffe 1993). This is expressed as :

$$\Delta / L = \text{constant} \quad \text{[equation 1.1]}$$

where:-

Δ = the differential threshold luminance

L = the prevailing background luminance

constant = Weber Fechner fraction

This is the most common definition of contrast and is used frequently in many visual psychophysical studies.

Although glare assessment is useful in predicting the effect of glare on visual performance, the quality of the retinal image can only be assessed adequately using double-pass techniques.

1.3.2.1 The point spread function

Light scatter is the principal component of straylight. Light rays from infinity in an emmetropic or corrected eye will be converged by the refracting surfaces of the eye to a focal point on the retina. In a normal young eye, approximately 90% of the light from a point source falls within the central one degree of the retinal image. Outside the central one degree, the remaining proportion is scattered. Its intensity decreases with distance from the centre of the image (Vos 1976) and is referred to as straylight or scattered light. This phenomenon causes a reduction in the quality of vision, because it interferes with the retinal image at the fovea (Vos 1976). The veil of light across the retina caused by the glare source will alter the state of adaptation of the retina, and reduce the contrast of the retinal image. This results in compromised visual performance, a loss often termed 'disability glare'.

The image of a point object formed by an aberration-free optical system of circular aperture consists of an 'Airy disc', which is a central bright circular disc surrounded by alternating dark and light rings of decreasing intensity. As the aperture of the system increases, the size of this diffraction pattern decreases and becomes a point. The point spread function (PSF), is used to describe the retinal light distribution resulting from an external point source. The PSF is a result of aberrations present in the optical system and diffraction by the pupillary aperture.

1.3.2.1.1 The functional point spread function

Straylight has been defined as the skirt (outside of $\theta = 1$ degree) of the PSF. The clinical testing of visual acuity (VA) depends only on the central peak of the PSF. As Snellen VA is of high contrast, it is relatively insensitive to changes outside one degree of the outer edges of the PSF (van den Berg 1986). The functional PSF is relevant for visual function, and differs from the optical PSF because of the directional selectivity of the retina (van den Berg 1991). The directional selectivity of the retina is known as the Stiles-Crawford effect, which influences the effectiveness of light scattered by the periphery of the cornea or lens. If light strikes the retinal cones at an angle, it is less effective at stimulating the receptors than paraxial rays. The glare effect is enhanced under scotopic light levels, when the Stiles-Crawford effect is weak.

The Stiles-Crawford effect may be explained by considering the fate of a point source of light when it enters the eye. All of the quanta travelling in paths within a cone on the retina, formed by the source at the apex and the edges of the pupil at the base, enter the eye and contribute to the retinal image of the source. A small hole placed in front of the pupil restricts the quanta striking the retina and only those travelling close to the visual axis will contribute to the retinal image. If this hole is moved, the quanta forming the image will move along a different path, but the location of the image on the retina will be unchanged, as will the physical intensity (figure 1.1). Therefore, as the hole is moved across the pupil, the subject reports a stationary bright point of light that changes in intensity, being brightest when the hole is centred over the pupil and dimmest at the pupil margin.

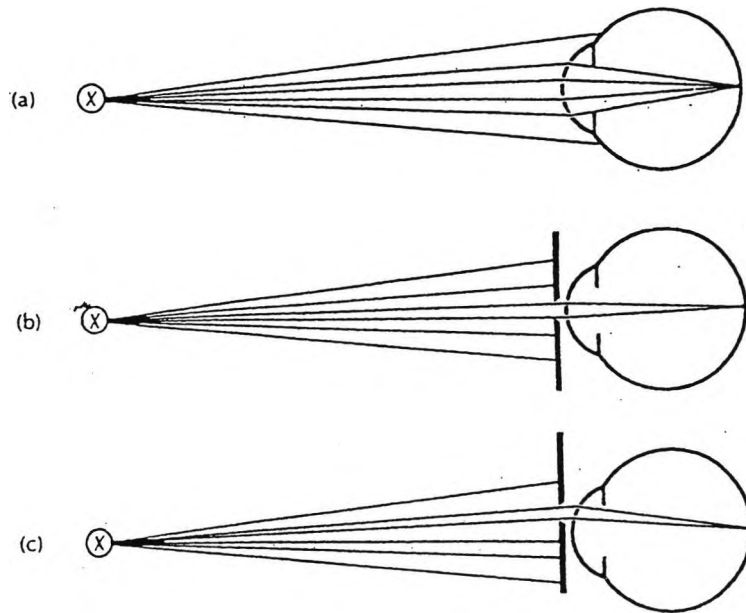


Figure 1.1 - An eye forming a retinal image of a source through different pupils where (a) represents a natural pupil, (b) shows a small artificial pupil centered on the natural pupil and (c) shows the same artificial pupil displaced to one side so that light enters the eye near the edge of the natural pupil. As the artificial pupil is moved from position (b) to (c), the retinal image is stationary with respect to the retina (providing the eye is correctly focused for distance) (Cornsweet 1970).

The visual system is thus more sensitive to quanta entering the eye near the centre of the pupil, and becomes progressively less sensitive as the quanta enter further away from the centre. However, this effect only exists when the stimulus is acting on the cone system. The cone system generally has a higher threshold than the rods, except during the first five mins of dark adaptation and the threshold for the test spot is thus determined by the cones. However, if the same measurements are made after 10 mins of dark adaptation, when the rod threshold is lower than the cone threshold, the Stiles-Crawford effect is diminished.

It may be postulated that light travelling near the edges of the pupil is strongly absorbed or reflected by the cornea, the lens or other media of the eye. However, the contributions from these areas are too small to account for such a large effect and must instead be due to properties of the retina. Also, since quanta are absorbed, information about the direction of incidence is lost and as a consequence it is likely that the Stiles-Crawford effect is caused by the properties of the receptors, or the pigment itself.

O' Brian (1951) hypothesised that the inner segment of a cone acts like a funnel, gathering all incident quanta on the end facing the cornea, and concentrating it at the area of most pigment. However, if the quanta enter the inner segment at an angle then they are less likely to be absorbed by the cone pigment. This theory assumes that the axes of the cones are pointed toward the centre of the pupil, that light entering through the edge of the pupil will be less likely to effect the area of the pigment, and therefore the threshold will be higher. This has been confirmed experimentally using foam 'model' cones and microwave rays; the ratio of the speed of microwaves in the foam to their speed in air being equal to the ratio of speed of light in cones to its speed in the surrounding ocular media (O' Brian 1951). The degree of penetration in the outermost segment of the 'model' cones was then measured. The sensitivity of the model reduced as the angle of incidence increased. This agreed with the findings of Stiles and Crawford (1937) and also Enoch and Fry (1958).

1.3.2.2 Indirect measurements of intraocular straylight

1.3.2.2.1 The equivalent veil technique

The first psychophysical technique used to determine the amount of intraocular light scatter was termed the *equivalent veil technique* and was developed by Cobb in 1911. The method examines the effect of peripheral straylight on the fovea. The Stiles-Crawford effect is accounted for since the technique is subjective. Cobb (1911) determined that the threshold luminance of a foveally viewed test flash is elevated by the application to the same eye of a peripheral glare stimulus. This threshold elevation can be attributed to straylight, or to neuronal interaction effects. The scatter estimate is found by the ratio of the luminances of the homogenous and the image fields. It involves determining an increment threshold at a distance from the image, and evaluating the level of a large homogenous field that results in the equivalent increment threshold. It was found that as the glare angle, θ , decreases, the amount of straylight increases.

Both Holladay (1927) and Stiles and Crawford (1937) concentrated on the peripheral part of the PSF. It was proven that for small sources, the angular dependence of scattered light in the eye can be described adequately by the PSF. This work was used as the basis for glare experiments.

Quantitative data on the masking effect of the visible halo around glare sources was published by Holladay (1927). Sensitivity of the eye to varying brightnesses, under low luminance conditions, was determined using large backgrounds (40 degrees or greater) and small test objects (2 degrees or less). The purpose of the experiment was to determine whether the addition of a light source alters the adaptation level of the fovea. This was expressed in terms of an equivalent veiling luminance (L_{eq}), that would produce the equivalent masking effect (that is, the amount of straylight falling at a given diameter from the centre of the retinal image). The technique estimates the amount of straylight falling at the fovea when the light source producing the straylight is at the glare angle, θ .

$$L_{eq}/E_{gl} = f(\theta) \quad \text{[equation 1.2]}$$

where:-

L_{eq} = equivalent veiling luminance.

E_{gl} (measured in lux) = illumination on the observer's eye.

Numerous researchers have investigated the relationship between L_{eq} and E_{gl} (e.g. Holladay 1926; Holladay 1927; Stiles 1929; Le Grand 1937; Stiles and Crawford 1937) and concluded that the proportionality between L_{eq} and E_{gl} is constant for varying values of illumination. Neural interaction would be indicated if the proportionality between L_{eq} and E_{gl} were not constant. Therefore, straylight is the limiting factor on the absolute threshold for a specific point on the retina (at a known glare angle θ). The adaptive brightness of the fovea was increased following addition of a glare source, thereby increasing the minimum perceptible brightness difference required for discrimination. The origin of the scatter causing the veil of straylight across the fovea could be either the image-forming rays coming from the glare source, or the result of multiple reflections and diascleral illumination.

The expression 'equivalent veiling luminance' is widely used and assumes that the visual effects of glare in the eye are entirely dependent on the quantity of straylight that reaches the fovea. It refers to an external veiling luminance, which is added to the luminances of both the object and its background. Strictly, it is the value of the external veiling luminance at the position of the test object. Every part of the external veiling luminance distribution will have some effect on the state of adaptation of the retina (Le Grand 1937).

Consequently, different equivalent veiling luminances at the test object would be expected with different external veiling luminances, except for the instance in which the distribution happens to coincide. In fact, the functions describing the visual effect of glare do not exactly correspond to those from measured illuminance using electronic recordings as reported by DeMott and Boynton (1958). Fisher and Christie (1965) suggested that the effect of glare is dependent on the distribution of the background illuminance. However, only a minor error results from ignoring this fact, because the graphs of visual effect and measured illuminance are similar (DeMott and Boynton 1958). The visual effect is greater for large angles and is less for small glare angles (Holladay 1927), than would be expected from the illuminance distribution results noted by DeMott and Boynton (1958). It was concluded that most of the psychophysical effects were attributable to straylight.

Vos (1962), using an experimental set-up that encouraged neural interaction, reported that linearity between L_{eq} and E_{gl} did not occur when luminance levels were low in the central retina. However, linearity was constant in the peripheral retina. The angle of the glare source from the line of vision was 30 minutes of arc and thresholds were measured when both the test object and the glare source were presented peripherally and centrally. Vos (1984) later concluded that cone and rod sensitivity to straylight might differ and as a result the linear relationship between L_{eq}/E_{gl} could alter when changing from one threshold level to another.

1.3.2.2.1.2 Angular dependence of scattered light

The angular dependency of L_{eq}/E_{gl} has also been studied (Holladay 1926; Holladay 1927; Stiles 1929; Stiles and Crawford 1937; Campbell and Gubisch 1966; Rushton and Gubisch 1966; Vos et al 1976, 1984), with the scatter function $f(\theta)$ found to be inversely proportional to the square of the glare angle (Holladay 1926):

$$f(\theta) = k\theta^{-n} \quad \text{[equation 1.3]}$$

where :-

n = scatter index (typically 2)

k = straylight coefficient

and θ is measured in degrees

This equation is called the Stiles-Holladay approximation (Holladay 1926; Holladay 1927; Stiles 1929; Stiles and Crawford 1937). Although the equivalent veiling method is satisfactory for measuring the scatter functions for values of θ greater than two degrees, it is less applicable for smaller angles (Fry 1965).

The central part of the PSF, up to 10 minutes of arc, was later studied by ophthalmoscopic recording of the retinal image (Campbell and Gubisch 1966; Rushton and Gubisch 1966). The investigators used a modified ophthalmoscope to measure the double-pass, reflected image (Rushton and Gubisch 1966) and determined the range of the image spread, and of the scatter in the central portion of the PSF ($\theta = 0$ and $\theta = 0.1$ degrees). Unfortunately, it gave little information about the weaker far scatter, due to the adverse signal-to-noise ratio, and it is the weaker peripheral part that is most concerned with straylight.

Vos et al (1976) first constructed the complete range of the PSF from 0 to 100 degrees by combining Campbell and Gubisch's (1966) data with the findings of Walraven (1973), who used colour induction experiments to investigate the angular dependency of straylight at small angles. Later, Vos (1984) produced an expression which describes the scatter function from 0 to 90 degrees, and integrates to 100% over the entire visual field.

$$L_{eq}/E_{gl} = 10/(\theta + 0.02)^2 + 10/(\theta + 0.02)^3 + 10^6/\exp(\theta/0.02)^2 \quad [\text{equation 1.4}]$$

A large percentage of documented work on straylight and glare uses the principle of the equivalent luminance concept.

1.3.2.2.1.3 Wavelength dependence of scattered light

A significant amount of work has been undertaken to elucidate the angular dependence of straylight, but much less is known about wavelength dependence. An early study conducted by Le Grand (1937), incorporating broad band filters, concluded that red (long wavelength) light scatters more than blue (short wavelength) light, for glare angles less than a few degrees. It further concluded that wavelength dependency was itself dependent upon visual angle. That is, at narrow angles long wavelengths predominated, whilst at greater angles the situation was reversed. This information was refined by Ivanoff (1947), who found that for a small glare angle ($\theta = 1.2$ degrees), yellow light (Wratton No.15)

scattered least, red (Wratton No.25) and green (Wratton No.58) about 1.3 times more than yellow, and blue (Wratton No.47) about 5.6 times more than yellow. Ivanoff (1947), therefore demonstrated experimentally the predominance of short wavelengths in straylight. However, direct comparison of the results of Le Grand (1937) and Ivanoff (1947) is difficult, due to poor experimental controls, and large errors. A later study by Boettner and Woltner (1962), experimenting on enucleated human eyes, demonstrated that short wavelengths produced increased scatter, though of a reduced extent compared with predictions from Rayleigh scatter. Once again, this research was subject to poor experimental technique, due to the known deformation of the tissue samples taken. Despite this, the authors were able to conclude that wavelength-dependency is secondary to the general increases in scatter.

The existence of significant amounts of wavelength dependent scatter has since been disputed (Vos 1963). Vos's findings were corroborated by Wooten and Geri (1987), who measured intraocular light scatter as a function of wavelength using the equivalent veil technique. It was concluded that intraocular light scatter is produced by particles, or cellular structures substantially larger than the wavelength of light. Further work by Vos (1984) proposed that the vast majority of forward straylight occurs due to larger scattering structures than the wavelength of light. However, van den Berg et al (1991) reported that for certain normal subjects, long wavelength light scatters more than shorter wavelength light. This was attributed to selective transmission of longer wavelengths through the largely opaque structures of the iris and sclera. However, such results were not observed in a study by Whitaker et al (1993), which indicated that wavelength dependent scatter in normal young and elderly eyes is of little or no significance. On the other hand, a small amount of wavelength dependence was demonstrated in subjects with cataract, but only four subjects were investigated. Therefore, neither Wooten and Geri (1987), or Whitaker et al (1993), were able to demonstrate the increase in long wavelength scatter found at large angles by van den Berg et al (1991).

It may be concluded that the dependence of disability glare on wavelength in the human eye has been shown to be much weaker than would occur if Rayleigh scatter was dominant. Therefore, ocular light scatter across the visible spectrum is predominantly Mie scatter, caused by structures which are large in comparison to the wavelength of light (Vos 1984;

Wooten and Geri 1987). Consequently, the angular distribution of the ocular light scatter approximately follows the direction of the beam.

1.3.2.2.2 Contrast sensitivity and glare testing (The Light Scattering Factor)

The Light Scattering Factors (LSFs) of Paulsson and Sjostrand (1980) were based upon the earlier work of Vos (Vos 1962; Vos and Boogard 1963; Vos et al 1976). CS measurements were made using a sinusoidal grating presented on a VDU screen, with and without a glare source (positioned at 1.7 degrees from the subject's line of sight). An expression was derived for an LSF, where:-

$$\text{LSF} = L/E * ((M_2/M_1) - 1) \quad [\text{equation 1.5}]$$

where :-

L = stimulus luminance

E = illuminance in the plane of the pupil

M₂ = detection contrast threshold with glare light

M₁ = detection contrast threshold without glare light

The authors state that the LSF depends only on the scattering angle, and that changes in L or E produce compensating changes in M₂, so that the overall LSF remains unchanged. Five normal subjects (aged 30-61), and six patients with posterior subcapsular cataract (aged 46-68 years) were examined using this method (Paulsson and Sjostrand 1980). The resulting decrease in the CSF was measured and the LSF was calculated. With the addition of a glare light, the normal subjects showed no significant decrease in contrast sensitivity. However, patients with cataract showed a loss of CS at low and medium spatial frequencies (Paulsson and Sjostrand 1980). Abrahamsson and Sjostrand (1986) and Karbissi et al (1993) confirmed these findings in subsequent experiments on a larger sample of cataract patients. The methodology used was challenged by Yager et al (1992), but the authors maintained that it was valid when the appropriate stimulus conditions were used.

1.3.2.2.3 The Miller-Nadler glare tester

The Miller-Nadler glare tester is a contrast test surrounded by a uniformly bright light source (Miller et al 1972; Le Claire et al 1982; Hirsch et al 1984a, 1984b; Nadler 1984). The glare tester uses 35mm slides, each containing a central black 20/400 Landolt C ring,

with a background annulus that becomes progressively darker with subsequent slide presentations. The orientation of the C changes in one of four directions and once the subject fails to detect the orientation of the ring opening, the contrast threshold is recorded. The results are expressed as the percentage contrast between the ring and background at the end point and converted to a VA value from a table provided by the manufacturer.

Many researchers have used the glare tester developed by Miller et al (1972). Le Claire et al (1982) demonstrated that glare sensitivity increased with age in normal subjects and was increased in aphakic patients, compared to normal subjects. High levels of glare sensitivity in patients with subcapsular and cortical cataracts were reported with the smallest increase in glare sensitivity produced by patients with pure nuclear sclerosis. No clear correlation was found between near VA and glare sensitivity (Le Claire et al 1982; Hirsch et al 1984a, 1984b; Neumann et al 1988a). Hirsch et al (1984a, 1984b) reported that glare scores using the Miller-Nadler glare tester were significantly better predictors of outdoor VA among cataract patients facing the sun than Snellen acuity. Later, Neumann et al (1988b) showed that some patients with pure nuclear sclerosis did not have reduced glare sensitivity, although they did have poor Snellen acuity outdoors. It should be noted that this test is disadvantaged by the fact that a significant reduction in glare intensity is produced if the subject moves off axis (Van Der Heijde et al 1985).

1.3.2.2.4 The Brightness acuity tester

The introduction of the Brightness Acuity Tester (BAT) (Holladay et al 1987), simplified glare testing because it can be used to provide a glare source whilst testing either VA or CS. The glare sensitivity score is recorded in terms of the number of lines of acuity lost with glare, compared to the value obtained without glare. The BAT is a hand-held illuminated hemispherical bowl, 60mm in diameter, with a 12mm aperture through which the patient views the eye chart in a darkened room. The bowl is illuminated by a shielded bulb. The glare source subtends from 5 to 50 degrees visual angle at a vertex distance of 25mm. The luminance of the glare source can be varied, having three levels of brightness (low, medium and high luminance level). The three settings simulate conditions of bright indoor lighting, overcast skies and bright sunlight respectively. The medium setting appears to predict most accurately the level of functional visual performance (Neumann et

al 1988a), whilst the highest setting has a tendency to overestimate the effects of disability glare (Holladay et al 1987).

Certain studies investigating the results produced by the BAT compared with outdoor acuity have proved contradictory. Holladay et al (1987), Neumann et al (1988a) and Elliott and Bullimore (1993) showed that results obtained with the BAT showed a high correlation with outdoor acuity. However, a later study stated that the BAT over-predicted glare problems in 76% of the subjects examined (Prasad et al 1991).

1.3.2.2.5 The Berkeley glare test

The Berkeley glare test consists of an opal plexiglass sheet containing a central 18% contrast Bailey-Lovie letter chart. Transillumination of the plexiglass (750 cd/m^2) provides the glare source. Measurements with and without a glare source are made at a distance of 1 metre and the patient scores 0.02 log MAR units for each letter correctly recognised.

1.3.2.2.6 The Vistech MCT8000

The Vistech MCT8000 is a glare test which utilises patches of sinusoidal gratings that are nominally equivalent to five Snellen acuities. The instrument permits control of target presentation, luminance and glare source position. Illuminance is held constant by a calibration circuit and by selecting high-intensity bulbs that surround the test chart, real-life conditions can be replicated e.g. "night-time" (3 cd/m^2), or "daytime" (125 cd/m^2) conditions. A central bulb can be activated to simulate an oncoming headlight.

1.3.2.2.7 The Baylor visual function tester

The Baylor visual function tester uses a Landolt C and an annulus of light to test glare (Koch et al 1986). Baseline VA is recorded and then repeated under two different glare conditions, (i) 450 foot-lamberts and (ii) 2000 foot-lamberts. The number of lines of vision lost at each glare setting determines the glare score.

1.3.2.2.8 The Stereo Optical glare tester

The Stereo Optical glare tester uses a bright point source to induce glare in order to mimic car headlights and other focal glare sources. It consists of a black background with five concentric back-illuminated white rings with radii of 3.6, 2.7, 1.8, 1.4 and 0.9 degrees. A

small focal glare source is positioned in the centre of the rings. Each ring has one or more breaks, equivalent to a 20/200 Snellen acuity letter. Subjects are asked to count the number of breaks in each ring beginning with the largest and proceeding to the smallest, with and without the addition of the glare source (Koch et al 1986).

1.3.2.2.9 The EyeCon 5

This glare test is a PC-based instrument that permits selection of both optotype (Landolt C, sinusoidal gratings or Sloan letters) and contrast. The target is presented at a viewing distance of 12 ft on a VDU with uniform luminance. The optotypes are surrounded by a 130 cd/m² glare field, which is equivalent to a bright overcast day.

1.3.2.2.10 The Penlight test

The penlight test is a simple, quick test used in clinical practice (Maltzman et al 1988). The penlight is positioned off the visual axis and acts as a glare source. There are obvious disadvantages to this test as many variables are difficult to control, including the angle and distance of the glare source from the patient, intensity of the penlight and the ambient luminance. In addition, the patient may momentarily lose fixation and view the glare source. These problems may result in the clinician conducting a 'photo stress test', as opposed to a disability glare test.

1.3.2.3 Direct measurements of intraocular straylight

There are several disadvantages inherent in the measurement of the equivalent veiling luminance. Principal among these is the fact that repeated threshold measurements are required, which increases the variance associated with the measurements. In addition, the measurements may be subject to changes in the patient's criteria and poor fixation may cause variable results (van den Berg 1986). Furthermore, variations in the adaptation of the retina, due to changes in retinal luminance, can affect threshold values. In order to minimise these disadvantages, the direct compensation technique for the measurement of intraocular light scatter was developed (van den Berg 1986; van den Berg and Spekreijse 1987).

1.3.2.3.1 The direct compensation technique

To distinguish between glare and straylight, van den Berg and Ijspeert (1987) expanded on the work of Le Grand (1937), and developed the direct compensation, or flicker compensation technique. The direct compensation technique determines the point at which the illuminance from the straylight and the target luminance are equal. van den Berg and Ijspeert (1987) used a straylight source (a ring) and a foveal test patch modulated in counterphase at the same temporal frequency as the scatter sources. The instrument assesses the equivalent veiling luminance of the glare source, using the retina as a detector (Ijspeert et al 1990).

The human visual system has both an optimal spatial frequency (i.e. there is an object size that can be seen most easily) and temporal frequency (i.e. there is a rate of flicker that can be seen most easily). To determine the temporal frequency, the intensity of a light is varied over time, usually in a sinusoidal fashion. At certain rates, flicker can be seen even when the intensity of the light fluctuates very little. At other rates, flicker can be seen only when the intensity of the light fluctuates by a large amount. The actual sensitivity of the human eye is defined as the smallest fluctuation in intensity that is detected as flicker, and is most sensitive when the light flickers at approximately 8 Hz (van den Berg 1995b). This value is used by van den Berg, who states that as long as the fovea can detect a sensitivity of 8 Hz, then a high level of accuracy can be obtained (van den Berg 1995b).

The authors claim the lack of any neuronal influence (van den Berg and Spekreijse 1987) and the lack of any threshold assessment measurement means that the state of retinal adaptation and the sensitivity of the fovea are relatively unimportant. Hence, retinal function is not critical as long as flicker can be appreciated (van den Berg and Spekreijse 1987). Since the requirement is to neutralise flicker, the sensitivity of the test is independent of the values of straylight obtained. Therefore, the direct compensation technique negates the disadvantages inherent in the equivalent veiling glare technique, since both light from the nulling source and the scatter source are scattered over the same angle, by the same structures. Also, due to the spatial relationship between the straylight source and the test patch, measurements using the direct compensation technique are relatively unaffected by fixational errors. Furthermore, correction of refractive errors is

not necessary, as long as the patient can identify the one degree central target, as refractive blur has a minimal effect on the perception of flicker.

1.3.2.3.1.1 The straylightmeter

van den Berg's technique for determining light scatter involves determination of luminance of a patch of homogenous light that is visually equivalent to the light scattered intraocularly from the bright source (van den Berg 1986). The straylight source is a concentric ring with the equivalent patch in the centre being fixated. The annular nature of the glare source not only aids fixation, but also gives greater accuracy than a point glare source. Essentially, it acts as numerous point sources, permitting a low luminance, whilst still producing a high level of scatter. The central dark test target is one degree in radius, surrounded by a bright outer circle, of two degrees in radius, with a steady luminance of 30 cd/m^2 . The direct surround is blocked by an annulus of five degrees outer diameter, contiguous with the test area. A separating annulus positioned around the central target provides a higher luminance than the straylight. This maintains flicker sensitivity by minimising lateral, inhibitory retinal effects (Diamond 1955).

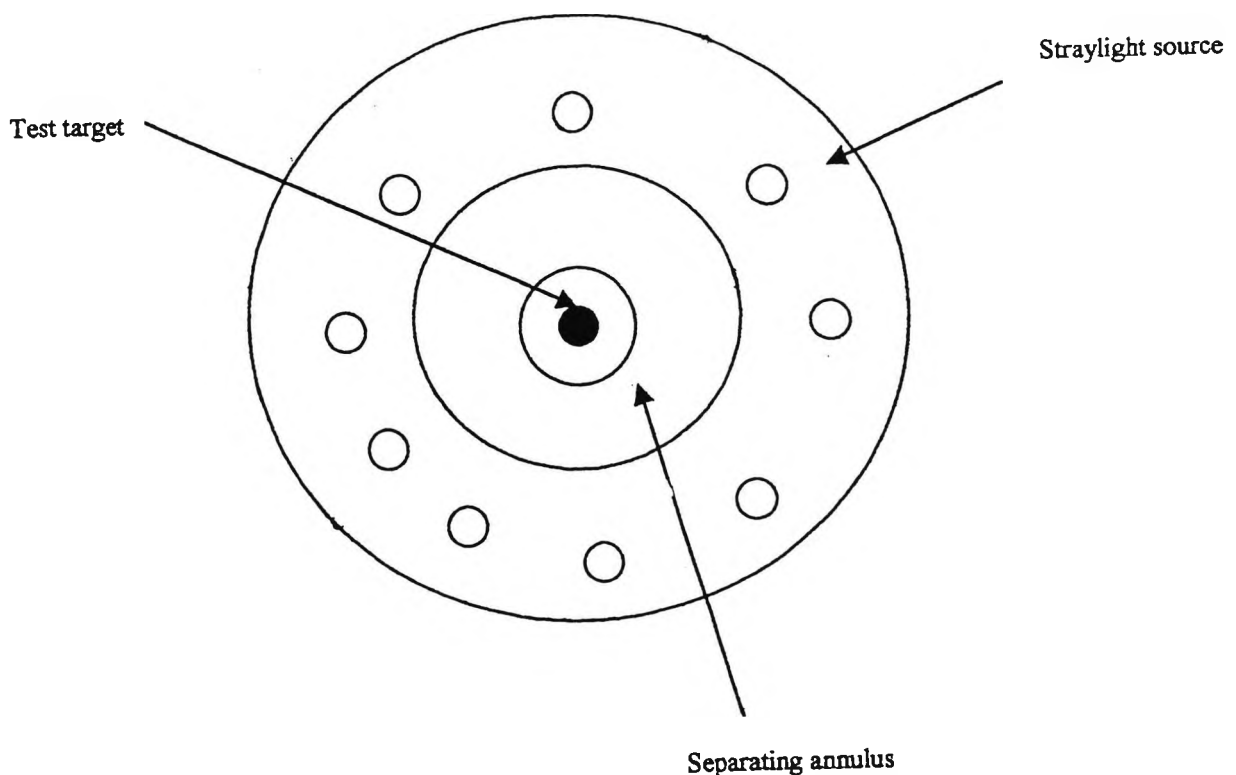


Figure 1.2 - The straylight source (van den Berg 1986).

The prototype straylightmeter was designed with four straylight rings with radii from 3.5 to 28 degrees, used in conjunction with a square wave flicker (van den Berg 1986). van den Berg has since simplified the design to three rings (3.5, 10 and 28 degrees from the centre) and changed to a sinusoidal flicker modulation, which can be modified to arrive at a desired suprathreshold level of straylight flicker at fixation.

The subject's task is to fixate the equivalent patch (test target) in the centre of the straylight source. Once the subject is positioned, an LED ring flickers at 8Hz, with a light/dark ratio of one. The straylight caused by the flickering annulus yields a flickering veil across the test target. The flickering is in phase with the flickering of the straylight source. A compensation light is presented over the central test target, of equal modulation, but in counterphase to the flickering of the glare source. When the luminance modulation of the equivalent patch is low, flicker caused by the straylight source can be perceived. The flicker can be nulled by varying the luminance modulation of the test target. The measured luminance, L_{eq} , matches the equivalent luminance caused by the scattered light. Therefore, straylight is directly compensated.

1.3.2.3.1.1 Accuracy of the straylightmeter

The size of the test patch, and the luminance of its surround, are the main factors that determine the accuracy of the straylightmeter. The size of the test target is a balance between a small enough target that still produces good flicker sensitivity, and a large enough target which still retains a specific eccentricity relative to the straylight source (Rovamo et al 1988). The accuracy of the test is reduced by the isolating annulus that surrounds the test target, as it scatters additional light across the retina.

Beckman et al (1991) evaluated the straylightmeter (Le Grand 1937; van den Berg and Spekreijse 1987) in order to determine the parameters required to obtain optimum accuracy. At a fixed glare angle, the equivalent veiling luminance of the glare source, L_{eq} , is proportional to the product of the luminance of the glare source, L and its area, A .

$$L_{eq} \propto LA$$

[equation 1.6]

The illuminance in the plane of the pupil should be tolerable for the patient, (1 - 1000 lux), but also needs to be large enough to yield sufficient scatter. The illuminance, E, depends on the luminance of the glare source L, its area and the distance between the scatter source and the eye. In general,

$$E = \frac{LA}{R^2} \quad \text{[equation 1.7]}$$

where :- L and A have been defined previously and R is the distance between the pupil plane and the scatter source.

To obtain a sufficient level of illuminance at the pupil, the glare source needs to be either a high luminance, narrow glare annulus, giving a well-defined glare angle, or alternatively a wider annulus of lower luminance. Less well-defined glare angles are sufficient as high luminances are difficult to achieve with a well-defined glare angle.

The accuracy of the direct compensation method has been reported to be 0.05 log units (Ijspeert et al 1990) and 0.12 log units (Elliott and Bullimore 1993). It is less accurate for small angles of glare (3.5 degrees), where the effect of inhomogeneity is greatest. The range of straylight values in normal subjects is reported to be 0.1 log units (Ijspeert et al 1990), and higher in abnormal subjects (van den Berg 1988; van den Berg and Boltjes 1988; van den Berg et al 1989).

1.3.2.4 Comparison of glare tests

The commonly used glare testers are each subtly different and there is a lack of standardisation. The type and size of the target together with the position, brightness and type of glare source used each influence the measures of glare sensitivity. Several researchers have attempted to compare the results obtained from the variety of glare instruments available.

Smith et al (1987) compared the results of testing cataract patients with the Miller-Nadler glare tester and the BAT. Patients with posterior subcapsular opacities showed a much greater glare sensitivity when the BAT was used compared to the Miller-Nadler glare

tester. Although the BAT produced a smaller pupil diameter than the Miller-Nadler glare tester, pinhole effects were reported to be insignificant.

The BAT, EyeCon 5, InnoMed true vision analyser, Miller-Nadler glare test and the Vistech VCT 8000 were evaluated by Neumann et al (1988a) in order to investigate which technique most accurately predicted outdoor Snellen acuity. Three measurements were taken (i) actual Snellen acuity (ii) outdoor Snellen acuity and (iii) using the glare tests. The glare tests were then classified according to their ability to predict outdoor acuity within one Snellen line. The following results were obtained: BAT (73%), InnoMed true vision analyser (69%), Vistech VCT 8000 (56%), Miller-Nadler glare test (47%), and EyeCon 5 (15%).

Elliott and Bullimore (1993) determined the reproducibility, discriminative ability and validity of several glare tests, namely, the Miller-Nadler glare tester, the Vistech MCT800, the Berkeley, the BAT used in conjunction with the Pelli-Robson and Regan charts, and the van den Berg straylightmeter (which was used as the 'gold standard'). Three groups of subjects were investigated - young normals (mean age 24.3 ± 3.3 years), older normals (mean age 66.3 ± 6.2 years) and cataract patients (mean age 70.6 ± 8.1 years). In all tests, cataract patients were seen to perform worst compared to other subjects tested. The Berkeley and Regan tests demonstrated good reliability whilst the straylightmeter gave a repeatability of 0.12 log units, which was reduced at large glare angles. The Pelli-Robson chart demonstrated the highest reliability compared to other contrast tests, whilst the Vistech MCT8000 and the Miller-Nadler glare test exhibited the poorest reliability compared to other glare tests.

The ability of these tests to discriminate between the three subject groups was greatest for those involving measures of CS or low contrast VA in the presence of a glare source. Under glare conditions, CS and low contrast VA scores from the Pelli-Robson, Regan and Berkeley tests provided similarly reliable, discriminative, and valid measures of visual assessment in cataract. Disability scores tended to give a poor discriminative ability. The Miller-Nadler and the Vistech MCT8000 glare testers demonstrated poor discrimination, which was thought to be due to large step sizes at low contrast thresholds. The Pelli-Robson chart, used with the BAT, gave good discriminative ability, and the results

demonstrated a high correlation with straylightmeter measures. However, the low spatial frequency content of the Pelli-Robson chart resulted in poor discrimination between cataract and older normal subjects compared with VA. For the Regan chart, 11% contrast with the BAT gave the highest discriminative ability, whilst 96% contrast gave the worst. However, certain cataract patients could not see any of the letters on the 11% chart in the presence of the BAT. Therefore, the 25% Regan chart was suggested as a more appropriate test when evaluating cataract patients. Results with the Berkeley test were similar to those for the 25% Regan chart or the BAT.

1.3.2.5 P_SCAN 100 Light Scatter Instrumentation

The instrumentation used in the present study was the P_SCAN 100 pupillometer apparatus designed by Alexandridis et al (1991) and Barbur et al (1991). The P_SCAN 100 scatter apparatus can be used to quantify the distribution of light scatter, to measure retinal function, and to investigate the integrity of the afferent/efferent systems. It can take simultaneous binocular measurements of pupil size and two dimensional eye movements. A schematic drawing of the P_SCAN 100 apparatus is shown in figure 1.3.

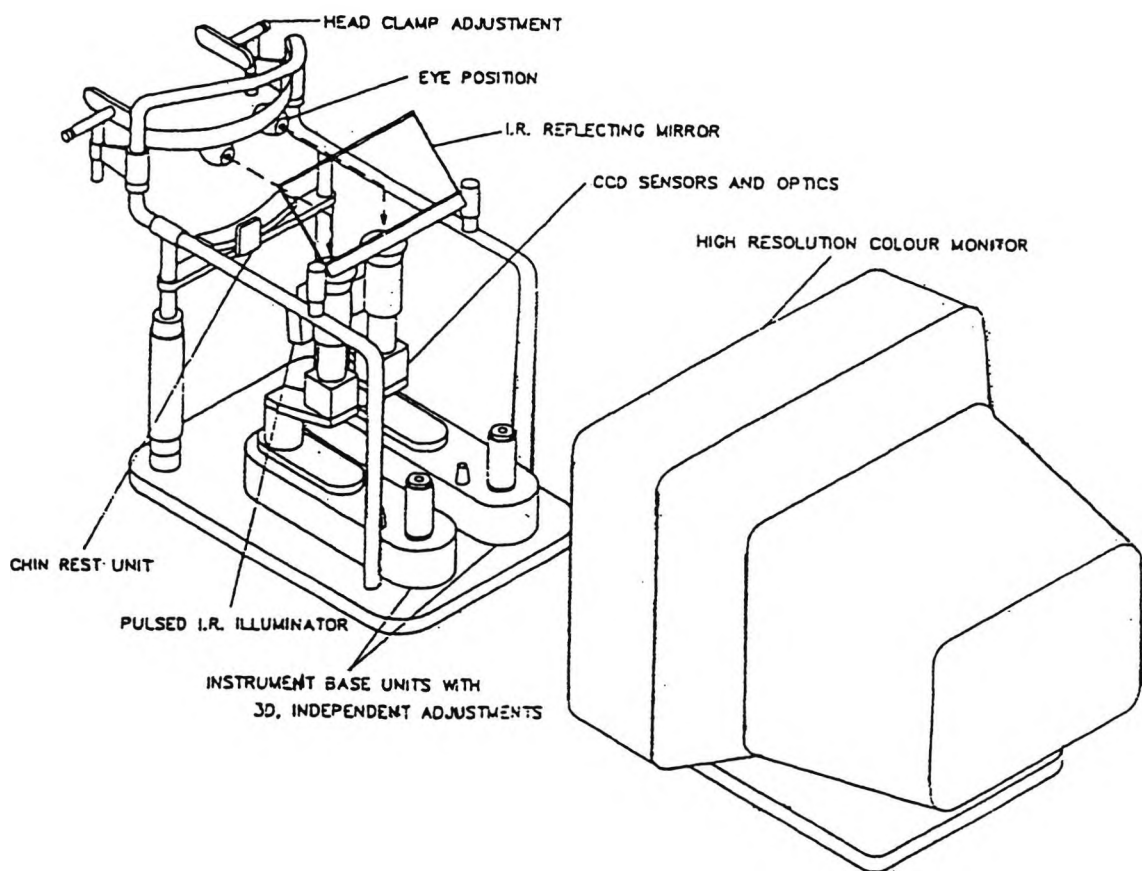


Figure 1.3 - Schematic drawing of the P_SCAN 100 scatter apparatus.

In order to make the scattered light measurable, the P_SCAN 100 scatter apparatus uses high display luminances and relatively large annuli areas. The central display unit has a normal resolution 19 inch monitor of 1280 x 1024 pixels, operated at a frame rate of 60 Hz. The luminance of the scattering source is modulated sinusoidally at a frequency of 8.6 Hz. This results in flickering over the central target, produced by the corresponding temporal modulation of retinal illuminance. The luminance of the central test target is also modulated sinusoidally, in counterphase with the scattering source, with the same temporal frequency. The mean luminance is adjusted to obtain a null flicker point using a modified staircase procedure. The sinusoidal modulation of the scatter source luminance is presented to the subject as a burst of flicker lasting for 350 ms. This 'nulling' of the scattered light is solely achieved by the counterphase modulation of the screen luminance. When the two components are equal, the modulation cancels out completely and no flicker is perceived by the subject. The modulation of the retinal illuminances at this end point is represented by the top line of the figure 1.4 below. This is seen as a resultant 'ripple'.

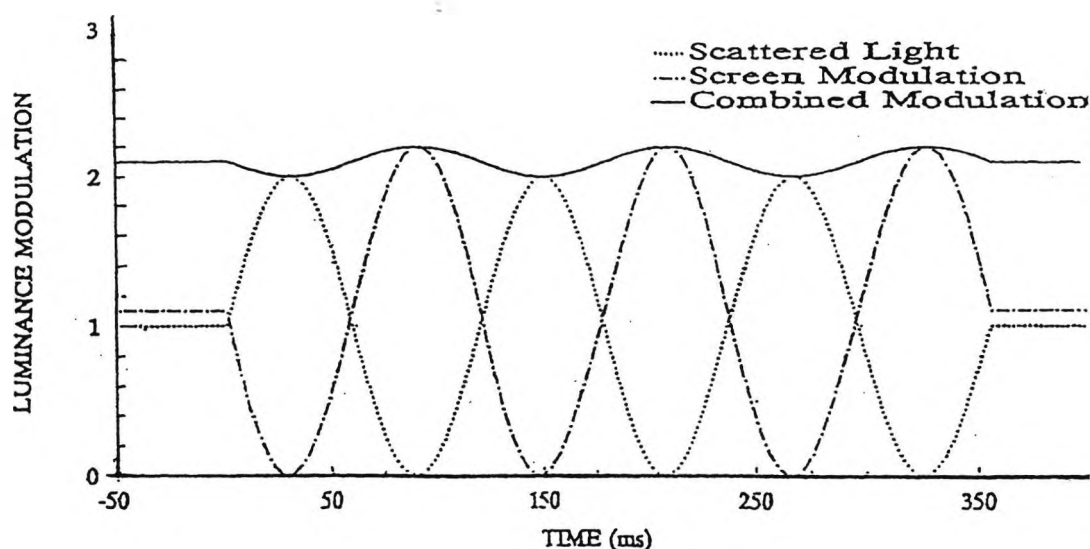


Figure 1.4 - Sinusoidal modulation of the scatter source.

The diameters of the scattering sources are separated from the central test area by isolation annuli of five fixed radii. These are yellow in colour to emphasise separation of the central test area and the scattering sources. The diameters of the scatter sources are such that a constant level of illuminance is measured in the pupil plane during the calibration procedures.

A video system, containing infra-red (IR) sensitive CCD sensors, above an IR reflecting mirror is situated below the head rest. The mirror is placed at an angle of 45 degrees and transmits 95% of visible light. A pulsed IR illumination system is used to illuminate the iris for 4 ms within each frame. This ensures that the iris is well illuminated with specular images outside the pupil area. The sampling rate can be set to 50 or 60 Hz and the electronic system provides asynchronised video frames of the monitored pupil. This system can extract the co-ordinates of intersection between the pupil margin and a series of pre-selected scan lines. Due to the fact that in a 'normal' population a circular pupil would be expected, filtering techniques can remove unnecessary 'noisy' intersections caused by eye movements that deviate from the expected result. By filtering the best circle to each set of data points, small elliptical variations in pupil diameter within the normal population do not appear to produce large experimental errors (Barbur et al 1993). As pupil size has been shown to affect measures of light scatter (Barbur et al 1995), subjects with an average pupil diameter of greater than 6.5 mm were excluded from data sets.

Repeatability of the results obtained using the P_SCAN 100 apparatus are shown in table 1.1. Repeatability was established using randomly selected consecutive pairs of data from 31 normal subjects (27 females and 4 males, mean age = 22.7 years, range 18 - 27). All subjects were healthy, ophthalmologically normal, non-contact lens wearers, with refractive errors of less than ± 2.00 DS, less than 0.50 DC and with Snellen acuities of 6/6 or better. Measurements were taken under mesopic conditions, using a 6/12 Snellen letter as a visual target and subjects were adapted for at least three minutes. Mean and difference values were calculated for the pairs of data, together with 95% confidence limits.

Table 1.1 - Repeatability results for pupil diameter comparing two sessions.

	Mean difference	Standard deviation	95% confidence intervals
Pupil diameter	-0.05mm	0.51mm	+0.97mm/-1.07mm

The P_SCAN 100 scatter apparatus has been adapted to measure pupil size at the point just before presentation of the scatter stimulus. The modulation of the scatter source lasts for 350 ms and the size of the pupil remains relatively constant during the modulation. The onset of flicker causes a constriction of the pupil but the latency of this constriction is normally greater than 350 ms. This instrument provides the patient with an unobstructed view of the scatter source and is easy to use (Barbur et al 1993). It provides reliable, reproducible data, without "noisy" results, and also takes into account large head movements and even blinks (Alexandridis et al 1991).

The method used to calculate the amount of light scatter in the eye is based on the Stiles-Holladay approximation. This is given by the following equation :

$$L_s = k E \theta^{-n} \quad \text{[equation 1.8]}$$

where:-

L_s = mean luminance of the compensating field, θ .

θ = the angle between the direction of a small scattering source and the point of interest on the retina.

E = illuminance level generated by the scattering source in the plane of the pupil (Stiles and Crawford 1937).

$$E = \Phi / A \quad \text{[equation 1.9]}$$

where:-

E = illuminance (lux)

Φ = incident flux (lumens)

A = area of the surface illuminated

n = the scatter index (describes the distribution of scattered light from the scattering source).

k = the straylight parameter (describes the overall level of light scattered).

(n and k are constants for a given eye).

$\log L_s$ has a linear relationship with $\log \theta$:

$$\log L_s = \log (Ek) - n \log \theta \quad \text{[equation 1.10]}$$

A knowledge of E makes it possible to compute k and n , by fitting the least squares line to $\log L_s$ vs. $\log \theta$.

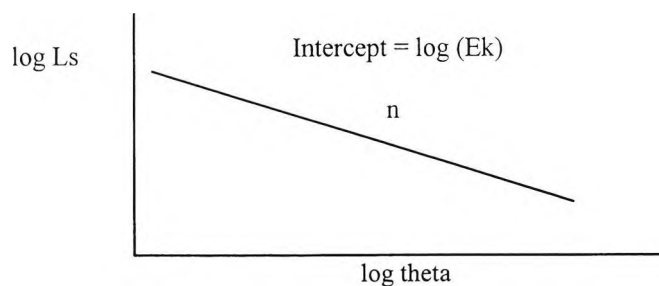


Figure 1.5 - Computation of k and n .

The value n can be taken from the gradient of the line, and the value of Ek computed from the intercept. If the illuminance due to the scatter source at the plane of the pupil, E , is known, then k , the straylight parameter, can be calculated.

Several researchers have examined the distribution of scattered light across the retina, and have produced diverse values for the constants n and k , at various glare angles (table 1.2):

Table 1.2 - Range of n and k values obtained by different researchers at various glare angles.

Author	Year	Glare angle measured	Value of n	Value of k
Holladay	1926	$2.5 < \theta < 25$	2	9.2
Stiles and Crawford	1937	$1 < \theta < 102$	2.1	11.5
Fry and Alpern	1953	$0.75 < \theta < 4.5$	2.5	22.4
Vos and Bouman	1963	$1 < \theta < 8$	2.8	29

Those studies that have attempted to quantify the amount of intraocular scattered light and its angular dependence have not yielded consistent results. Furthermore, in current clinical tests, it was assumed that any variability between individuals was due to changes in the amount of scatter (the straylight parameter, k) alone and that n remains constant (typically 2). The scatter index, n , has now been identified as an important variable which can influence visual performance, and can affect significantly the computed value of k (Barbur et al 1993). A smaller value of n suggests that smaller scattering centres are involved and they may account for the subject's disability glare. Smaller values of n predict a large angular spread. Conversely, larger values correspond to a narrower spread. Clinically, k is often regarded as the most important measurement because it is wrongly assumed that changes in n are not significant. However, figure 1.6 shows the relationship between the straylight parameters k and n , for a single subject, the measurements having been taken over a period of several days. The continuous line shows the predicted relationship between n and k on the basis that the total light scattered in the eye remains constant, and that the only changing variable is its angular distribution. Therefore, it can be seen that both n and k determine the total amount of scattered light in the eye (Barbur et al 1993). A new parameter has been calculated termed k' (the integrated straylight parameter), which is obtained from the integral of the scatter function of the eye. This parameter is, therefore, proportional to the total light scatter in a given eye. k' shows little variation when repeated measurements are made in the same eye (Barbur et al 1995).

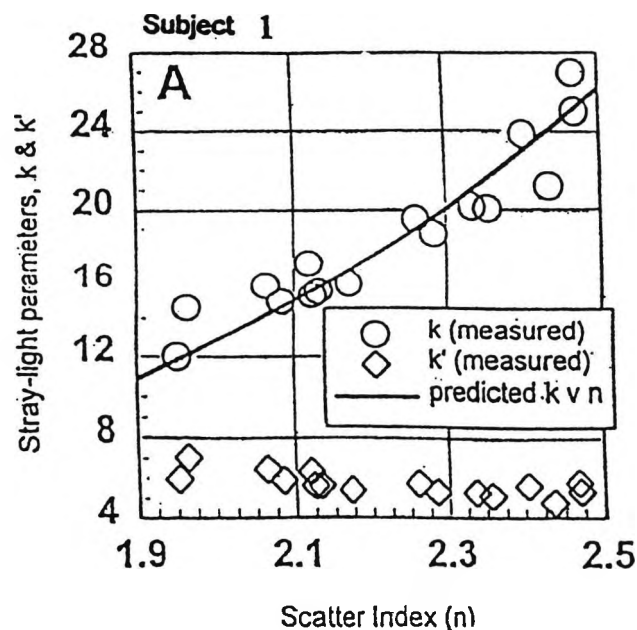


Figure 1.6 - Relationship between n , k and k' (Barbur et al 1995).

Therefore, it is not sufficient to measure only the straylight parameter k , as is done in most clinical tests, since changes in the scatter index, n , may also affect visual performance (Barbur et al 1993). Secondly, these results suggest that there is a significant variation in n over several days. When the scatter function is integrated so as to obtain a parameter proportional to the total scatter in the eye (i.e. parameter k'), little or no variation is observed. This means that k' is independent of fluctuations of n and k .

The variability associated with values of n and k can be further demonstrated by repeated measurements (figure 1.7 a, b and c). Three male subjects were recruited (subject 1, aged 41 (Rx = +0.25/-0.25 x 150), subject 2, aged 31 (Rx = -0.25 DS), subject 3, aged 45 (Rx = -2.00/-2.50 x 170) and tests were completed on a randomly chosen eye. All subjects were healthy, ophthalmologically normal with Snellen acuities of 6/6 or better. Sixteen estimates were made under optimum conditions over several days. The scatter values obtained from the three individuals can be seen in table 1.3, where the coefficient of variation (CV - s.d./mean x 100) of each set of measurements is also shown.

Table 1.3 - n , k and k' values obtained from three subjects.

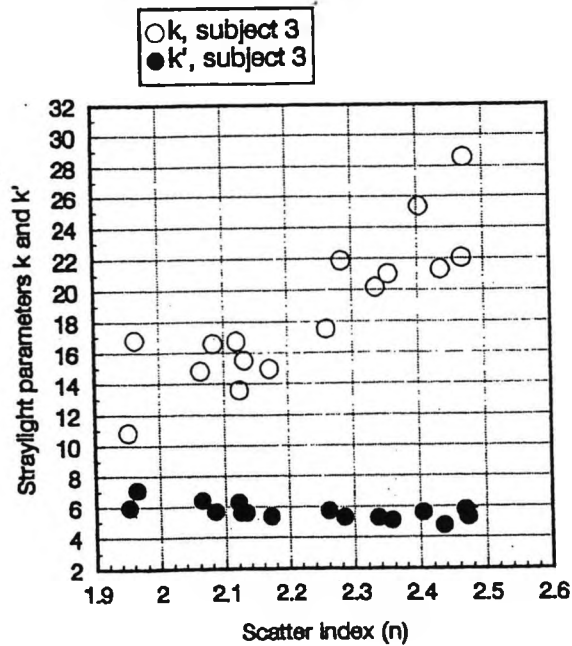
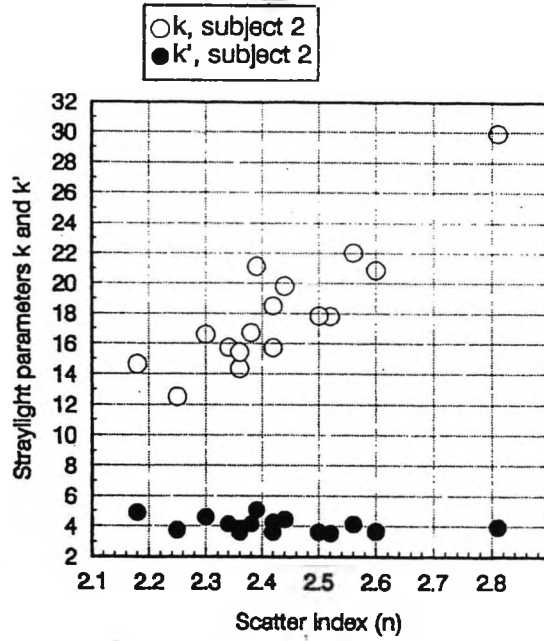
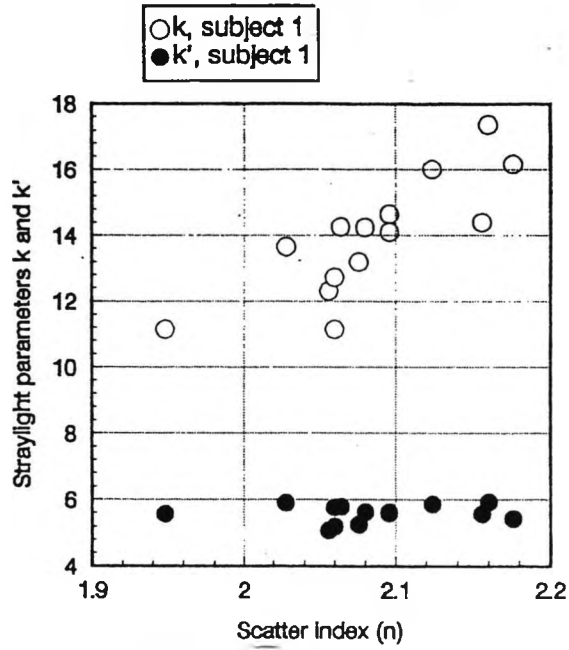
Subject	n	sd	CV (%)	k	sd	CV (%)	k'	sd	CV (%)
1	2.06	0.07	3.4	12.75	4.15	32.5	5.25	0.27	5.14
2	2.43	0.15	6.17	18.1	4.13	22.8	4.71	0.47	9.97
3	2.23	0.17	7.62	18.63	4.46	23.9	5.69	0.55	9.66

The average CV for k is 26.40% compared to 8.26% for k' . It can therefore be seen that the variability associated with k is high in comparison with that associated with k' . The results demonstrate that k' is a more appropriate parameter to measure and to use clinically to describe the amount of light scatter in a given eye.

Figure 1.7 also demonstrates that similar k' values can be obtained from very different values of n and k . For example, subject 1 revealed a k' value of 5.95 having yielded an n value of 1.95 and a k value of 11.22, whilst subject 3 revealed a similar k' value (5.70) having yielded an n value of 2.48 and a k value of 22.01. Following analysis of the effect

Figure 1.7

Straylight parameters plotted against n for three subjects



of random error fluctuations, it has been shown that n does vary systematically over time, although the cause of this variation is as yet undetermined (Edgar et al 2000).

The P_SCAN 100 scatter apparatus employs extended annular sources of light scatter to increase the light flux entering the eye, which is necessary when the scatter source is of relatively low luminance and generated on a visual display unit. The central display monitor, as outlined above, has been a source of problems when the measurement of light scatter was considered. Firstly, errors in light scatter parameters can be introduced if the light level entering the eye does not remain constant for different scatter source eccentricities. This problem is addressed by varying the diameters of the scatter sources, so that a constant level of illuminance is measured in the pupil plane by the photometer during the calibration procedure. The effective eccentricities of the large annuli are computed to give the equivalent eccentricities (θ) of the narrow annuli which would produce the same level of illuminances in the pupil plane, and cause the same amount of light scatter over the central test area. The basic diagram for the calculations involved is shown in figure 1.8.

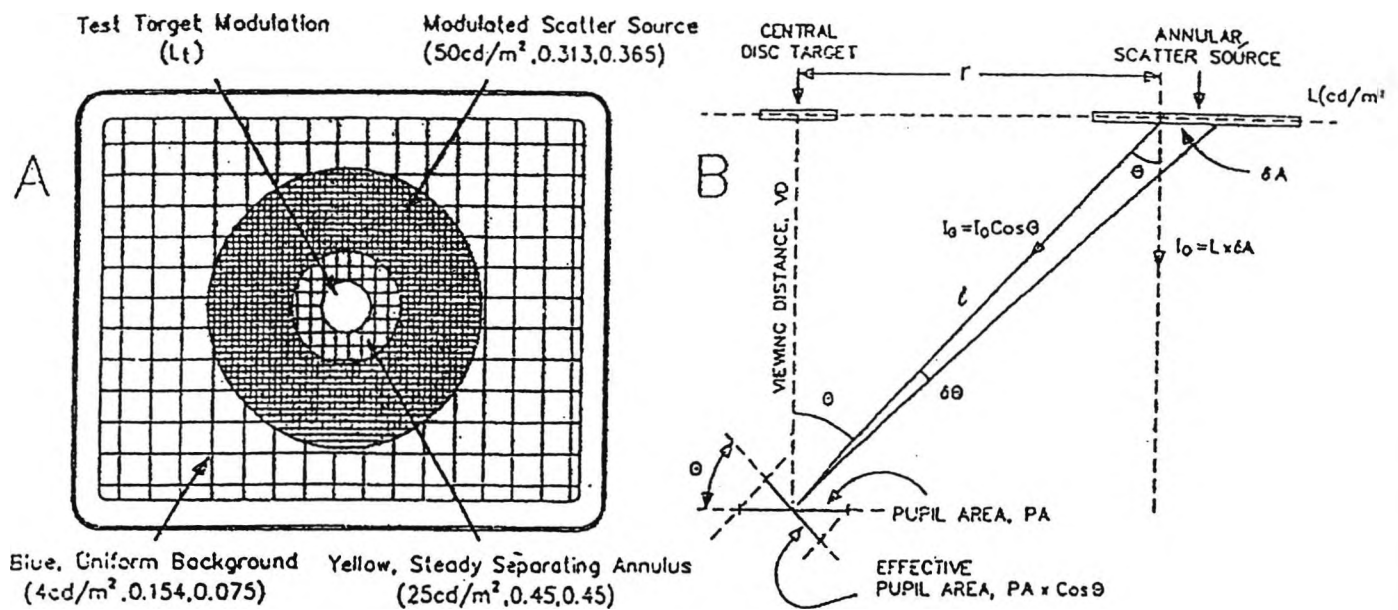


Figure 1.8 - Diagrams showing the schematic representation of the stimulus configuration used for the measurement of scattered light on a visual display unit (A), and the geometry of the display required for the computation of annulus size as a function of eccentricity (B) (Barbur et al 1993).

The effective eccentricity, θ , of each annulus is a function of the scatter index, n . Therefore, for a given value of n , one can compute the effective eccentricities of each

annulus employed. Weighted linear regression of the measured L_s values yields values of k and n . The weight assigned to each point is inversely proportional to the standard deviation obtained. Therefore, if one point has a large standard deviation, it will be given less weight in the statistical analysis. The best fit scatter model parameters are obtained when the value of n extracted from this analysis matches that used in the computation of effective eccentricities.

The P_SCAN 100 scatter program also employs a photometric calibration procedure to measure the internal scatter in the display for each annulus. Appropriate corrections are then applied automatically to each measured L_s value. By using this procedure, it is possible to use visual displays with extended annuli, and hence increase the illuminance level in the plane of the pupil. In addition, this obviates the disadvantage of earlier instrumentation (e.g. van den Berg and Spekreijse 1987), which does not necessarily compensate for the internal scatter occurring within the equipment.

1.4 Summary

A number of researchers have examined the distribution of scattered light across the retina, and produced a variety of estimates for n and k for different positions of the glare source. However, past studies to quantify the amount of intraocular scattered light and its angular dependence have not yielded consistent results, due to the assumption that n has a constant value of about 2. An additional assumption was that any variability between individuals was due to changes in k alone. The scatter index, n , has now been identified as an important variable that can influence visual performance. The computerised straylight program assesses the full scatter function and allows for the calculation of the parameter, k' , from the integral of the scatter function. This parameter shows reduced subject variability and is proportional to the total amount of light scattered.

In summary, the availability of the computerised straylight program which assesses the full scatter function and a researcher available to collect and analyse the data generated by this equipment permits:-

- direct measures of forward light scatter
- measurements of k'

- comparison between measures of visual performance (e.g. CS) and levels of intraocular light scatter
- comparison between backscatter and forward scatter.

The P_SCAN 100 scatter apparatus, which allows the full scatter function to be measured, will be utilised to investigate:-

- normal subjects of different ages
- diurnal and longitudinal variations within the normal population
- subjects with corneal abnormalities
- long-term contact lens wearers.

CHAPTER 2

Sources of intraocular straylight

2.1 Introduction

The crystalline lens and cornea are thought to contribute more entoptic light scatter than other ocular structures (DeMott and Boynton 1958; Vos and Boogaard 1963; Olsen 1982; Weale 1986; Smith et al 1990). The retinal tissue is also known to backscatter light (van den Berg et al 1991) and transillumination of the iris and ocular wall has been reported in eyes with little pigmentation (van den Berg 1991). The overall level of scatter in the normal human eye has been estimated at approximately 1 - 2% (Walraven 1973; Wooten and Geri 1987).

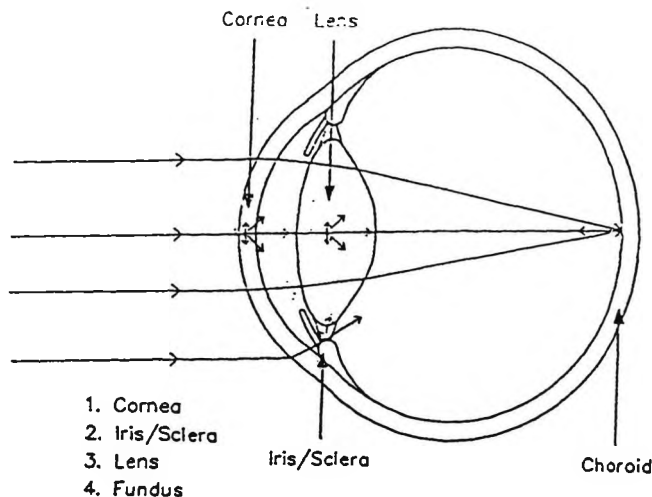


Figure 2.1 - Schematic diagram showing sources of forward light scatter in the human eye.

The principal method for evaluation of ocular structures is using a slit lamp biomicroscope, which yields a variety of information about the quality of these structures, including components that contribute to scatter in the eye. However, the vitreous and anterior chamber cannot be visualised using a slit lamp biomicroscope in normal subjects. Likewise, these structures do not contribute a significant amount to the light scatter in the normal eye.

The first method to quantify relative contributions of intraocular scattered light was performed by DeMott and Boynton (1958), using a photographic technique and excised steer eyes. Scattered light from a beam was directed towards the fovea and reflected by a mirror onto a photographic plate. The density of the exposed film was proportional to the luminance in the direction of the film of a source of scatter, and the position of any point in the photographic image was geometrically related to the anatomical location of the source. It was concluded that approximately 70% of scattered light originated from the cornea and aqueous, and 30% from the lens. However, the precise amount of scatter from these structures was dependant on pupillary aperture, because scatter can only arise from those regions illuminated by the glare source. As the incident light is restricted by the pupil to a cone on the retina, the scatter sources must lie in a disc coincident with the pupil. However, this conclusion may not be directly relevant to the situation in the human eye, due to differences in physiology and the changes brought about by excision. To overcome some of these problems, Boynton and Clarke (1964) used the equivalent veiling method (as described in section 1.3.2.2.1) in two human subjects. Scatter due to the cornea was reported to be $25 \pm 5\%$, with the majority arising from the crystalline lens. However, both studies failed to account for the fundus contribution of entoptic scatter (DeMott and Boynton 1958; Boynton and Clarke 1964).

Certain studies have attempted to ascertain the exact scattering properties of, and the effect of wavelength on each structure in isolation (e.g. Bettelheim and Vinciguerra 1971; Stevenson et al 1983; Hemenger 1990, 1992, 1996). In order to understand what causes light scatter in the eye, it is necessary to first consider the anatomy and physiology of structures that may affect the measurement of scattered light in the eye, in particular (because they are the principal sources of straylight), the cornea and the lens.

2.2 The cornea

The cornea is the main refracting surface of the eye. It is avascular and has a regular arrangement of stromal collagen lamellae, both factors that render the cornea highly transparent. The cornea forms the anterior 1/6th of the circumference of the outer coat of the eye. Due to conjunctival overlap of the peripheral cornea in the vertical meridian, the adult cornea is 10.5 mm vertically and 11.5 mm horizontally. The cornea can be described in terms of its five distinct layers, being:-

- The epithelium
- Bowman's layer
- The stroma
- Descemet's layer
- The endothelium

75% of the cornea is water and the metabolic activity of the cornea maintains the tissue in its proper state of deturgescence. Even a small increase in the water content will result in some loss of transparency. The epithelium and endothelium play a major role in the metabolic maintenance of corneal transparency, exerting their influence by an active as well as a passive process (Lerman 1980b). The peripheral cornea (limbal portion) receives its major nourishment from the perilimbal vessels located in the episclera and conjunctiva. The aqueous humour provides a significant amount of nourishment to the cornea, particularly to the inner layers, and completely nourishes the lens. The tear film is a third source of nourishment for the cornea. The cornea obtains its oxygen supply from the atmosphere.

2.2.1 The epithelium

The cells of the corneal epithelium are held tightly together by desmosomes. Only a small variation in RI exists between, and within these cells. As a consequence, the epithelium scatters little light, and transmits light in a manner similar to a fluid.

The epithelium accounts for approximately 1/10th of the total corneal thickness (CT), and is composed of three different cell types. The **basal columnar** cells form a single layer attached to the basement membrane by hemidesmosomes and are the source of two other cell types. The **wing** cells, arranged in two or three rows, are so-called due to their 'wing like' extensions. The **surface** cells are long and thin, which possess microvilli and microplicae to promote adsorption of goblet cell mucin. As a result, the cornea is kept constantly moist. Occasionally, non-native cells, such as lymphocytes and Langerhan's cells may also be present, principally during the occurrence of pathology.

The epithelial cells have a life span of seven days and are constantly shed into the tears. Cell division in the cornea is limited chiefly to the basal layer, however, corneal epithelial cells are ultimately derived from the corneal epithelial stem cells. These stem cells are thought to reside in the basal layer of the limbal conjunctival epithelium. Due to this process of disintegration and shedding, the superficial cells may be at different stages of development (Tseng 1962). Desmosomes are situated at the intersections of the cell wall and these also disintegrate as the cells move towards the surface.

2.2.2 Bowman's layer

Bowman's layer is an acellular structure that forms the superficial part of the stroma. It is a uniformly thick layer (8 - 14 μm), which underlies the basement membrane of the epithelium. It consists of collagen fibres devoid of keratocytes, in a randomly orientated arrangement (Hogan et al 1971). Generally, individual fibres are smaller than those in the remainder of the stroma (Jakus 1961; Harris 1962; Klyce and Beuerman 1987). Occasional interruptions in Bowman's layer occur in areas where corneal nerves pass from the stroma to the epithelium. Disruption may also occur during chronic pathological processes, such as corneal dystrophies or various types of keratitis which lead to scarring. The termination of Bowman's layer demarcates the beginning of the limbus.

2.2.3 The stroma

The stroma makes up 90% of the CT (approximately 500 μm thick) and consists of approximately 200 sheets of lamellae, each 1-2 μm thick, made up of type I collagen fibrils approximately 36 nm in diameter (Sayers et al 1982; Craig et al 1987). The refractive index (RI) of the collagen fibrils is 1.555 compared with the RI of the matrix, which is 1.345.

The collagen fibrils of the stroma are uniform in size and stretch across the length of the cornea as bundles, otherwise known as lamellae. Within each lamella, the collagen fibrils run parallel to each other, interlacing with regular interfibrillar spacing (Maurice 1957; Hart and Farrell 1969; Farrell et al 1973; Fratzl and Daxer 1993).

Keratocytes are interspersed between the lamellae and are collagen-producing fibroblasts. They form an interlinking network throughout the cornea, occupying 3% and 5% of the stromal volume (Jakus 1961; Harris 1962; Klyce and Beuerman 1987).

2.2.4 Descemet's layer

Descemet's layer forms the basal lamina of the corneal endothelium. It originates at the posterior aspect of the stroma and terminates at the trabecular meshwork. Ultrastructure examination shows that it is a two layered structure, composed of fine collagen fibrils and consisting of an anterior zone, which is developed in embryo and a posterior zone which is made continuously by the corneal endothelium throughout life. The innermost (endothelial) layer increases in thickness by $1\mu\text{m}$ with each decade of life.

2.2.5 The endothelium

The corneal endothelium consists of a single layer of polygonal cells and is responsible for maintaining the transparency of the cornea, by regulating corneal hydration. In essence, it acts as a pump, actively interchanging water and ions to and from the corneal stroma. The endothelial cells are packed with mitochondria, which satisfy the energy requirements for active pump mechanism. Tight junctions exist between adjacent cells, ensuring that transport of water or ions is through the cells, rather than between them.

It is generally accepted that the adult corneal endothelium responds to trauma by sloughing dead, or dying endothelial cells. Adjacent healthy cells then move to cover the denuded area, forming an endothelial barrier. Whilst it was once assumed that mitosis did not occur in the mature corneal endothelium, it has since been observed in cultured human endothelium cells (Zagorski 1980), and also in organ cultured corneas, following wounding (Treffers 1982). Indeed, preliminary specular microscopic evidence for mitosis has been reported (Laing et al 1983). Later, in 1984, the same author confirmed the earlier observation of mitosis and suggested that if proper conditions are met, then mitosis can occur in the adult human corneal endothelium. However, the factors that trigger mitosis in these cells are still not known (Laing et al 1984).

2.2.6 Corneal transparency

The physical basis of corneal transparency has been the subject of much interest amongst researchers. Several highly mathematical hypotheses have been presented, in support of different theories of corneal transparency. A much greater understanding of the structure has developed since the advent of the electron microscope.

The transparency of the ocular media was originally attributed to the homogenous nature of constituent elements (Duke-Elder 1932) and the absence of opaque structures. Other work has suggested that transparency was the result of the alignment of rows of fibrils within the stroma, with the diameter of the fibrils corresponding to a peak in the absorption spectrum of the cornea at 300 nm (Caspersson and Engerstrom 1946). Light rays were thought to pass down rows of fibrils, being refracted, to emerge undeviated. Reflection was thought to be limited by graduation in RI between the collagen fibril and the ground substance. However, this theory did not account for rays of light entering the cornea at various angles. Maurice (1957), considering measurements of birefringence, assumed that there was a large difference in RI between the collagen fibrils and ground substance, and concluded that individual collagen fibres in the lamellae could not scatter light independently of one another. If each collagen fibre did scatter light independently of any other fibres, then more than 90% of incident light would be scattered and hence the stroma would be opaque. It was therefore proposed that the physiological condition which accounted for corneal transparency was one in which the collagen fibres were equidistant, that is, arranged in a lattice. This arrangement would result in destructive interference and hence, corneal transparency. It was suggested that during stromal swelling, the regular arrangement of fibres became disrupted and thus scattering increased significantly. The increased scatter under conditions of mechanical stress was therefore explained by geometrical displacements in each cell centre. However, this theory was shown to be deficient following studies investigating other transparent ocular structures. For example, Goldman and Benedek (1967) noted that in the Dogfish, the fibres in Bowman's layer were not in a lattice arrangement and yet it scattered less light than the rest of the stroma. The authors concluded that a lattice arrangement of collagen fibrils was not a necessary condition for corneal transparency, and that transparency existed in Bowman's layer since it is optically homogenous over distances comparable to approximately half the wavelength of light. Later work supported this theory (Goldman et al 1968).

Further work using mathematical probability functions attempted to reveal the proximity between stromal fibrils that resulted in destructive interference (Hart and Farrell 1969). It was stated that the position of pairs of collagen fibres remained correlated only over a maximum of two near-neighbours, representing a partially ordered array. The mathematical summation of the phase of waves produced by such an arrangement was in good agreement with that found experimentally (Benedek 1971).

Benedek (1971) simplified the earlier work with Goldman (Goldman and Benedek 1967) and stated that scattering of light is only produced by those fluctuations in RI whose Fourier components vary over a distance equal to, or larger than, half the wavelength of light in the medium.

Feuk (1970) also considered the theoretical relationship between wavelength and different light scattering characteristics and drew similar conclusions to Maurice (1957). However, Feuk (1970) suggested that Maurice's lattice theory was not necessary for transparency and that a displacement from ideal fibril positions of up to one-third of a fibril diameter would produce only 1% scatter. Later, Farrell et al (1973) suggested that the cornea exhibited short-range ordering of fibrils rather than a strict lattice. The fibrils were suggested to be slightly displaced from the regular lattice, with the lamellae running randomly across the cornea, but parallel to the corneal surface. This arrangement results in the destructive interference of light, in all directions apart from forwards and backwards. Therefore, the geometric arrangement of the collagen fibrils plays a significant role in corneal transparency.

Orientation of the fibrils is constant within each lamella but varies throughout successive layers in a way that may depend on species, as well as other conditions (Coulombre and Coulombre 1975; Gordon 1976; Meek et al 1987; Komai and Ushiki 1991). Although the regular arrangement of the fibrils within each lamella is considered to be responsible for the transparency of the tissue (Maurice 1957; Benedek 1971; Twersky 1975), orientation of the successive fibril layers throughout the entire cornea is an important factor which determines the mechanical properties of the cornea (Nyquist 1968; Nash et al 1982).

Although many local details of the corneal structure have been obtained by electron microscopic methods (e.g. Komai and Ushiki 1991), information about typical structural characteristics of the entire cornea, such as preferred or random orientation of the layers, is more readily obtained through measurements of scatter (McCally and Farrell 1982; Meek et al 1987; Fratzl and Daxer 1993). In particular, Meek et al (1987) reported x-ray scattering patterns from normal human corneas, indicating preferred orientation of collagen fibrils along the horizontal and vertical meridians. A subsequent study by Daxer and Fratzl (1997) reported orthogonal four-fold symmetry, indicating that the preferred orientation of the collagen fibrils was along the horizontal (nasal - temporal), and the vertical (inferior - superior) directions. It was determined that 66% of the fibrils were within the horizontal and vertical sectors, whereas only 34% were found in the oblique sectors between. This behaviour was found not only in the centre of the cornea but also at every other investigated position (nasal, inferior, temporal and superior) at the margin of a central 7 mm zone (Daxer and Fratzl 1997). The authors further stated that the collagen fibril orientation was completely disrupted in keratoconic corneas.

2.2.7 The origin of corneal light scatter and its angular dependence

Feuk and McQueen (1971) examined the angular dependence of light scattered from normal rabbit corneas and showed that as the scattering angle increased, the amount of light scattered decreased. The stroma was found to be the main structure responsible for scattering in the backward direction, whereas the epithelium scattered more strongly in the forward direction. Epithelial oedema was shown to greatly increase scattering in the forward direction. It was suggested that collagen fibrils of the corneal stroma are displaced from the lattice arrangement by up to 10% of the centre to centre distance between fibrils. Such a model would produce 1% scatter and the wavelength dependence of scatter would be inversely proportional to the 5th power of wavelength (Feuk and McQueen 1971). Subsequent work cast doubt on the accuracy of this model, with the wavelength dependence of scatter shown to be inversely proportional to the 3rd power of wavelength (Farrell et al 1973).

Lindstrom et al (1973) reported that the greatest intensity of scattered light came from those regions closest to the limiting layers in rabbit corneas, particularly anteriorly. The author suggested that this was due to the reduced regularity of the collagen fibrils in this

area. Subsequent work by McCally and Farrell (1976) confirmed this finding. Normal rabbit corneas were examined using a slit lamp biomicroscope, a photocell and an X-Y recorder. The results showed that as the scattering angle increased, the amount of light scatter decreased over a range of scattering angles (between 20 - 145 degrees). 60% of the total light back scattered originated from the stromal region and intensified scattering was noted at the stromal borders. It was suggested that the fibril arrangement in these border areas is rather irregular, when compared to the central stromal region.

Lovasik and Remole (1983) measured forward light scatter in excised corneas and investigated (i) the angular dependence of scattered intensity over a 140 degree angle and (ii) CT. Corneas were submerged in saline solutions ranging from isotonic, to hypertonic. The results corroborated previous findings (Kikkawa 1960; Feuk and McQueen 1971), showing that as the scatter angle increased, corneal light scatter decreased.

2.2.8 The corneal contribution to light scatter in the eye

The principal sources of information regarding scatter from ocular structures have been obtained from excised eyes, which provide only limited information because of the significant changes that occur post-mortem. As previously described, DeMott and Boynton (1958) suggested that 70% of light is scattered by the cornea. In a subsequent study, Vos and Boogaard (1963) attempted to determine the contribution of the cornea to entoptic scatter. A thin pencil of light was used as the glare source which, as the light entered the eye, caused the cornea to act as a point source of straylight, producing a luminance veil across the retina. This in turn transilluminated the pupil, casting a shadow of the iris on the retina. The discrepancy in retinal illuminance between the area affected by the luminous veil and the shadow was considered to represent the corneal contribution to entoptic light scatter. The jump at the border was either (i) compensated by the pattern, by the addition of a dark circle of uniform background, whose size and intensity could be altered (figure 2.2 (b)) or (ii) imitated by the pattern, by adjusting a white circle on a dark background to simulate the same luminance profile as the glare source (figure 2.2 (c)). Comparable results were obtained using both techniques (Vos and Boogaard 1963). The equivalent luminance versus the glare angle was plotted for various pupil sizes. As the glare angle increased, corneal light scatter reduced. The distribution was similar to that measured for total intraocular light scatter.

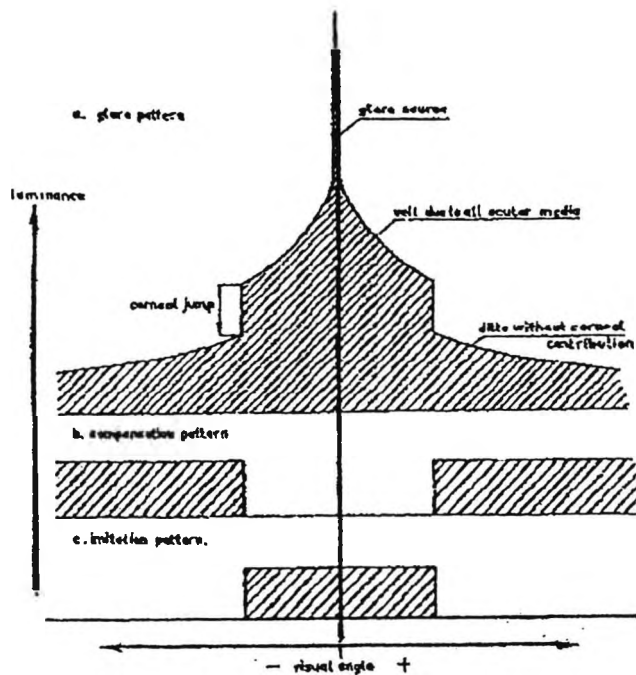


Figure 2.2 - The luminance distribution in the entoptic veil round the glare source (a). The jump at the border is either compensated by the pattern (b), or imitated by the pattern (c) (Vos and Boogaard 1963).

This technique gave high reproducibility. However, there was large intersubject variation, due to difficulties with the experimental set-up. The study concluded that for glare angles between 30 and 70 degrees, the cornea contributes up to 30% of entoptic straylight. This is in close agreement with the 25% determined by Boynton and Clarke (1964), using the equivalent veiling method. In order of magnitude, this is also in agreement with the findings of DeMott and Boynton (1958). The apparent difference in findings of a factor of two may be attributed to the lack of consideration of the fundus contribution of entoptic scatter, and also to the use of excised steer eyes.

Allen and Vos (1967) tested the hypothesis that forward light scatter was related to backscattered light using a variable contrast Landolt C test. Back scatter was measured using slit lamp photographs (30 degrees from the incident light). The results showed that less than 1% of the incident light was backscattered. Data from young normal observers, with clear optical media revealed that approximately 30% of total intraocular scattered light

originates from the cornea, a finding in agreement with previous work (Vos and Boogaard 1963).

2.3 The crystalline lens

The lens has long been considered an important source of straylight, especially with ageing and when affected by cataract. The normal human lens contains approximately 65% water and 35% organic matter, the latter being chiefly structural proteins. Since the structural proteins (alpha, beta, gamma crystallins, and insoluble protein fraction) constitute most of the dry weight of the lens, they play a major role in the transmission, as well as in the absorption, scattering and refraction of light through the organ. A knowledge of the morphology and composition of the lens will not only explain its transparency to visible light but also indicate the potential for increases in the light scattering characteristics of the eye.

The crystalline lens is an optically dense, biconvex, flexible living structure located between the refracting surface of the cornea and the light sensitive retina. New lens fibres arise by cell division in the germative zone in the pre-equatorial region of the lens and so the lens grows at a steady rate through life by the process of surface accretion which is partially compensated by central compaction of fibres towards the nucleus (Huggert 1946). The rate of lens growth is thought to be approximately 0.03 mm per year (Brown 1976). This growth may account, at least in part, for the zones of discontinuity observed with the slit lamp biomicroscope. Zones of discontinuity are essentially cortical layers which differ in light scattering properties and width. When the lens is observed using the slit lamp, the adult lens can be divided into five layers: C1 alpha/beta, C2, C3 and C4. These layers are most easily observed around the age of 40 (Niesel et al 1976; Sparrow et al 1986). Zones C1 and C2 are located in the superficial cortex and C3 and C4 are located in the deep cortex. C1 is divided into two layers, one of which is essentially clear (C1 alpha) and the other is a light scattering zone (C1 beta). C2 is also a clear zone. As the lens increases in sagittal width, C2 becomes increasingly thick. As fibres are added to the surface (C1), the fibres located adjacent to C2 scatter less light and become part of C2 (Sparrow et al 1986). Zone C3 increases in light scatter and width with age (Sparrow et al 1992). The last zone (C4) is relatively clear.

The lens of a normal eye has refractive power, providing accommodation and optical transparency. However, the refractive power of the lens reduces with age (Stafford 1996). The lens has anterior and posterior surfaces which approximate to parabolas. At birth, the equatorial lens diameter is approximately 6.5 mm but increases to approximately 10 mm by the ninth decade. The sagittal thickness increases from 3 mm at birth, to 5 - 6 mm by the ninth decade (Stafford 1996; Bron et al 2000). It is suspended radially from the ciliary body by the zonular fibres attached on either side of the equator.

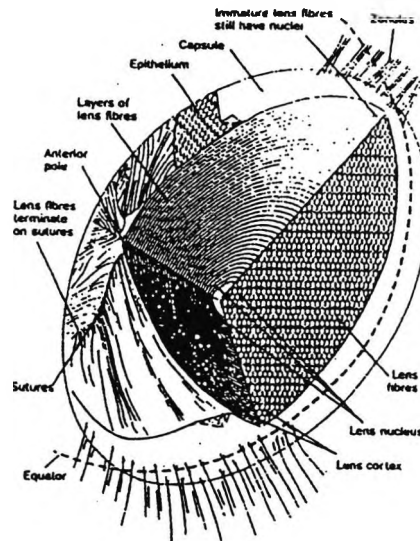


Figure 2.3 - Three-dimensional representation of the human lens (Stafford 1996).

The lens is avascular, and lacks both a nerve supply and cellular contact with other structures within the eye. Consequently, although the lens tissue is less metabolically active than most tissues, it depends on absorption of metabolites and removal of waste products via the aqueous. The most metabolically active site lies within the epithelium, which is adjacent to the aqueous. Glycolysis is the main source of energy, permitting cell division and growth (Lerman 1980b).

2.3.1 The lens capsule

The capsule encases the lens elements (figure 2.3). It is a highly elastic, replicated basal lamina, formed by the basement membrane of the epithelium. Although the capsule appears structureless, electron microscopy reveals a laminar structure. Each lamina consists of parallel collagen filaments. There is a denser outer layer which contains

capsular filaments and zonular elastic microfibrils. Zonular fibres run tangentially to the lens surface at their attachment to the capsule. As lens volume increases, the capsule thickens anteriorly and equatorially, due to the deposition of new lamellae.

2.3.2 The lens epithelium

The cells of the epithelium are joined to each other by desmosomes and gap junctions which permit communication between cells. The basal surfaces of the epithelial cells joining the capsule show interdigitation with the basal lamina at each lateral cell border. The epithelial cells are involved in the synthesis of lens crystallins, ion transport, secretion of capsular precursors and they are also rich in cytoplasmic organelles. Epithelial cells divide pre-equatorially moving to the posterior equator, where they elongate and become lens fibres. The apical end of the cell (away from the lens capsule) pushes forward, and the basal process (next to the capsule) moves backwards beneath the posterior capsule until the cells meet at posterior sutures. As the cells elongate, they lose organelles, retaining only mitochondria. The nucleus breaks down and interdigitation increases. There is an increase in the density of the cytoplasm, and also changes in the cytoskeleton.

2.3.3 The lens cortical fibres

Lenticular cortical fibres are thin, long, and roughly hexagonal in cross-section, increasing in width as they cross the equator. The fibres from the young lens are approximately 7-10 μ m in length, whilst the nucleus fibres tend to be longer and thicker. Gap junctions are more prominent between the capsule and the outermost layer, maximising the potential for metabolic communication. All lens fibres have a cytoskeleton made up of microtubules and cytoplasmic filaments. Microtubules give lens fibres their elastic properties and increase in number as the new lens fibres elongate (Stafford 1996). The mature strap-like fibre cells lose their nuclei, and few organelles remain (Lerman 1980a). The lens fibres grow from all around the equatorial region and meet at radiating lines or sutures. With time, the lens fibres that are initially formed at the periphery migrate inward, and become more sclerotic. This results in relatively abrupt changes in the RI of specific regions in the lens. Electron micrographs indicate that the morphological basis for this phenomenon is a generalised decrease in the number of specific intracellular organelles, with a concomitant increase in the amount of low-density material in the lens fibres of the deeper cortical layers (Lerman 1980a).

In addition to the structures that constitute the lens, it is also necessary to discuss other lenticular properties that may influence the light scattering characteristics of the eye.

2.3.4 Lens fluorescence

A number of investigators have reported fluorescent peptides and proteins in the human lens (e.g. Lerman et al 1970; Bando et al 1975; Lerman et al 1976; Lerman and Borkman 1976; Larsen 1993; Pau et al 1993). These proteins contain one or more fluorescent chromophores, or "flourogens". In vitro purple fluorescence has activation wavelengths of approximately 290 nm and an emission maximum at 340 nm (Pirie 1968; Satoh et al 1973; Lerman 1980a; Bleeker et al 1986; Mosier et al 1986; Occipinti et al 1986). This type of fluorescence is most likely to be due to the amino acid, tryptophan (Satoh et al 1973), and its fluorescence is not thought to have a consequence on vision, remaining as it does at a relatively constant level throughout life. Indeed, excitation wavelengths are in fact absorbed strongly by the cornea (Zulich et al 1992). Other flourophores are the result of photooxidation reactions involving prolonged exposure of tryptophan to UVR. Blue/green flourogens have activation wavelengths of approximately 420 to 435 nm and emission maxima at around 520 nm (Lerman 1980a; Bleeker et al 1986; Mosier et al 1986; Occhipinti et al 1986). This fluorescence increases in diabetes (Mota et al 1992; Sparrow et al 1992; Bron et al 1993; Larsen 1993; Eppstein et al 1995) and with age (Yappert et al 1992). UV/blue excitation has activation wavelengths of approximately 360 nm, and emission around 440 nm (Pirie 1968; Satoh et al 1973; Bando et al 1975; Lerman 1983) and is related to the yellow pigment of ageing and nuclear brunescence cataract (Monnier and Cerami 1982; Hemenger et al 1989; Lerman et al 1989). Long wavelength fluorescence has also been reported, red (activation - 647/emission - 672), near red (568/633), and orange (568/591) (Yu et al 1979).

The visual consequences of lenticular fluorescence have not been well documented in the literature but it is thought that fluorescence may contribute to forward light scatter by acting as a source of veiling luminance (Henker 1924). Therefore, lenticular fluorescence may add a uniform component to the retinal PSF, reducing visual performance. Elliott et al (1993b), using the Regan chart at various levels of contrast, measured the visual deficit associated with UV induced lenticular fluorescence for 61 normal subjects between the

ages of 21 and 80 years. UVR was shown to reduce low contrast acuity and this loss increased linearly with age.

Changes in lens fluorescence have an important role in ageing, which in turn will increase the amount of scattered light in the eye. These changes will be discussed in more detail in section 5.2.2.

2.3.5 Lenticular transparency

When light enters the eye and passes through the lens, some absorption, and/or scattering of light is inevitable. However, the lens must optimise passage of wavelengths required by the retina, whilst at the same time hindering passage of other wavelengths that may cause retinal damage. The normal clear lens transmits approximately 90% of the incident light between the wavelengths of 500-1000 nm (Lerman and Borkman 1976). Light scatter in the lens not only reduces the incident intensity of the light, but also leads to glare and distortion of the image formation of the retina (Phillipson 1973). Lenticular light scatter is minimised by the perpendicular arrangement of the lens fibre layers, which results in little extracellular space. Light scatter from the lens fibres is further reduced, as only a few organelles are present, and their intracellular proteins are soluble.

Even in the normal transparent lens, a certain amount of light entering the eye is scattered. When light enters the eye, the total light scattered in the young normal lens is less than 5% (Allen and Vos 1967). Naturally, a certain amount of light is scattered from the surface of the lens, due to the large difference in RI between the aqueous humour and the lens capsule (Phillipson 1973). However, this is minimised by the smoothness of the outer surface of the capsule. In addition, the lens sutures and fibre walls also contribute a significant amount of light scatter, because the interdigitations of the cell membranes form bodies as large as 0.5 μm in diameter, acting as centres for light scatter (Phillipson 1973).

Trokel (1962) proposed that lens transparency is a consequence of the paracrystalline structure of the soluble proteins. These proteins are arranged in an ordered manner within each lens fibre thus minimising light scatter. Localised alterations in the density of the packing of lens proteins, be they due to aggregation and/or configurational changes developing in various portions of the lens, will lead to changes in transparency and yield

small scatter sources, resulting in Rayleigh scatter. Although the lens fibre walls were identified as large scatter sources, it was suggested that their regular spacing serves to minimise light scatter. This was later confirmed by Benedek (1971) and Miller and Benedek (1973). In addition, Benedek (1971) suggested that the sizes of the spatial Fourier components contained in the crystalline lens were smaller than the wavelength of light.

Delaye and Tardieu (1983) expanded on the 'transparency theory', proposing that the crystallin proteins exhibit short-range, "liquid-like" order. Subsequent studies, which investigated light scatter and protein content in young and old lenses, confirmed this arrangement (e.g. Yaroslavsky et al 1994). The lens core exhibited a large variation in light scatter, which was attributed to alterations in protein configuration.

The lenticular fibre cells also contribute to scatter in the normal eye. As discussed, fibre cells are packed regularly, so that light scattering gives rise to a diffraction pattern. The calculated spacings from such patterns compared well with the thickness of cortical fibre cells (Phillipson 1973). This implies that the membranes causing the diffraction have only periodic density fluctuation, and little optical anisotropy. The nature of optical anisometry in the crystalline lens has been studied by Bettelheim using laser diffraction patterns (Bettelheim and Vinciguerra 1971; Bettelheim et al 1973). Light scatter was found to increase if the variation of RI orientation increases. In fact, the lens halo resulting from RI fluctuations in the fibre lattice has been shown to contribute to disability glare in experiments using monochromatic light (Mellerio and Palmer 1972).

Smith et al (1992) investigated the relationship between backscattered light and the width of various regions of the anterior cortex of human lenses. Fifty eyes from 50 subjects were examined using computerised linear scanning densitometry of Scheimpflug images. The study showed that light scatter increased in the three major zones (C1 - C3) with age (section 5.2.2). The zone pattern observed was thought attributable to a number of factors. Most notably, not only do the refractive indices vary between zones, but the fibre cell membranes have a higher RI than the cytoplasm which they border (Huggert 1946; Bettelheim 1985). In addition, Travers (1990) showed that the fibre cell interdigitations vary from 'finger like protrusions' in the superficial fibres to 'ball and socket' in the deeper cortex. Thus, these changes in fibre interdigitations may cause varying amounts of light

scatter in the zones of discontinuity. Finally, Brown (1976) and Brown et al (1988) have shown that compaction of the lens fibres occurs in the cortex and nucleus in young subjects but that the compaction is confined to the cortex in middle age and older. This finding may explain the increase in light scatter found in the three major zones of discontinuity.

Hemenger (1992) showed that by inversion of the disability glare function, RI fluctuations in the lens extend over distances of tens of micrometers. This implies that the fluctuations that occur were over large distances, compared to the wavelength of light. Consequently, randomly placed inhomogeneties (e.g. protein aggregates) were excluded as a cause of light scatter. It was concluded that the primary cause of small angle intraocular light scatter are RI fluctuations associated with the periodic lens fibre lattice, as these structures provided the necessary large spatial extent (Hemenger 1990, 1992). Later, Hemenger (1996) reported that calculations based on scatter by lens fibres were in good agreement with measurements from donor lenses (van den Berg and Ijspeert 1995).

van den Berg and Ijspeert (1995) investigated the angular distribution of scattered light in vitro. Sixteen donor lenses (age range 21-86 years) were investigated using a high pressure mercury lamp, a series of diaphragms and a photomultiplier. Changes in light scatter in the lens were not due to scattering type, but instead were due to the number of scattering sources (i.e. cataract formation scatterers are added with the same type of scattering characteristic that would normally be found in a transparent lens). van den Berg and Ijspeert (1995) suggested that if the number of scatterers was relatively low, light was scattered only once (single scattering). The intensity of this scattering is proportional to the number of scatterers. This may explain the relatively constant angular dependence of intraocular scattered light despite cataract formation. However, if the number of scatterers is high, such as in advanced cataract, light may undergo multiple scattering. When this occurs, the scattering characteristics of the eye change and the angular distribution of scattered light becomes flattened.

2.3.6 Lenticular wavelength dependence

Whitaker et al (1993) investigated the wavelength dependency of light scatter, in order to demonstrate that large scattering centres, such as the variation in RI at the lens fibre intersections, caused the majority of intraocular light scatter. As discussed in section

1.3.2.2.1.3, Whitaker et al (1993) examined straylight in normal young, elderly and cataractous eyes, taking CS measurements, with and without a glare source. The resulting decrease in the CSF was measured and the LSF was calculated. No significant wavelength-dependency was demonstrated in normal eyes, confirming the lack of any significant Rayleigh scatter. However, in eyes with cataract, a slight wavelength dependence was found, with increased straylight values at long wavelengths. However, only four subjects were investigated. It was suggested that the increased scatter at long wavelengths may be caused by the development of yellow pigment within the lens, masking a proportion of the short wavelength light.

Subsequent work by van den Berg studied the wavelength dependence of the lens (van den Berg and Spekerijse 1997). Despite little *in vivo* evidence, van den Berg (1997) suggested that different parts of the lens have different scattering characteristics and that lenticular light scattering in the forward direction is dependent on wavelength. It was reported that the lenticular scatterers are not much smaller than the wavelength of light, and so demonstrate weak wavelength dependence. Also, the scattering of the superficial layers of the lens was relatively stable, compared with those of the nucleus (van den Berg 1997). The changes in the nucleus cause an increase in straylight and also produce a change in the light scattering characteristics of the eye. This can be demonstrated in the *in vivo* situation: after the age of about 50 straylight increases, with a doubling observed by the age of 70 (Vos 1984; van den Berg 1991) (Chapter 5). In agreement with Whitaker et al (1993), it was suggested that the increase in nuclear scattering produced a lenticular long-wavelength dependence.

2.4 Effect of iris and ocular wall pigmentation

Straylight is dependant on iris colour (van den Berg 1990), and is found to be greatest in blue-eyed Caucasians. Brown-eyed non-Caucasians have least scatter, less than is found in brown-eyed Caucasians (Ijspreet et al 1990). van den Berg (1990) stated that brown-eyed Caucasians exhibit 18% less light scatter than blue-eyed individuals. Significantly lower levels of forward light scatter have been reported in highly pigmented eyes, especially at large angles (Elliott et al 1991).

The colour of the iris is chiefly determined by melanocytes. In the brown iris, the melanocytes are pigmented and abundant. In contrast, the blue iris, contains few melanocytes in addition to amelanotic cells which contain non-pigmented granules (Yanoff and Fine 1989). The colour of the iris indicates the level of pigmentation throughout the eye. As iris colour varies between subjects, so does the pigmentation of the ocular wall which affects the amount of light transmitted. Intracocular light scatter will increase if the amount of transmission of light through the ocular wall increases. In fact, the amount of pigmentation decreases with age (Schmidt and Peisch 1986). Therefore, by allowing some light to be transmitted to the retina, the relatively opaque structures of the iris and sclera act as further sources of scattered light. Light scattered by these structures has not generally been accounted for in most studies investigating intraocular light scatter. Therefore, this suggestion may provide an explanation for the conflicting reports regarding the wavelength dependency of intraocular light scatter (van den Berg and Ijspeert 1991). van den Berg and Ijspeert (1991) reported greater long wavelength scatter that could be attributed to the selective transmission of light through the blood vessels of the iris and the sclera. This phenomenon would allow more red light through the ocular wall whilst absorbing green and blue light. The authors prevented any light from entering the pupillary aperture and projected an annulus of light through the iris or ocular wall. The subjects were then tested using the van den Berg straylightmeter. Transmission through a blue iris for red light was found to be 1%, and 0.2% for green light. As predicted, highly pigmented eyes transmitted less light through the iris and ocular wall than eyes with little pigment. This was thought to be due to the absorption of light by melanin. van den Berg and Ijspeert (1991) stated that there was little relationship between scattered light and wavelength. The dependence of scattered light on wavelength was small, especially in more pigmented eyes and at small scatter angles. In less pigmented eyes, at larger glare angles, the wavelength effect could prove more significant.

2.5 Retinal contribution to scattered light

Polarised light was used by Vos and Bouman (1964) in order to determine the retinal contribution to intraocular light scatter. Two methods of assessing the contribution of retinal light scatter to overall intraocular light scatter were employed. The imitation technique required the observer to adjust the intensity of a set of imitation brushes until they matched the entoptic brushes, whilst the compensation technique involved the

projection of compensation brushes to fill the dark gaps between the entoptic brushes. The intensity of the brushes was altered in order to obtain an even veiling field. Using both techniques, the purpose was to find the equivalent veiling luminance. It was found that when the glare light was linearly polarised, the veiling glare took on a “winged” formation and by continuously changing the direction of polarisation, in order to give rotation, the wings were refined. The wings became more apparent when the glare source was projected onto an extra-foveal area. This was due to the increased scattering of light caused by the thicker retinal tissue. The study concluded that parafoveal fixation gave an estimate of 40% of total scatter due to the increased thickness of the retina, whilst foveal fixation produced an estimation of 12% retinal scatter. However, these values assume that all the polarised scattered light was due to the retina. In addition, since DeMott and Boynton (1958) concluded that the retina played no significant part in forward light scatter in the eye, it is possible that Vos and Bouman (1964) were in fact measuring retinal backscatter, rather than forward scatter.

2.6 Summary

The cornea and crystalline lens are thought to contribute more entoptic light scatter than other ocular structures (DeMott and Boynton 1958; Vos and Boogaard 1963; Olsen 1982; Weale 1986; Smith et al 1990). The transparency of the cornea and lens is due to the minimal absorption and scattering of light across the visible spectrum. Although these structures are essentially considered transparent, they are known to scatter light, since backscatter allows them to be visible.

The transparency of the lens has been the subject of much research. Trokel (1962) proposed that an even distribution of lens proteins within the fibre cells could account for lenticular transparency. Subsequently, Benedek (1971) suggested that the sizes of the spatial Fourier components within the normal lens were smaller than the wavelength of light. Hence, it is a transparent structure. Consequently, either the absence of large fluctuation in RI (Phillipson 1973), or the absence of scattering units comparable to the wavelength of light, provide lenticular transparency (Hemenger 1992). (Hemenger 1990, 1992, 1996) also demonstrated that the primary cause of small angle intraocular light scatter are RI fluctuations associated with the periodic lens fibre lattice. Therefore, an

increase in light scatter may result from changes to the size and number of the lens proteins within the lens or changes in RI.

Hypotheses of corneal transparency have discounted a random collagen fibril arrangement, since this would result in high levels of scatter (Maurice 1957; Hart and Farrell 1969; Feuk 1970). An entirely regular lattice with highly ordered collagen fibrils, as proposed by Maurice (1957) has also been questioned, since this would result in no scatter. Later, Farrell et al (1973) suggested that the cornea exhibited short-range ordering of fibrils rather than a strict lattice. The fibrils are thought to be slightly displaced from the regular lattice, the lamellae running randomly across the cornea, but parallel to the corneal surface. A later study by Daxer and Fratzl (1997) reported orthogonal four-fold symmetry, indicating the preferred orientation of the collagen fibrils along the horizontal (nasal - temporal), and the vertical (inferior - superior) directions. If the regular collagen fibril arrangement is disrupted, an increase in light scatter will result.

Other ocular structures may also act as scatter sources within the eye. Transillumination of the iris and ocular wall has been noted in eyes with little pigmentation (van den Berg 1991) and the retinal tissue is known to scatter light (van den Berg 1991). In addition, the aqueous and vitreous humours may also add a small amount to the level of scattered light. However, their contribution is difficult to quantify.

The lack of light scatter in the eye is fundamental to visual performance. Changes in any ocular structure, be it due to oedema, contact lens wear or pathology, are likely to result in an increase in light scatter, as the structures maintaining transparency will be adversely affected.

CHAPTER 3

The contrast sensitivity function

3.1 Introduction

The relationship between the contrast sensitivity function (CSF) and the PSF means that measurements of CS are of relevance to studies investigating intraocular light scatter. The retinal PSF and the optical transfer function of the eye are Fourier transforms of one another (Campbell and Gubisch 1966), and are directly related to the CSF. As such, examinations of the shape and form of the PSF have a direct bearing on studies involving the CSF. In addition, when compared to VA measurements, CS more adequately reflects visual capabilities. Measurement of VA defines the highest spatial frequency (or smallest detail), that can be resolved by the eye at high contrast levels. The test is universally known, simple to perform, and well proven in assessing refractive errors. However, measurement of VA does not fully describe the quality of vision and thus does not always reveal the full extent of visual changes attributable to pathology (Abrahamsson and Sjostrand 1986). In fact, patients with similar VA may differ significantly from one another in terms of CS (Ginsburg et al 1980). Furthermore, an individual's ability to see large, low contrast objects can be predicted from an individual's CS, but not from his VA (Ginsburg 1978; Ginsburg 1981).

The human visual system is able to recognise objects if they differ from their surroundings by either luminance, colour, motion, texture, or disparity. To distinguish an object from its background, the visual system must respond to a change around a steady level of illumination. This change is known as contrast and responses of retinal, geniculate, and some primary cortical neurones, are dependent on this factor. Therefore, CS testing gives a more complete description of the spatial resolution of the visual system than VA testing. Grating CS tests have been used to study the physiology of the visual system in normal subjects (Campbell and Green 1965; Banks and Salapatek 1976), and those with pathology (Regan et al 1977; Atkin et al 1979). Measurement of CS has revealed sensitivity loss in patients with cerebral lesions (Bodis Wollner and Diamond 1976), multiple sclerosis (Regan et al 1977; Bodis Wollner et al 1979), macular disease (Sjostrand and Frisen 1977; Stangos et al 1995), glaucoma (Arden 1978; Atkin et al 1979; Vaegan and Halliday 1982;

Bron et al 1984), ocular hypertension (Ross et al 1987), cataract (Hess and Woo 1978), amblyopia (Hess 1979) and keratoconus (Hess and Carney 1979; Carney 1982; Zadnik et al 1984). CS is particularly useful for the detection of subtle visual loss (Arden 1978; Arden 1988; Regan 1988; Tytla and Buncic 1988) and has been used to identify differences in visual capabilities not revealed by more traditional procedures (Ginsburg 1981b; Ginsburg et al 1982; Evans and Ginsburg 1985).

3.2 Psychophysical basis for measuring contrast sensitivity

Schade (1948) was among the first to report investigations that employed sinusoidal functions based on the modulation transfer function (MTF). The MTF for an optical system is the ratio of the image contrast formed by the device, to that of the object contrast for different spatial frequencies. Schade (1948) studied the MTF of a diffraction limited optical system, together with the effects of spatial interactions within the nervous mechanism of the retina. Essentially, it was shown that any object can be broken down into a series of sine waves of various frequencies and phases, by the application of Fourier analysis. Therefore, any given pattern can be synthesised by superimposing a sufficient number of sine waves of the appropriate spatial frequencies, amplitudes and phases. Since CS is a smooth continuous function, it is not necessary to measure the system's response to every spatial frequency.

3.3 The contrast sensitivity function

The CSF is the threshold needed for the detection of gratings of different spatial frequencies (Abrahamsson et al 1988). Sinusoidal gratings vary in frequency, contrast, and phase. The number of light-dark cycles of the grating patch which subtend a one degree visual angle is a measure of the spatial frequency of the grating and is expressed in cycles per degree (cpd). A low spatial frequency consists of broad black and white bands; whereas a high spatial frequency grating has thin black and white bands.

The contrast of a sinusoidal grating is based on the maximum luminance (L_{max}) and the minimum luminance (L_{min}) in the grating. It is a dimensionless variable with values ranging from 0.0 (a uniform field), to 1.0 (the maximum possible). The minimum contrast at which a grating can be distinguished from a uniform field with some fixed level of

accuracy, is the contrast threshold. Sensitivity at each spatial frequency is defined as the reciprocal of the contrast threshold.

Modulation of the sine waves is defined by the following equation, which is independent of mean luminance (Campbell and Maffei 1974). The dependent variable which is the basis of the CSF, is the contrast of the sinusoidal test grating.

$$C = \frac{(L_{\max} - L_{\min})}{(L_{\max} + L_{\min})} \quad \text{[equation 3.1]}$$

Where :-

L_{\max} = the maximum luminance level at the peak of the sine wave measured in cd/m^2

L_{\min} = the minimum luminance level at the trough of the sine wave measured in cd/m^2

C = contrast

The CSF is a graph which plots CS as a function of spatial frequency. Sjostrand (1979) defined the normal CSF as an inverted 'U' with a well defined peak of maximum sensitivity. The intercept of the curve with the spatial frequency axis approximately corresponds to VA (Campbell and Green 1965; Arden 1978). Highest contrast sensitivity is normally obtained at a spatial frequency of approximately 3 cpd, but can vary between 2 and 5 cpd (Bailey 1993). Sensitivity falls off for lower spatial frequencies, and falls off rapidly for higher spatial frequencies. Eventually, a high spatial frequency is reached which requires a contrast of 1.0 for detection (the high frequency cut-off) and higher spatial frequencies cannot be detected by the observer. The human visual system is highly sensitive to gratings of intermediate spacing because less than 1% contrast can be detected. CS is lowest for very fine gratings, when 100% contrast is needed. The human visual system is able to detect spatial frequencies up to about 40 cpd. (Wolfe 1990). There is no lower limit, but measurements are not generally made below about 0.1 cpd, because of the practical limits of display size.

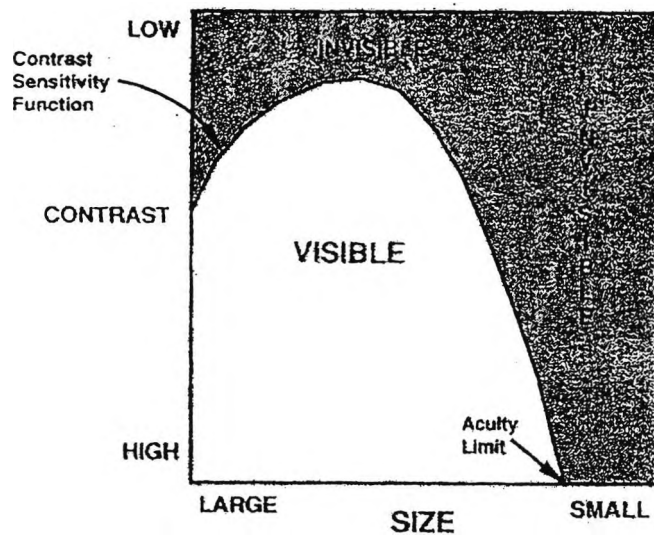


Figure 3.1 - Graph to show that visibility depends on both the size (spatial frequency) and the contrast of the stimulus (Wolfe 1990).

3.4 Interpretation of the contrast sensitivity function

The most popular interpretation of CSF is that spatial gratings are detected by multiple spatial frequency 'channels' (Campbell and Robson 1968; Blakemore and Campbell 1969; Sachs et al 1971; De Valois 1977). It has been shown that if a channel is stimulated by a specific spatial frequency, then that channel is rendered less sensitive to subsequent stimulation. However, the sensitivity to gratings of other spatial frequencies is unaffected, or may even be improved. In this way, the concept has arisen of visual channels, each handling information relevant to specific bands of spatial frequency. Each channel is sensitive to a restricted range of spatial frequencies, and the CSF is assumed to be the envelope of the separate sensitivity functions of all these narrow channels. If this view is accepted, traditional screening methods (e.g. Snellen acuity) assess the functioning of only a very limited subset of these channels, particularly those sensitive to very high spatial frequencies (Ginsburg 1980, 1981b; Ginsburg et al 1982; Evans and Ginsburg 1985).

Several researchers have employed different methods to investigate the existence of spatial frequency channels such as adaptation, discrimination at detection thresholds, subthreshold summation and masking. Although the number of channels that exist is subject to controversy, it is thought that the number varies between six and eight (Blakemore and Campbell 1969; Watson and Robson 1981).

Graham and Nachmias (1971), using a sub-threshold summation technique, concluded that gratings show summation if their spatial frequencies differ by less than a 2:1 ratio. Thus, if two sinusoidal gratings are presented to the same patch of retina at sub-threshold contrast, they will summate the same underlying spatial frequency channel. Alternatively, inhibition may occur if the spatial frequencies differ by more than a 2:1 ratio (Olzak and Thomas 1981).

The concept of separate channels for various spatial frequencies is a restatement of the fact that the retina is non-uniform (Arden 1978). Only the fovea is specialised for high acuity and must, therefore, handle the information about high spatial frequencies. The lower spatial frequencies are preferentially handled by the retinal periphery. For coarse gratings, the central and more peripheral retina has an equal CS per unit area of retina, however, the larger the retinal area stimulated (up to 45 degrees for very coarse gratings), the greater the sensitivity.

3.5 Factors affecting the measurement of spatial contrast sensitivity

Because of the protective mechanisms to prevent damage inherent in the ocular system, the contrast of the retinal image of a grating will be less than that of the target grating (Campbell and Robson 1968). Even if one assumes that the dioptric mechanism of the eye is ideal, image formation is still limited by diffraction at the pupil. In addition, there exist a number of methodological issues which complicate measures of CS. Essentially when measuring the CSF, one is determining the minimum detectable contrast. However, it is incorrect to assume that a stimulus below threshold will never be perceived and a stimulus above threshold will always be perceived. In fact, attempts at finding a threshold will not yield a single value, but instead a distribution of values. If the threshold is assumed to vary randomly according to a Gaussian distribution, the probability of detection assumes the

shape of a normal ogive often referred to as a 'probability of seeing curve'. The threshold is usually defined as the stimulus value that corresponds to 50% probability of detection. The absence of a clear criterion has been attributed to a number of factors. Detection of a weak stimulus will be dependent on a weak neural event occurring amidst fluctuations in the neural response. Conversely, internal neural noise may be mistaken for the presence of a stimulus, especially in an enthusiastic subject (Wolfe 1990). Therefore, reliable tests of CS require a method to counteract the effects of criteria. The two-forced alternative choice method minimises the effects of guessing and is discussed in section 3.6.3.

3.5.1 Stimulus variables

CS is subject to many variables all of which will affect the shape of the CSF. Therefore, if measurements are to be comparable, it is vital that stimulus variables are kept constant.

3.5.1.1 Stimulus size

The size and position of the grating presented affects the peak of the CSF curve. If a 1 degree foveal field size is used, a peak as high as 10 cpd may be found (Hoekstra et al 1974; Sjostrand 1979). With an eccentrically viewed target, the peak of the CSF curve can be as low as 1 cpd (Rovamo et al 1978).

Essentially, like most measures of visual sensitivity, the sine wave CS increases with the area of the retina stimulated. If one wishes to measure CS as a function of spatial frequency, then each target should be large enough, such that a larger target would not significantly change the result. CS increases with area at small grating areas, but becomes independent of area at large grating areas (Hoekstra et al 1974; Savoy and McCann 1975; Howell and Hess 1978). Virsu and Rovamo (1979) have shown that, in bright light, spatial integration in grating detection obeys a single saturating function of relative grating area at all spatial frequencies. Human visual performance obeys the DeVries - Rose law in dim light, but Weber's law in bright light. At intermediate light levels, performance falls between these laws (Kelly 1972; Savage & Banks 1992).

3.5.1.2 Mean luminance of the sinusoidal gratings

The mean luminance of the sinusoidal gratings has a profound effect on the CSF. At high photopic levels of mean luminance, the normal CSF has a peak sensitivity at about 5 cpd,

and a high frequency cut-off at about 60 cpd. As mean luminance is lowered, the frequencies of the peak sensitivity and the high frequency cut-off become lower. In addition, the height of the peak is reduced. At the mesopic level, the peak in the CSF practically disappears. This peak, which is prominent at high luminances, is generally believed to reflect the dynamic interaction between excitatory and inhibitory influences in the visual system. At low luminance levels, the shift of the peak towards lower spatial frequencies is considered to be caused by the use of larger receptive fields (Kulikowski 1971; Bodis-Wollner 1980). Low frequency neural effects appear at a fixed adaptation level but the CSF also shows non-optical behaviour at high spatial frequencies, when the mean retinal illuminance is varied.

3.5.1.3 Effect of background luminance level

Generally, CS varies in a gradual, non-linear manner with background luminance. This compensates for the constant component of the stimulus pattern. As the background luminance is increased, CS remains constant at low spatial frequencies, but increases at high frequencies, causing the sensitivity peak to move toward higher frequencies at higher luminances. As the diameter of the gratings is increased, the reverse occurs, (that is, the CS remains constant at high spatial frequencies, but increases at low frequencies). This causes the peak sensitivity to move toward lower frequencies. Each of these trends level-off for large, bright targets. This limiting function is governed by foveal vision at high frequencies, but at low frequencies it derives from a large retinal area and so from many receptive field sizes (Kelly 1977).

3.5.1.4 Temporal characteristics of the contrast sensitivity function

The exposure duration of the grating target and the time course of its onset will influence the CSF, especially at lower spatial frequencies. Low frequency sine wave thresholds represent a balance between antagonistic processes. At spatial frequencies below 1 cpd, adaptation effects are induced, but can be suppressed by presenting the grating in short flashes. This transient presentation tends to flatten the CSF curve at low frequencies, increasing the measured sensitivity to about four times its steady state value at 0.25 cpd (Kelly and Savoie 1973). Therefore, with brief exposure duration, or with rapid onset of the grating stimulus, sensitivity to low spatial frequency is enhanced compared with that to longer duration, more gradual onset stimuli (Kelly 1977). Presenting the stimuli in one

second flashes of contrast has little effect on normal sensitivity at frequencies greater than 1 cpd but as the flash duration is reduced the CS eventually ceases to increase at low frequencies. This results in a reduction in contrast threshold at all spatial frequencies.

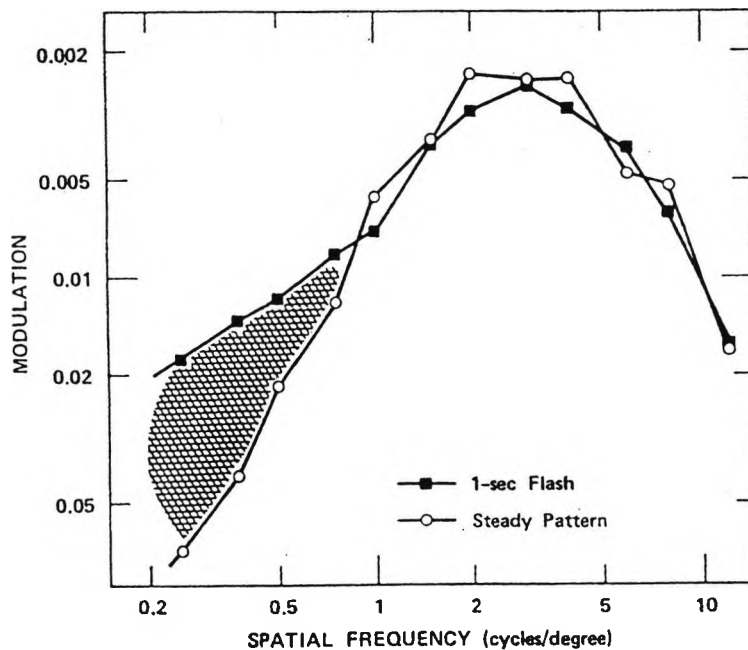


Figure 3.2 - Effect of a 1 second flash presentation on the grating sensitivity at low spatial frequencies (■) compared to the steady state (o). The crossed-hatch area shows stimuli that are visible when a transient stimulus is switched on, but disappear after a few seconds of steady fixation (Kelly 1972).

The effect of eye movements on the CSF can be demonstrated at low spatial frequencies. The frequencies and contrasts within the shaded area of figure 3.2 represent gratings that appear when first turned on, and then disappear after a few seconds, remaining invisible until the subject makes a larger eye movement. This phenomenon is unique to coarse, sinusoidal gratings.

3.5.1.5 Effect of observation distance

The observation distance used to test the CSF is not generally considered a parameter that will significantly influence the result (Hernandez et al 1996). However, this assumption is a matter of some dispute (De Palma and Lowry 1962; Schober and Hilz 1965; Capilla et al 1993). Reports of fluctuations in the CSF with observation distance have often considered whether the optical or neural part of the visual system, or a combination of the two, is to blame. Work by Cavonius and Hilz (1973) and Hennessy and Richards (1975) showed that neural CSF does not vary when the distance from the stimulus changes and it was concluded that the observed differences in CS, resulting from changes in distance, are due to optical parts of the visual system. Such factors include changes in pupil diameter, spherical aberration, astigmatism inherent in the convergence of binocular vision, and astigmatic accommodation.

3.5.1.6 Effect of accommodation

Ciuffreda et al (1990) reported that the configuration of the CSF test has considerable influence on the accommodative response. It is well known that if there is a decrease in either the luminance and/or the contrast of an object, the accommodation error increases in such a way that, under extreme conditions (i.e. in the absence of an adequate visual stimulus, for example nocturnal myopia, empty field myopia), accommodation remains at an intermediate stage (dark focus) around 1.5 D (Johnson 1976; Rosenfield et al 1993). If contrast and blurring are a function of spatial frequency, this will in turn influence the accommodative response, and thus accommodative errors are dependent on spatial frequency (Charman and Heron 1979). In addition, as accommodation increases, pupil diameter and retinal illumination decrease (Toates 1972). Hernandez et al (1996) carried out experiments using a computerised CSF test (Navarro et al 1990), with an artificial 3 mm pupil in order to keep retinal luminance constant for each of the studied distances of 6, 3, and 1 metres. It was reported that sensitivity values differed greatly among the observers, and therefore were not directly comparable. The study concluded that at low and medium frequencies there are fewer accommodation errors at a distance of 1 m, than at 6 m.

3.5.1.7 Effect of pupil diameter

Kay and Morrison (1987) reported that CS (up to 30 cpd) in younger adults was remarkably similar despite variations in pupil diameter. In a study on spatial vision, Campbell and Green (1965) examined the role of the pupil size in CS. The study compensated for changes in pupil diameter with changes in illumination, in order to keep retinal illuminance constant. It was reported that under these circumstances, pupil size did not have a significant effect on the CSF. In fact, smaller pupils yielded improved high spatial frequency sensitivity, since optical aberration was minimised. Sloane et al (1988) tested CS at different light levels, and in agreement with Kay and Morrison (1987) reported that in younger adults CS was relatively unaffected by changes in pupil size. However, tests in older adults with miotic pupils showed CS losses. The older adults were tested again using artificially dilated pupils (to match the pupil size that naturally occurs in young adults at that light level) and still exhibited approximately the same magnitude of vision loss. Therefore, the older adults' CS loss cannot be compensated for by a simple increase in the diameter of the pupil. In fact, senile miosis slightly improved the CS result in certain cases, compared to artificially dilated pupils because miosis limits optical aberration and improves depth of focus (Woodhouse 1975) (section 5.2.3).

3.5.1.8 Effect of refractive error

Low spatial frequencies are affected less by refractive error than high spatial frequencies. The effect of common aberrations of the optical system of the eye is preponderantly upon the higher spatial frequencies, which pass through the system with a loss of contrast (Campbell and Green 1965). However, subjects with a relatively high degree of myopia often cannot reach a normal VA when refracted, even with the full optical correction, due to degenerative effects in the retina (Duke Elder 1973). The impairment of VA may be due to the fact that myopic individuals, during the early period of life, lack experience of high spatial frequencies compared to normal subjects. In normal subjects, the CSF at photopic levels has a peak around 3 - 6 cpd and a high frequency cut-off around 45 - 50 cpd. For myopic subjects, the cut-off may be at a lower spatial frequency (i.e. the CS in the high frequency range should be lower than normal), whilst at lower spatial frequencies the CS may remain essentially the same as for 'normal' subjects. Fiorentini and Mahhei (1976) tested this hypothesis by investigating the effect of myopia on the CSF in ten fully corrected myopic subjects (all subjects had a refractive error of at least -5.00 DS and/or at

least -0.50 DC). It was determined that the myopic subjects, possessing a lowered VA, also had impaired overall CS. However, the impairment was not restricted to the highest spatial frequencies, but instead it occurred over the whole spatial frequency spectrum.

It is possible that the wearing of spectacle lenses affects the CSF due to changes in retinal image size. To investigate this, Enoch et al (1979) studied normal observers made artificially ametropic with plus or minus lenses, and aphakic patients using their prescribed spectacles or contact lenses. An interference acuity method was employed, coupled to a two-point interference device. The authors reported that a high plus trial lens caused a modest low frequency fall-off in CS, with a shift in the peak CS to a higher frequency in normal subjects. A high minus trial lens caused an apparent low frequency CS enhancement, and an apparent reduction in the frequency exhibiting greatest CS (i.e. the lowest threshold). It was suggested that in the longer myopic eye, the retinal line frequency may differ, due to retinal stretch. In a second study using aphakic eyes, Enoch et al (1979) measured the CS in three subjects with their spectacle prescription, and wearing PMMA contact lenses. In all three cases, the use of aphakic spectacles caused an apparent shift of the CSF to higher frequencies. It also led to a small reduction in measured CS. The aphakic contact lens resulted in a shift of the entire function to lower frequencies, and to a more normal position on the frequency continuum. This was explained as a magnification effect. That is, if one magnifies the image, the retina sees a lower frequency and the response varies accordingly. As the eye's response is frequency-dependent, it was concluded that aphakic or highly myopic patients should be fitted with contact lenses during assessment of CS to limit artifactual responses.

3.6 Methods of testing contrast sensitivity

Measurements of CS are useful in vision research and during clinical assessment of visual function because the CSF can reveal sensitivity losses that go undetected with VA. For instance, measurement of CS will reveal sensitivity losses in patients with cerebral lesions (Bodis Wollner and Diamond 1976), multiple sclerosis (Regan et al 1977; Bodis Wollner et al 1979) and macular disease (Sjostrand and Frisen 1977; Stangos et al 1995). This has led to a proliferation of instrumentation and techniques for measuring CS (e.g. Westheimer 1960; Cornsweet 1962; Campbell and Green 1968; Arden and Jacobson 1978; Ginsburg and Cannon 1983; Regan and Neima 1983; Barbur et al 1986; Pelli et al 1988; Wilkins et

al 1988) despite the fact that CS testing is dependent on the method employed to present the spatial frequencies.

Clinical measurements of CS are usually taken using grating or letter charts, as opposed to more research-based techniques which require costly VDU monitors and computer software. Below is a summary of the CS charts most commonly used in the U.K.

3.6.1 Grating charts

3.6.1.1 Vistech and 'Functional Acuity Contrast Test' charts

The original Vistech and second-generation functional acuity contrast test (FACT) charts assess the entire CSF curve, and can be used at 3m, or at near. The charts consist of grating patches, which are orientated vertically or tilted to the left or right, ranked in five rows of increasing spatial frequency (1.5, 3, 6, 12 and 18 cpd) and nine columns of decreasing contrast (Ginsburg 1984). The FACT contrast step sizes are a constant 0.15 log units, whilst the contrast step sizes on the Vistech chart vary, but approximate to 0.23 log CS steps (Reeves et al 1991). The subject is required to read along each row of the chart and state the orientation of each grating patch, with the final grating seen correctly being compared to normative values (Latham 1998). Elliott and Whitaker (1992b) recommended that the subject should only be classified as abnormal if spatial frequencies of 1.5, 3 and 6 cpd are outside the normative values.

3.6.1.2 Cambridge low contrast gratings

The Cambridge low contrast gratings are presented as a booklet that is viewed from a distance of 6 m (Wilkins et al 1988). The Cambridge test uses a two alternative forced choice detection task and is based on Michelson contrast. Two pages of the same mean luminance are presented to the subject: one page is blank, the other has a square wave grating (4 cpd). The subject is required to state the page containing the grating, guessing if necessary. The contrast reduces from 13% to 0.11%, as the pages are turned. Once a mistake is made by the subject, the test is repeated, starting four pages before the page where the error was made. Once four repeats of the test have been completed, the value is converted to a CS scale. Comparison is then made to validated normal limits (Wilkins et al 1988; Elliott and Whitaker 1992a).

3.6.2 Letter charts

3.6.2.1 Pelli-Robson chart

The Pelli-Robson chart (Pelli et al 1988) consists of 16 letter triplets of constant size, spread over eight lines of chart and is based on Weber contrast. At the recommended working distance of 1m, the spatial frequencies of the letters are about 0.5 - 2 cpd. Each triplet of letters has the same contrast, which reduces in 0.15 log CS steps between triplets from 0.00 log CS units at the top of the chart, to 2.25 log CS units at the bottom. The subject is required to state the lowest letter that can be identified. Each letter correctly identified after the first three, scores 0.05 log units (allowing misreading of C for O and vice versa) (Elliott et al 1990). Elliott and Whitaker (1992a) recommend that the subject be given sufficient time to look at the letters near threshold, otherwise scores tend to be inaccurate by at least 0.15 log units.

3.6.3 Research-based methods for measuring contrast sensitivity

In most studies, CS is measured by increasing the threshold amplitude from zero, or decreasing it from a large value, until the threshold of visibility is reached. The threshold is not exclusively determined by sensitivity because it is also dependent on the subject's criteria, and the response requirements (Green and Swets 1966; Woods and Thomson 1993). In addition, learning effects vary according to the method used (Long and Tuck 1988) and subjects with ocular pathology or reduced vision may demonstrate larger intra-subject and inter-subject variability (Ross et al 1984; Woods 1993).

3.6.3.1 'Method of adjustment'

A number of investigators have employed the 'method of adjustment' to determine CS (e.g. Bernstein and Broderick 1981; Travis and Thompson 1989). Subjects are given control of the grating contrast until the grating is either "visible" or "not visible". Although the method is straightforward, there are several inherent disadvantages. Firstly, thresholds are prone to fluctuations caused by variability between different subject's criteria for detection. In addition, differences in the adjustment strategy may result in variability, leading to different levels of adaptation to the stimulus (Woods and Thomson 1993).

3.6.3.2 'Method of limits'

The 'method of limits' has been employed by numerous researchers (e.g. Applegate and Massof 1975; Arden and Jacobson 1978; Ginsburg and Cannon 1983). The subject or examiner varies the pattern (ascending and descending) to target the threshold. The 'method of limits' is fast and simple, and can be used with inexperienced subjects (Arden and Jacobson 1978; Ginsburg and Cannon 1983). However, it is the subject who decides what the threshold level is and so it depends on the subject's criteria for detection (Higgins et al 1984). Furthermore, the threshold may also depend on the investigator (Reeves et al 1988). In addition, spatial frequency adaptation effects (Kelly 1972), and after-images produced by the suprathreshold stimuli (Ginsburg and Cannon 1983) will affect the measurements. If the investigator only increases the contrast to measure threshold, then the detrimental effects described by Kelly (1972) and Ginsburg and Cannon (1983) will be avoided. Woods and Thomson (1993) investigated two versions of the method of limits (i) discrete ascending method of limits and (ii) continuous ascending method of limits using experienced observers. The study reported a low test-retest correlation and a large repeatability coefficient for both methods compared to the method of constant stimuli.

3.6.3.3 Constant stimuli

This method involves the presentation of a pattern at various contrast levels but at the same spatial frequency. After the threshold is established, a pattern of a different spatial frequency is presented (Storch and Bodis-Wollner 1990). 'Yes/no' or 'forced-choice' responses may be employed. Both false-positive and false-negative responses are recorded and a psychometric function can be constructed for each spatial frequency. Many adaptations of the forced-choice procedure have been developed due to the number of inherent advantages. Essentially, the observer is forced to make a response and guessing will yield correct answers 50% of the time. An estimation of the 75% detectability of the pattern is usually derived as the threshold level and so more reliable comparisons for the same observer or different observers can be made. Despite the large number of responses required, this method has been shown to be one of the most reproducible psychometric methods (Guilford 1954; Storch and Bodis-Wollner 1990; Woods and Thomson 1993).

3.6.3.4 Adaptive procedures

Adaptive procedures are comparable to conventional constant stimuli procedures, but require fewer stimulus presentations (Woods and Thomson 1993). The subject's response is recorded and the next presentation of the stimulus is adjusted according to pre-determined intervals. Staircase methods (Cornsweet 1962) and Parameter Estimation by Sequential Testing (PEST) (Taylor et al 1983) are examples of adaptive procedures. In essence, each presentation of the stimulus is determined by the preceding response and the contrast level is increased or decreased according to perception of the stimulus. For example, the contrast modulation may start at 100% and reduce to 40% following two correct responses. After a further two correct responses, the contrast modulation may reduce to 20%, then to 2% and so on. If the subject fails to detect the stimulus at 2%, the staircase will return to 20% and so on. The staircase will eventually fluctuate close to the subject's threshold (Wolfe 1990). A staircase may be run for a fixed number of peaks or troughs. The technique increases in accuracy with the number of reversals.

3.6.3.5 von Bekesy procedure

This method of testing CS has been used by Ginsburg and Cannon (1983) and Long and Tuck (1988). Subjects control a two-position switch that either raises or lowers contrast at a fixed rate. If the contrast is below threshold at the beginning of a run, the subject positions the switch to increase the contrast. As soon as the grating is detected, the switch is reversed to reduce contrast until the grating is invisible. This method is not often used as it has been shown to produce poor repeatability and has a high inter-subject variance.

3.6.4 Repeatability of the methods used to test contrast sensitivity

Numerous studies have compared the repeatability of the various methods employed to assess CS (e.g. Long and Tuck 1988; Woods and Thomson 1993). The method of adjustment is considered to be more repeatable and to have a lower inter-subject variance than the von Bekesy procedure (Long and Tuck 1988). However, the method of adjustment can be greatly affected by fluctuations in the subject's criteria for detection. A four-alternative forced-choice procedure is considered to be more repeatable than the method of limits, which in turn is superior to the method of adjustment (Corwin and Richman 1986).

3.7 Summary and aims

The CSF has several important virtues. It summarises a subject's ability to see a wide range of target sizes and it is sensitive to changes in vision that are difficult to detect by standard clinical means. In addition, it tests optical and neural properties of the visual system that acuity measures cannot test.

For these reasons, a technique of assessing the CSF was employed in the present study, in addition to a scatter test. In the present study, CS testing will permit:-

- a measure of visual performance
- a comparison between measures of light scatter and the results of testing visual performance using CS
- the effect of increased light scatter on the CSF to be investigated.

3.8 The City University contrast sensitivity test

A random 'yes/no' staircase using a 250 ms square pulse, with variable step size was used to obtain contrast threshold. Contrast threshold was measured at seven spatial frequencies - 1.5, 3, 5, 7, 10, 16 and 22 cpd, and six measurements taken at each spatial frequency. Measurements were taken at a distance of two metres (see section 5.7.2). The parameters used to conduct the CS test can be seen in table 3.1.

Table 3.1 - The parameters used to conduct the City University CS test

Staircases:	Coarse	Fine
No of reversals:	6	6
Reversals ignored:	4	4
Start increment:	0.15	0.05
End increment:	0.04	0.01

To establish the repeatability of the CS method employed, two normal subjects were recruited and six runs were taken. The results can be seen in table 3.2.

Table 3.2 - Mean and standard deviation of six CS measurements at spatial frequencies of 1.5, 3, 5, 7, 10, 16 and 22 cpd for two observers.

Subject	22 cpd (sd)	16 cpd (sd)	10 cpd (sd)	7 cpd (sd)	5 cpd (sd)	3 cpd (sd)	1.5 cpd (sd)
1	3.91 (1.02)	10.48 (2.34)	51.02 (10.74)	90.42 (10.20)	132.55 (29.53)	133.93 (26.37)	125.97 (25.13)
2	19.18 (14.66)	18.79 (5.37)	65.65 (25.03)	101.23 (18.49)	164.52 (44.07)	171.93 (62.38)	170.37 (40.21)

Although the intra- and inter-subject variability is high, such variability in CS measurements is well documented (Virsu et al 1975; Cohen et al 1976; Ginsburg et al 1984; Arden 1988). It is thought that variability is unlikely to be an artifact, but rather it reflects genuine biological variability. Despite this, CS is still useful in the context of the present study, in order to investigate the relationship between measures of light scatter and the CSF.

CHAPTER 4

Rationale for the research

4.1 Introduction

Using a novel technique to measure intraocular light scatter in the eye, the primary aim of this research was to investigate the light scattering characteristics of the contact lens-wearing eye. Although contact lenses have been in use for approximately 40 years, little research has been conducted into the effects of such long-term lens wear. Given the number of physiological responses that occur during contact lens wear, it is not unreasonable to hypothesise that such changes may manifest as increased intraocular light scatter. Therefore, the author carried out a study to establish whether long-term contact lens wear causes increased levels of light scatter when compared to age-matched controls. Furthermore, the author wished to determine whether long-term contact lens wear results in altered visual performance. Therefore, CS testing was also employed to examine the effects of long-term contact lens wear on the CSF.

Before examining contact lens wearers, it was first necessary to investigate the light scattering characteristics of eyes that have not experienced contact lens wear. Therefore, light scatter and CS were measured in normals of different ages. This study generated a normal database used for comparison with long-term contact lens wearers. Furthermore, this study extended the knowledge of ocular changes that occur with age. Of additional interest was whether light scatter in the normal eye is subject to diurnal or longitudinal variations. Knowledge of the normal variations in light scatter which occur over time assisted the protocol design, the patient selection process, and the interpretation of results in the later study on subjects wearing contact lenses. Having established the range of values expected from a normal population, investigation of subjects with anterior eye disease allowed the author to establish whether contact lens wearers achieved light scatter values within a normal, or an abnormal range.

Although the changes in visual performance that occur during contact lens wear have been well documented, most studies have concentrated on changes in Snellen VA or CS. The principal method for assessing changes in visual performance in UK optometric and

ophthalmologic practice is Snellen VA. However, Snellen VA is only sensitive to conditions that produce a loss of CS at high spatial frequencies and does not necessarily reflect degenerative changes that may be occurring elsewhere in the visual system. In physiological terms, the method most commonly used for the evaluation of ocular structures is slit lamp biomicroscopy. However, this method only provides information on structures which contribute to backscatter. Numerous researchers have concentrated on measuring levels of backscatter on the incorrect assumption that backscattered light is representative of forward scattered light. However, measures of backscatter may not adequately reveal visual problems caused by forward light scatter. In the clinical and research environment, indirect measurements of light scatter, known as glare tests, have been employed. It is assumed that such tests reflect levels of forward light scatter. However, the commonly used glare testers are each subtly different and there is a lack of standardisation. The type and size of the target together with the position, brightness and type of glare source used, each influence measures of glare sensitivity.

The majority of scatter studies performed to date have lacked the benefits of modern computing techniques and experimental apparatus. A number of researchers have examined the distribution of scattered light across the retina, and have produced a variety of estimates for the constants n (the scatter index, which describes the angular distribution of scattered light in the eye) and k (the straylight parameter, which is proportional to the amount of light scatter in the eye) for different positions of a point glare source. However, past studies to quantify the amount of intraocular scattered light and its angular dependence have not yielded consistent results. Any variability between individuals was assumed to be due to changes in the amount of scatter (k) alone and that n remained constant (typically two). The scatter index, n , has since been identified as an important variable that can influence visual performance. n has been shown to fluctuate from day to day and this causes significant changes in the measured k values. In fact, the relationship between n and k can be predicted from the assumption that the total amount of light scatter in the eye remains constant and that the only parameter that changes is its angular distribution. k' (the integrated straylight parameter) is seen to be independent of fluctuations of n and k . k' has reduced variability and is, therefore, a more appropriate parameter to measure and to use clinically to determine light scatter in the eye. Although the straylight meter designed by van den Berg (1986) also uses a flicker compensation technique (van den Berg 1986), the

instrument does not allow the full scatter function to be calculated, therefore studies using this instrument assume that n has a constant value of two.

The P_SCAN 100 scatter apparatus utilises extended annular sources and is able to assess the full scatter function, which allows for the calculation of the parameter, k' , from the integral function of the scatter function. Therefore, more accurate measures of intraocular light scatter can be obtained. With regards to visual performance, changes in contrast sensitivity were investigated using a random 'yes/no' staircase, with variable step size and the contrast threshold was measured at seven spatial frequencies: 1.5, 3, 5, 7, 10, 16 and 22 cpd.

4.2 Aims and plan for experimental work

The availability of a range of sophisticated equipment and a researcher who could spend the long periods of time required to collect and analyse the data generated by this equipment permits:-

- direct measurements of forward light scatter using the P_SCAN 100 scatter apparatus
- measurement of k' , (in addition to n and k)
- comparison between measurements of scatter and the CSF over a wide range of spatial frequencies
- comparison between measurements of back scatter and forward scatter.

The broad aim of the studies described in this thesis was to quantify the scattering characteristics of the eye in a number of subject groups, with particular emphasis on long-term contact lens wearers, using the P_SCAN 100 scatter apparatus. Previous studies have not measured the full scatter function as a function of age. Therefore, normal subjects of various ages with little refractive error were recruited, to establish whether k' or CS varies with age (Chapter 5). Not only did this study generate a database of normal values that was used for comparison in subsequent studies, but it also allowed a better understanding of the physiological changes that occur with age.

Subjects were also recruited to investigate whether light scatter is subject to diurnal (Chapter 6) or longitudinal variations (Chapter 7). This facilitated the protocol design, patient selection and interpretation of results in subsequent chapters.

Once the light scattering characteristics of the normal eye have been established, subjects with a variety of corneal conditions (which may exacerbate scatter) were recruited. Subjects included those with keratoconus (prior to and following surgery) and other corneal abnormalities (Chapter 8). Investigation of these subjects allowed quantification of the effect of a range of corneal abnormalities, with varying levels of severity, on measures of forward light scatter and the CSF. These findings, together with those from normals, have particular relevance to the investigation into the effects of long-term contact lens wear, on scatter and CSF, by allowing comparison of the magnitude of these effects between lens wearers, normals and those with corneal abnormalities.

Having determined the light scattering characteristics of the abnormal eye, long-term contact lens wearers were recruited (Chapter 9). The subjects had worn PMMA, hydrogel and RGP lenses for approximately 5, 10, 15, 20, 25 and 30 years. Scatter and CS measurements were taken to establish whether long-term contact lens wear produces increased light scatter or a reduction in the CSF compared to non lens wearing age-matched controls. A comparison is made with the results obtained from subjects with corneal abnormalities.

CHAPTER 5

The light scattering characteristics of the normal eye and how these are affected by ageing

5.1 Introduction

A main focus of this thesis is the effect of long-term contact lens wear on scatter, as measured by the integrated straylight parameter k' . In order to compare the light scattering characteristics of different populations (in particular in this thesis, long-term contact lens wearers and those suffering from a range of anterior eye disease), it is important to establish the range of values that one would expect from a physiologically normal population, with little refractive error.

The rising mean age of our population has increased the need for understanding the physiologic consequences of ageing on visual function. In UK optometric and ophthalmologic practice, Snellen VA remains the principal method of assessing changes in visual performance. However, VA does not necessarily reflect degenerative changes that may be occurring elsewhere in the ocular system. Therefore, a second main aim of this thesis is to increase knowledge of changes in visual function that occur with age. This will help to anticipate the visual needs and limitations of the elderly, and may also assist the detection of age-related pathological conditions.

Age-related changes in visual function, such as VA, visual fields, colour vision and dark adaptation, are well documented (Pitts 1982). Cross sectional age-related changes have also been reported for sensitivity at absolute threshold (Birren and Shock 1950; Gunker and Gouras 1963), colour discrimination (Verriest 1963), short term adaptational dynamics (Lovasik 1983; Wright and Drasdo 1985), spatial (Owsley et al 1983; Morrison and McGrath 1985) temporal CS (Morrison and McGrath 1985), and light-sense perimetry (Lachenmayr et al 1994). There may also be age-related changes in perceptual organisation, and in the speed of the processing of information (Botwinick 1978). Light scatter in the eye has also been reported to increase with age (Allen and Vos 1967; Wolf and Gardiner 1965; Sigelman et al 1974; Siew et al 1981; Ijspeert et al 1990; Whitaker et al

1993). However, the full scatter function (i.e. the amount of scattered light and its angular distribution), has not been measured as a function of age. This is the aim of the present study.

A decline in visual function may result from changes in a variety of ocular structures. For instance, the lens may develop opacification, or colouration, and lens fluorescence may increase with age. Changes in the cornea or vitreous can cause reduced transparency. The most important of these age-related changes, in terms of the eye's function, are the increased yellowing and opacification of the crystalline lens (Kline and Scheiber 1985). Other structures may also contribute to decreased contrast and retinal illuminance. Unfortunately, our knowledge of how these changes affect performance of complex, real-world tasks is woefully inadequate.

In studying the effects of ageing and vision, it is important to distinguish, as far as possible, those effects related to ocular disease, from those effects due to ageing *per se* (Owsley et al 1983). This is particularly important in studying the CSF, since several ocular diseases affect the shape of the CSF curve. These conditions include macular disease (Sjostrand and Frisen 1977), cataract (Hess and Woo 1978), and glaucoma (Atkin et al 1979). It is, however, difficult to separate biological changes that are due to old age, from those that are due to disease processes (Ludwig and Smoke 1980). Indeed, ageing may be considered to be a non-specific disease process. However, it is also a time-dependent process, which predisposes us to disease as we age.

5.2 Ocular changes with age

Normal age-related changes in the optical media of the eye increase scatter, and alter the spectral composition of incident light, contributing to age-related losses in acuity, sensitivity, and task performance. Such losses are particularly evident under conditions of poor illumination. Although some of the scatter can be attributed to alterations in the cornea and vitreous humor, the most functionally important of the age-related optical media changes appear to be the increased opacity of the lens, and the reduced diameter of the pupil (Sekuler et al 1982; Kline and Scheiber 1985).

As light scattering is the principal cause of disturbances of vision in the ageing population (Ben-Sira et al 1980), it is necessary to consider what mechanisms underlie the increase in straylight.

5.2.1 Corneal changes with age

Specific changes to the endothelial cells have been reported. Laing et al (1979a) examined the endothelial mosaic of sixty-one normal subjects (age range 20-89 years), with a specular microscope. In young subjects (20-30 years), the mean endothelial cell size was normally distributed around a mean of 20 μm . However, the mean size of these cells increased to 30 μm by the age of 70, with morphological and thickness changes in Descemet's membrane (Capella 1971; Laing et al 1979a). These results were explained by changes in corneal hydration, or by cell loss (Carlson et al 1988; Doughty and Dilts 1994). Later, Yee et al (1985) using specular microscopy and pachometry, examined 60 subjects with an age range of 12 to 85 years. The study reported that there was a definite increase in cellular polymegathism and polymorphism due to cell loss. In addition, older subjects exhibited more irregular hexagonal shapes compared to young subjects. This was later confirmed by Malik et al (1992). Controversy exists as to whether CT changes with age (section 6.9.1). In addition, Savage et al (1993) reported that stromal density increases with age which in turn causes an increase in light scatter in the eye. The changes in stromal density and endothelial cell number/regularity have an impact on corneal physiology. Wigham and Hodson (1987), who investigated donor human corneas, suggested that donor age correlates with some loss of endothelial pump activity.

5.2.2 Crystalline lens changes with age

The media of the eye are susceptible to a number of age-related changes, and the most important of these in terms of the eye's function are the increased yellowing and opacification of the crystalline lens (Kline and Scheiber 1985). In addition, there is a reduction in retinal illuminance (Said and Weale 1959; Sample et al 1988) because light absorption in the lens increases with advancing age (Bron et al 2000). The increase in the optical density of the crystalline lens with age increases intraocular light scatter, thereby degrading the retinal image, and reducing image contrast (Weale 1963; Savage et al 1993). Hence, normal age-related changes in the crystalline lens of the eye, increase scatter, and

alter the spectral composition of incident light, contributing to age-related losses in acuity, sensitivity and task performance (Kline 1987).

Ageing causes morphologic changes in structures controlling the optics of the lens (Harding 1997). This results in changes in lens transmittance (Coren and Girgus 1972; Zeimer and Noth 1984; Pokorny et al 1987; Weale 1987; Siik et al 1992), lens scatter (Weale 1986, 1987; DeNatale et al 1988; Costagliola et al 1989), lens absorption (Johnson et al 1989; Bron et al 2000), and lens fluorescence (Zeimer and Noth 1984; Weale 1987; Siik et al 1992; Bron et al 2000). The principal cause of such changes are modifications to the lens proteins. With advancing age, intermolecular changes in lens proteins cause an increase in molecular weight and the proteins lose their compact shape (Benedek 1971). This results in the disturbance of the soluble protein:water balance which causes changes to the water content within the cytoplasm of the lens fibres. Consequently, transparency will be lost. Fluctuations of refractive index (RI) may also result from damage to the cell membrane or cytoskeleton, aggregation or loss of solubility of crystallins. Additionally, increases in extracellular space, or the deposition of light scattering or absorbing particles within the fibres or extracellularly, may alter the RI. The resulting fluctuations in RI represent the physical basis for increased light scattering with age, and are more important than resonance absorption in lens pigment (Philipson 1973) (section 2.3).

Wolf and Gardiner (1965) reported a 16-fold increase in lens opacification between the ages of 40 and 80 years, and a doubling between the ages of 10 and 40 years. One hundred and sixty eight subjects were recruited and divided into eight groups according to age. Each subject was required to identify the orientation of Landolt rings, positioned at 4, 7, or 10 degrees from a circular glare source subtending a visual angle of 2 degrees. Five glare luminances were employed. At each glare level, the target screen luminance necessary to identify the rings was determined. The logarithms of glare luminance were plotted against the logarithm of the target screen luminance. The results demonstrated that the target screen luminance increased with age (Wolf 1960; Wolf and Gardiner 1965). For ages up to 45 years, the curves were very similar, whereas the curves for the older age groups were much higher. The oldest age group (76-85 years) produced the highest curve. Therefore, up to 45 years of age, there was little change in glare sensitivity but above this age there was a positive linear relationship between back scatter and glare sensitivity. Wolf and

Gardiner (1965) concluded that a correlation existed between age, glare and the amount of backscattered light.

Smith et al (1992) used computerised linear scanning densitometry of Scheimpflug images to investigate the relationship between backscattered light and the width of various regions of the anterior cortex of human lenses. Zone C2 demonstrated the greatest increase in width with age, but zone C3 showed the largest rise in backscattered light with age, with the scatter increasing even after width changes had ceased. A positive correlation was demonstrated between scatter from each of the cortical regions and the age of the subjects (Smith et al 1992).

The proportion of Rayleigh scatter has also been shown to increase with age (Said and Weale 1959; Cooper and Robson 1969; Mellerio 1971), although the precise cause has not been identified. An alteration in the peak wavelength of maximum absorption occurs from the age of 40 years (Cooper and Robson 1969), and is related to the gradual yellowing of the crystalline lens (Said and Weale 1959).

Fluorescence studies on normal human lenses have demonstrated that UV/blue fluorogens (emission maxima of 440 nm) are not present in the first year of life. However, their fluorescence then becomes apparent and increases in intensity with age (Yappert et al 1992). The fluorogen blue/green (emission maxima of 520 nm) also increases progressively as the lens ages (Yappert et al 1992). Fluorescence and nuclear brunescence are thought to be linked (Lerman 1980a; Bleeker et al 1986; Larsen et al 1989; Sparrow et al 1992). Recently, a new fluorogen which increases with age has been identified, namely, glutathione-3-hydroxykynurenine glycoside (GSH-3-OHKG) (Garner et al 1999). This compound is derived from tryptophan and is thought to play a significant role in increasing fluorescence of the lens nucleus which occurs with age. This compound is also thought to cross-link with the lens crystallins (Bron et al 2000). Therefore, GSH-3-OHKG may influence the formation of high-molecular weight aggregates (Benedek 1971), which in turn, increase light scatter in the eye (Bron et al 2000).

5.2.3 Pupil diameter changes with age

Senile miosis refers to the tendency of the aged pupil to remain at a smaller diameter despite decreases in ambient illumination (Kornzweig 1954; Loewenfeld 1979). Woodhouse (1975) demonstrated that the pupil of a young adult assumes a diameter which optimises spatial resolution by balancing the positive versus negative effects of retinal illuminance changes and optical aberrations. A large pupil will increase retinal illumination, thereby improving resolution. However, this is balanced with the resulting increase in optical aberrations, which will reduce resolution. In the older eye, where the pupil tends to remain at a small, relatively fixed size, this delicate balance is disrupted.

Senile miosis does not adversely influence visual performance in older observers at high luminance levels (e.g. 100 cd/m²), since younger and older adults typically have similar pupil diameters (usually between 2 and 4 mm) under these conditions. Furthermore, Woodhouse (1975) has shown that spatial resolution at these high luminance levels is unaffected by pupil size changes within this range. However, the situation is quite different at lower luminance levels. As luminance decreases, the younger adults' pupil increases in size, thereby increasing retinal illuminance. However, the older pupil remains largely unchanged in the presence of low luminance. For example, at 0.1 cd/m² the young pupil is typically around 6 mm in diameter, whereas the older pupil is around 2 - 4 mm. Woodhouse (1975) demonstrated that spatial resolution in younger adults deteriorates significantly at this luminance level when the pupil diameter is experimentally decreased from 6 to 2 mm. More recently, Winn et al (1994) established that pupil size decreases linearly as a function of age, over a wide range of illuminance levels. The pupil diameters of 91 subjects (age range 17 to 83 years) were measured using an objective infra-red based continuous recording technique at five luminance levels (9, 44, 220, 1100 and 4400 cd/m²). The accommodative status of each subject was precisely controlled at a constant level. Although the effect of age was highly significant at each luminance level ($p < 0.001$), the gradient of the regression line became smaller as the luminance increased (figure 5.1).

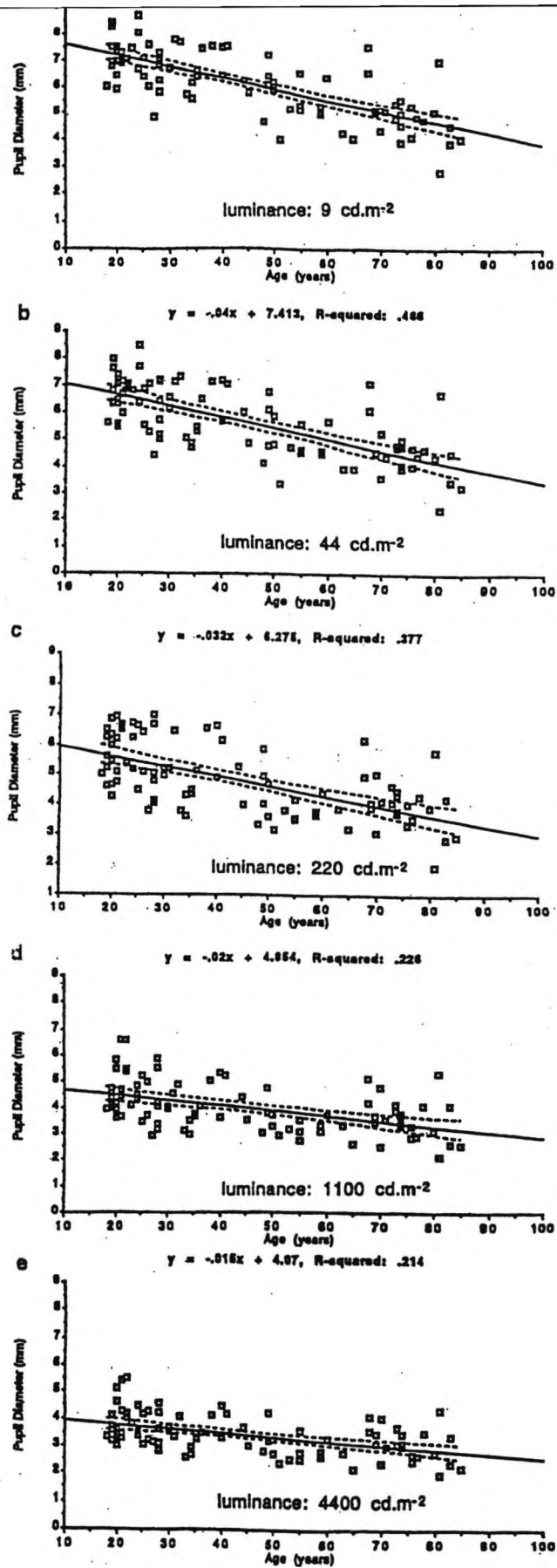


Figure 5.1 - Pupil diameter as a function of age for each luminance condition. Data are fitted by linear regression with the 95% confidence limits indicated by the dotted line. There is a reduction in slope with increasing luminance (Winn et al 1994).

The findings of this study were in close agreement with those of Said and Sawires (1972), Loewenfield (1979) and Koch et al (1991). Winn et al (1994) concluded that senile miosis results in lower retinal illuminance levels, thereby affecting visual performance under low levels of ambient illumination. However, it was noted that a small pupil has the advantage of approaching the optimum size for image formation (Campbell and Green 1965) and may serve to reduce the amount of light scatter produced by an ocular lens that invariably becomes less transparent with age. It has been proposed that this counteracts the expected decline in visual performance as a result of lower retinal illumination (Woodhouse 1975; Sloane et al 1988a; Elliott et al 1990). In addition, depth-of-focus is increased as pupil size is reduced. Finally, a smaller pupil may serve to protect the already vulnerable elderly retina from further phototoxic damage.

5.2.4 Retinal and neural changes with age

The vessels within the retina are subject to the same processes of ageing and sclerosis that affect vessels elsewhere in the body. Retinal pigment cells collect the degenerative yellow ageing pigment lipofuscin, and melanin begins to degrade. Lipofuscin released from the RPE causes the Bruch's membrane to become hydrophobic resulting in impaired transport of materials (Marshall 1997). With increasing age, the number of rods decreases linearly (Curico et al 1993). In addition, cell bodies from the outer nuclear layer displace into the outer plexiform layer and into the layers of rods and cones (Gartner and Henkind 1981). This is accompanied by changes in the morphology of the human cones (Marshall 1987), and also in the density of the cone photopigment (Kilbride et al 1986). These changes result in a decreased quantum catching ability of photoreceptors in the older retina. The lateral geniculate bodies and cortex reveal cell loss and lipofuscin accumulation. Devaney and Johnson (1980) report that between the ages of 20 to 87 years, the neurone population density of the macular projection areas decreases by 54% in the striate cortex.

Eisner (1987) found that for eyes with 6/6 or better acuity, sensitivity mediated by the blue sensitive cones decreased with age. The rate of decrease was greater for females than for males. This gender-related difference was associated with different rates of lenticular change. Absolute sensitivity at long wavelengths also decreased with age, but at the same rate for each gender. The time constant describing the rate of photopic dark adaptation did

not appear to change with age. The sensitivity loss at long test wavelengths correlated with increasing age, and was thought to be due to increased intraocular light scatter, or to physiological compromise at, or central to, the photoreceptor level (Gartner and Henkind 1981).

5.2.5 Temporal processing changes with age

The most prominent functional decline in the older visual system is in its ability to detect temporal change, or to resolve detail in that change. Temporally contiguous visual stimuli that would be seen separately by younger subjects, are often seen as 'fused' or 'smeared' by older persons (Kline 1987). In fact, Walsh (1976) showed that central processing of visual images reduces with age. Although no single mechanism appears to account for the diminished temporal processing capacity of the senescent visual system, it is clear that changes in the ocular media explain little of this change, and that most of it is 'neural' in origin. Among the significant contributors to this decline there appear to be changes in the temporal response characteristics of the visual channels, and in the effectiveness of the oculomotor system responsible for smooth pursuit eye movements.

5.3 Age and its effect on visual function

In summary, the media of the eye are susceptible to a number of age-related changes. The most important of these, in terms of the eye's function, are the increased yellowing and opacification of the crystalline lens (Sekuler et al 1982; Kline and Scheiber 1985; Weale 1987). Additional structures may also contribute to lowering the illuminance on the retina, including the cornea, the vitreous and the macular pigment. However, their involvement may only be minimal (Boettner and Wolter 1962; Werner et al 1987).

All these factors contribute to alterations in an older person's visual function. VA reflects the behaviour of only 1 to 2% of the area of the visual field, and does not adequately reflect degenerative changes that may be occurring throughout the visual system. For example, an individual may achieve a VA of 6/6, even when 44% of the normal number of foveal neuroretinal channels are inoperable (Frisen and Frisen 1981).

5.3.1 Effect of age on visual acuity

Having examined 35,000 refraction records, an early study by Slataper (1949) reported that VA declines with age. The study stated that Snellen VA increases until the age of 18 when it reaches a maximum of 6/5. VA remains stationary until the age of 62, when it reduces to 6/6. From the age of 70, VA declines further due to age-related changes in the eye. Weale (1975) reported a linear decline in VA with age which was thought to be due to cumulative cell loss. However, Pitts (1982) reported that between the ages of 20 and 50 years of age, mean VA does not change. These results were disputed by Elliott et al (1993b) who remarked that the data reported by Pitts (1982) were truncated to 6/4.5, 6/5 or 6/6 due to the Snellen chart design. Elliott et al (1993b) investigating 61 normal subjects between the ages of 21 and 80 years of age reported that equivalent Snellen values fall from 6/4 at 20 years of age to 6/6 at 80 years of age.

5.3.2 Effect of age on luminance levels

Richards (1977) measured letter acuity at a range of luminance levels in normal subjects ranging from 16 to 90 years of age. Results indicated that whilst adults of all ages had acuity reductions with decreases in chart luminance, older adults suffered greater acuity reductions compared with younger adults. Richards (1977) suggested that increases in light level are not needed to resolve high and medium contrast letters at an age of 40, but about twice as much light is then needed for low contrast letters. At age 60, luminance increases of 1.3 times would be helpful to resolve high and medium contrast letters, and 2.8 times luminance increases for low contrast letters. At age 80, increases in luminance of 1.4 times are needed to resolve high contrast material, 1.5 times for medium, and 5 times for low. Therefore, the ageing eye needs more light to detect contrast. However, it is difficult to ascertain from this study the actual severity of an older adult's visual loss, or the mechanisms which underlie it, since subjects were not screened for cataractous lens changes and were not refracted for the test distance. Despite this, the most likely cause of the increased light necessary to achieve the same performance in older subjects is senile miosis (Woodhouse 1975).

5.3.3 Effect of age on measurements of light scatter

Everyday experience confirms that age-related visual problems, such as susceptibility to glare, strongly impair visual task performance (Wolf 1960). However, there is no standard

clinical instrument for measuring how visual performance is affected by glare, or by other related phenomena. Glare appears to be a more significant problem for older observers than for younger ones. Wolf (1960) found the inability to identify a target under veiling glare increased with age, except in older eyes which had the lens removed, suggesting that the age-related susceptibility to veiling glare is attributable largely to changes in the lens. The contrast reduction effects of veiling glare are likely to be most disadvantageous to older persons under conditions of low illumination (Kline 1987).

The mean total increase in intraocular light scatter is seen to vary between the ages of 20 years and 70 years and estimates range from 2.11 times (Yager et al 1992) to 2.57 times (Whitaker et al 1993). Fisher and Christie (1965) investigated the effect of age on the constants n and k of the Stiles-Holladay approximation (equation 1.3). The parameter n (which describes the angular distribution of intraocular light scatter) was found to be a constant independent of the age of the observer and the distribution of luminance over the background against which the test object was seen, with a mean value of 2.2 (Fisher and Christie 1965). A correlation, significant at the 0.1% level was found between k , and the age, A , of the subject in years. The authors also quoted a regression equation:

$$k = (0.2A + 0.4)\pi \quad \text{[equation 5.1]}$$

However, as discussed in section 1.3.2.5, it may not always be correct to assume a constant value, independent of age, for the scatter index, n .

5.3.4 Effect of age on contrast sensitivity measurements

CS has been extensively studied in order to investigate the change in visual performance with age. One of the earliest studies was conducted by Arden (1978). The study measured CS to low and intermediate spatial frequencies in subjects between the ages of 11 and 70 years. Stimuli were presented on photographic plates, with each plate presenting a different spatial frequency. Contrast varied from a subthreshold level at the top of the plate, to a suprathreshold level at the bottom. CS threshold for each frequency was measured by an uncovering process, in which the experimenter slowly uncovered the grating, exposing increasingly higher contrasts until the observer said that the grating was visible. Arden (1978) reported a much greater variability of CS in older patients than in the

younger age groups, but reported that no age-related changes in sensitivity were detected at any of the frequencies tested. However, a similar study reported a slightly decreased sensitivity at older ages at each tested frequency (Arden and Jacobson 1978).

There are serious flaws in both studies, which may explain their contradictory findings. The authors do not describe the number of subjects, or the various age ranges. Also, it is unknown if the subjects wore their optimum optical correction for the test distance of 50 cm, or if the subjects received an ocular health examination to exclude pathology. Therefore, it is possible that the results may reflect refractive error or changes due to pathology. With regard to the Arden plates, the threshold can be influenced by the rate at which the examiner uncovers the test grating. This rate may not only vary between examiners, but may also vary for the same examiner on repeated tests. Furthermore, variations in the illumination level of the plates will significantly affect the threshold (Arden and Jacobson 1978). Despite this fact, there is no standard procedure for measuring CS with the Arden plates. This technique is also disadvantaged by the fact that when older subjects are tested, they tend to give a higher number of false positives, especially to higher frequencies (Sokol et al 1980). This may lead to errors in estimating the threshold. Finally, one might predict older individuals to have a more pronounced loss of sensitivity at high frequencies. Yet at the recommended viewing distances, the Arden plates only test as high as 6.4 cpd. In fact, Skalka (1980), using the Arden plates, reported that older subjects had elevated thresholds at all six frequencies tested. However, this study did not present data separately for each frequency and decade of age.

Arundale (1978) using computer generated sine wave gratings found that the principal difference in CSF between young and older adults in their 40s and 60s, was that the latter had reduced mid and high frequency sensitivity. Contrast thresholds were taken at 0.25, 0.5, 1, 2, 4, 8, 16 and 28 cpd and 31 normal subjects were investigated in total (age range 8 - 66 years). However, the older sample (45 - 66 years) only consisted of five subjects.

Derefeldt et al (1979) presented gratings on an oscilloscope in order to measure CSF from childhood to 60 years of age. Thirty-three subjects were screened for ocular abnormalities, and wore their best prescription. It was revealed that children and young adults had a

similar CSF. Over the age of sixty, there was a reduced sensitivity for all spatial frequencies of 4 cpd and above, when compared to the younger subjects.

Sekuler et al (1980) measured CS in ten individuals in their 60s and 70s, and compared results with those from 25 college aged subjects (18 - 21 years old). All subjects were checked for ocular abnormalities, and had good acuity. The results showed that older observers had decreased sensitivity at low and intermediate frequencies, compared to young observers, but had similar sensitivity at 16 cpd, the highest frequency tested. This similarity at the higher frequency is to be expected, given the high acuity of both sets of observers (Owsley et al 1983). There were considerable individual differences in sensitivity at low frequencies. Although the mean sensitivities of the two age groups were well separated at low frequencies, there were a number of older individuals whose low frequency result fell within the range of the younger subjects tested. However, a sample of only ten older subjects was used, and consequently it is difficult to say with confidence how prevalent the low spatial frequency loss actually is within the older population.

McGrath and Morrison (1981) tested CS in 66 subjects ranging in age from 5 to 94 years. Gratings were presented on an oscilloscope at a mesopic mean luminance of 2 cd/m². It was not stated whether subjects were screened for ocular pathologies. An overall shift downward in the CSF with increasing age was reported. The frequency at which the sensitivity was maximal was approximately equal for all age groups.

Owsley et al (1981), using a face perception task, determined that older subjects had perceptual difficulties which would not be detected by conventional Snellen acuity. Eight slides of single faces were projected one at a time onto a translucent screen, 115 cm from the subject. The older subjects (mean age 74.2 years) revealed good acuity at high contrast. However, the subjects were significantly impaired, relative to young observers (mean age 20.5 years) in perceiving faces under low contrast. In a subsequent study, Owsley et al (1983) attempted to clarify age changes in a larger sample (91 subjects), with individuals over 60 receiving a thorough eye examination, and all measurements taken using the best possible optical correction. Most older subjects tested had traces of cataract, which is to be expected in this age group (Leibowitz et al 1980). CS measurements were taken using an Optronix Vision Tester (Model 200), a part-programmed micro-computer controlled

television display. The subjects were tested at spatial frequencies of 0.5, 1, 2, 4, 8 and 16 cpd. There was a decrease in CS to intermediate and high spatial frequencies with age (between 20 and 80 years) that became increasingly more pronounced with age (Sekuler et al 1982). Contrary to previous reports, low frequency sensitivity was unchanged throughout adulthood (Arden and Jacobson 1978; Sekuler et al 1980; Skalka 1980; McGrath and Morrison 1981). However, the data were in good agreement with Derefeldt et al (1979).

Ross et al (1985) measured the CSF in 70 subjects divided into two groups of normal subjects ('young' - 20 - 30 years, and 'old' - 50 - 87 years) to examine the pattern of CSF. All subjects had a VA of at least 6/9 and were screened for ocular abnormalities. The study used stationary vertical sine wave gratings of variable frequency, generated on a display oscilloscope. It was determined that older observers had reduced CS for all spatial frequencies, compared with younger subjects. This effect was particularly marked for medium and high spatial frequencies. Between the ages of 50 and 87 years, there was a linear decline in CSF with age, for medium and high spatial frequencies. The responses to low spatial frequencies (0.4 and 0.95 cpd) appeared to be independent of age within this age range. These findings were in close agreement with many of the existing data obtained using oscilloscope generated gratings (Arundale 1978; Derefeldt et al 1979), and printed tests (McGrath and Morrison 1981; Owsley et al 1983).

Elliott (1987), using a psychophysical technique (Ginsburg and Cannon 1983), reported that there was a significant decrease in overall CSF with age at medium and high spatial frequencies (> 4 cpd). Sixteen 'young' subjects (mean age 21.5 ± 2.7 years) and 16 'older' subjects (mean age 72 ± 4.3 years) were tested. The decrease in the CSF reported became more significant with higher spatial frequencies.

5.4 Summary

The media of the eye are susceptible to a number of age-related changes, and the most important of these in terms of the eye's function are:

- the increased yellowing and opacification of the crystalline lens (Kline and Scheiber 1985)
- the reduced diameter of the pupil (Sekuler 1982; Kline 1985).

The resulting increase in the optical density of the crystalline lens increases intraocular light scatter, thereby degrading the retinal image and reducing image contrast (Savage et al 1993).

Age-related changes in visual function measures are well documented, such as

- VA (Slataper 1949; Weale 1975; Elliott et al 1993b)
- visual fields (Pitts 1982)
- colour vision (Pitts 1982; Lachenmayr et al 1994; Knoblauch et al 1995).

Light scatter has also been reported to increase with age (Allen and Vos 1967; Whitaker et al 1993) but the full scatter function (i.e. the amount of scattered light and its angular distribution) has rarely been measured as a function of age.

The results from studies investigating the effects of age on the CSF have tended to be somewhat conflicting. Previous reports have indicated:-

- no change with age (Arden 1978)
- preferential CS loss with age at low and medium spatial frequencies (Sekuler et al 1980)
- preferential loss at medium and high spatial frequencies (Arundale 1978; Derefeldt et al 1979; Sekuler et al 1982; Owsley et al 1983; Elliott 1987)
- CS loss at all spatial frequencies (Skalka 1980; McGrath and Morrison 1981; Ross et al 1985).

Some of the contradictions can be explained by methodological differences (Arden 1978), the use of small samples, age-related criteria differences (Arundale 1978), or concurrent undisclosed ocular pathologies (Sekuler et al 1980).

5.5 Aim

The aims of the present study are to establish a normal database for k' (the integrated straylight parameter) and to investigate the effects of age on k' and n (which describes the angular distribution of scattered light) as measured by the P_SCAN 100 scatter apparatus. In addition, the study aims to assess any similarities between the effects of age on scattered light (as measured by k') and CS. Knowledge of the values obtained from testing scattered light and CS in a normal population will allow a greater understanding of the visual

problems that may be associated with ageing and also provide a normal database for comparison with other population groups.

The availability of novel equipment and a researcher who was able to spend long periods of time collecting and analysing the data has allowed the current study to:-

- investigate normal subjects of different ages
- obtain a direct measure of forward light scatter using the P_SCAN 100 scatter apparatus
- measure k' , in addition to n and k
- compare measurements of scatter and the CSF over a wide range of spatial frequencies.

5.6 Subjects

Thirty-one normal subjects participated in the scatter study and twenty-eight participated in the CS study. Before inclusion, a slit lamp examination was carried out in order to exclude significant cataract, using LOCS II (Chylack et al 1989). A fundus examination was carried out by hand held direct ophthalmoscope in order to exclude disease of the posterior segment. Subjects had a Snellen VA of at least 6/6, a spherical refractive error between +0.50 DS and -0.25 DS, and astigmatism of less than 0.50 DC. All subjects had no history of ocular disease, and were between the ages of 16 and 60 years. Subjects were divided into five groups according to age. Subjects were included in the study if:-

- they had a VA of at least 6/6
- they were ophthalmologically normal
- they had no significant lenticular changes (i.e. less than Grade 1 as measured by LOCS II).

Subjects were excluded from the study if :-

- they had a VA of less than 6/6
- they were not ophthalmologically normal
- they had significant lenticular changes (i.e. more than Grade 1 as measured by LOCS II).

5.7 Methods

Changes in the light scattering properties of the eye were evaluated using the P_SCAN 100 scatter apparatus (Barbur 1991) (as described in section 1.3.2.5). CS measurements were also taken using the City University CS test (as described in section 3.8).

5.7.1 Scatter apparatus

The experimentation room allowed control for constant conditions of illumination and an isolated environment in which to perform the psycho physical study. Measures of light scatter are independent of background luminance. The equipment involved consisted of:

- Controlled illumination from a low 11.5 volt halogen lamp
- Adjustable seating, chin and head positioning for the subject
- A P_SCAN 100 pupillometer, with which the pupil diameter was measured and centration monitored
- A computer which programmed the scatter source to be generated on a high resolution visual display unit
- A recording system linked to the computer for data processing.

A large uniform background field of low luminance was used to maintain a constant state of light adaptation. In order to obtain diffuse ambient illumination, the halogen lamp beam was kept constant, and reflected from a matte white surface placed directly above the screen. The subjects' eye was centred at a distance of 70 cm from the monitor and the head position fixed against the head rest. Pupil diameter was simultaneously measured as the stimulus was presented, using infra-red sensitive charged couple device sensors on the P_SCAN 100 system. The experimenter used a hand-held box for control of the central test area luminance on the screen, and also for recording the reported null end-point. The push-button controls of the unit were labeled 'YES', 'NO', 'REPEAT' or 'GO'. The luminance of the central test target was increased by pressing the 'YES' button, decreased with the 'NO' button, re-presented at the same luminance by the 'REPEAT' button, or if the threshold had been reached, recorded by pressing the 'GO' button. A uniform step size interval was used if the change of luminance was in the same direction as before, however, following a reversal the step size was reduced by 40%. This 'bracketing' technique, used

in conjunction with the reduction in step size at each reversal, allowed for accurate determination of the nulling luminances. The nulling luminances of the central test target which were sufficient to balance the retinal illuminances caused by the scattered light were recorded for each of the five eccentricities. The test programme was repeated five times at each of the five scatter source eccentricities, and the average nulling luminances were recorded. Standard errors were calculated, and the light scatter parameters were computed using error-weighted regression analysis of the recorded data.

5.7.1.1 Experimental procedure

The apparatus was switched on at least 30 minutes before the beginning of a light scatter investigation in order to allow the equipment to 'warm up' and screen luminance to become constant. The scatter parameters were displayed upon the monitor and confirmed as optimal for the test run before proceeding.

5.7.1.2 Experimental set - up

The optimal conditions for the study were considered to be the following measurement and scatter parameters:

MEASUREMENT PARAMETERS

Number of averages	5
Initial step size of test luminance	0.12 (cd/m ²)
Reduction in step size after each reversal	40%
Presentation time of flicker stimulus	350 ms

SCATTER PARAMETERS OF THE SOURCE

Modulation temporal frequency	8.57 Hz
-------------------------------	---------

LUMINANCES

Background luminance	5 (cd/m ²)
Scatter source luminance (mean)	50 (cd/m ²)
Initial isolation annulus luminance	35 (cd/m ²)

CHROMATICITY CO-ORDINATES

Background	x 0.164	y 0.075	blue
Scatter source	x 0.2978	y 0.3438	white
Isolation annulus	x 0.45	y 0.45	yellow
Test target	x 0.2978	y 0.3438	white

OUTER RADII

Scatter source	405 (pixels)
Isolating annuli	72, 105, 155, 200 and 300 (pixels)
Test target	22 (pixels)

The flux entering the eye from the scattering source was constant in the pupil plane. Viewing conditions were monocular in all subjects so that the level of scattered light from each eye could be ascertained.

A two minute adaptation period to the background screen illuminance was included. The subject was asked to scan over the screen during this period. The eye under investigation was focused on the P_SCAN 100 display equipment. At the beginning of the programme, the central test target on the monitor had a luminance of 0 cd/m², and thus the subject was able to perceive central flicker over this disc caused by scattered light in the eye. The flicker source was presented for a period of 350 ms, and the subject was instructed to report 'yes' if flicker was detected in the central test target, or 'no' if none was detected. The experimenter increased the luminance of the central test target to a value above that of the scattered light so that flicker was again perceived after passing through the null point. The luminance was then reduced in small increments, in order to null the luminance of the scattered light from the eccentric source. The end-point was indicated by no perception of flicker (to which the subject reported 'no'). However, a more accurate value of the nulling luminance is obtained using the computer controlled reduction in 'luminance step size interval' on reversal. Thus, the central test target luminance was increased again until flicker was reported, and the nulling luminance reassessed using the 40% reduction in step size interval automatically introduced as a result of reversal. The level of the screen luminance which fully compensated the light scattered from the eccentric source was recorded by pressing the 'GO' button. The programme was then re-run for the next scattering source.

A subject completing the experiment would normally take approximately 15 minutes to complete a single run. Wherever possible, three runs were taken from each subject participating in the study.

5.7.1.3 Calibration of luminance

Calibration of the central test target was performed at two-monthly intervals. The luminance of each gun is proportional to voltage, and luminance was measured at each step size interval, using an LMT photometer set-up. Each of the red, green and blue phosphors of the display was measured separately and the luminance versus applied voltage relationship was stored in a file for use by all experimental programs. These data files are used by the scatter programme to calculate the luminance values of each required phosphor.

5.7.2 Contrast sensitivity apparatus

A high resolution CRT display (1280 x 1024 pixels) was used to generate vertical sine wave grating stimuli. The test field subtended a visual angle of five degrees, at a viewing distance of 2 metres and had a surround luminance of 34 cd/m². The background illuminance was set at 11.5 amps. The subjects were adapted for at least three minutes to the grey background. The subject was then asked to fixate the central target test area (a yellow cross on the visual display unit), and instructed to inform the examiner whether any vertical lines were observed. As the measurement of CS may be influenced by the number of tests, each subject completed a training session, to reduce potential practice effects.

A random 'yes/no' staircase, with variable step size and stimulus presentation time of 250 ms, was used to obtain contrast threshold. Contrast threshold was measured at seven spatial frequencies - 1.5, 3, 5, 7, 10, 16 and 22 cpd, and six measurements taken at each spatial frequency. All measurements were taken monocularly.

5.8 Results

Table 5.1 - Variations in the integrated straylight parameter k' and n for subjects grouped according to age.

Group (Age Range)	Number of subjects	Mean k' (s.d.)	Mean n (s.d.)
Group 1 (16-23)	8	6.80 (0.87)	2.04 (0.18)
Group 2 (30-31)	5	6.77 (1.26)	2.15 (0.13)
Group 3 (40-43)	5	6.72 (0.75)	2.05 (0.19)
Group 4 (48-50)	8	12.75 (1.68)	1.88 (0.12)
Group 5 (58-60)	5	18.38 (1.70)	1.78 (0.10)

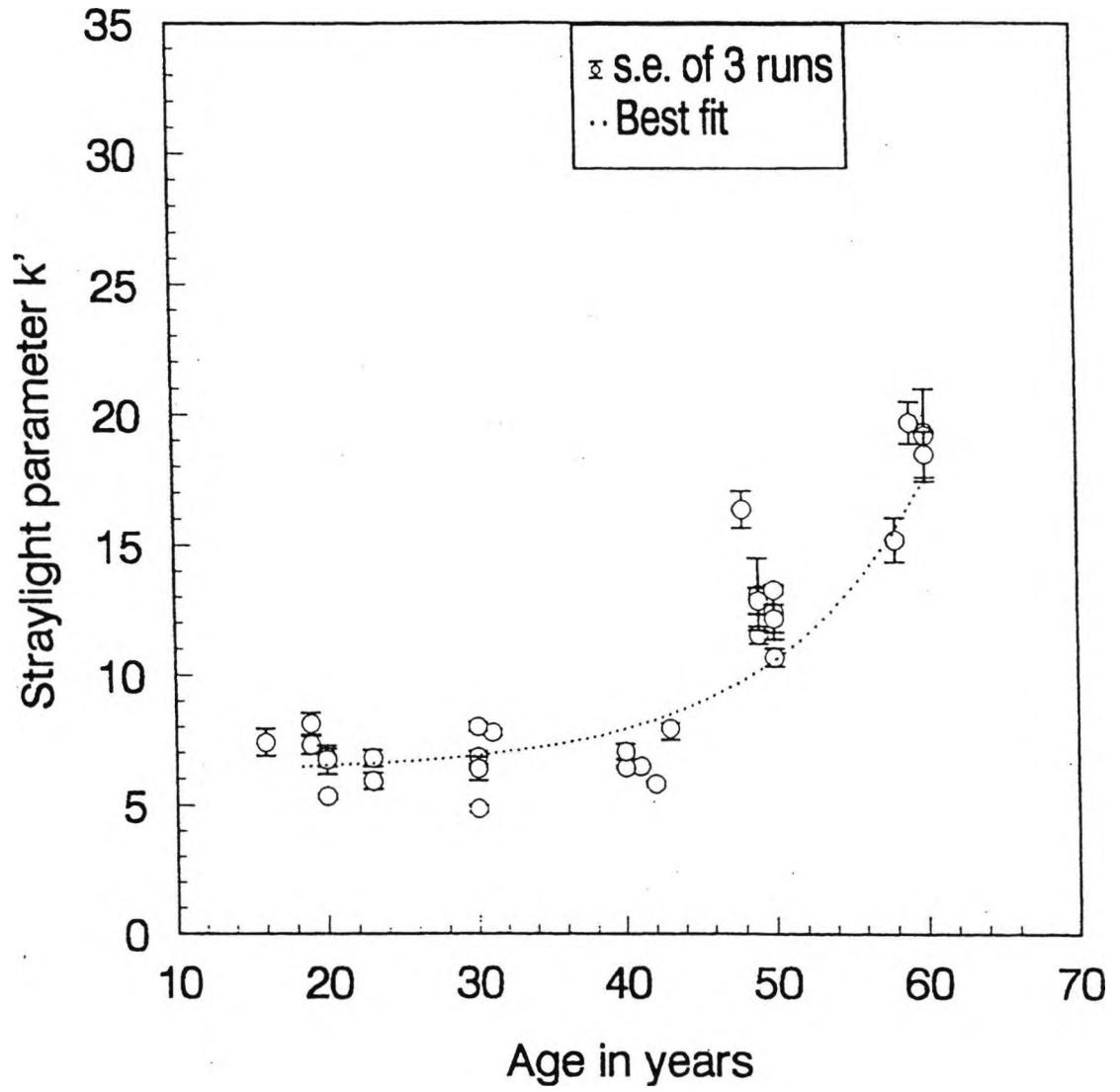
The scatter graph of k' against age (figure 5.2), shows that for this sample of 31 normal subjects, k' varies little with age for younger subjects in the sample (up to 43 years). The data can be described by a function of the form:-

$$k' = 6.6 + 0.1 \exp(a^{0.1025} - 1.1) \quad \text{[equation 5.2]}$$

where k' represents the integral of the scatter function between $\theta = 2.2$ degrees and infinity, and a represents the age of the subject in years. Equation 5.2 is used throughout the remainder of the thesis to generate the age-matched normal values for k' used for comparison with different groups of subjects, such as long-term contact lens wearers.

Using the P_SCAN 100 scatter apparatus, k' , the integral of the scatter function, shows no significant change up to about 45 years of age. However, a rapid increase in scatter follows above 45 years of age. For subjects less than 45 years of age, k' ranged from 4.85 to 8.13 (mean = 6.75, s.d. = 0.91). For older subjects, k' ranged from 10.69 to 19.71 (mean = 14.92, s.d. = 3.28). To facilitate statistical analysis, subjects were classified into five groups according to age (Table 5.1). Whenever possible, the subjects selected had ages close to 20, 30, 40, 50, and 60 years. One way analysis of variance showed Group 5 (60 year olds) to have significantly greater k' than all other groups, and Group 4 (50 year olds)

Figure 5.2 The integrated straylight parameter (k') as a function of age.



The standard errors of three runs are indicated. The line of best fit is also plotted.

to have significantly greater k' than 20, 30 and 40 year olds ($p < 0.001$, $F+85.65$, Fishers LSD).

The scatter graph of the parameter, n (which describes the angular distribution of scattered light) against age (figure 5.3) shows that for this sample of 31 normal subjects, n varies both within and between subjects. However, for older subjects there is a decline in the value of n compared to younger subjects. The data can be described by a function of the form:-

$$n = 1.95342 + 0.01633A^{-0.00034}A^2 \quad \text{[equation 5.3]}$$

where n represents the angular distribution of light scatter between $\theta = 2.2$ degrees and infinity, and A represents the age of the subject in years.

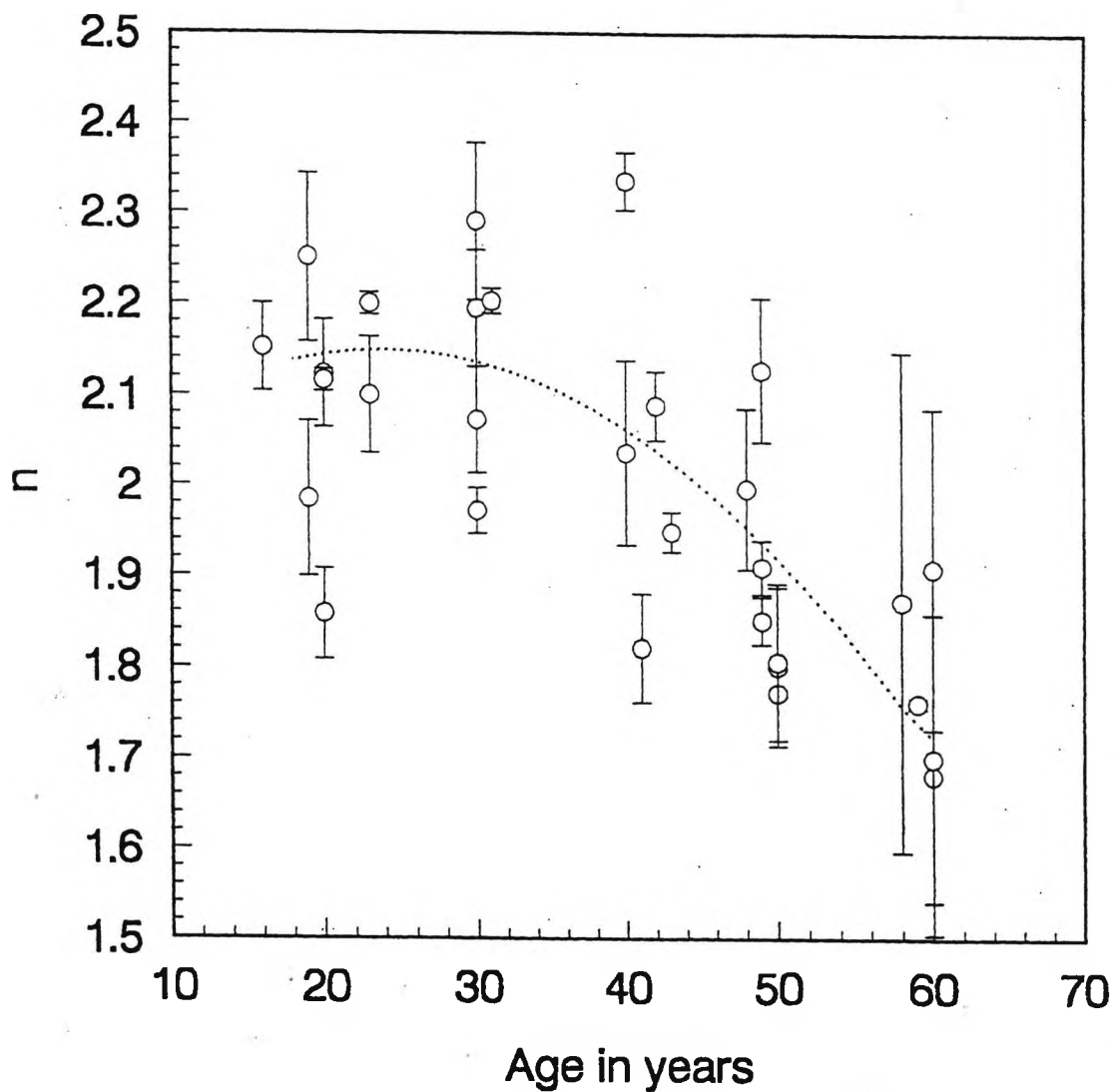
There is no significant change in n up to about 45 years of age. For subjects less than 45 years of age, n ranged from 1.86 to 2.34 (mean = 2.15, s.d. = 0.25). For older subjects, n ranged from 1.70 to 2.13 (mean = 1.85, s.d. = 0.12). One way analysis of variance showed that both Groups 4 (50 year olds) and 5 (60 year olds) have significantly lower n values than the 20, 30 and 40 year olds ($p < 0.001$, $F+7.48$, Fishers LSD).

Table 5.2 - Variations in CS thresholds for 3 cpd, 10 cpd and pupil diameter for subjects grouped according to age.

Group (Age Range)	Number of subjects	Mean CS at 3 cpd (s.d.)	Mean CS at 10 cpd (s.d.)	Mean Pupil diameter (s.d.)
Group 1 (16-20)	6	122.80 (15.75)	25.83 (14.56)	5.59 (1.10)
Group 2 (30-31)	5	141.40 (18.06)	58.96 (9.45)	5.24 (1.20)
Group 3 (40-43)	5	133.90 (4.09)	46.18 (9.40)	4.66 (0.94)
Group 4 (48-50)	8	130.26 (17.81)	28.73 (10.86)	4.48 (0.77)
Group 5 (58-60)	4	101.77 (9.18)	32.29 (5.67)	4.04 (0.90)

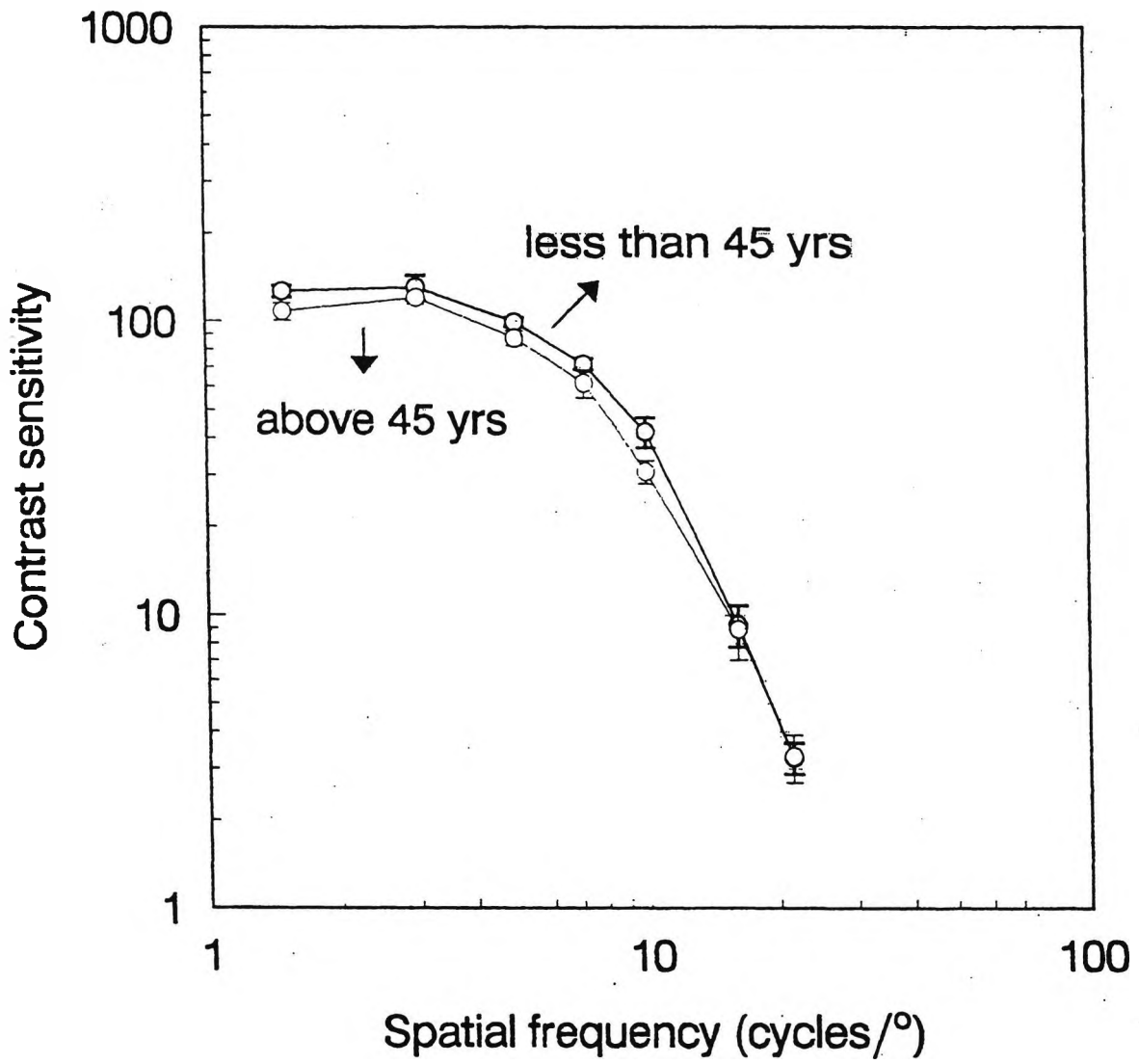
The CSF revealed a high degree of intra- and inter-individual variability, but for subjects older than 45 years there was a slight downward shift at all spatial frequencies, apart from

Figure 5.3 Parameter n , (describing the angular distribution of scattered light) as a function of age.



The standard errors of three runs are indicated. The line of best fit is also plotted.

Figure 5.4 The mean contrast sensitivity function for subjects aged less than 45 years and above 45 years.



The standard errors are indicated.

22 cpd (figure 5.4), when compared with those under 45. There was a significantly higher threshold for detection at 3 cpd in Group 5, than in Groups 1 to 4 ($p = 0.01$, $F+4.65$, Fishers LSD). At a spatial frequency of 10 cpd, the 20, 50 and 60 year olds had significantly higher thresholds for detection than the 30 and 40 year olds ($p < 0.001$, $F+9.27$, Fishers LSD). There were no significant differences between Groups for all other spatial frequencies tested.

As expected, pupil diameter reduced with age (figure 5.5). A mean diameter of 5.59 mm was found in Group 1, compared with 4.04 mm in Group 5. However, inter-subject variability was high, and when tested statistically there was no significant difference between Groups ($p = 0.12$, $F+2.05$, Fishers LSD).

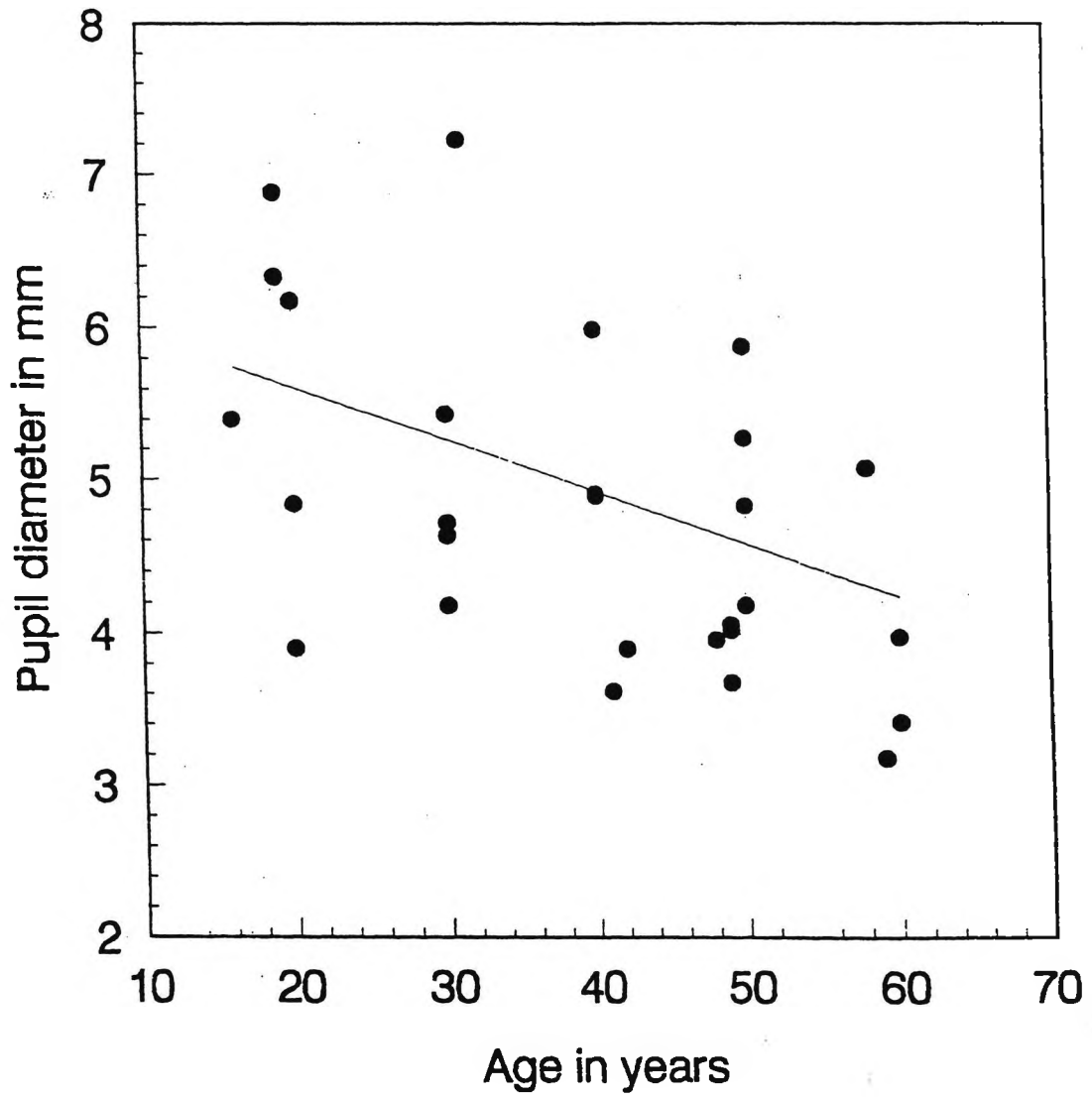
5.9 Discussion of Chapter 5

5.9.1 Changes in light scatter with age

It can be concluded that the integrated straylight parameter k' varies little with age for subjects under 45, but increases in older subjects. An increase in scattered light with age has also been found using alternative techniques (Wolf and Gardiner 1965; Allen and Vos 1967; Sigelman et al 1974; Siew et al 1981; Ijspeert et al 1990; Whitaker et al 1993). In the present study, k' , the integrated straylight parameter, is seen to increase by nearly three times between the ages of 16 and 60 years.

Previous studies investigating forward light scatter have assumed that n has a constant value of 2. In the present study, values of n were measured and were found to vary between individuals. Also, n decreased with age, implying that light scatter becomes more widely distributed or becomes more spread, with age. This finding is in contrast to the results of Fisher and Christie (1965) who investigated the effect of age in 15 subjects on the constants n and k of the Stiles-Holladay approximation (using a test spot and a glare source at various angles). The parameter n was found to be a constant (2.2) independent of the age of the observer (Fisher and Christie 1965). The finding that n varies between individuals with age (as measured by the P_SCAN 100 scatter apparatus) raises questions regarding the practice, common in scatter research, of assuming a constant value of 2 for n .

Figure 5.5 Changes in pupil diameter with age



5.9.1.1 Age at which visual performance begins to decline

The increase in straylight for subjects over the age of 45 agrees broadly with the findings of Said and Weale (1959) and Moreland (1978), who state that the decline in visual function after the age of 50 may be due to increased ocular lens absorption and increased lenticular light scattering. Other studies of visual function in older normal individuals also indicate that visual function does not change at a constant rate with age, but rather is fairly static until about age 50 - 60, e.g. VA (Weymouth 1960), stereopsis (Jani 1966), colour matching (Moreland 1978) and CS (Owsley et al 1983). Johnson and Choy (1987) stated that at around the age of 50, for all the functional measurements (i.e. stereopsis, perimetric increment threshold sensitivity, colour vision, CS, and VEP latency), except VA, there appears to be an abrupt change in the function that describes the relationship between visual performance and age.

Other tests of visual function reveal a more linear decline with age. In subjects aged 20 and 60 years, McFarland and Fisher (1955) measuring dark adaptation thresholds, found that the intensity of a test light at threshold had to be approximately doubled for each additional 13 years of age. It was reported that from the age of 20 years, there was an increase in threshold of approximately 1.7 log units to the 70s, and 2.5 log units to the 80s. More recently, Lachenmayr et al (1994) demonstrated that the results of flicker perimetry decreased linearly with age, and suggested that this was a result of the flickering stimulus being independent of the disturbing effects induced by ocular media changes with age.

Increased scatter is known to reduce visual performance with age (Fisher and Christie 1965; Elliott 1987; de Waard et al 1992; Whitaker et al 1993) and produce increased sensitivity to glare (Bailey and Bullimore 1991). The increases in scatter progress at a slow rate, and as a consequence, subjects adapt to the reduced contrast of the retinal image resulting in a lack of subjective complaints (Ijspeert et al 1990; Barbur et al 1991). Assessment of the changes in glare sensitivity with age have shown a gradual increase in glare up to the age of 40 years, followed by a more rapid increase, approaching a maximum at around 80 years of age (Wolf 1960; Allen and Vos 1967; Le Claire et al 1982). This is in agreement with the findings of this study, although subjects older than 60 years were not tested. Although increases in scattered light with age are well documented, it is necessary to consider the origins of straylight which cause this change in visual function.

5.9.1.2 The origins of light scatter in the ageing eye

The origins of the increased straylight in the ageing eye found in this study are difficult to determine. An early study by Allen and Vos (1967) attempted to relate forward light scatter to backward light scatter. A variable contrast Landolt C test of 0.5, 1, 3 and 6 min of arc was employed to assess visual performance and back scatter was measured using slit lamp photographs (30 degrees from the incident light). Between the ages of 10 to 80 years, a four-fold increase in backscatter was noted. However, the level of inter-individual variation was significant. Visual performance measures revealed that an increase in contrast was required with older subjects. However, the level of backscatter could not predict the change in visual performance.

5.9.1.2.1 Corneal light scatter and age

Unfortunately, very few studies have elucidated the amount of forward light scatter derived from the cornea as a function of age. As previously described, Allen and Vos (1967) assessed backscattered light from the crystalline lens and cornea as a function of age, and attempted to relate the results to forward light scatter (section 2.2.8). Allen and Vos (1967) demonstrated that the normal cornea scatters only about 1% more light at the age of 80 years compared with the younger eye (figure 5.6). However, as discussed, the hypothesis that backward light scatter equates to forward light scatter is incorrect.

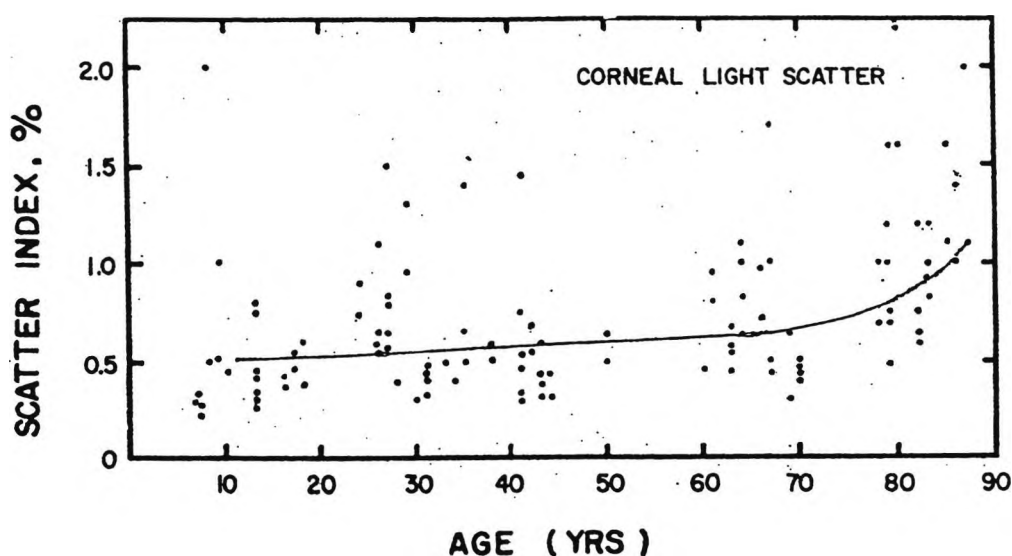


Figure 5.6 - The results from light scatter measurements on 124 corneas plotted against age (Allen and Vos 1967).

Olsen (1982), using similar techniques to Allen and Vos (1967), determined that there was an increase in back scatter with age. Corneal scatter and CT as measured by pachometry were recorded in 93 normal eyes. For normal corneas, a significant correlation was found between the scatter and the age of the subject (figure 5.7). CT did not parallel these age-related changes.

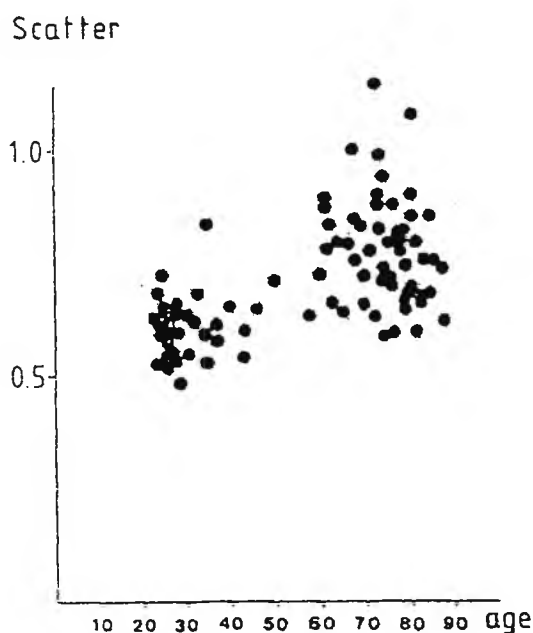


Figure 5.7 - Corneal scatter versus age in 93 normal subjects. Spearman's rank coefficient $r = 0.55$ ($p < 0.001$) (Olsen 1982).

The author concluded that the increase in scatter with age was due to the increasing irregularity of the spacing of collagen fibrils as the eye aged. The day-to-day variation in corneal backscatter was approximately 7%, and the inter-individual variation increased with age (Olsen 1982).

In a later study, Smith et al (1990) measured light scatter from the central human cornea in 60 eyes of 60 subjects using Scheimpflug photography (age range seven to 88 years). The Scheimpflug slit image photographs had originally been taken to study lens changes in subjects with varying types of cataract and so in order to compare the results of normal subjects, images of subjects with diabetes or corneal abnormalities were excluded. The remaining normal photographs underwent computerised image analysis. The study concluded that the amount of scatter was not uniform throughout the thickness of the

cornea and the intensity of light scattered was greater from the anterior and posterior surfaces than from the stroma. No correlation between the age of the subjects and the amount of corneal light backscatter was reported.

As it has been known for some time that backscattered light does not equal forward light scatter (Chapter 1) it is difficult to predict the effect of any increase in light scatter with age. However, the corneal contribution to forward light scatter has been reported to be independent of age (van den Berg 1995a). Studies that have investigated the contribution of corneal forward light scatter have concentrated on the light transmission of the human cornea. Boettner and Woltner (1962) using isolated human cornea measured light transmittance using a small acceptance angle (of 1 degree), which was termed 'direct transmittance', as well as a large acceptance angle (170 degrees) which was termed 'total transmittance'. It was thought that forward light scattering causes these two quantities to differ. From the results of nine patients (age range - 4 weeks to 75 years) it was demonstrated that corneal spectral transmissivity reduced with age. Lerman (1984) also reported a decreasing amount of light transmission in human corneas of increasing age *in vitro*. However, Beems and van Best (1990) showed that the data from Boettner and Woltner (1962) was incorrect and in fact no age-related changes in corneal transmissivity exist. A later study by van den Berg and Tan (1994) investigated the scotopic spectral sensitivity function for 10 aphakic subjects aged between 14 - 75 years (aphakic subjects were chosen as it was assumed that the cornea will dominate in the pre-retinal transmittance function). From the results of this study, it was concluded that the spectral transmittance function of the human cornea was dominated by forward light scattering processes and that this function was independent of age. It is therefore not clear whether increases in light scatter with age are correlated with decreases in corneal transmissivity as a result of corneal forward light scatter.

5.9.1.2.2 Lenticular light scatter and age

The most likely cause of increased forward-scattered light in the ageing eye is the crystalline lens. A strong correlation has been reported between glare sensitivity and the transparency of the crystalline lens (Wolf and Gardiner 1965). This implies that the lens is probably the principal cause of increased glare sensitivity. The subjects in the present study were examined using the LOCS II, and no significant lens changes were noted.

However, the ability of the LOCS II to detect subtle changes in backscatter is unlikely. In fact, Allen and Vos (1967) reported that although there was a clear deterioration of visual performance with age, it could not be predicated by measuring back scatter. Therefore, the measurement of forward scattered light more adequately reflects visual function.

The light scatter produced by the lens increases more or less linearly during adult life up to about 60 years, and then increases exponentially (Franklin et al 1990). Moreland (1978) stated that the greater variability in light scattering in individuals over the age of 60 was principally due to lenticular light scatter. Short wavelength increases in ocular lens absorption and increased lenticular light scattering may be partially responsible for the accelerated decline in visual function and increased variability that occurs after the age of 50. Moreland (1978), Weale (1980) and Pokorny et al (1987) have each shown that lens absorption increases dramatically after the age of 60. Through analysis of data in the literature, Pokorny (1987) has shown that lens density at 400 nm increases at a rate of 0.12 density unit per decade of life before the ages of 20 and 60, and by 0.40 per decade thereafter. Epidemiological data from the Framingham Eye Study indicates that the prevalence of senile cataract in the normal population quadruples between 60 and 70 years of age. Early lens changes, which may go undetected in the selection of subjects for normative visual function studies, increase from a prevalence of 27% in individuals under 65, to 50.3% in individuals between 65 and 74 years of age (Sperduto and Hiller 1984).

5.9.2 Changes in contrast sensitivity with age

The results of CSF testing revealed a high degree of intra- and inter-individual variability. Such variability in CS measurements is well documented (Virsu et al 1975; Cohen et al 1976; Ginsburg 1984; Arden 1988). It is thought that variability is unlikely to be an artifact, but rather it reflects genuine biological variability. In fact, Johnson and Choy (1987) state that because of a large number of factors conspiring to produce age-related changes in visual function, there is often greater variability in data obtained from older individuals. Such variability decreases the sensitivity of any test which is designed to identify early pathology.

Although the mean sensitivities of the two age groups investigated in this study were fairly well separated at lower frequencies, there were some individuals whose sensitivities fell

within the range of the younger subjects and vice versa. This has previously been reported by Sekuler et al (1982).

A downward shift in the CSF was apparent in this study in subjects over the age of 45. Older subjects had decreased sensitivity at all spatial frequencies apart from 22 cpd, when compared to young subjects. This is in general agreement with Skalka (1980), McGrath and Morrison (1981), and Ross et al (1985). However, little change was noted for the highest spatial frequencies tested (16 and 22 cpds). The significantly decreased sensitivity in Group 5 subjects (58-60) compared with the other younger groups at 3 cpd is in broad agreement with Sekuler et al (1980). They also found a reduction at medium spatial frequencies, and the current study did find significant differences between Groups 4 and 5 and younger subjects in Groups 2 and 3 at 10 cpd. However, the 10 cpd finding must be treated with caution as Group 1 subjects (16-20) also performed significantly worse than Groups 2 and 3. However, other studies have reported losses of CS confined to spatial frequencies 4 cpd and above (Arundale 1978; Derefeldt et al 1979; Elliott 1987), loss at all spatial frequencies (Skalka 1980), or changes in medium to high spatial frequencies (Sekuler et al 1982; Owsley et al 1983).

5.9.2.1 Factors involved in reducing the contrast sensitivity function with age

There is little consensus about the mechanisms which underlie the loss of spatial CS in the aged eye. Issues of controversy include the frequency range at which age effects start (Derefeldt et al 1979; Owsley et al 1983; Kline and Scheiber 1985), and to a lesser degree whether the sensitivity decrease is related linearly to age (Morrison and McGrath 1985).

A number of investigators have suggested that high spatial frequency losses in the elderly may be primarily due to optical, rather than neural factors (Owsley et al 1983; Hemenger 1984; Wright and Drasdo 1985). Owsley et al (1983) found that the CSF of seven young (20 year-old) subjects with a 0.5 neutral density (ND) filter in front of the eye (in order to imitate the loss of retinal illuminance between 20 and 60 years of age), was reduced to the level found in 60 year-old subjects. It was concluded that a significant portion of the loss of CS with age was attributable to retinal illuminance reduction in the aged eye, due to a decreased lens transmission and senile pupillary miosis.

Sloane et al (1988a) attempted to eliminate senile miosis as a contributing factor in the reduction of CS with age. The loss in spatial CS as a function of luminance level was determined with increasing age. In so doing, the contribution of senile miosis observed to CS losses could be calculated. The study concluded that their group of normal older adults (11 subjects, mean age 73 years, age range 67 - 79), tended to experience significant losses in spatial CS which were exacerbated under low environmental light levels. Older adults exhibited CS reductions at all light levels tested when compared to younger observers (13 subjects, mean age 24 years, age range 19 - 35). However, vision loss was especially significant at the lowest luminance. Under 0.107 cd/m² conditions, older adults required three times more contrast to detect an intermediate spatial frequency than younger subjects. In addition, when older adults matched the pupil size that naturally occurs in young adults, at 0.107 cd/m², older observers still exhibited approximately the same magnitude of vision loss. Therefore, the older adults' CS loss at any of the tested light levels cannot be compensated for by a simple increase in the diameter of the pupil. In fact, in certain subjects, senile miosis slightly improved the CS result. However, the aged eye exhibits increased optical density of the ocular media, particularly the crystalline lens (Weale 1963). This increases intraocular light scatter, thereby degrading the retinal image, and reducing image contrast. Therefore, in this situation a small pupil may be beneficial as it limits optical aberration, and improves depth of focus (Sloane et al 1988a).

The increased levels of forward light scatter found with age can be thought to act as a veiling luminance on the retina (Stiles 1929; Fry and Alpern 1953), decreasing the contrast of any pattern imaged on the retina. Owsley et al (1983) suggested that if light scatter was the sole cause of a reduced CSF then the scattered light would reduce the effective contrast of any pattern, and thresholds for targets of all spatial structures would be elevated to the same degree. For this reason, Owsley et al (1983) suggested that it is inappropriate to hold increased light scatter in the older responsible for young-old threshold differences, since these threshold differences are specific to certain spatial and temporal characteristics.

In contrast to Owsley et al (1983), Hemenger (1984) argued that increases in intraocular scatter in the aged eye can indeed account for increases in contrast thresholds. It was assumed that disability glare increases uniformly in proportion to age for all glare angles, and therefore any change in CS should represent the increase in light scatter (Fisher and

Christie 1965). In a mathematical argument based upon disability glare data (Vos 1965; Walravren 1973), it was argued that an older adult's loss in CS may be caused by intraocular light scatter, since the ratio of the MTFs of the ocular media for older subjects and younger subjects is in good agreement with the ratio of their CS. However, this conclusion is open to criticism. Firstly, some of the data points from Derefeldt et al (1979) plotted in Hemenger's figure seem to be plotted incorrectly (Sloane et al 1988a). Also, the data from Owsley et al (1983) referred to in the Hemenger paper are not included in the graph. A new graph was subsequently generated by Sloane et al (1988a) to include the aforementioned data and corrections.

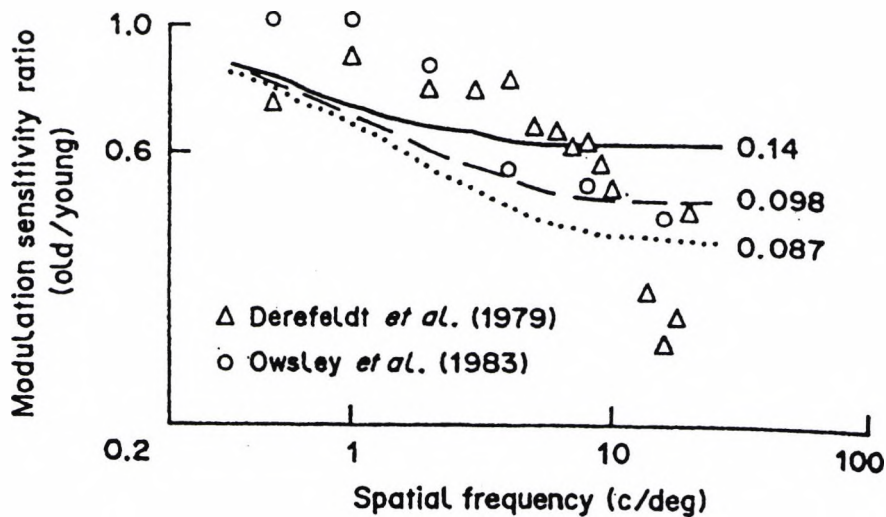


Figure 5.8 - Based on Hemenger's Fig. 1 (1984). The three curves were digitised from Hemenger's graph and re-plotted. The curves represent the ratio between the modulation transfer function (MTF) of the older eye (age 65) and the MTF of the younger eye (age 30), where a term for intraocular light scatter is contained in the calculation of the MTF. Each function represents a different width of the light scatter function. Δ = Derefeldt et al's (1979) CS data, plotted as the ratio of older adults' sensitivity (age 60-70) to the younger adults' sensitivity (age 20-40), \circ = Owsley et al's CS data (1983) (Sloane et al 1988a).

From figure 5.8, Sloane et al (1988a) suggested that it is not apparent that a light scatter explanation closely fits the pattern of the CS data. The light scatter functions initially fall quite rapidly as a function of spatial frequency, and then plateau at around 10 cpd. In contrast, the CS data initially falls progressively. As the spatial frequency increases, there is a more rapid decline in the light scatter functions. Whilst light scatter may produce an elevation in contrast thresholds, there appear to be other factors involved. It is also uncertain how the increased intraocular light scatter accounts for an older adult's increased impairment in sensitivity at low light levels (Sloane 1988a).

In addition to the increased scatter produced by the lens with age, there is an increase in light absorption which reduces retinal illuminance (Said and Weale 1959). This would have the effect of reducing the absolute light level reaching the photoreceptors, thereby reducing the adaptation level of the retina, and thus decreasing CS, particularly at higher spatial frequencies (Kelly 1972). If increased lens absorption was solely responsible for older adult's CS loss, one would expect that the slope of the function relating CS and luminance would be equal for younger and older adults. The older adult's function simply displaces downward on the sensitivity axis. A further study by Sloane et al (1988b) suggests that an explanation based solely on light absorption differences in the young versus the old eye is inadequate in explaining the older adult's CS loss. Figure 5.9 illustrates how the functions for CS versus luminance would differ for young and old adults, if increased light absorption were to be solely responsible for the sensitivity loss (Sloane et al 1988b).

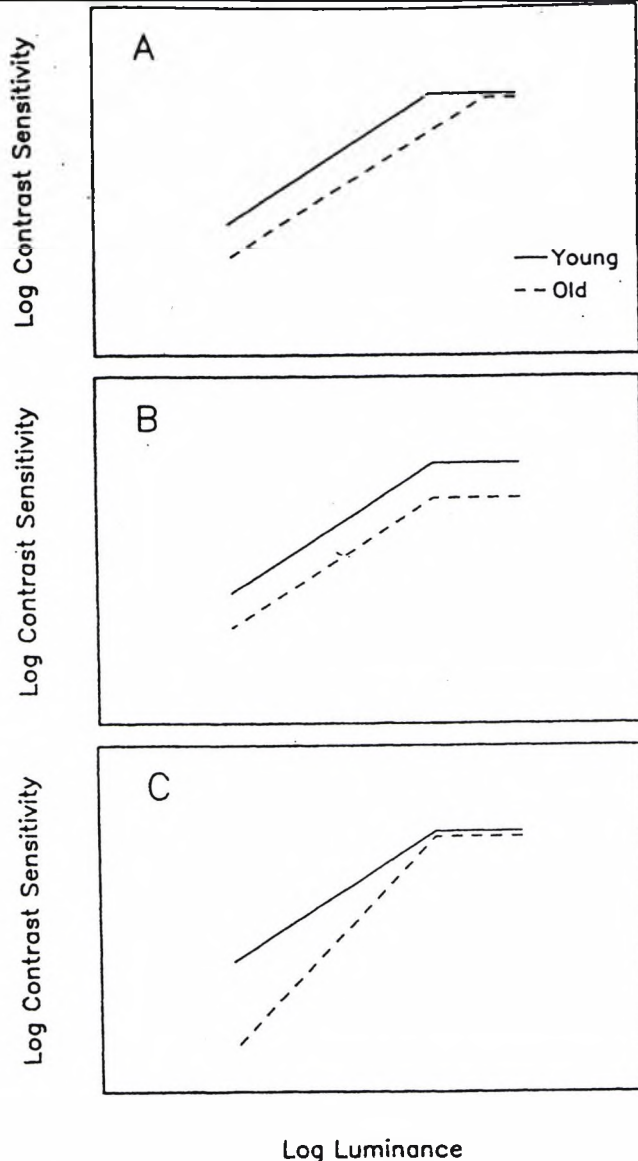


Figure 5.9 - Hypothetical function illustrating how CS and luminance are related for younger adults (-) and older adults (--). Graph A represents the effect of light absorption, Graph B represents the effect of light scatter, and Graph C represents the effect of changes in neural mechanisms (Sloane et al 1988b).

The CSF for older adults would be shifted rightward on the x-axis with no change in slope, since the light level reaching the photoreceptors in older adults would be a constant fraction of the light level in younger adults. In addition, because the function for younger adults levels out at high luminance, there should be a point at which the function for older adults meets that for younger adults (Sloane et al 1988b).

Other lenticular changes apart from increased light scatter and absorption have been postulated as a cause of a reduced CSF with age. Research has indicated that the modulation transfer function (MTF) of the excised aged lens is markedly diminished at intermediate and high spatial frequencies compared to the MTF of the young adult lens

(Block and Rosenblum 1987). It is thought that the older lens attenuates the image contrast of higher spatial frequencies to a greater degree than the young lens, implying that older adults would require more contrast to detect a higher frequency target. This concurs with psychophysical data (Derefeldt et al 1979; Owsley et al 1983). Block and Rosenblum (1987) argue that the MTF changes in the lens are likely to be due to increased intraocular light scattered by the aged lens. Theoretically, this MTF change in older adults may increase the contrast threshold at a given light level. However, it cannot account for the fact that older adults' loss in spatial vision worsens with decreasing luminance, since the MTF of the lens is invariant. Thus, it seems that additional factors must underlie the loss in spatial vision experienced by older adults.

A subsequent report by Owsley et al (1985) contradicted the 1983 study (Owsley et al 1983), and concluded that CS loss with age is not in fact due to optical factors. This was based on the finding that ten patients who had undergone cataract extraction and intraocular lens (IOL) insertion (and in most cases capsulotomies), had similar mean CS values to ten normal age-matched eyes. However, Owsley et al (1985) assumed that the optical state of the eyes after cataract extraction and IOL insertion would be better than that of a normal older eye. The results of VA would not appear to justify this claim (Elliott 1987), as subjects with IOLs achieved a mean VA 6/7.5, whilst normal eyes achieved a mean VA 6/6+. That said, the results were consistent with Zuckerman et al (1973) indicating that lens opacity must be substantial (involving at least 40% of the lens) before image contrast is significantly reduced.

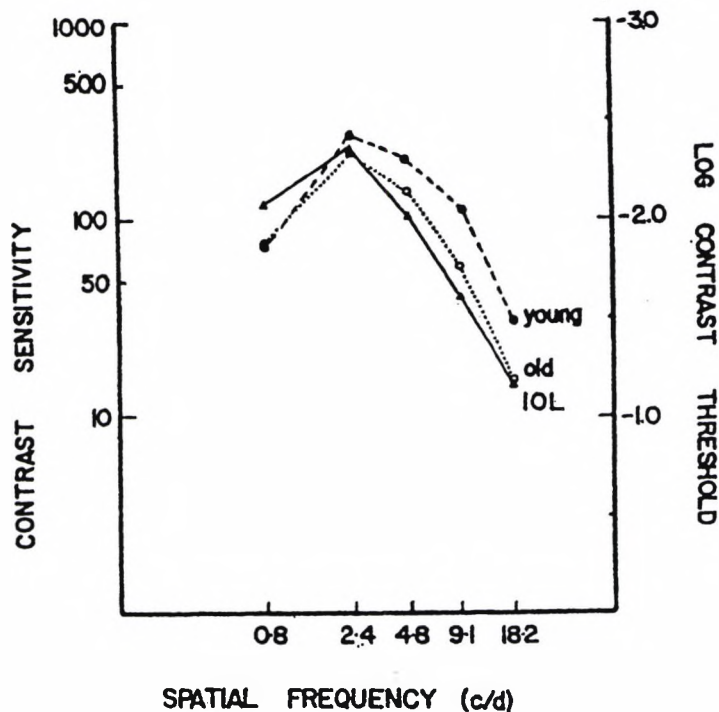


Figure 5.10 - Mean CS as a function of spatial frequency, displayed for each group (Owsley et al 1985).

In agreement with Owsley et al (1985), Sloane et al (1988a) claimed that neural factors must also contribute to a decline the CSF. In addition, Morrison and McGrath (1985) demonstrated significant neural-based losses in CS in elderly observers, using laser interferometry to bypass the optics of the eye. Morrison and McGrath (1985), employing a 0.5 ND filter with five young subjects, indicated no mean change in the CSF. Certain subjects showed an improvement in CS, some a significant loss, and others no change at all. Morrison and McGrath (1985) demonstrated a continuous decline of retinal and neural CS with age. The authors concluded that the deterioration in CS with age is primarily caused by changes within the central nervous system, rather than the optical media. However, no full screening for ocular pathology was undertaken and alternative studies,

using similar laser techniques, reported no age-related sensitivity losses (Dressler and Rossow 1981; Kayazawa et al 1981). Dressler and Rossow (1981) and Kayazawa et al (1981) suggested that there is no change in neural or retinal CS throughout adulthood. However, these studies did not document the method, or results in either case. The studies did not present the data stated by age, nor did they present sample sizes by age group.

Later, Elliott (1987) also attempted to determine the source of the loss in CSF. Sixteen 'young' subjects (mean age 21.5 ± 2.7 years) and 16 'older' subjects (mean age 72 ± 4.3 years) were tested. The overall CS (OCS) was measured conventionally by using a computer-based monitor system, while retinal and neural CS (RNCS) was measured using a modified Rodenstock Retinometer. This system bypasses the effects of the eye's optical system and measures the CS of the retinal and neural system alone. In addition, glare sensitivity measurements were taken by repeating the OCS procedure with a circular fluorescent glare source. The study reported a significant decrease in the OCS with age at medium and high spatial frequencies (> 4 cpd). The decrease in CS became larger, the higher the spatial frequency. There was no significant difference between the OCS and the RNCS, as both revealed a reduced CSF. Glare sensitivity scores were found to significantly increase with age, for all spatial frequencies. The results indicated that the reduction in CS with age could not be due to optical factors alone as the RNCS scores did not show an improved CSF. The loss of sensitivity was thought to be predominantly retinal and neural, most probably due to cell loss and degeneration. The optical media was found to have a lesser effect, decreasing the CSF marginally, and then only for the high spatial frequencies. For both young and old subjects, glare sensitivity scores were significantly lower at higher spatial frequencies. This was supported by Paulsson and Sjostrand (1980). As the overall CS loss due to optical factors only appears at the highest spatial frequency, this would suggest light scatter was not a major factor. The study concluded that the decrease in OCS due to optical changes with age is likely to be due to reduced retinal illumination, resulting from senile miosis and increased lenticular absorption (Elliott 1987).

In summary, the increased forward scatter of light may act as a veiling luminance on the retina (Stiles 1929; Fry and Alpern 1953). In so doing, the contrast of any pattern imaged on the retina is decreased. In addition, the reduction in pupil diameter noted with age may also contribute to reducing CS by reducing retinal illumination. However, previous studies

have found this change to be insignificant (Campbell and Green 1965; Sekuler et al 1980; Sloane et al 1988a). In fact, Sloane et al (1988a) state that a small pupil diameter is likely to improve subjects' performance, as it limits optical aberration, and improves depth of focus. This serves to facilitate image formation in the older eye. The reduction in CS may also be due to retinal and neuronal factors, as previously described.

5.10 Conclusions

In conclusion, the integrated straylight parameter k' varies little with age for younger subjects (under 45 years), but increases in older subjects (over 45 years). n also varies little with age for younger subjects (under 45 years), but decreases in older subjects (over 45 years). These findings indicate that both the amount and angular distribution of light scatter increase with age. These increases are accompanied by a reduction in the CSF, despite apparently good VA. An increase in the amount of scattered light with age has also been found by alternative techniques (Wolf and Gardiner 1965; Allen and Vos 1967; Sigelman et al 1974; Siew et al 1981; Ijspeert et al 1990; Whitaker et al 1993). The increase in the straylight revealed for subjects over the age of 45 agrees broadly with the findings of Said and Weale (1959) and Moreland (1978), who state that the decline in visual function after the age of 50 may be due to increased ocular lens absorption and increased lenticular light scattering.

A downward shift in the CSF was apparent over the age of 45. Older subjects had decreased sensitivity at all spatial frequencies apart from 22 cpd, when compared to young subjects. This is in general agreement with Skalka (1980), McGrath and Morrison (1981) and Ross et al (1985). The largest reduction in CS was found at low to medium spatial frequencies and is in agreement with Sekuler et al (1980).

The increased forward scatter of light may act as a veiling luminance on the retina (Stiles 1929; Fry and Alpern 1953). In so doing, the contrast of any pattern imaged on the retina is decreased. In addition, the reduction in pupil diameter noted with age may also contribute to reducing CS by reducing retinal illumination. However, previous studies have found this change to be insignificant (Campbell and Green 1965; Sekuler et al 1980; Sloane et al 1988a). The reduction in CS may also be due to retinal and neuronal factors, as previously described.

As the subjects used in the present study had excellent VA, and apparently no pathology, the results obtained are likely to be accounted for by advancing age. These changes may originate from any ocular structure, but the most likely cause of increased scatter and reduced CS is the lens i.e. optical in origin. Even though all subjects were investigated using LOCS II, it has been previously demonstrated that backward light scatter (as seen with the slit lamp), does not equal forward light scatter. Therefore, the results of this study suggest that k' is a useful parameter to quantify changes in light scatter with age.

The results of this chapter have established the range of k' values to be expected from a physiologically normal population. Knowledge of the changes in light scatter that occur with age now facilitates comparative studies of subjects with anterior segment eye disease and contact lens wear. Equation 5.2 will be used in Chapters 8 and 9 to generate age-matched k' values for each subject examined. By subtracting the values of k' obtained from normal age-matched subjects, the data obtained from such populations can be compared, whilst accounting for the effects of age. The CS results obtained in this chapter will also be used for comparison purposes in later chapters.

CHAPTER 6

Factors causing a variation in light scatter in normal subjects

6.1 Introduction

The aim of the experiments described in Chapter 6 was to investigate whether measurements of light scatter in the eye using the P_SCAN 100 scatter apparatus are subject to diurnal or longitudinal fluctuations. Pachometry was also employed in order to investigate the cause of any observed increases in light scatter. This information will assist the protocol design, patient selection process and interpretation of results for the later studies on subjects wearing contact lenses.

When human functions are assessed longitudinally, many behaviours fundamental to life are found to exhibit regular cyclical variations. For instance, body temperature has been shown to become reduced at night and increased during the day (Tomlinson 1992). Within the eye, intraocular pressure (IOP) and corneal thickness (CT) are known to exhibit diurnal variation (Fujita 1980; Harper et al 1996).

Corneal oedema is associated with a number of pathological ocular conditions, and occurs in response to a variety of physiological stresses. For instance, the normal human cornea experiences oedema on a daily basis beneath the closed eyelid during sleep (Efron and Carney 1979; Johnson et al 1985). Measurement of CT allows the extent of corneal oedema to be estimated, and by way of the established relationship between hydration and thickness, provides a useful indicator of the physiological integrity of the cornea (Mishima and Hedbys 1966). As the cornea becomes oedematous, light scattering increases (Maurice 1957; Potts and Friedman 1959; Kikkawa 1960; Potts 1962; Hart and Farrell 1969; Feuk and McQueen 1971). As such, the measurement of CT may reveal physiological and/or pathological changes which influence measurements of intraocular light scatter.

6.2 Corneal physiology

In order to transmit and refract light, the cornea must maintain its structure. As discussed in section 2.2, the corneal stroma is composed mainly of collagen fibrils, glycosaminoglycans (GAGs) and a glycoprotein ground substance. The GAGs are

hydrophilic and absorb fluid in a manner similar to a gel (Maurice 1984). 'Lakes', or separations, between the stromal lamellae and a wide range of collagen fibril densities can be seen in oedematous corneas. Each of these changes will lead to increased light scatter, and the corneal epithelium and endothelium must provide a low enough level of stromal hydration such that light scatter is minimised (Tomlinson 1992).

Active fluid pumps and the passive barrier properties of the cell layers maintain stromal hydration. On its own, the barrier function merely slows down leakage of water across the cell layers in response to the stromal imbibition pressure. The rate of leakage must be compensated by active fluid pumping if constant stromal hydration is to be maintained. Interfering with energy production causes the cornea to swell (Davson 1955; Dikstein and Maurice 1972). Although initial research implicated the epithelium as responsible for maintenance of corneal hydration, later work clearly demonstrated that the primary site is the endothelium (Maurice 1972). The majority of corneal biophysicists agree with Maurice's theory, however, the precise mechanism of corneal hydration is still disputed. Hodson and Miller (1976) proposed that the endothelium actively transports bicarbonate (HCO_3^-) ions into the anterior chamber, and water tends to follow osmotically, however, the validity of this theory has since been challenged (Doughty and Maurice 1988; Doughty 1990). Doughty (1990) postulated that the stroma is the likely site of corneal hydration control, with the endothelium merely regulating the HCO_3^- flow into the stroma.

Insult to the endothelium, whether physical or metabolic, will become clinically manifested as corneal oedema and scattering of light. It is believed that excess lactate is produced by the hypoxic epithelial cells when the epithelium is compromised. Lactate cannot diffuse anteriorly between the tight-bordered epithelial cells, and so instead diffuses back across the stroma to act osmotically, and counterbalance the effect of the endothelial pump. This results in stromal swelling.

6.2.1 Maintenance of corneal transparency

In order to fully discuss the mechanisms involved in corneal oedema, it is important to clarify the parameters necessary to maintain corneal transparency. Since Smelser and Ozanics (1952) discovered that atmospheric oxygen was necessary to maintain a normal level of corneal hydration, a number of attempts have been made to determine the

minimum oxygen tension required to prevent corneal oedema (e.g. Polse and Mandell 1970; Carney 1974; Mandell and Farrell 1980). Polse and Mandell (1970) estimated that a minimum oxygen concentration of 1.5 - 2.5% is necessary to prevent corneal oedema. This conclusion was based on results from three subjects exposed to a narrow range of hypoxic conditions (0 to 2.5%). Despite this, a study by Carney (1974) of four eyes exposed to 2% oxygen for two hours supported the Polse-Mandell criterion. Subsequently, Mandell and Farrell (1980) investigated 28 subjects using gases with oxygen partial pressures of 6.9, 17.1 and 20.2 mmHg (oxygen concentrations of 0.95%, 2.34% and 2.77% respectively). The authors concluded that the minimum oxygen tension required to maintain a normal CT was 3.3 - 5.5%, although there were marked individual variations in this threshold. It is noted that the authors extrapolated beyond their data to predict the minimum oxygen tension. Further experiments by Holden and Mertz (1984) and Holden et al (1984) used a wider range of oxygen concentrations within the goggle (1 - 21%) and extended exposure times (up to 8 hours). These experiments suggested that steady-state oedema takes approximately 4 to 5 hours to develop (figure 6.1), and confirmed that there was wide variation in both the corneal swelling response with various oxygen concentrations, and also in the atmospheric oxygen concentration required to avoid oedema. One subject required 7.5% oxygen concentration, four subjects required 10.1% and three subjects required 21.4%. The mean oxygen tension necessary to prevent corneal swelling was stated as being 74 mmHg (10.1%). This critical oxygen tension is considerably higher than that calculated by Mandell and Farrell (1980).

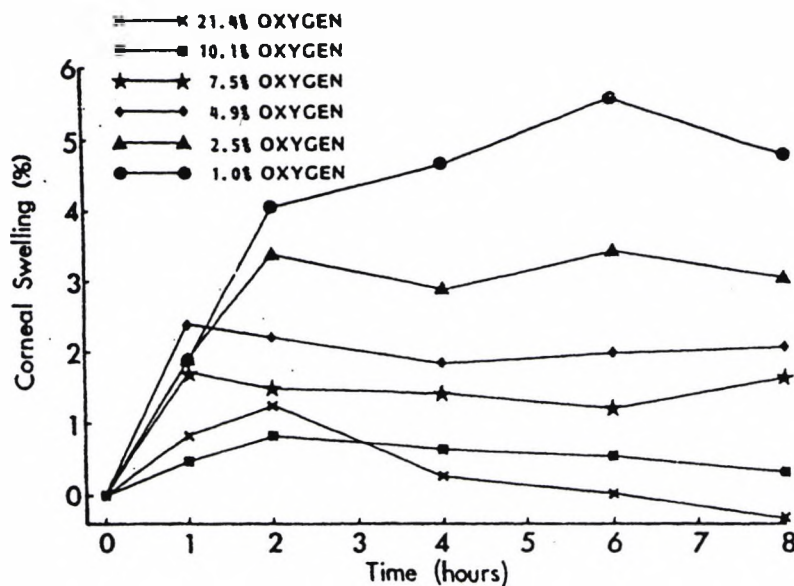


Figure 6.1 - The average corneal swelling for a group of eight subjects exposed for different time intervals to various oxygen concentrations within a gas goggle (Holden et al 1984).

The high variability in the oedematous response is in line with previous findings, namely, that corneal oxygen distribution is widely distributed between individuals (Larke et al 1981; Quinn and Schoessler 1984).

6.3 Corneal oedema

Although corneal oedema may ultimately result in an overall increase in CT, the precise cause of the oedema may determine the effect on individual structures of the cornea. There are three known causes of corneal oedema, namely anoxia, hypoxia and osmotic imbalance.

6.3.1 Effect of anoxia on corneal integrity

One of the first comprehensive studies into the effect of anoxia on the cornea was reported by O' Leary et al (1981). The authors used nitrogen to replicate anoxic conditions in six subjects (four males aged between 20 - 40 years and two females, each aged 24 years) and measurements were taken using a micropachometer developed by Wilson et al (1980). Following six hours of oxygen deprivation, the epithelial thickness was relatively unchanged. The authors proposed that the corneal epithelium is able to maintain a homeostatic 'steady state' in anoxia. However, once oxygen supply was restored, the

epithelium shrank by up to 20%, before returning to normal thickness. It was suggested that the shrinkage was due to the removal of electrolyte from the epithelial cell at a faster rate than it could leak back during the first hour or so of recovery. Thus, inter-epithelial fluid is removed faster than the rate at which cells return to normal size and shape. Although no fluorescein staining of the epithelium was visible during the experiments, two of the four subjects who were subjected to two hours of anoxia, and all three subjects who were subjected to six hours of anoxia reported faint halos. The authors concluded that homeostasis is maintained in the corneal epithelium for up to 6 hours of anoxia but that the intercellular spaces within the epithelium become altered. This results in little change in CT, but a significant change in visual performance, as measured using halometry.

In addition to epithelial changes due to anoxia, both O' Leary et al (1981) and Lambert and Klyce (1981) reported an associated stromal thickening. As the stromal oedema appeared to be greater posteriorly, it was suggested that the thickening was the result of altered endothelial function, rather than a leakage of fluid into the stroma from the epithelium (Goldmann and Kuwabara 1968; Bergmansson and Chu 1981).

6.3.2 Effect of hypoxia on corneal integrity

Hypoxia causes stromal thickening, but in so doing it may leave epithelial thickness unaltered (Lambert and Klyce 1981; O' Leary et al 1981). Lambert and Klyce (1981) studied the mechanisms underlying stromal oedema subsequent to epithelial hypoxia, using rabbit corneas. The results support the theory that stromal lactate accumulation, and the consequent osmotic imbalance, are the major initial factors in corneal oedema caused by hypoxia. With regard to clinical epithelial oedema, significant changes in light scatter were produced by hypoxia, and were shown to be capable of causing the subjective appearance of halos around a point source of light (Sattler's veil phenomena - section 9.3.1). These changes occur without significant change in epithelial thickness. As such, measurements of CT may not reflect epithelial changes in response to hypoxia. Thus, CT measurements may remain normal, despite significant light scatter from the epithelium. Increased glare sensitivity that occurs following hypoxically-induced corneal oedema is due to the formation of light scattering sites within the epithelium (Lambert and Klyce 1981). There is little increase in stromal scattering of light with hypoxia until a substantial increase in stromal thickness occurs.

6.3.3 Effect of osmotic imbalance on corneal integrity

Normal corneal transparency depends on the osmotic pressure of the tears. Cogan and Kinsey (1972) theorised that the pre-corneal tear film and aqueous humour are normally hypertonic with respect to the cornea, resulting in a continuous flow of water across the semi-permeable epithelium and endothelium. Oedema will result from a change in this osmotic gradient. Osmotically-induced corneal oedema shows a characteristic biomicroscopic appearance, distinguished by greater epithelial light scattering than that present in oedema resulting from hypoxia.

Feuk and McQueen (1971) investigated the angular dependence of light scattered from normal rabbit corneas. Saline solution was used to replicate oedematous situations. Light scattered from the cornea was collected by a fibre optics light guide. The authors concluded that the corneal stroma is responsible for the vast majority of backward light scattering from the cornea during oedema, whilst epithelial changes tended to produce increased forward scatter (Feuk and McQueen 1971). It is the forward scatter of light from the cornea which is considered to be more visually debilitating (Zucker 1966; Lancon and Miller 1973). Stromal oedema was seen to be responsible for small angle scattering, whilst epithelial oedema caused larger angle scattering (Feuk and McQueen 1971). These findings were subsequently demonstrated in humans (Wilson et al 1981).

6.4 Histopathological changes in response to corneal oedema

Corneal swelling is usually associated with loss of transparency in the area affected by oedema (Goldman and Kuwabara 1968). This is because the structural elements that constitute the cornea become separated from each other during swelling. This pattern of oedema has been described in human corneal pathology by Goldman and Kuwabara (1968), who characterised the oedematous cornea by an increase in the anteroposterior dimension.

Oedema can affect the structures of the cornea in different ways, however, the resulting structural changes contribute to an increase in intraocular light scatter in the eye. In order to understand the changes that result in a decline in visual performance, it is first necessary to consider the response of the individual corneal structures to oedema.

6.4.1 Oedema of the epithelium

Fluid fills the intercellular spaces of the basal epithelium in the oedematous epithelium, forming an intricate three dimensional meshwork around the cells. The RI surrounding the cells is different to the RI of the cells themselves and if the fluctuation in RI has sufficient spatial regularity, it will serve as a diffraction grating. This produces a diffraction pattern or halo (Finkelstein 1952; Miller and Benedek 1978).

Finkelstein (1952) was one of the first researchers to calculate the angular radius of halos produced by epithelial cells after inducing epithelial oedema with scleral contact lenses. Epithelial cell diameter was measured as approximately $10\ \mu\text{m}$ with the diffraction maxima corresponding to 3.19° . Subsequently, Miller and Benedek (1978) confirmed these findings. Hence, epithelial changes in response to oedema may be more usefully evaluated by measures of visual performance, in particular scatter testing. Since Finkelstein's (1952) early study, halos caused by corneal epithelial changes have been accepted as a useful means of evaluating corneal epithelial oedema (Remole 1981; Stevenson et al 1983).

Remole (1981) measured forward scatter of the *in vivo* cornea, following immersion in hypotonic saline solutions. Measurements were taken during an immersion period of one hour, and following a recovery period of 30 minutes. Scattering was found to increase as the solution became more hypotonic (Polse et al 1990). Stevenson et al (1983) bathed the *in vivo* cornea in hypotonic saline solutions using similar methodology to Remole (1981). Increases in light scatter were recorded by the presence/brightness of halos and pachometry was performed. Maximum halo brightness was recorded following a 9% increase in CT but no significant decrease in CT was detected as the halo diminished. The authors concluded that halos resulting from oedema were epithelial in origin since pachometry principally monitors changes in stromal thickness (Lambert and Klyce 1981; Lovasik and Remole 1983).

6.4.2 Oedema of the stroma

Although extensively studied, the histopathological basis of stromal oedema has been the subject of much controversy. Maurice (1957) expanded upon the lattice theory (section 2.2.6), suggesting that under hypoxic conditions, collagen fibrils separate. This results in decreased transparency, and increased light scattering (Maurice 1957). Hart and Farrell

(1969) reported that the ordering of collagen fibres was short ranged, that is, the regularity of spacing did not extend over many wavelengths in any given region. When the cornea becomes even more inhomogeneous, wavelength dependence of stromal light scatter changes from γ^3 to γ^4 (Maurice 1957).

Twersky (1975) suggested that correlated pairs of randomly distributed small scatterers were the cause of increased light scatter resulting from hypoxia. The loss of transparency that occurs during oedema was thought to be due to increased spacing between particles. This decreases the destructive interference effect which normally results in little light scatter (Twersky 1975). A subsequent study by Malik et al (1992) found little change in fibril diameter of swollen stromas. Farrell and McCally (1975) postulated that two histological factors may influence oedema. Firstly, the distribution in ordering of the fibrils, and secondly the increasing difference in RI between fibrils and the surrounding medium. It was concluded that the disorientation of collagen fibrils in the corneal stroma had the more significant effect on light scatter during oedema (section 2.2.6).

The sequence of events that results in stromal oedema is a matter for some speculation. In the initial stage of oedema there is an increase in the interfibrillar distance. As oedema continues, small interruptions appear as 'lakes' between the lamellae, and around the keratocytes (Goldman and Kuwabara 1968; Kanai and Kaufman 1973). The changes that occur between the lamellae and the increase in lamellae thickness may have a significant effect on measurements of light scatter.

6.4.3 The endothelial response to oedema

The endothelium is the site of the physiological pump for maintaining corneal hydration, and is therefore of particular relevance to the discussion of the oedematous cornea (Hodson and Miller 1976). Numerous studies have shown that during contact lens wear the endothelium responds with the formation of 'blebs' (Zantos and Holden 1977, 1978). In this context, bleb is a term used to describe the apparent increase in separation of endothelial cells and the development of areas of loss of membrane reflectivity. Chapter 9, section 3.3 provides a comprehensive review of blebs as a consequence of contact lens wear. The mechanism of bleb formation is not clear, and endothelial irregularities are also evident following removal of an eye patch (Khodadoust and Hirst 1984). The irregularities

were scattered and unicellular, or in some instances coalesced as patches involving several endothelial cells. The resulting irregular distribution of the endothelial cells may result in scattering centres within the cornea.

6.5 Summary of the effects of oedema on the cornea

Corneal oedema is caused by a reduction in oxygen levels in the ocular tissues as a result of anoxia, hypoxia, or osmotic changes. Although oedema may affect any corneal structure, it mainly manifests in two sites, namely the epithelium and the stroma. Epithelial oedema, (characterised by large increases in forward scattering of light (Feuk and McQueen 1971)), is usually considered to be more visually debilitating than stromal oedema (Zucker 1966; Lancon and Miller 1973). The appearance of halos and the increased glare sensitivity that occur following hypoxically-induced corneal oedema result from the formation of light-scattering sites within the epithelium (Lambert and Klyce 1981). There is little increase in stromal scattering of light until a substantial increase in stromal thickness occurs.

6.6 The effect of oedema on measurements of visual function

Due to the number of histological changes that occur as a result of corneal oedema, it is not unreasonable to predict that these changes will have a detrimental effect on measures of visual function. Although visual disability from corneal oedema is a well-recognised clinical finding, it is not easily confirmed by measures of visual function.

6.6.1 Visual acuity

It is possible to retain normal VA in the presence of relatively marked corneal swelling (Elliott et al 1991). A study by Zucker (1966), (using calf corneal buttons), reported only a 23% reduction in acuity resulting from a 70% increase in the thickness of the corneal stroma. Supporting this, Lancon and Miller (1973) and Carney and Jacobs (1984) found that VA may remain unchanged despite an increase in stromal thickness of as much as 19%. Lancon and Miller (1973), using corneal buttons at various turbidity levels, concluded that glare sensitivity tests follow corneal changes more accurately than measures of VA, as VA only became reduced in the presence of extreme increases in oedema levels. The latter study also compared the effects of stromal and epithelial oedema (the epithelium was removed from the corneal buttons). For corneal buttons without epithelium, VA

dropped below 6/6 when CT increased to 30% above the base value, whilst glare sensitivity increased when CT increased to 10% above the baseline value. For oedematous corneas with epithelium, VA dropped below 6/6 when total CT increased by 10%, whilst glare sensitivity changed significantly when total thickness increased by 5%. Such studies demonstrate that VA testing is not a particularly sensitive means of detection of the presence of corneal oedema. Thus, a patient with stromal oedema may perform well visually when tested using VA but may be significantly handicapped in instances of high glare e.g. bright sunlight.

6.6.2 Contrast sensitivity

Like VA, CS measurements may be unchanged in the presence of a significant level of oedema. For instance, CS has been shown to be insensitive to 9% of stromal oedema (Carney & Jacobs 1984). Following oedema of anoxic origin, CS reduction was not severe, even in the presence of a glare source, and the loss was more apparent at higher spatial frequencies. With regard to oedema resulting from osmotic imbalance, the CS reduction was more marked than under anoxic conditions and present at all spatial frequencies (Carney & Jacobs 1984). Consequently, under conditions of osmotic imbalance, a more significant visual loss ensued (Hess et al 1972).

Hess and Garner (1977) considered the effect of oedema (regardless of origin) on the CSF to be frequency-dependant. That is, the higher the spatial frequency, the greater the visual loss. The study also compared the effect of oedema with the equivalent defocus, defined as the defocus which produced the same high frequency loss. This defocus (+1.25D) had no measurable effect upon the low spatial frequencies. With small levels of oedema, the scattering effect was considered as equivalent to defocus, however, with greater levels of oedema, the defocus equivalent was not applicable.

6.6.3 Effect of oedema on other measures of visual performance

Numerous studies have investigated the effect of oedema on a variety of different visual and physiological tests. In order to assess whether corneal oedema can be adequately quantified, Cox and Holden (1990) investigated the effect of unilaterally induced oedema in five subjects (aged between 20 and 24 years). The study employed osmotic (0, 0.3, 0.6, 0.9% NaCl solutions) and anoxic (100% nitrogen gas) stimuli. Stromal changes were

evaluated using the Holden-Mayer micropachometer, and epithelial changes using halometry with an incandescent light source. Subjects were asked to report whether halos were detected, and if so, the apparent diameter of the halo. The brightness of the halo was then measured using a threshold technique. Visual changes were recorded using a CS technique (Nicolet Vision Tester, Model 2000). A strong positive relationship was found between the relative halo brightness and the CS loss, with the degree of visual loss being relative to the magnitude of the epithelial changes. The study concluded that vision loss with physiologically-induced levels of oedema is primarily epithelial in origin, with stromal thickness increases up to 10% having little effect on vision. As corneal swelling did not show a significant relationship with visual loss, it was suggested that light scatter originating from the corneal epithelium was responsible for the loss of vision found with physiological levels of corneal oedema.

Elliott et al (1993a) investigated hydrophilic contact lens-induced oedema in 19 subjects (mean age 25.9 years). The effect of oedema on visual function was assessed by the van den Berg Straylight meter, Bailey-Lovie LogMar VA, slit lamp biomicroscopy (noting the presence or absence of vertical striae), a modified optical pachometer, and two glare tests, the BAT used with (i) 10% contrast VA and (ii) Pelli-Robson CS. Following baseline measurements (all subjects were awake for at least three hours), the subjects wore a thick hydrogel lens on one eye, which was patched tightly for three hours. Following removal of the patch and contact lens, the battery of tests were rotated for a period of two hours. Pachometry revealed a mean swelling of $10.95 \pm 1.79\%$, with a range of 8.0 to 14.60%. Most subjects returned to within about 2% of baseline CT values within the two hour monitoring session. Glare test results (BAT used with (i) 10% VA and (ii) Pelli-Robson CS) returned to their baseline values approximately 35 minutes after contact lens removal in 16 subjects. At this time, corneal swelling was still approximately 8%. This result is similar to the findings of Carney and Jacobs (1984) who studied the sensitivity of glare tests to hypoxia-induced oedema. The average time taken to return to baseline for LogMar VA and the two glare tests was consistently two to three times shorter than the straylight meter score. The average time for the straylight meter scores to return to baseline was 86 minutes, whereas the average time for the epithelial vertical striae to disappear was 97 minutes. When the results of the straylight meter were investigated, there was little correlation between CT change and straylight. It was concluded that the straylight meter

does not detect increased forward light scatter which results from stromal swelling. This is consistent with the findings of Lambert and Klyce (1981), Carney and Jacobs (1984), and Cox and Holden (1990). Therefore, the authors investigated the relationship between the presence of epithelial vertical striae and measurements of forward light scatter. However, little correlation was found between measurements of forward light scatter and the number of striae (Elliott et al 1993a). As the striae were visible due to reflections from the troughs and folds in Descemet's membrane, it was suggested that they do not cause forward light scatter. Therefore, the study concluded that the straylight scores primarily reflected oedema-induced changes in the epithelium caused by the contact lens (Zucker 1966; Carney and Jacobs 1984; Carney 1990; Cox and Holden 1990), as epithelial changes tend to produce more forward light scatter than backscattered light (Feuk and McQueen 1971).

In summary, a variety of methods may be employed to evaluate the effect of corneal oedema on visual function. Unfortunately, commonly used methods lack reproducibility and reliability, and are relatively insensitive to the onset of oedema. The measurement of forward light scatter may be a more accurate indicator of corneal oedema than the more commonly used methods.

- In order to evaluate the effect of corneal oedema on light scatter it is also necessary to provide a reliable indication of corneal hydration. Therefore, pachometry was employed in the present study as a means of determining corneal hydration.

Essentially, pachometry allows the *in vivo* measurement of CT, and thus gives an indication of the metabolic status of the cornea (Hedbys and Mishima 1966). Although a variety of techniques exist for the measurement of the CT (e.g. specular microscopy, ultrasonography, photographic techniques), optical pachometry has proven to be the most popular method over the last two decades.

6.7 Optical pachometry

The word pachometry (or pachymetry) is derived from the Greek word '*pachys*', meaning 'thickness' or 'clotted'. In recent years, *in vivo* measurements of human CT have been increasingly employed to determine corneal hydration for clinical purposes.

The first CT measurement was performed by the French surgeon Petit in 1723. A CT of 400 μm in enucleated cadaver eyes was reported. Since Blix (1880) first performed an optical measurement of the human (in vivo) central CT (CCT), numerous investigators have published the results of the measurement of the human cornea. A summary of the methodology and results of previous researchers is presented in table 6.1. The mean CCT is approximately 530 μm , and the frequency distribution is shown to be similar to a normal Gaussian distribution (Kruse Hansen 1971).

There are several possible explanations for the significant variation in results observed between researchers with regard to CT. Although corneal measurements have been made with the slit lamp and the split corneal image for more than 30 years, no standardisation of equipment has taken place and a variety of procedures are used to obtain the measurements. Variables affecting CT measurement have included different techniques for horizontal and vertical alignment, patient fixation, anatomical pachometrical measurement position, angle of the light source during measurement, focus of the corneal structures and the method of the final measurement (Molinari and Bonds 1983). Additional variables may be introduced if the timing of measurements is not kept constant, due to diurnal variations in CT (section 6.9.5). Despite this, most studies do not state the time of day that measurements were taken. Furthermore, variations exist between observers, even using the same equipment and alignment technique, making comparison problematic (Edmund 1985).

6.7.1 Alignment techniques

In addition to the inherent variability resulting from the use of different pachometrical instruments used to measure CT, investigators have also used different techniques to visualise the depth of the cornea. The investigator may just touch the endothelial surface to the epithelial surface whilst viewing the split image. This is termed the 'end to end alignment', or the 'touch method'. Alternatively the 'slit width independent', or 'overlapping' method may be employed, in which the endothelial and epithelial surfaces are overlapped.

Table 6.1 - Review of the literature pertaining to corneal thickness measurements

KEY TO TABLE

Wherever possible methods were defined as the following:

FB - (Blix 1880). This apparatus consists of two microscopes with identical horizontally positioned microtubes which converge at an angle of 40 degrees in front of the tubes. An illuminated diaphragm was contained within one tube and its image is situated at the point of intersection of the two microscope axes. By moving the tubes simultaneously and symmetrically along the line bisecting the angle, the image of the epithelium can be seen. Adjustment of the apparatus is required to view the endothelial reflex. The distance moved located the apparent distance between the two surfaces. When the anterior corneal radius and corneal index are known, the actual thickness is calculated.

GULL - (Gullstrand 1924). This apparatus consists of one microscope and two vertical slit light sources. The perpendicular common to the corneal surfaces is determined. Then the lamps are placed 25 degrees on one side of this perpendicular and the telescope 25 degrees to the other side. Thus, the lights are reflected by the posterior surface of the cornea. A weak light source is reflected on the anterior surface of the cornea and moved until it is aligned with the posterior vertical slit images. The angle between the weak light source and the common perpendicular is measured and from this value the CT is calculated.

VB - (von Bahr 1950). This method involves the rotation of parallel plates simultaneously. One plate is in front of the slit lamp beam and the other in front of the microscope. This is a modification of Blix's principle using two rotating glass plates, coupled by gearing, which are mounted in front of a condensing lens and microscope of a slit lamp, so that the aperture of each is half covered by one of these plates. On rotation, the reflection of the slit in the corneal endothelium may be displaced in the field of view of the microscope and brought into coincidence with that in the epithelium. By noting the angle of rotation, the thickness of the cornea is obtained from a curve derived by calculation and a light source.

MG - (Maurice and Giardini 1951). This is a modification of the von Bahr method using only one plate with parallel sides in the path of the slit beam. The plate has a cut out in the centre which has a coloured celluloid plate mounted in it. The investigator sees a slit section with a clear part and a coloured part. As the plate is rotated the coloured part is stationary while the clear part moves. The epithelial and endothelial reflexes are coded and using a perspex plate in front of the slit lamp beam, the alignment of the two reflexes is accomplished. The angular rotation of the plate is scaled to indicate the CT. The arms of the microscope are at 50 degrees between the beam and the microscope.

JAEG - (Jaeger 1952). This refers to an instrument attached to the Haag Streit 900 slit lamp and consists of a head unit with a rotating parallel plate. As the plate is rotated the top half of the split corneal section moves to the left of the investigator's view and the bottom half is stationary. CT is read directly from the dial. The optical arrangement positions the illumination beam normal to the corneal surface and the observation at 40 degrees to this beam. The Haag Streit pachometer is designed such that CT may be read directly from a scale on the pachometer. This is the design Haag Streit AG has adopted for their standard pachometer.

DON - (Donaldson 1966). This design has the ocular of a slit lamp replaced by a split lens for use with the Haag Streit 360 slit lamp. The ocular replaces the ordinary slit lamp ocular and the device creates a horizontal prismatic effect when one-half of one convex lens is moved over the other half in the opposite direction. A micrometer screw moves the two halves in opposite directions resulting in a split optical section of the cornea. CT is a linear function of the lens movement. Two lights are attached to the front of the slitlamp objective and positioned to reflect off the anterior corneal surface to enable the observer to obtain alignment. Donaldson placed the microscope at an angle of 45 degrees with respect to the light source. Patients are asked to fixate the two lights described so as to assure normal alignment to the corneal apex.

MH - (Mishima and Hedbys 1968). The optical arrangement of the pachometer was similar to the von Bahr and Jaeger apparatus but alignment of the slit corneal images in the viewing eyepiece is achieved with the use of the new Haag Streit slitlamp and standard pachometer. The two plates are aligned one on top of another. Like the Jaeger apparatus, the lower plate was fixed while the upper was free to rotate about a central point common to both plates. The plates are placed directly in front of the microscope objective. The metal diaphragm was extended and two small 'pin lights' 10 mm apart were placed on a vertical line equidistant from the plates of the pachometer. The angle between the light source and the microscope is set at 35 degrees. A split image eyepiece was introduced to facilitate alignment of the displaced images of the epithelium in the upper half of the optical section, and of the endothelium, in the lower half. As the patient fixates a horizontal target, alignment is obtained in the viewing eyepiece. The CT is calculated from the angle of rotation of the upper glass plate, using the thickness and RI of the cornea.

MP - (Mandell and Polse 1969). This was an adaptation of Donaldson's and Mishima and Hedbys' system. They placed two fixation lights above and below the objective lens and a third light (the patient's fixation light), exactly in the centre of the two vertically aligned lights. These investigators used a potentiometer with an electronic recording system to convert the mechanical position of the glass plate into an electrical signal proportional to the CT.

Table 6.1 - Review of the literature pertaining to corneal thickness measurements

ULTRA - (Kremer et al 1985). Ultrasound pachometers rely on the detection of pulse echo levels to determine the corneal thickness. A transducer probe emits high frequency sound wave pulses. Upon lightly touching the corneal surface with the probe tip, a sound wave pulses through the corneal tissue. These waves are reflected at interfaces, such as at the anterior and posterior surface of the cornea. A sensor receives the echo pulses and measures the time between the two pulse signals. The CT can then be calculated from the product of the time delay between echoes, and the velocity of sound in the human cornea.

VP - (McLaren and Bourne 1999). The slit beam of a photographic slit lamp is monitored with a video camera through one half of the biomicroscope. When the slit is properly aligned with the cornea, the operator triggers a flash, and one video frame that included the flash is captured. A custom software package detects epithelial and endothelial edges. CT is calculated from the median corneal image width and image widths from similar measurements of contact lenses of known thicknesses.

M - Male, F - Female, R - Right eye, L - Left eye, ? - information was not available.

Researcher	Year	Method	No. of subjects	No. of eyes	Eye used	Age (yrs)	Gender	Race	Time of measurement	Mean CCT (mm)
Blix	1880	FB	8	10	?	?	?	? (German study)	?	0.541 (Range 0.482-0.668)
Gullstrand	1924	GULL	?	2	?	?	?	?	?	0.485 (Range 0.460-0.510)
Juillerat and Koby	1928	FB Microscope axis placed parallel to the optical system. The slitlamp beam was placed at an angle of 45 degrees	20	?	?	?	?	? (French study)	?	0.583 (Range 0.466-0.703)
Fincham	1930	GULL	12	?	?	?	?	? (French study)	?	0.531 (Range 0.480-0.590)
Sobanski	1934	GULL	20	?	?	?	?	? (German study)	?	0.531 (Range 0.400-0.670)
von Bahr	1948-1956	VB	?	224	R & L	?	?	Caucasian	?	0.565 ± 0.035 (Range 0.460-0.670)

Table 6.1 - Review of the literature pertaining to corneal thickness measurements

Researcher	Year	Method	No. of subjects	No. of eyes	Eye used	Age (yrs)	Gender	Race	Time of measurement	Mean CCT (mm)
Maurice and Giardini	1951	MG The overlap method was employed.	44	?	R & L	M-20-35 F-18-30	24 M 20 F	?	?	0.507 ± 0.028
Cook and Langham	1953	MG	10	?	?	?	?	?	?	0.536 ± 0.04
Lavergne and Kelecom	1962	Goldmann pachometer	198	?	?	?	?	Caucasian (Dutch study)	?	0.510 ± 0.04
Donaldson	1966	DON Touch method. Used glass in the calibration procedure. Five readings	268	?	?	?	?	?	?	0.522 ± 0.041
Forsius et al	1967	Goldmann's (Haag Streit) device (Methodology not stated)	686	?	?	School age	?	343 Skolts 151 Skelts 97 Half-breed Skolts 95 Lapps	?	No actual values are given-Skolts corneas $0.07\text{mm} <$ than Lapps and Finns. Half-breed Skolts are in between these two groups.
Martola and Baum	1968	DON 5 readings	121	209	?	5-89	?	Caucasian	?	0.523 ± 0.039
Mishima and Hedbys	1968	MH	49	?	?	?	?	?	?	0.518 ± 0.02
Peterson	1968	JAEG	27	?	R	?	?	?	?	0.571 ± 0.029
Lowe	1969	MH (Modified) 3 Readings	80	157	?	?	?	? (Australian study)	?	0.517 ± 0.034

Table 6.1 - Review of the literature pertaining to corneal thickness measurements

Researcher	Year	Method	No. of subjects	No. of eyes	Eye used	Age (yrs)	Gender	Race	Time of measurement	Mean CCT (mm)
Mandell and Polse	1969	MP First to calibrate with PMMA CLs. Touch method	16	?	?	?	?	? (USA study)	?	0.506 ± 0.040 (range 0.43-0.56)
Kruse Hansen	1971	VB Used PMMA lenses to calibrate Touch method 5 readings	113	150	R & L	10-89	68 M 45 F	Caucasian	?	R = 0.520 ± 0.018 for 76 eyes L = 0.524 ± 0.020 for 74 eyes
Tomlinson	1972	MH	65	?	R	18-27	30 M 35 F	? (English study)	?	M = 0.556 ± 0.022 F = 0.549 ± 0.044
Stone	1974	Haag Streit and slit lamp with an aperture thickness setting slit width No. 7. Touch method	?	?	?	?	?	?	?	No data on human subjects
Binder et al	1977	MH Electronical pachometer Touch method	16	?	R & L	18-27	3 M 13 F	15 'White' and 1 'Black'	?	MH = 0.544 ± 0.013 Electronic = 0.644 ± 0.013
Ehlers and Kruse Hansen	1976	VB	126	?	R	18-21	?	? (Danish study)	?	0.514 ± 0.027
Ehlers et al	1976	? Haag Streit and pachometer	26	?	R	5-14	?	? (Danish study)	?	0.520 ± 0.007
Alsirk	1978	? Optical pachometry using attachment No. 1 of Haag Streit slitlamp 900	117	?	R & L	7-15	?	Greenland Eskimos	?	0.533 ± 0.030
Alsirk	1978	As above	118	?	R & L	16-39	?	Greenland Eskimos	?	0.521 ± 0.028

Table 6.1 - Review of the literature pertaining to corneal thickness measurements

Researcher	Year	Method	No. of subjects	No. of eyes	Eye used	Age (yrs)	Gender	Race	Time of measurement	Mean CCT (mm)
Alsbirk	1978	As above	173	?	R & L	40+	?	As above	?	0.505 ± 0.032
Alsbirk	1978	As above	53	?	R & L	?	?	Danish	?	0.542 ± 0.024
Hirji and Larke	1978	Topographic pachometer similar to the one described by Mandell and Polse	23	?	?	?	19 M 4 F	M - Caucasian F - race not stated	?	M = 0.550 ± 0.04 (Range 0.480-0.610) F = 3 subjects-0.540 1 subject-0.530
Azen et al	1979	a - Haag Streit, b - Mishima Hedby's technique overlap method	8	?	?	?	?	?	?	a = 0.572 b = 0.489
Crook	1979	? Overlap method used with flourescein	52	?	?	?	?	?	?	0.515 ± 0.025 0.519 ± 0.031
Soni and Borish	1979	MP	5	100	?	18-39	?	?	?	R = 0.491 ± 0.035 L = 0.490 ± 0.035
Molinari and Bonds	1983	MH Touch (T) and overlap (O) method 5 readings	6	12	R & L	24-40	2 M 4 F	?	?	RO = 0.491 ± 0.036 RT = 0.525 ± 0.036 LO = 0.498 ± 0.032 LT = 0.529 ± 0.030
Olsen & Ehlers	1984	VB Modification applied to a photographic technique End to end alignment	115	?	R & L	10-90	46 M 69 F	Random sample from Denmark	10:00-14:00	0.515 ± 0.033
Kremer et al	1985	ULTRA (Kremer corneo-ometer)	175	?	?	?	?	?	?	0.512 ± 0.0354

Table 6.1 - Review of the literature pertaining to corneal thickness measurements

Researcher	Year	Method	No. of subjects	No. of eyes	Eye used	Age (yrs)	Gender	Race	Time of measurement	Mean CCT (mm)
Novak et al	1985	ULTRA (Kremer corneo-ometer) Specular microscope MH	68	?	R & L	?	?	?	?	0.554 ± 0.028 0.551 ± 0.037 0.542 ± 0.035
O' Neal & Polse	1985	Haag Streit pachometer connected to an electrical digital unit. The angle between the slit beam and ocular was set at 75 degrees 10 readings	10	10	L	26.7±4.8	9 M 1 F	?	At least three hours after awakening	0.509 ± 0.024
Serup & Serup	1985	Haag Streit pachometer with two pinlights	17	34	R & L	44.3 (11-69)	4 M 13 F	?	?	0.511 ± 0.0094
Edmund and La Cour	1986	Haag Streit pachometer attached to a Haag Streit 900 slit lamp End to end pachometrical alignment procedure	29	?	R & L	Median age 26 (range 22-39)	16 M 13 F	? (Danish study)	10:00-14.00	0.581 ± 0.031
Edmund and La Cour	1986	Optical pachometry	37	?	?	?	?	?	?	0.570 ± 0.040
Edmund	1987	Haag Streit pachometer with a modification as described by Ehlers and Sperling (1977)	40	R & L	?	Median age 31 (range 17-66)	19 M 21 F	?	?	0.570 ± 0.002
Polse et al	1989	Modified slit lamp and Haag Streit pachometer linked to a microcomputer 10 readings Angle at 47.5 degrees	8	?	?	24.4±4.3	?	?	?	0.516 ± 0.034
Polse et al	1989	As above	8	?	?	71.9±7.3	?	?	?	0.538 ± 0.030

Table 6.1 - Review of the literature pertaining to corneal thickness measurements

Researcher	Year	Method	No. of subjects	No. of eyes	Eye used	Age (yrs)	Gender	Race	Time of measurement	Mean CCT (mm)
Giasson & Forthomme	1992	MP (ELECT) 10 readings Flourescein used Touch method	31	62	R & L	10-80	31 M	?	07.00-19:00 Measurements taken at the same time of day.	0.541 ± 0.027
Herse and Yao	1993	MH Optical pachometry using a Haag Streit pachometer mounted on a Topcon SL-5 slit lamp. The pachometer was modified by the addition of alignment lights and a digital readout. Touch method used.	775	1082	L	5-20	515 M	European	10:00-14:00	0.540 ± 0.025
Herse and Yao	1993	As above	76	?	L	5-20	?	Asian	10:00-14:00	0.545 ± 0.024
Herse and Yao	1993	As above	40	?	L	5-20	?	Indian	10:00-14:00	0.544 ± 0.026
Herse and Yao	1993	As above	133	?	L	5-20	?	Polynesian	10:00-14:00	0.542 ± 0.220
Herse and Yao	1993	As above	58	?	L	5-20	?	Maori	10:00-14:00	0.535 ± 0.023
Gromaki and Barr	1994	ULTRA	14 (7 were CL - wearing subjects)	28	R & L	Mean age 28 ± 9.3	8 M 6 F	? U. S. A. study	?	0.560 ± 0.020 (Range 0.500-0.610)
Hitzenburger et al	1994	Partial coherence laser Doppler interferometry	9	18	R & L	?	?	?	Measurements taken at least two hours after awakening	0.531 ± 0.016

Table 6.1 - Review of the literature pertaining to corneal thickness measurements

Researcher	Year	Method	No. of subjects	No. of eyes	Eye used	Age (yrs)	Gender	Race	Time of measurement	Mean CCT (mm)
McLaren and Bourne	1999	VP	25	50	R & L	?	?	?	?	R = 0.512 ± 0.020 L = 0.515 ± 0.021

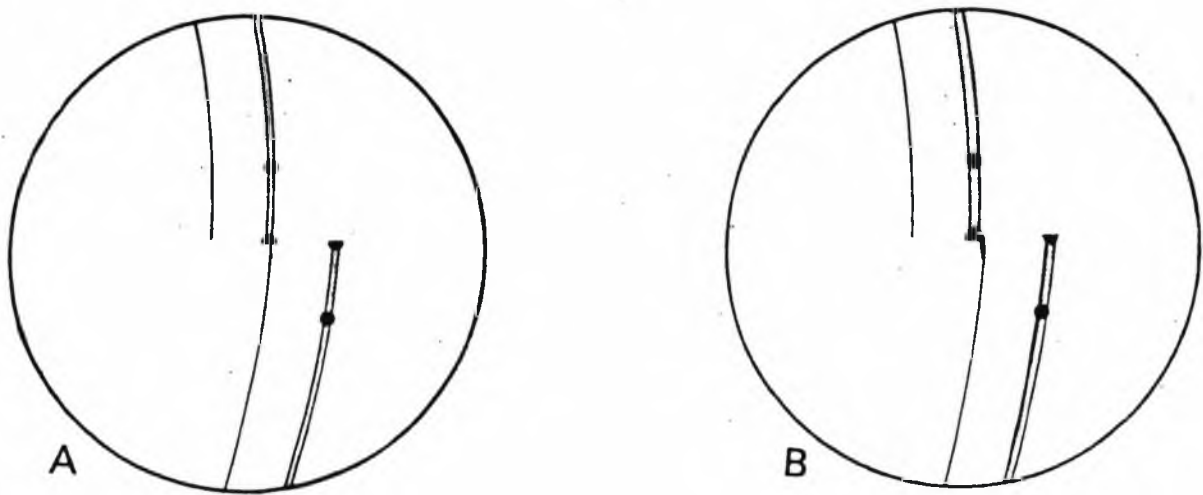


Figure 6.2 - Schematic showing A: overlap (alignment) of CT profile, B: touch (juxtaposition) of CT profile.

The variability between the 'touch' and 'overlap' methods is reported to be statistically significant (Molinari and Bonds 1983), however, most published research into CT fails to declare which technique was employed (table 6.1). Despite the potential for causing an exaggeration of the CT, the 'touch' procedure is thought to be more repeatable than the overlap technique (Olsen et al 1980). For this reason, the 'touch' technique was employed in the present study.

6.7.2 Angle kappa

According to the optical principle of the pachometrical measurement, the incident light should fall perpendicular to the cornea. However, as the patient fixates the incident light, the measurement is made along the line of sight, rather than along the perpendicular to the cornea. A small but systematic difference between right and left eye may be demonstrated, caused by the angle kappa between the optical axis of the eye and the line of sight (von Bahr 1948; Ehlers and Kruse Hansen 1971). Ehlers and Kruse Hansen (1971) reported that CT was significantly greater in the left eye. This was confirmed by Alsbirk (1978a) who reported that CT in the left eye may exceed the right by between 0.019 mm and 0.04 mm. When the thickness difference between the left and right eye was plotted against the sum of

the angle kappa of the two eyes, a linear relationship was found, with a significant correlation ($p = 0.001$, $r = 0.84$).

No correction need be made for angle kappa, however, if measurements are made along a line perpendicular to the cornea, when the observed difference is eliminated. Mishima and Hedbys (1968) introduced a modification to the pachometer in which the perpendicular incidence of light was secured. This method is discussed in table 6.1. Other modifications were made after a manner first suggested by Donaldson (1966) and further modified by Mandell and Polse (1969). These serve to eliminate right and left eye thickness differences. The instrument used in the present project was the modified version of the Haag Streit Pachometer, which ignores right and left eye thickness differences due to the angle kappa as the optical axis of the observation system is perpendicular to the cornea. Obviously, angle kappa may result in a different CT for the right and left eyes, and this provides an additional source of error when comparing results from different researchers. The majority of CT studies do not state whether the difference due to angle kappa has been accounted for (if using equipment other than the modified Haag Streit pachometer) and this may result in incorrect mean CT for a given population.

6.7.3 Accuracy of optical pachometry

The accuracy of CT measurements using optical pachometry may be affected by a number of errors, and the precise causes of these errors remains in dispute. Differences in the RI of the cornea could lead to a change of approximately 3% in the estimate of CT at the extremes of RI encountered physiologically (1.333 to 1.419). A decrease in RI would make the cornea appear thicker, while an increase in RI would make the cornea appear thinner. Nevertheless, Fatt and Harris (1973) and Patel (1987) suggest that a variation in RI has a negligible effect on the measurement of CT. The errors introduced by differences in anterior curvature of the cornea are also reported to be negligible, amounting to less than 0.2% of CT. However, accuracy will also be affected by the thickness of the precorneal tear film as the cornea changes its apparent thickness by 0.001 or 0.002 mm in the period between two blinks (Ehlers et al 1971).

The precision of the Haag Streit pachometer is equal to the adjustment precision, with typical precision values between 0.006 and 0.008 mm (Ehlers & Kruse Hansen 1971; Hirji

& Larke 1978; Olsen 1980) (although Alsbirk (1974) reported that the precision of the mean of three pachometer adjustments was 0.012 mm). The reliability of a single measurement of CT, expressed as a standard deviation (sd), (including the biological day to day variation) was found to be 0.015 mm. This may be improved by repeated measurements (Edmund and la Cour 1986). The study concluded that triplicate readings are rational when employing the Haag Streit pachometer. A sd of 0.005 mm (approximately 1%) corresponds to an accuracy of 0.01 mm at the 95% confidence level, a standard of reproducibility requiring a highly experienced examiner. According to Hirji and Larke (1978), a novice can only expect to achieve a sd of 0.032 mm, improving eventually to 0.005 - 0.006 mm. Maurice and Giardini (1951) quoted an accuracy of 1% to 2% for CT measurement of normal corneas. Donaldson (1966) claimed to measure CT with an accuracy of 2 to 3%, and oedematous corneas to within 8 to 10%. It should be stressed that these studies employed different pachometrical techniques, which will influence the level of accuracy obtained.

6.8 Corneal topography

In order to accurately translate the pachometrical reading into a measure of CT, it is useful to have an understanding of corneal topography.

6.8.1 Corneal apex

Often the optic axis is displaced from the line of sight (Mandell 1965; Mandell and St. Helen 1969). The exact displacement of the corneal apex is the subject of some controversy. Clark (1974) studied fifty pairs of eyes, but drew no specific conclusions about apex position. In contrast, Tomlinson and Swartz (1979) measured a larger number of normal eyes (500 right and 500 left) and concluded that the corneal apex is most frequently situated at, or near, the visual axis. Where the corneal apex is not found to be near the visual axis, it is four times more likely to be temporally rather than nasally displaced. A trend of 0.5 mm temporal displacement was reported in 60% of subjects. No strong vertical bias in apex location has been reported (Midelfart 1987).

6.8.2 Corneal thickness profile

The thickness of the normal human cornea varies significantly across the cornea. The CT is at a minimum over the central 3 mm diameter of the cornea, and increases towards the

periphery where the anterior surface flattens (Maurice and Giardini 1951). A number of studies have attempted to quantify the difference between central and peripheral CT. Martola and Baum (1968), used a Donaldson split ocular pachometer mounted on a Haag Streit 900 slit lamp, and measured at nine o' clock and three o' clock positions, immediately central to the limbal vessel loops in 209 normal eyes. A mean peripheral CT of 0.660 ± 0.076 mm, and a mean CCT of 0.523 ± 0.039 mm, were reported. Mandell and Polse (1969), measured CT in 16 subjects using an electronic optical pachometer, and stated that a difference between the central and peripheral thickness (measured at 35° in the periphery) of less than 0.085 mm could be classified as being normal. The mean difference between central and peripheral CT for normals was reported to be 0.062 mm. Tomlinson (1972) investigated 65 subjects using optical pachometry, and measured along the visual axis and at 25° temporal to this direction. A gender difference in peripheral corneal measurements was observed, with male subjects having a difference of 0.055 mm between central and peripheral thickness, compared to 0.050 mm for female subjects.

Hirji and Larke (1978) studied nineteen male Caucasian subjects using optical pachometry and reported a peripheral thickness of 0.600 ± 0.050 mm and 0.570 ± 0.030 mm at 15° nasal and temporal to the centre, respectively. Superior and inferior thicknesses (at 15° from the centre) were reported as 0.610 ± 0.030 mm and 0.580 ± 0.040 mm, respectively.

Soni and Borish (1979) measured the CT centrally and at 15° temporally and nasally from the central area using an electronic digital pachometer. The mean CCT for 100 eyes was found to be 0.491 mm, with a value of 0.522 mm nasally, and 0.516 mm temporally.

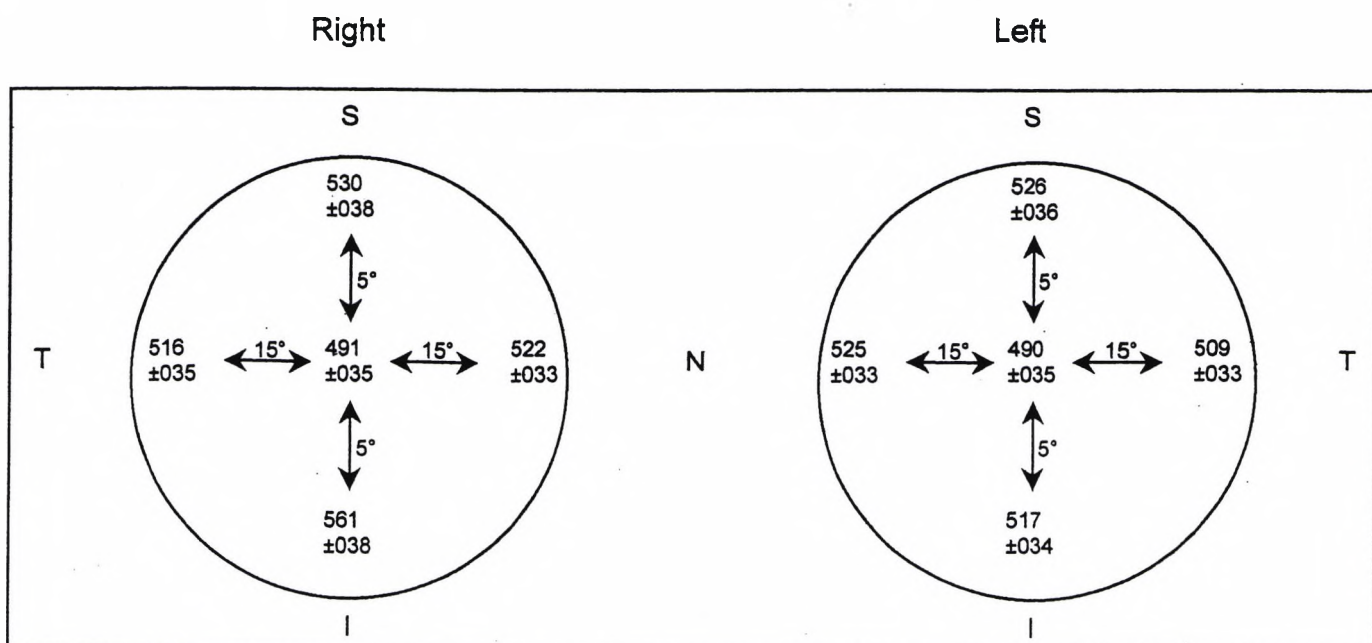


Figure 6.3 - Mean thickness (mm) at five different positions as measured in the right and left corneas of 50 subjects. T = temporal, N = nasal, I = inferior, S = superior (Soni and Borish 1979).

The temporal and inferior values were found to be less than the corresponding nasal and superior thickness values. This was thought to be a consequence of greater and longer lid coverage in the nasal and superior areas. The temporal and nasal CT results reported in the study by Soni and Borish (1979) were lower than those previously reported by Martola and Baum (1968) and Tomlinson (1972). This may have been a consequence of the fact that Soni and Borish (1979) measured CT at 15° in the periphery (nasal and temporal) as opposed to the extreme periphery. In addition, Mertz (1979) challenged the measurement locations reported by Soni and Borish (1979), proposing that angle kappa had not been accounted for. If this was the case, then the measurements reported by Soni and Borish (1979) were in fact taken at 10° nasally and 20° temporally.

In a more recent study, Gromacki and Barr (1994) employed ultrasonic pachometry to study 28 normal eyes. CT was measured at 0.625 mm from the limbus nasally and temporally. The study concluded that the thickness of the cornea was 0.810 ± 0.04 mm (nasally) and 0.830 ± 0.04 mm (temporally).

Hitzenberger et al (1994) was the first to obtain a measurement of the CT profile using an interferometric procedure. This method employs a laser Doppler interferometer scanner for

rapid electronic detection and contrast measurement of interference fringes. Interferometry with partially coherent light has been used to obtain tomographic images of the human retina in vivo (Fercher et al 1993) and has been used to measure the axial length of eyes with cataract (Hitzenberger et al 1993). The first measurements of CT were carried out using a dual beam version of the partial coherence interferometry technique and yielded a precision of $7 \mu\text{m}$. Using a superluminescent diode as the light source increased the precision to $1.5 \mu\text{m}$. The dual beam technique is insensitive to relative motions between eye and instrument and obtains micrometer precision readings of CT (Hitzenberger 1992). Figure 6.4 illustrates the results of the investigation of 18 normal subjects, measured from 20° nasal to 25° temporal.

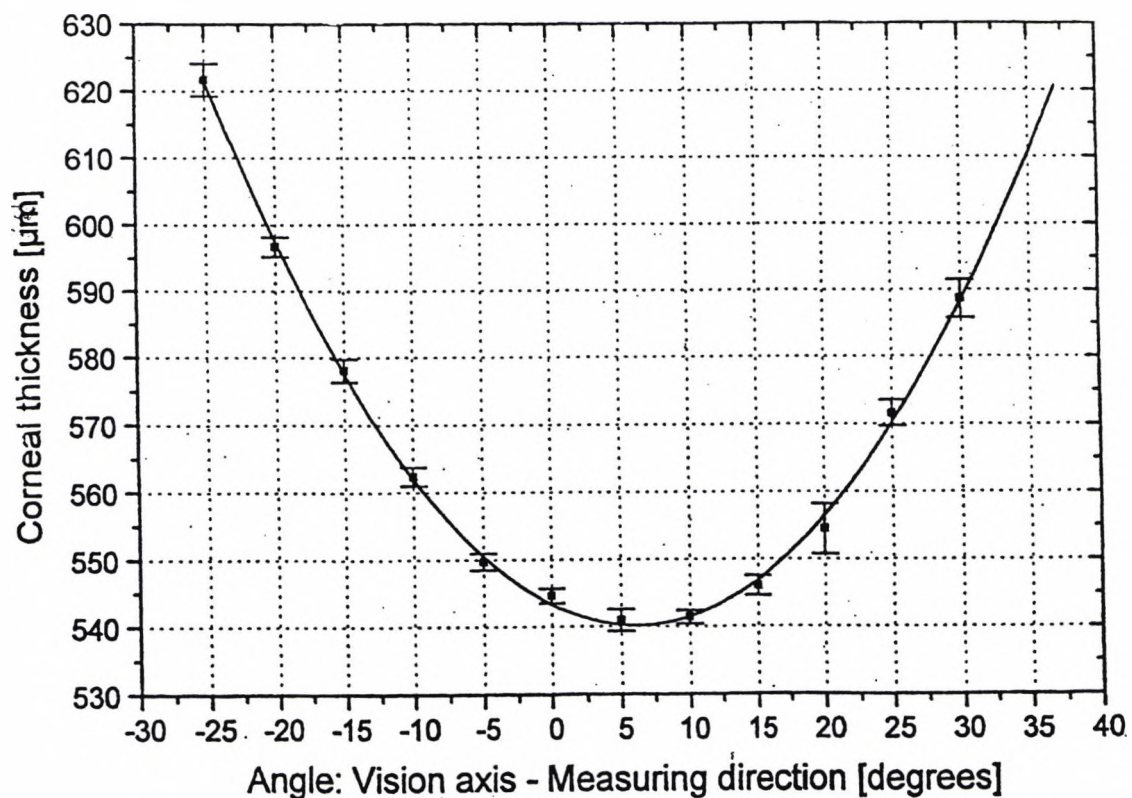


Figure 6.4 - The geometric CT is plotted as a function of the angle between the visual and the axis-measuring direction. The solid line represents the parabolic fit to the measured points (Hitzenberger 1992).

6.9 Factors affecting corneal thickness

CT is independent of axial length (Lowe 1969; Kruse Hansen 1971), corneal radius of curvature (Lowe 1969; Kruse Hansen 1971), corneal astigmatism (Ehlers et al 1976), depth of anterior chamber, lens thickness and vitreous length (Ehlers et al 1975). Controversy

exists as to whether CT is dependant upon factors such as age (Martola and Baum 1968), gender and environment (Alsbirk 1978b). There is also a suggestion of a genetic influence (Alsbirk 1978b). Each of these factors will be considered in turn.

6.9.1 Corneal thickness changes with age

Conflicting data has been published regarding the influence of age on CT (Martola and Baum 1968; Lowe 1969; Kruse Hansen 1971; Alsbirk 1978a; Olsen and Ehlers 1984). An early study by von Bahr (1948) (investigating the CT of 224 Caucasian eyes using optical pachometry), reported a mean CT of 0.571 ± 0.007 mm, for subjects over 65 years, compared with a mean of 0.559 ± 0.005 mm for subjects below 25 years. The apparent increase in CT with age was not reported to be significant. However, Martola and Baum (1968) concluded that the peripheral CT had a tendency to decrease with age in Caucasians over the age of fifty (table 6.2).

Table 6.2 - Peripheral and CCT in different age groups (Martola and Baum 1968).

Age (in years)	No. of eyes	Peripheral thickness (in mm)	Central thickness (in mm)
0-10	7	0.660	0.504
11-20	30	0.688	0.507
21-30	17	0.726	0.532
31-40	17	0.707	0.534
41-50	28	0.669	0.519
51-60	41	0.667	0.540
61-70	24	0.629	0.518
71-80	39	0.618	0.518
81-90	6	0.520	0.528

Although central thickness did not appear to vary significantly with age, the ratio of central thickness to peripheral thickness revealed a thinning in older age groups (Martola and Baum 1968). In contrast to these findings, certain studies in Caucasians have concluded that CT is in fact independent of age (Lavergne and Kelecom 1962; Kruse Hansen 1971). However, age-related corneal thinning has been demonstrated in a study of Finns, Lapps and Skolts (Forsius et al 1971). These findings were supported by Alsbirk (1978a) who reported a thinner cornea with increasing age in Japanese and Eskimos. Indeed, Eskimo men showed a highly significant reduction of CT with age (0.007 mm decrease per year)

(Alsbirk 1978a). Danish subjects also appear to develop corneal thinning with age, however, this was not reported to be significant (Alsbirk 1978a). Later, Olsen and Ehlers (1984), (using a specular method to determine CT), investigated 115 Danish subjects (46 males and 69 females), aged between 10 and 90 years. A significant decrease in CT was reported with age (0.0045 mm per decade).

Polse et al (1989) reported differences in hydration control between eight young subjects and eight older normal subjects using three composite tests which permitted reliable assessment of corneal control. The tests used were the 'Stress-Patch' test (which involved the fitting of a 'stress' lens with patching in order to induce corneal oedema), the 'Stress-Natural' test (no patch used and measurements taken after sleep), and the 'Stress-Direct' open eye steady state (OESS) test (measurements taken in the evening after the subject's eyes had been open for at least 6 hours). It was concluded that recovery from induced corneal swelling is approximately exponential for older and younger individuals, however, older individuals had a substantially slower recovery rate, on average requiring three times longer in order to make a 95% recovery to the OESS thickness level. A greater morning residual swelling was also observed in the older subjects. From these results, it was concluded that corneal hydration control decreased with age.

In summary, most studies report a trend towards corneal thinning with age, however, the extent of thinning is a subject of controversy. The analysis of age-related thinning is complicated by the numerous factors which may also influence CT (e.g. genetic and environmental effects).

6.9.2 Genetic and environmental effects on corneal thickness

Forsius et al (1967) reported a pronounced familial resemblance in CT between offspring and parents, suggesting that genetic pre-determinants influence CT. As previously stated, Alsbirk (1978b) reported a highly significant ethnic influence on CT (Eskimo's CT 0.024 mm thinner than Danes). However, Herse and Yao (1993) (using optical pachometry in 1082 male and female students), concluded that no significant difference existed between cultural groups (European, Polynesian, Asian and Indian) between the ages of 5 - 20 years.

Alsbirk (1978b) reported that subjects from families with an indoor occupation tended to have thicker corneas than those with an outdoor occupation, and a trend towards a correlation between the CT of husband and wife was described. Familial resemblance with respect to CT was found to be high. CCT between first degree relatives showed a resemblance which indicated a high degree of genetic influence. It is likely that genetic effects to some extent determine CT, however, it is difficult to differentiate the genetic effects from socio-economic factors related to age, location, and common familial environment (Alsbirk 1978b).

6.9.3 Effect of gender on corneal thickness

In an early study, von Bahr (1948) reported that no significant gender difference existed with regard to CT. The mean CCT was calculated following the examination of 224 corneas (112 males), and was reported to be 0.565 ± 0.004 mm in males and 0.564 ± 0.003 mm in females. In contrast, a subsequent study by Martola and Baum (1968) reported a gender-related trend with regard to the mean central and peripheral CT, with females having a thinner CT than males.

Table 6.3 - CT measurements in male (M) and female (F) Caucasian subjects (Martola and Baum 1968).

Location of measurement	Gender	No. of eyes	Central thickness (in mm)
Central	M	98	0.530 ± 0.040
Central	F	111	0.517 ± 0.036
Peripheral	M	98	0.668 ± 0.062
Peripheral	F	111	0.654 ± 0.085

Kruse Hansen (1971), Tomlinson (1972) and Olsen and Ehlers (1984) each concluded that there was no significant relationship between CT and gender in Caucasians. This conclusion was later supported by Herse and Yao (1993), who found no significant difference between male and female Caucasian subjects using optical pachometry (0.541 ± 0.026 mm and 0.540 ± 0.025 mm respectively). Interestingly, Alsbirk (1978a) reported an increasingly significant gender difference between male and female Eskimo adults as age increased (0.019 mm difference above the age of 40).

In summary, there is scant evidence to suggest that in general a gender difference with regard to CT exists, however, differences in CT may indeed exist for certain non-Caucasian races.

6.9.4 Correlation of weight and height with corneal thickness

A correlation between CCT and birth weight of new-borns was revealed in studies undertaken by Ehlers and Kruse Hansen (1976) and Ehlers et al (1976). The relationship was not found to be significant. Kruse Hansen (1971) had previously reported a tendency for CT to decrease with increasing height in adults.

6.9.5 Diurnal variations in corneal thickness

The human CT has been shown to vary significantly with time of day (Mandell and Fatt 1965; Hirji and Larke 1978; Fujita 1980; Mertz 1980; Kiely et al 1982) and also from day to day (Kikkawa 1973). Consequently, the repeatability of pachometry is limited by the biological day-to-day and diurnal variation of the CT. Knowledge of this variability is thus an important prerequisite for the establishment of an optimal procedure of CT measurement.

The literature regarding diurnal variations of CT has not always distinguished between complete studies of diurnal variation over a 24 hour period (or longer), and those studies which have concentrated on overnight swelling. In this introduction, these two aspects of physical variation in CT will be treated separately. Table 6.4 shows the findings of previous studies investigating the diurnal variation in CT.

A study by Peterson (1968) reported that the thickness of the human cornea varies rhythmically throughout the waking hours, with a thickening of the central portion of the cornea early in the morning, a thinning in the early afternoon, and a thickening in the late afternoon. Measurements were taken at 09:50, 11:30, 13:30, 15:15 and 16:45, from four subjects. The maximum extent of the corneal thickening was found to be 13%. However, no pre-sleep measurements were taken and a thickness measurement was not taken immediately on waking.

Table 6.4 - Results of previous measurements of diurnal variation

Researcher	Year	Method	No. of subjects	No. of eyes	Eye used	Age (years)	Gender	Race	Diurnal variation	Range of diurnal variation	Time of maximum increase	Timing of measurements	Errors
Peterson	1968	JAEG	4	?	R & L	?	?	?	11.4%	8 - 14%	Thicker a.m., then thinning and again thicker in late p.m.	Measurements taken at 09:50, 11:30, 13:30, 15:15 & 16:45	Measurements not taken after sleep. Small number of subjects
Mertz	1980	ELECT	9	9	?	22 - 54	3 M 6 F	?	4.33%	0.83 - 9.7%	Thickest following sleep at 06:00	Measurements taken pre-sleep, immediately following eye opening, 10, 20, 30, 45, 60, 75, 90, 120 and 300 minutes following eye opening	-
Fujita	1980	ELECT	32	32	?	19 - 23	17 M 15 F	? (Japan study)	No values stated	No values stated	05:00	Subjects were instructed to maintain their normal sleep/wake cycle before and during experimental days.	-
Kiely et al	1982	Optical pachometry	21	21	R & L	mean = 21.2 (18 - 32)	11 M 10 F	? (USA study)	?	?	After sleep	Every 1 hr for 12 hours	-
Gromaki and Barr	1994	ULTRA	14	28	R & L	28±9.3	8 M 6 F	? (USA study)	No variation reported	?	?	08:00 and 17:00 for 2 consecutive days	Measurements only taken twice a day, nine hours apart
Harper et al	1996	ULTRA	8	8	R	10 - 63	4 M 4 F	? (UK study)	7.2%	2.1 - 14.3%	Variable -at different times of the day	Readings were taken during the hour before night time sleep, immediately upon waking and then at 15, 30, 45 minutes and 1.0, 1.5, 2.0, 2.5, 3.0 hours and thereafter every 2 hours up to a period of 24 hours.	-

One of the first comprehensive investigations into a possible diurnal variation in CT was conducted by Kikkawa (1973) using rabbit corneas. Measurements were taken using a Maurice and Giardini pachometer. The corneas were reported to be thickest in the morning hours, followed by continuous thinning. CT often became thinnest in the afternoon, but sometimes this occurred at noon. The decrease in thickness was reversed at night. The amount of diurnal variation was not consistent, but the average change in CT during the day was 0.014 mm. Kikkawa continued this study in 1974 investigating the extent of the diurnal variation under controlled 12 hour cycles of light and darkness in the open and closed eye state. The CT was significantly greater during a 12 hour cycle of light and dark, compared with that under continuous (24 hour) light. The average thinning during the day was 0.022 mm, compared with 0.014 mm under continuous light. Since the adrenal corticoid activity has an important controlling influence on diurnal processes (Bunning 1967), the effect of a corticosteroid on the diurnal variation was also studied. An intravenous injection of a corticosteroid was administered in the morning hours, which augmented the daytime thinning. When administered at midnight, the corticosteroid caused a reversal of the night-time hydration process. Kikkawa (1974) postulated that CT is under a strong influence of the light-dark cycle, and may be associated with changes in the plasma level of endogenous steroids.

Fujita (1980) was the first to study CT over a 24 hour period in humans. Data were collected from 32 Japanese subjects (17 males and 15 females) of different ages. CT measurements were taken using a Haag Streit slit lamp 900 biomicroscope, with an extended diaphragm as described by Mishima and Hedbys (1968). Tonometry was also performed following pachometry using an Alcon pneumatic applanation tonometer in order to investigate the relationship between CT and IOP. The subjects maintained a normal sleep-wake cycle and, for overnight experiments, were permitted to sleep in between testing. The experiments were divided into five parts, with ten measurements taken at each sitting. Experiment 1 involved ten subjects (5 male and 5 female), with measurements taken at one-hourly intervals beginning at 07:00 until 09:00 the next day. Experiment 2 involved five out of the ten subjects (three males and two females) who participated in experiment 1. The procedure was the same for experiment 1, but was repeated on a different day with an interval of one week to two months. Experiment 3 involved three male subjects (who had not been involved in previous experiments) and a similar

procedure was performed on three successive days (i.e. beginning at 05:00 on the first day, through two overnights, and finishing at 17:00 on the third day). Experiment 4 involved twelve subjects (6 male and 6 female) with an age range of 19 to 40 years. CT was measured at one-hourly intervals from 07:00 to 17:00 of the same day. One eye was kept naturally open, whilst the other was intentionally closed with patching. Experiment 5 involved two young subjects (gender not stated) who had a temporal shift of sleep-wake cycle, consisting of several days with an ordinary pattern, followed by subsequent days with a reversed pattern. The CT was measured at hourly intervals on two occasions with a different sleep-wake cycle.

The results of these studies revealed a diurnal variation in CT. The cornea was relatively thick in the early morning, followed by a gradual thinning during the subsequent daytime hours until late afternoon. Thereafter, the cornea became gradually thicker during the onset of the night hours. This pattern of variation appeared to be reproducible. The IOP also showed a rhythmic change during the day, although its timing was different from that of the CT. The IOP was relatively low in the early morning hours, followed by a gradual elevation during the forenoon hours. IOP reached the highest level by the early or mid-afternoon. Thereafter, the pressure became gradually reduced during the night hours, reaching the lowest level at about midnight. CT was found to be greater following patching of the eye, compared to the results for the unpatched eye. Thinning upon eye opening accounted for 1% of the total thickness. After short-term reversal of the sleep-wake cycle (experiment 5), CT maintained its normal pattern of diurnal variation. It should be noted that the diurnal variation in IOP reported in this study is not the accepted view of IOP fluctuations. Many other authors (e.g. Phelps et al 1974; Henkind et al 1973; Kitazawa and Horie 1975; Weitzman et al 1975; Henkind and Walsh 1981) report that there is a peak in IOP upon waking for normal and glaucomatous subjects followed by a decline in pressure until late afternoon.

In conclusion, Fujita (1980) reported that the cornea did not maintain a constant thickness but varied significantly with time of day. The results were in agreement with Kikkawa (1973, 1974), in that the cornea was found to undergo cyclical diurnal variation, during which the cornea was relatively thick in the early morning (maximal CT at around 05:00), followed by gradual thinning during the daytime hours until late afternoon, and, thereafter,

thickening during the night. A non-linear correlation between CT and IOP at a given time was observed, with the latter peaking at noon and reaching a minimum at midnight. It was suggested that the diurnal CT cycle was elliptically correlated with IOP. This rhythm was repeated over two days, indicative of a circadian rhythm over a 24 hour period.

Fujita (1980) used a cosine curve to describe the diurnal variation in CT obtained from 10 young adult subjects within a 24 hour period. The average values of the rhythm parameters were 0.548 mm for the mean CT, 0.0085 mm for the mean amplitude of the rhythm and 04:83 hours for the acrophase of the rhythm (i.e. the time of day that the cornea was thickest). The circadian rhythm of the CT remained unchanged in its phase and amplitude when subjects had reversed sleep-wake cycles for a period of two days.

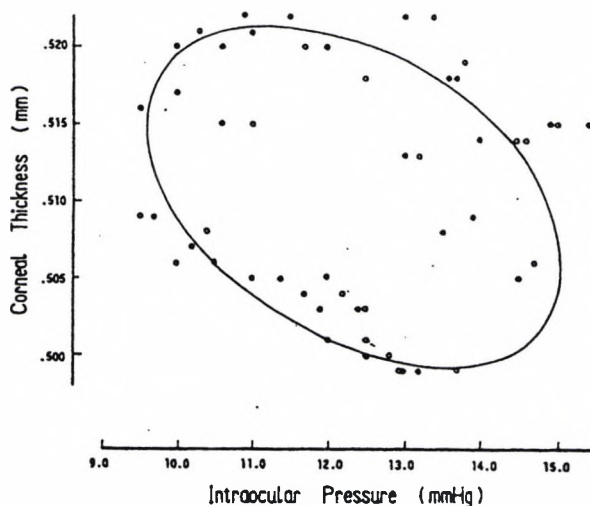


Figure 6.5 - Relation between CT and the IOP in a subject. Data points (open circles; right eye; closed circles; left eye) represent two variables at a given time of the day (Fujita 1980).

Ehlers et al (1975) noted that thick corneas can result in artificially high IOP readings because of the difficulty in applanating the cornea. Later, Bron et al (1997) reported a mean CT of 0.585 ± 0.043 mm for subjects with ocular hypertension, compared with 0.544 ± 0.033 mm for control subjects using the Goldmann tonometer and an ultrasound pachometer. This difference was found to be statistically significant, and the study concluded that corneal pachometry was a valuable tool for the investigation of patients in

whom IOP does not correlate to other clinical findings (such as visual field and optic nerve changes). Hence, CT is a factor of clinical importance in the evaluation of IOP.

In contrast to Fujita, Frampton et al (1987), (using a Non Contact Tonometer (NCT)), reported a rapid increase in IOP following sleep (ranging from a 37 - 248% increase). IOP was recorded over a 24 hour period in thirteen normal subjects (mean age 21 years, range 15 to 41 years). In a second study, IOP decreased when 15 subjects remained upright and awake throughout the night. When sleep was not permitted IOP was lowest at 03:00; when six of these subjects were permitted to sleep from 06:00 to 08:00, they showed a rapid and significant increase in IOP of up to 150%, whereas the remaining nine subjects showed posturally induced increases of up to 38%. Many authors have reported that thick corneas can result in artificially high IOP readings because of the difficulty in applanating the cornea (e.g. Ehlers et al 1975; Bron et al 1997). The relationship between IOP and CT was investigated by using two tightly fitting soft contact lenses to induce corneal oedema (Frampton et al 1987). The oedema produced a 16% increase in CT and was associated with a 2 mmHg increase in measured IOP. This increase was not significant. Variability was high in the hourly fluctuations reported for each subject and there were very large rises in IOP during sleep found in some subjects. Consequently, it was concluded that the rise in IOP noted during sleep was unlikely to be an artefact produced by sleep-induced corneal oedema.

Kiely et al (1982) investigated diurnal variation in CT in 21 subjects (11 males). CCT and measurements at 20 and 40° nasally and temporally were taken at one-hourly intervals for 12 hours (table 6.4). CT (as measured by optical pachometry) was found to be thickest on first awakening. Once this maximal thickness had been reached there was progressive corneal thinning throughout the day. The rate of this thinning was the same in all locations. The subject data revealed a mean decrease in CT of 2% during the day.

Gromacki and Barr (1994), (using ultrasonic pachometry on 14 normal patients - 8 male), measured the CCT at 08:00 and 17:00 for two consecutive days, but found no significant diurnal effect. In contrast, Harper et al (1996) reported individual differences in the extent of diurnal variation, following examination with ultrasound pachometry. Data were collected from 8 subjects (4 male) over a 48 hour period. Measurements were taken in the

subject's home (to limit interference with normal sleep patterns) with readings taken during the hour before night time sleep, immediately upon waking, and then at 0.25, 0.50, 0.75, 1.0, 1.5, 2.0, 2.5, 3.0 hours afterwards. Readings were then taken every two hours up to a period of 24 hours. An increase in CT was observed overnight, which then decreased upon waking. Also, CT varied throughout the day. In fact, for each subject, the degree of daytime variation was greater than the overnight thickening. A maximum mean diurnal increase of 7.2% in CT was reported with a range of 2.1 - 14%. This is in agreement with Gertsman (1972). The timing of the maximal diurnal variation varied between individuals (figure 6.6). The authors concluded that the overnight changes in CT are not truly representative of diurnal variations in human CT i.e. the maximum CT is not necessarily found following sleep, and a much greater diurnal variation occurs than previously reported.

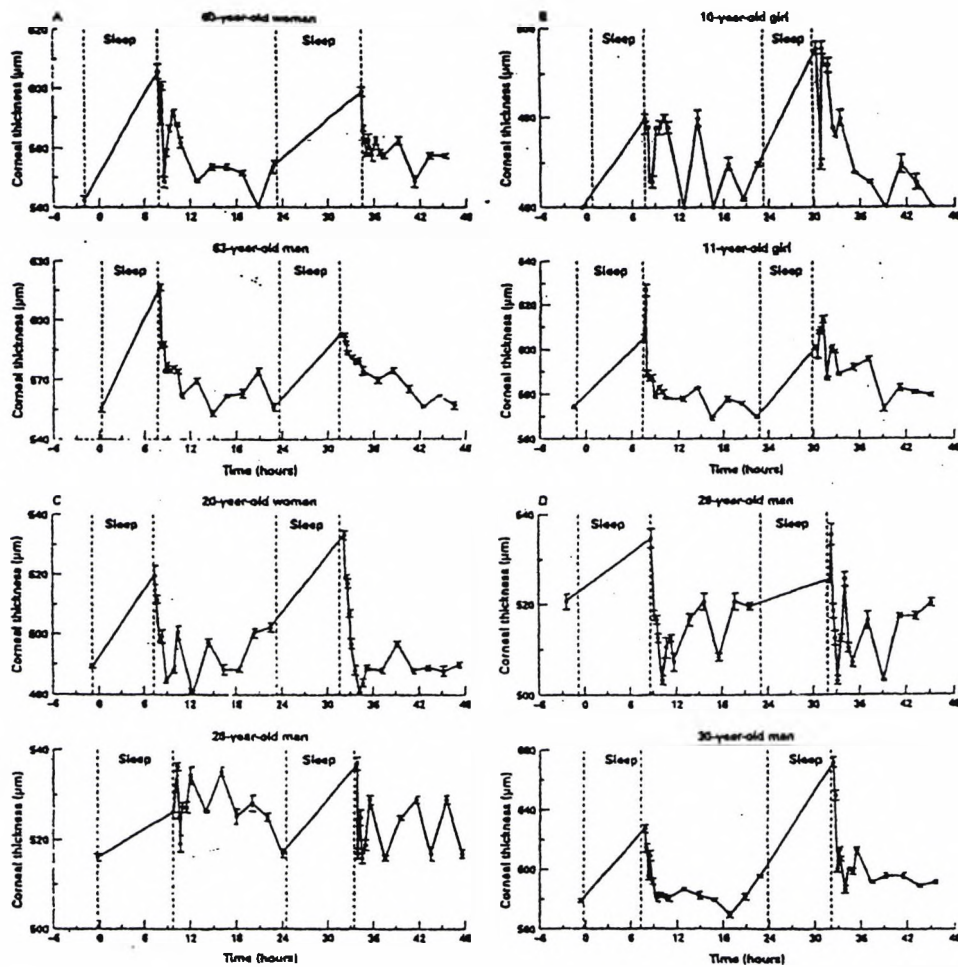


Figure 6.6 - The diurnal variation in CCT of eight subjects ranging from 10 to 63 years of age. Measurements were taken at different time intervals over a 48 hour period. Vertical bars = sd (Harper et al 1996).

6.9.6 Overnight corneal swelling

Numerous studies have shown that the maximum increase in CT occurs after awakening (rather than at other times of the day) (Mandell and Fatt 1965; Gertsman 1972; Hirji and Larke 1978; Mertz 1980; Kiely et al 1982). A review of previous researchers' findings is given in table 6.5.

Mandell and Fatt (1965) (using optical pachometry on one subject) reported that the thickness of the central cornea increased by 3.6% after 6 to 8 hours of sleep, followed by a gradual thinning to reach a steady state within 2 to 4 hours. A similar increase in CT of 4.33%, or 0.026 mm (range of 0.83% to 9.70%) was reported by Mertz (1980), in a study of 9 subjects using optical pachometry. The author concluded that a logarithmic recovery to baseline occurred within the first hour of opening the eye.

Table 6.5 - Results of previous measurements of overnight swelling

Researcher	Year	Method	No. of subjects	No. of eyes	Eye used	Age (yrs)	Gender	Race	Time spent asleep and methodology	% swelling	Range (%)	Errors
Mandell and Fatt	1965	VB Vickers optical beam splitter fitted into one tube of a binocular microscope on a Thorpe type slit lamp. Calibration with five contact lenses of known thickness and refractive index	1	1	?	20	1 F	Caucasian	Taped left eye, immediately on awakening in the a.m. after 6 hours sleep. Experiments began half an hour later. Measurements taken over four days - every 5 mins for first 80 mins and every 15 mins for remaining 80 mins.	Up to 4	?	Only one subject used. Tape fitted after awakening.
Gertsman	1972	DON Vickers image splitting eyepiece. The eyepiece was inserted into the left viewing tube of a Gamb's Photo Slit Lamp.	3	3	L	25 - 59	2 F 1 M	Caucasian	Upon awakening the subjects were brought immediately to the laboratory from their homes. Actual sleep time not stated. Subjects were allowed to pursue their usual daily activities.	7.8	?	No pre-sleep measurements. No measurement immediately on awakening. Flourescein instilled.
Hirji and Larke	1978	Topographic pachometer similar to the one described by Mandell and Polse.	8	8	R	?	8 M	Caucasian	Right eye taped prior to sleep. Measurements taken every 2 hrs for 16 hrs	?	?	Measurements taken every 2 hr for 16 hrs
Mertz	1980	ELECT Electronical digital pachometry	9	?	?	22 - 54	3 M 6 F	?	Subjects woken at 7 hrs of sleep at 06:00. Post sleep measurements were taken at 10, 20, 30, 45, 60, 75, 90, 120 and 300 minutes following initial eye opening.	4.33	0.83 - 9.7	2 subjects were daily wearers of hydrogel lenses. 2 subjects were occasional wearers of hydrogel contact lenses.
Holden et al	1983	ELECT Electronical digital pachometry (15 readings taken)	10	?	?	19.5 ± 0.8	8 M 2 F	?	Measurements taken over 36 hour period at 08:00, 09:00, 10:00, 12:00, 14:00, 16:00 and 20:00 on the first day, and immediately upon waking (usually 07:00) and 1, 5, and 12 hours later on the second day.	3.0 ± 1.2	1.4 - 5.1	-

Table 6.5 - Results of previous measurements of overnight swelling

Researcher	Year	Method	No. of subjects	No. of eyes	Eye used	Age (yrs)	Gender	Race	Time spent asleep and methodology	% swelling	Range (%)	Errors
Harper et al	1996	ULTRA	8	8	R	10 - 63	4 M 4 F	?	Woken naturally. Night sleep only. Normal sleep pattern - measurements taken in the home. Left eye taped to avoid evaporation.	5.5	1.9 - 12.6	-

Gertsman (1972) stated that 7.8% thinning of the human cornea occurs during the waking hours. Measurements were taken between 06:00 and 21:00 every hour, on the hour, for the first three hours and subsequently every two hours. Ten readings were taken from each of the three subjects, and the measurement cycle repeated twice on non-consecutive days. The thickest corneal measurement was reported to be on awakening (after half an hour of lid opening), with a subsequent thinning of 4.75% during the first three hours, and continued thinning during the remainder of the day. It should be noted that the study was flawed in that it did not take pre-sleep measurements and a thickness measurement was not taken immediately on waking.

Harper et al (1996) reported extensive individual day-to-day differences in the extent of overnight swelling in 8 subjects (4 male). An examination of overnight swelling revealed a mean increase of 5.5% (range of 1.9 - 12.6%). Five individuals had overnight increases in CT that were in excess of the 3 - 4% previously reported (Mandell and Fatt 1965; Mertz 1980). In fact, two of the male subjects (30 and 63 years old) showed overnight CT increases of at least 10%. The magnitude of the overnight swelling in the subjects tested differed on consecutive days for each individual (figure 6.6).

6.9.6.1 Causes of observed variations in corneal thickness

It is well known that CT is controlled by a balance between passive movement of water into the stroma under the swelling force and active movement of fluid out of the cornea by metabolic action (Maurice 1969). However, it is yet to be established how the endogenous diurnal rhythm influences these factors. When subjects were kept awake at night in the light and asleep in the daytime, the normally observed CT diurnal rhythm was unaffected (Fujita 1980). It appears that the initial stage of corneal thinning is approximately correlated with the subject's time of awakening, and thus the time of lid opening. Therefore, it is possible that corneal thinning is a result of evaporation from the precorneal tear film (Mishima 1965). However, gradual corneal thinning during the day was also noted in subjects, whether the eye was kept open, or closed between readings. Fujita (1980) suggested that the exact mechanism through which CT varies with time of day is controlled by the circadian clock in the brain. This hypothesis was investigated by measuring the serum corticosteroid level at several times during the day in ten subjects (five males and five females). The daytime thinning of the cornea correlated well with the

daytime decrease in serum corticosteroid, a finding which agrees with previous observations in animal models (Kikkawa 1974; Horie and Kitazawa 1979).

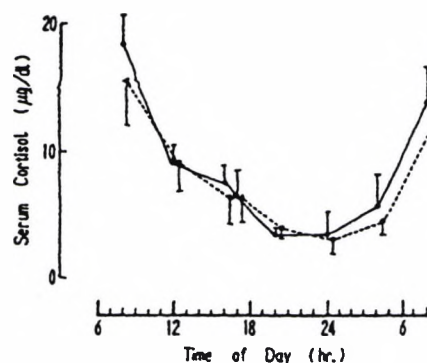


Figure 6.7 - Serum cortisol measured at several times of the day in ten young adult subjects. Open circles: mean of five males; closed circles; mean of five females. The serum cortisol is highest in the early morning, followed by a gradual decrease during the daytime (Fujita 1980).

In summary, there is much dispute as to the precise timing of the diurnal variation in CT. Nonetheless, there is clearly an increase in CT during sleep as a result of lid closure. What is less clear is the cause of subsequent changes that occur throughout the day. Certain authors report a continuous thinning throughout the day (e.g. Gerstman 1972), whilst others report a mid-afternoon increase in CT which may be greater than that associated with overnight swelling (e.g. Harper et al 1996). It is thus important that CT measurements are taken at the same time of day in comparative longitudinal studies, in order to minimise the effects of diurnal variation. That said, significant CT variations may still occur even if measurements are taken at the same time of day (Edmund 1980).

6.9.7 Intra-individual day-to-day variation

The literature gives no exhaustive clarification of intra-individual day-to-day variation of CT, and consequently, the basis for observed intra-individual variation remains obscure. Edmund and la Cour (1986) (using optical pachometry (performed by one observer) in 16 male and 13 female subjects, median age 26 years, range 22 - 39), took measurements of CT between 10:00 and 12:00 on two separate days with a median interval of 12 days (range 1 - 57) and reported significant day-to-day differences in CT. Edmund and la Cour (1986)

(using a statistical variance component model) showed that three components produce variability in CT measurements. These were errors due to the slit lamp and pachometer adjustment, and due to genuine biological variability. Variation attributed to lamp adjustment was estimated as 0.005 mm, whilst that due to adjustment of the pachometer was 0.013 mm. The biological day to day variation was reported to be 0.006 mm (1.1%). As measurements were taken between 10:00 and 12:00, overnight swelling could not explain the intra-individual day-to-day variation.

6.10 Summary

The technique of pachometry has advanced significantly since its introduction by Blix in 1880. At present, ultrasonic and optical pachometry are the two most viable techniques for CT measurements. It is possible to measure CT with 5-6 μm accuracy (using a Haag Streit optical pachometer, with certain instrument modifications). Within a normal population, CCT is found to vary between 0.430 and 0.560 mm (Mandell and Polse 1969). As a result, detection of corneal oedema must rely on changes relative to an individual baseline thickness. Previous workers have noted a significant diurnal variation in CT in the corneas of humans (Mandell and Fatt 1965; Fujita 1980). Overnight corneal swelling in the human cornea varies between 2 and 12.60% (Mandell and Fatt 1965; Gertsman 1972; Mertz 1980; Harper et al 1996). Studies on the recovery from corneal swelling upon eye opening have shown that the cornea de-swells logarithmically and recovers to baseline CT within 1 to 2 hours of eye opening (Mertz 1980). Therefore, the timing of CT measurement is critical, due to the number of factors that influence CT. By delaying pachometry for at least 2 hours after eye opening, the effects of diurnal variation are minimised. That said, more recent studies (e.g. Harper et al 1996) have shown that the maximal diurnal variation may not be found following sleep, rather this may occur at other times during the day.

6.11 Aims

To determine whether measurements of light scatter in the eye using the P_SCAN 100 scatter apparatus are subject to diurnal or longitudinal fluctuations, and to investigate the factors which may result in changes in scattered light, especially changes in CT. The results of these data will inform future studies investigating anterior eye disease and contact lens wear.

6.12 Methods

6.12.1 Pachometrical method

An electronic Haag Streit slit lamp biomicroscope with attachment I, modified in a manner first suggested by Donaldson (1966), was used to measure CT. This is the most commonly used optical pachometry apparatus, as it is one of the most reliable for measuring CT (Ehlers and Kruse Hansen 1971). The principle that forms the basis of the equipment was first described by Juillerat and Koby (1928), and further developed by Jaeger (1952). The apparatus consists of an attachment to the Haag Streit slit lamp, containing two glass plates in front of the right microscope, a lower fixed and an upper rotatable around a vertical axis. The incident light passes through a vertical aperture in a diaphragm extending from the attachment, with an angle of 40° between the incident light beam and the axis of the right microscope. The right ocular of the slit lamp biomicroscope is replaced by a split image ocular (Huygen's eyepiece), dividing the visual field into upper and lower halves. The light passing through the upper rotatable, and the lower fixed, glass plates is seen in the upper and lower visual field, respectively. The optical section through the cornea is seen in the microscope. Rotation of the upper plate displaces the light path and moves the upper half of the image of the cornea in relation to the fixed lower half. The angle of rotation of the glass plate to produce the 'touch' endpoint is a measure of the CT, and is read on a scale directly calibrated in mm. The microscope magnification does not influence the measurement (Jaeger 1952), and a high objective magnification (x 1.6) may be used.

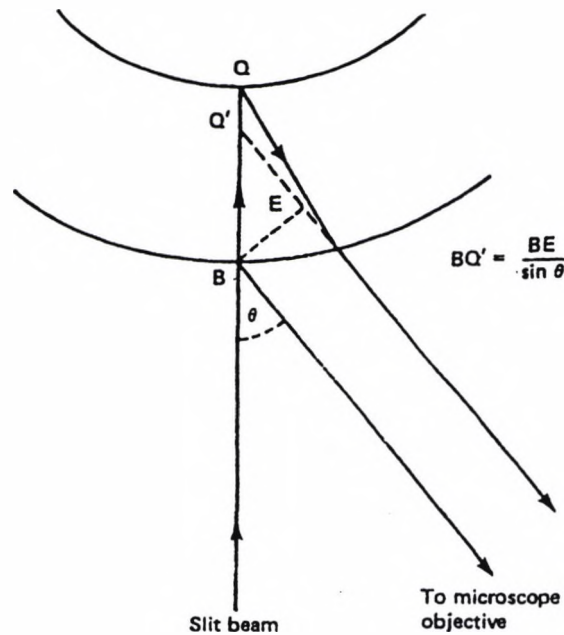


Figure 6.8 - Optical principle of pachometry (Sheridan 1989).

In the present study, the Haag Streit slit lamp 900 and Huygen's eyepiece were used in conjunction with a Diagnostic Concepts Digital Data Analyser. Although digital readouts were not possible (due to uncorrectable instrument malfunctioning) the central light emitting diodes (LEDs) were used as fixation targets. The electronic pachometer uses eleven fixation LEDs - nine in the horizontal plane, and two in the vertical. The images of the two vertical lights formed by the corneal surface are seen in the centre of the visual field through the slit lamp observation system. When these images are seen on the epithelium of the corneal optical section, the microscope is vertical to the corneal surface.

The light source was placed 40° to the experimenter's left, in relation to the microscope. The subject was instructed to fixate the central LED of the fixation apparatus. The plane glass plates of the measuring device necessitated the addition of +2.50 dioptres to the x10 right split ocular eyepiece. The slit lamp was focused on the central section of the cornea with vertical alignment of the three vertical diodes. Correct alignment was achieved when the image of the central red light bisected the superimposed slit beam. Thus, the upper section of the slit beam was lined up over the upper vertical alignment light, with the lower light over the lower section of the slit beam. The beam intensity of the slit lamp was

increased to a maximal level prior to each measurement to clearly juxtapose the endothelium of the lower section. The apparent thickness of the corneal optical section is equal to the amount of displacement of the light path by the rotated glass plate. When the posterior endothelium of the upper field and the anterior epithelium of the lower field were aligned, a measurement was read from the micrometer scale (section 6.7.1).

6.12.1.2 Calibration of the pachometer

Whether by direct calibration, or by ratios using glass or plastic curved surfaces (Maurice and Giardini 1951; Donaldson 1966; Mandell and Polse 1969), the investigator is limited to a measurement of the *apparent* CT, since the *actual* CT cannot be measured in vivo. Actual values of CT depend upon the method of calibration, since CT is either calculated from the given optical arrangement, or calibrated using shells of known thickness, RI and curvature. Errors due to RI and curvature of the cornea are slight and only important when the cornea imbibes water. The apparent thickness is a function of the true thickness, the RI and the anterior curvature readings of the cornea.

The simplest method for calibrating the pachometer is to use contact lenses of known thickness. A correction must then be made for the difference in refractive indices between the contact lens and the cornea. It has been demonstrated that the RI of the cornea is not a constant (Patel et al 1995). Furthermore, an average figure based on our knowledge of the variability of the RI of the cornea is yet to be accepted. That said, the generally accepted figure used in paraxial calculations that require CT is 1.376 (Bennett and Rabbets 1998). The method chosen for the present study was based on that developed by Mandell and Polse (1969). Four contact lenses were used with known standard thicknesses of 0.420 mm, 0.505 mm, 0.620 mm and 0.730 mm. The lenses were mounted on a panel attached to a vertical bar of the slit lamp framework, and measurements were taken. The measurement of the contact lens thickness had two purposes. Firstly, it enabled the examiner to gain practice with the instrument, which is necessary in order to develop the standard of performance necessary to obtain data of accuracy sufficient for the purpose of the experiment. Secondly, it enabled construction of a standard calibration graph. It thus allowed the conversion of the pachometer reading into the true CT, having taken into consideration the RI of the contact lenses and the cornea.

CT measurements were taken with the viewing systems at right angles to the contact lenses. For each lens, a set of six readings were taken, the Donaldson lights being re-centered before each reading. A mean thickness, with the associated sd, was thus obtained.

Calibration Data :

Table 6.6 - Measured thickness (mm) of four afocal contact lenses.

Contact lens thickness (mm)	Mean pachometer measurement	sd
0.420	0.630	0.008
0.505	0.730	0.008
0.620	0.830	0.006
0.730	0.950	0.006

The differing refractive indices of the cornea and the contact lenses also has to be accounted for.

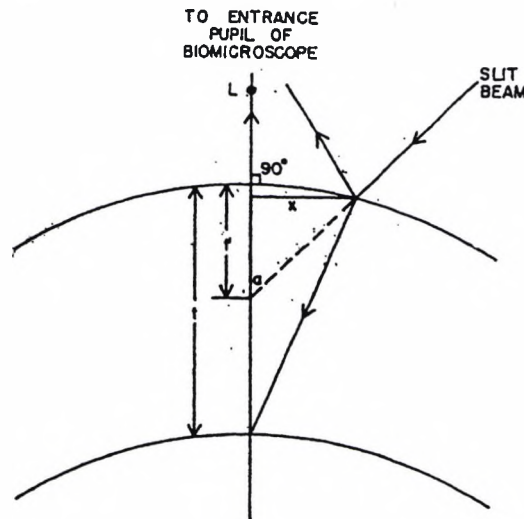


Figure 6.9 - Optical path of slit beam and reflected light (Mandell and Polse 1969).

where :-

r = radius of anterior corneal surface

t = true thickness

x = apparent thickness of the slit lamp section

t' = paraxial image of the true thickness

The apparent thickness x is proportional to the paraxial image t' -

[equation 6.1]

$$x = \frac{1}{t'} - \frac{1.376}{t}$$

$$x = \frac{-0.376}{r}$$

1.376 = RI of the cornea

1.490 = RI of the contact lens

[equation 6.2]

$$t = \frac{1.376t'r}{0.376t' + r}$$

Repeating the procedure to find the thickness of a contact lens of $n = 1.49$:

[equation 6.3]

$$t = \frac{1.490t'r}{0.490t' + r}$$

Thus the ratio of the CT to contact lens thickness when the apparent thickness is equal is :-

$$\frac{t_{cor}}{t_{lens}} = \frac{1.376 (0.490t' + r)}{1.490 (0.376t' + r)} \quad \text{[equation 6.4]}$$

Assuming an apparent thickness (t') of 0.450 and an average value of $r = 800$ mm

simplifies the relation to :

$$\frac{t_{cor}}{t_{lens}} = \frac{1.376 (0.490 \times 0.450 + 8)}{1.490 (0.376 \times 0.450 + 8)} \quad \text{[equation 6.5]}$$

$$= 0.925$$

This conversion factor of 0.925 was used to convert the artificial plastic corneae to the equivalent CT.

Table 6.7 - Mean pachometry readings and equivalent CT following use of the conversion factor to transpose actual contact lens thicknesses.

Contact lens thickness (mm)	Mean pachometer reading (mm)	Equivalent CT (mm)
0.420	0.630	0.389
0.505	0.730	0.467
0.620	0.830	0.574
0.730	0.950	0.675

This results in the standard curve seen in figure 6.10.

The graph was found to have the equation $y = 1.096(x) + 0.209$ [equation 6.6]

where:-

y = pachometer readout

x = CT

6.12.2 Light scatter method

Subjects underwent scatter testing using the P_SCAN 100 scatter apparatus as described in section 5.7.

To facilitate analysis of the results obtained in Chapter 6, the experiments have been divided into individual studies.

6.13 Study 1 - Variation in light scatter during one day

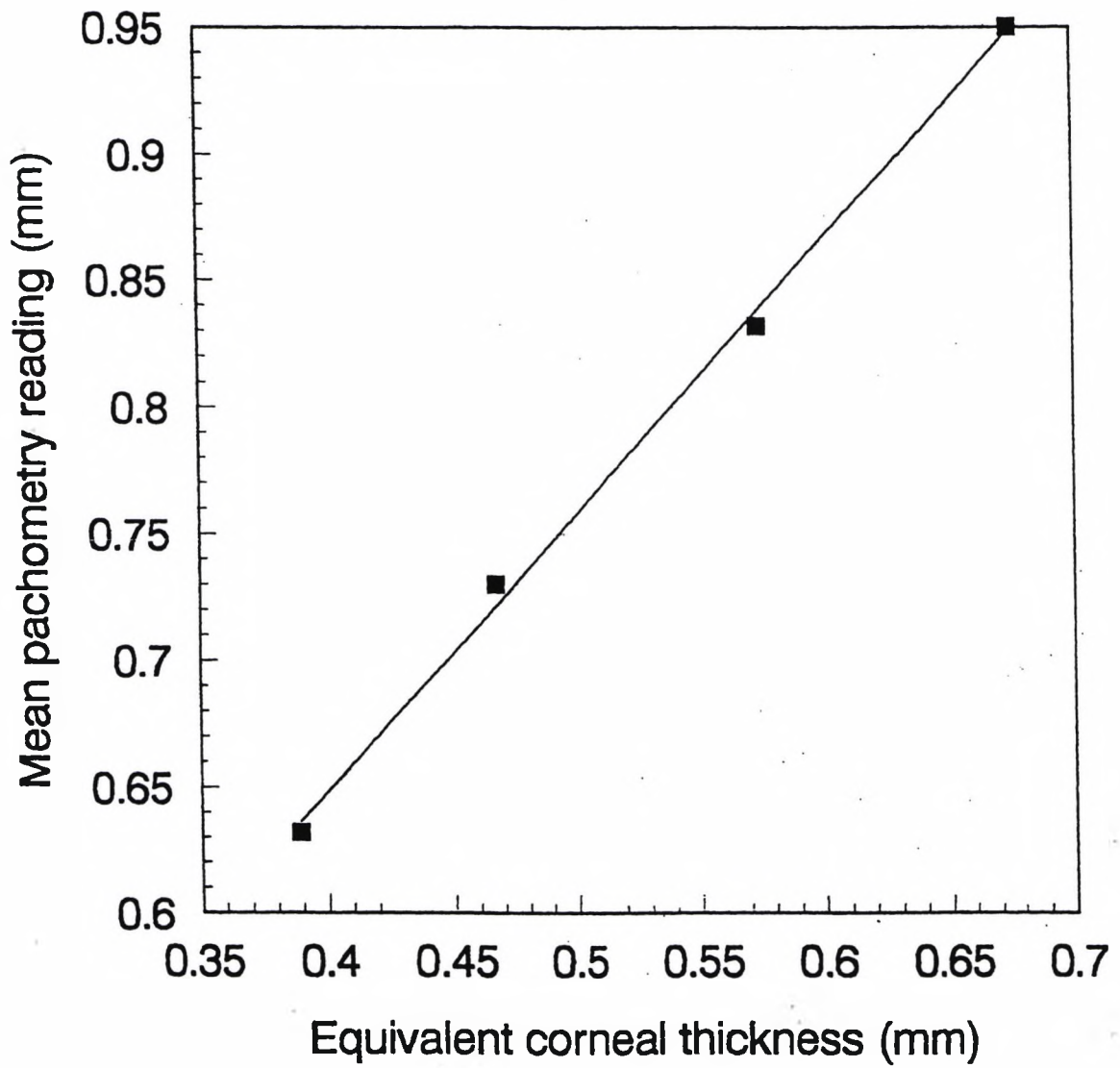
6.13.1 Aim

To determine whether light scatter is subject to temporal variations within one working day. This knowledge is useful because it will affect the measurement timing of longitudinal studies. In addition, it is well documented that CT is subject to diurnal variations and so it would be useful to elucidate whether the corneal changes resulting from biological variations affect the measurement of light scatter in the eye.

6.13.2 Method

One healthy male subject (42 years old) was recruited to investigate the variation in the straylight parameter k' with time. Before inclusion in the study, a slit lamp examination excluded lens opacities using the LOCS II system (Chylack et al 1989) and a fundus examination excluded disease of the posterior segment. The subject had a refraction of

Figure 6.10 *Mean pachometry reading from contact lenses plotted against equivalent corneal thickness*



-2.00/-2.50 x 170 and a Snellen VA of 6/5. Spectacles were worn for the duration of the test and measurements were taken from the subject's right eye. The P_SCAN 100 scatter programme was used, as described in section 5.7. The subject completed two hourly measurements for 10 hours (starting at 08:00).

6.13.3 Results

Table 6.8 - Timing of minimum and maximum k' values following two hourly measurements for ten hours.

Subject	1
Mean maximum k' (sd)	7.60 (0.10)
Time of maximum k'	08:00
Mean minimum k' (sd)	6.10 (0.57)
Time of minimum k'	10:00

The highest k' value (7.60) was recorded at 08:00 (figure 6.11), falling after this to reach a steady (minimum) value of approximately 6.10. The value of k' at 08:00 is approximately 25% higher than the values recorded for the rest of that day.

6.13.4 Discussion

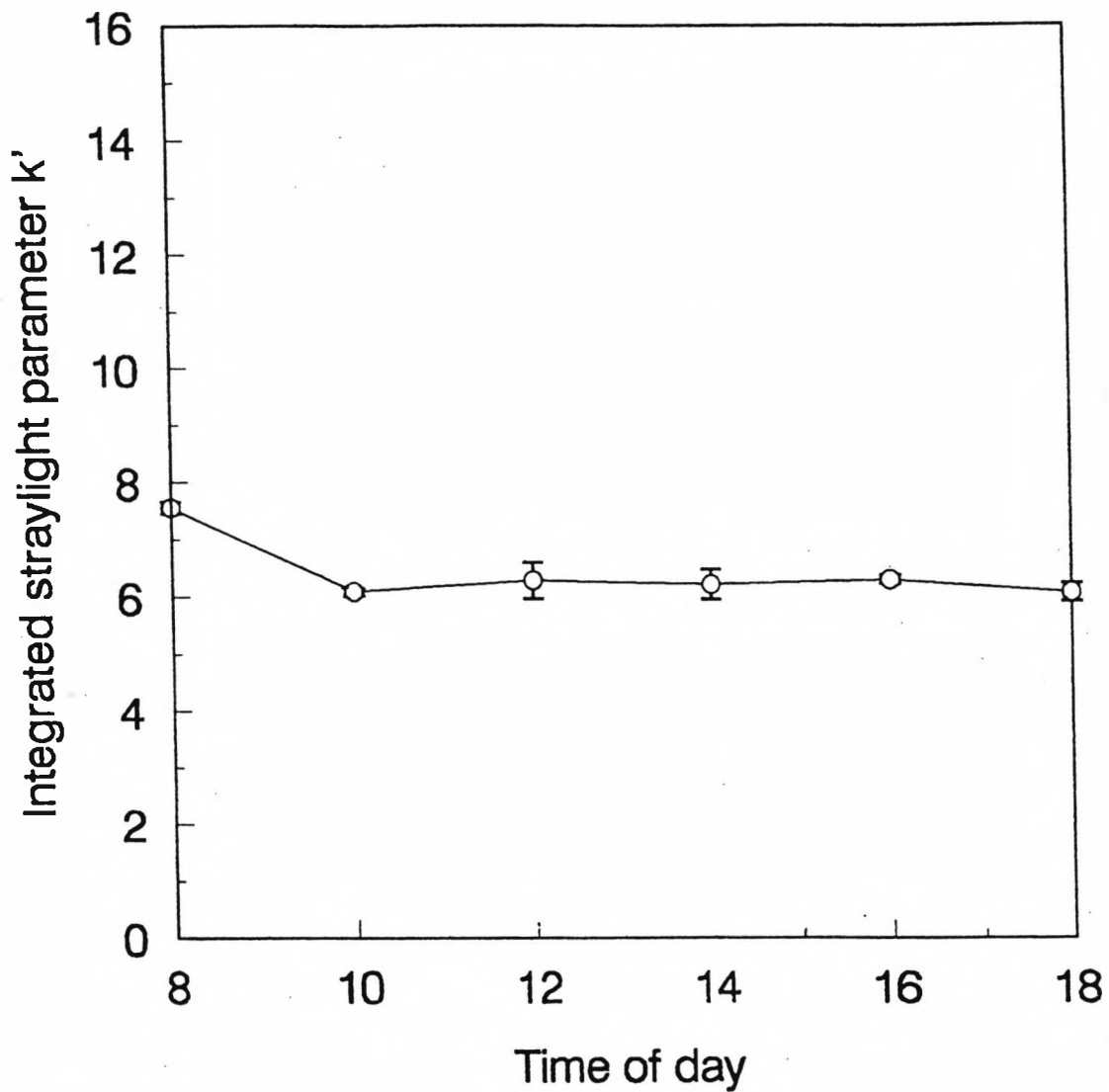
There was a diurnal variation in k' , with a morning peak. The subject had been awake for no longer than 30 minutes before testing. If the peak in k' is related to the length of time between waking and taking the measurements, then higher k' values may be recorded if a smaller interval between waking and testing was adopted.

The possible causes of the elevated light scatter at the initial time point are numerous, however, the most likely is as a result of corneal oedema following sleep. As previously discussed, the eye is subject to reduced oxygen tension during sleep due to the effect of lid closure. This results in an increase in CT, which in turn increases light scatter. To check the repeatability of this finding, the subject was retested on an additional day beginning at 08:00.

6.14 Study 2 - Repeatability of Study 1

6.14.1 Aim

Figure 6.11 Results for subject DE following scatter measurements taken over a ten hour period.



Variation in k' over one working day for subject DE. Measurements were taken at two hourly intervals beginning at 08:00. The plotted data points represent the mean k' obtained over four 'runs'. Error bars represent standard errors.

To repeat the morning scatter measurements to confirm that light scatter in this eye was at a maximum in the early morning.

6.14.2 Method

Subject 1 repeated hourly measurements from 08:00 to 10:00 on a further visit. Scatter measurements were taken at 08:00, 09:00 and 10:00.

6.14.3 Results

Table 6.9 - Timing of minimum and maximum k' values following hourly measurements for two hours.

Subject	1
Mean maximum k' (sd)	7.67 (0.13)
Time of maximum k'	08:00
Mean minimum k' (sd)	6.40 (0.20)
Time of minimum k'	10:00

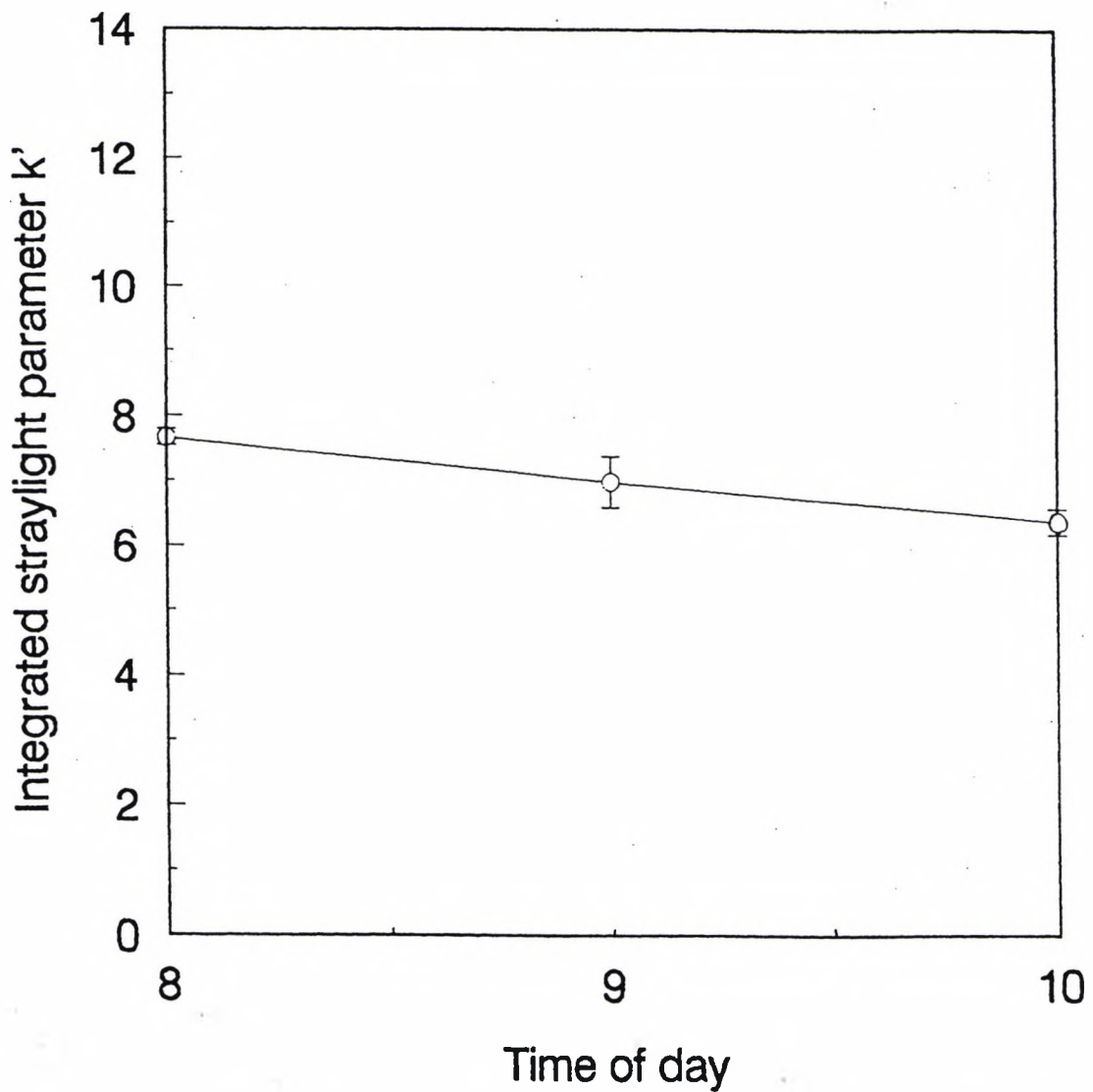
The maximum value of k' was again at 08:00 (7.67) (figure 6.12). As in the initial study, this value was reduced (to 6.40) when the measurement of light scatter was taken at 10:00 (a 20% reduction in scattered light over time).

6.14.4 Discussion

The results of scatter testing Subject 1 again revealed a peak k' at 08:00. As in Study 1, the subject had been awake for less than 30 minutes prior to testing. The increase in k' compared to the subsequent minimum at 10:00 was slightly less than that recorded in the initial study (20% compared to 25%), however, the reduction in k' after 08:00 was reproducible for this male subject, with a fall of approximately 20% being recorded on each occasion.

The results of Studies 1 and 2 reveal that k' does not remain constant throughout the day. In fact, the timing of the measurement is critical, as k' appears to be, at least for this subject, related to the length of time between waking and taking the measurements. Few conclusions can be drawn from the results of one subject, therefore, three further subjects were recruited. Pachometry was employed to explore whether changes in straylight are due to corneal oedema.

Figure 6.12 Results for subject DE following scatter measurements taken over a two hour period.



Variation in k' over two hours for subject DE. Measurements were taken at one hourly intervals beginning at 08:00. The plotted data points represent the mean k' obtained over four 'runs'. Error bars represent standard errors.

6.15 Study 3 - Changes in light scatter and corneal thickness following eye patching

6.15.1 Aim

To investigate the effect of eye patching on CT and measures of forward light scatter using the P_SCAN 100 scatter apparatus.

6.15.2 Method

Three male volunteers, Subject 1 (30 years old), Subject 2 (19 years old), and Subject 3 (30 years old) were recruited to further investigate diurnal variation in CT and test the hypothesis that any change in the straylight parameter k' during the early hours of the day was due to corneal oedema. Before inclusion, a slit lamp examination on each subject excluded significant lens opacities using the LOCS II system (Chylack et al 1989) and a fundus examination excluded disease of the posterior segment. All subjects had a Snellen VA of at least 6/6, a spherical refractive error of between +0.50 DS and -0.25 DS, and astigmatism of less than -0.50 DC. Baseline pre-patch measurements were taken on the evening before the studies, between 17:00 and 18:00 hours. The subjects were instructed to tape one eye closed and place a bandage patch over the eye before going to sleep, which they could not remove until arrival in the experimental room the following morning. Pachometry and scatter measurements were taken immediately following removal of the patch and continued until either the CT or the scatter results returned to within 10% of the baseline values. The scatter testing programme was employed as described in section 5.7.

Pachometry measurements were taken following the procedure outlined in section 6.12. The objective magnification was set to x1.6. The slit lamp illumination was switched to 6 volts, and the slit width was standardised at 0.3 mm. This was the narrowest setting which gave a bright enough image to see coincidence of the measured points. The angle between the microscope and the slit lamp was set at 40 degrees. The room lights were switched off and the eye patch was removed. The subject was asked to fixate the central of the three vertical lights so that CT measurements could be taken.

6.15.3 Results

Table 6.10 - Scatter and CT results from three subjects following patching.

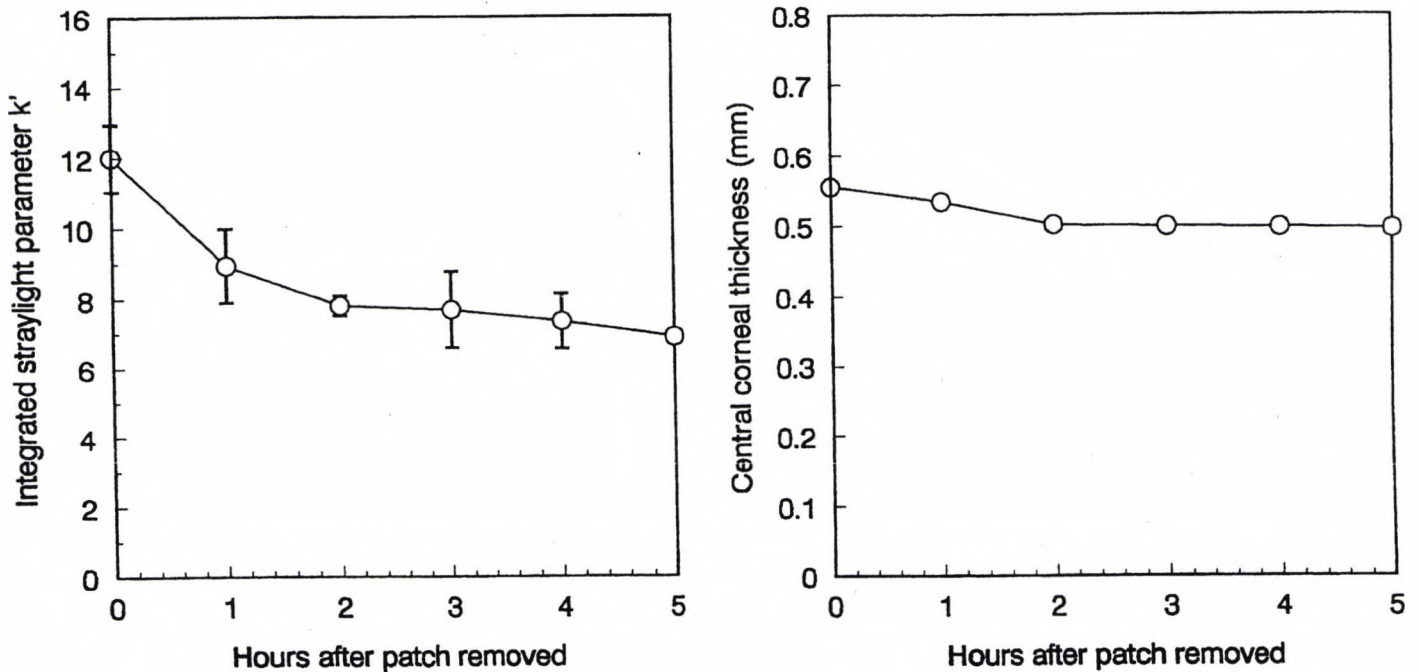
Subject	1	2	3
Pre-patch k' (sd)	6.61 (0.85)	7.31 (0.59)	7.30 (0.62)
Pre-patch CT in mm (sd)	0.503 (0.007)	0.543 (0.005)	0.580 (0.005)
k' immediately following removal of patch (sd)	12.01 (0.95)	11.58 (0.43)	7.50 (0.56)
CT in mm immediately following removal of patch (sd)	0.546 (0.005)	0.582 (0.006)	0.587 (0.005)

Subject 1 revealed a maximum value of k' (12.01) immediately following removal of the patch. k' then decreased throughout the subsequent five hour period following the removal of the patch (figure 6.13a), when it reached the minimum value of 6.89, a value approximately equal to the baseline value before patching ($k' = 6.61$). Eye closure during sleep followed by patching until testing caused a 81.7% increase in light scatter. Pachometry measurements revealed that the increased k' was accompanied by an increase in CT (figure 6.13b). The cornea was also at its maximum thickness immediately following removal of the patch, with an increase of 8.5% compared to baseline measurements.

Subject 2 also showed an increase in the straylight parameter k' immediately following removal of the patch. k' increased to 11.58 following eye closure during sleep and subsequent patching until testing. This maximal k' value fell to 7.74 after two hours (figure 6.14a), a value approximately equal to the baseline (i.e. before patching, $k' = 7.31$). This represents an increase in light scatter of approximately 58.4% as a consequence of eye closure during sleep and subsequent patching. CT also increased with patching (figure 6.14b). The overall increase in CT as a result of patching was approximately 7.2%.

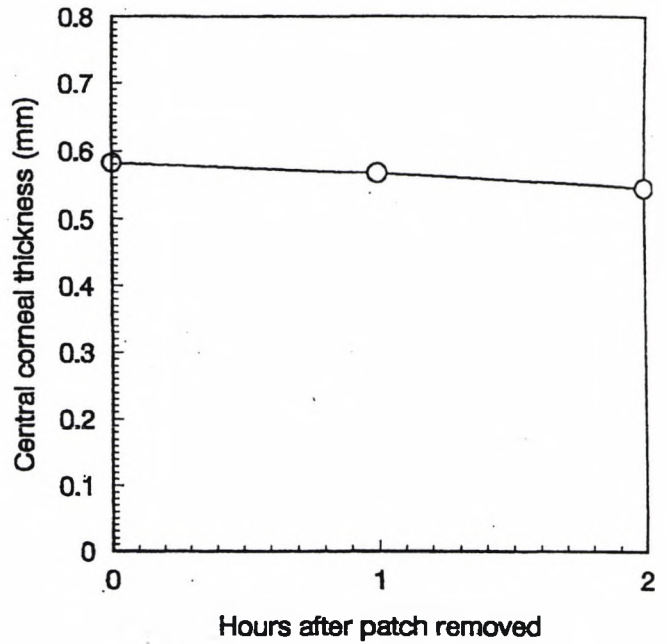
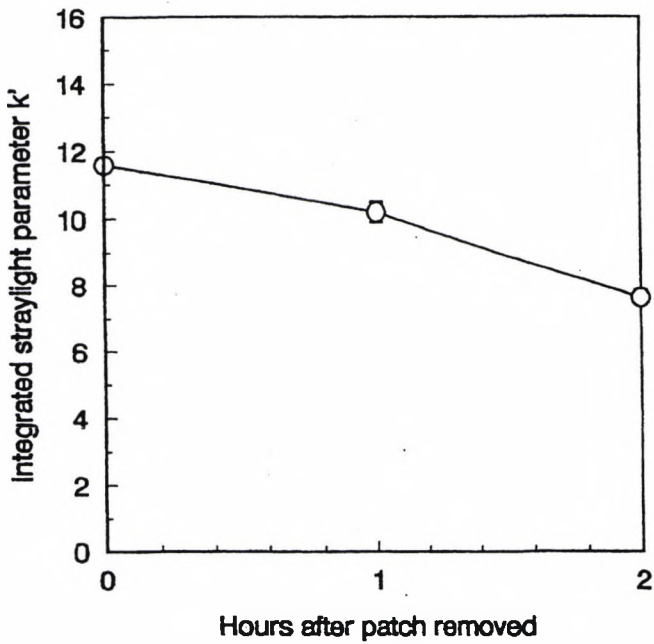
Subject 3 revealed a small increase in light scatter immediately following removal of the patch. (figure 6.15) A 2.7% increase in k' was noted between pre-patch and post-patch measurements. However, this value was approximately equal to the baseline value before patching ($k' = 7.30$). CT measurements also showed an increase, corresponding to an increase of 1.2% following patching.

Figure 6.13 (a) scatter results and (b) central corneal thickness following eye patching for Subject 1



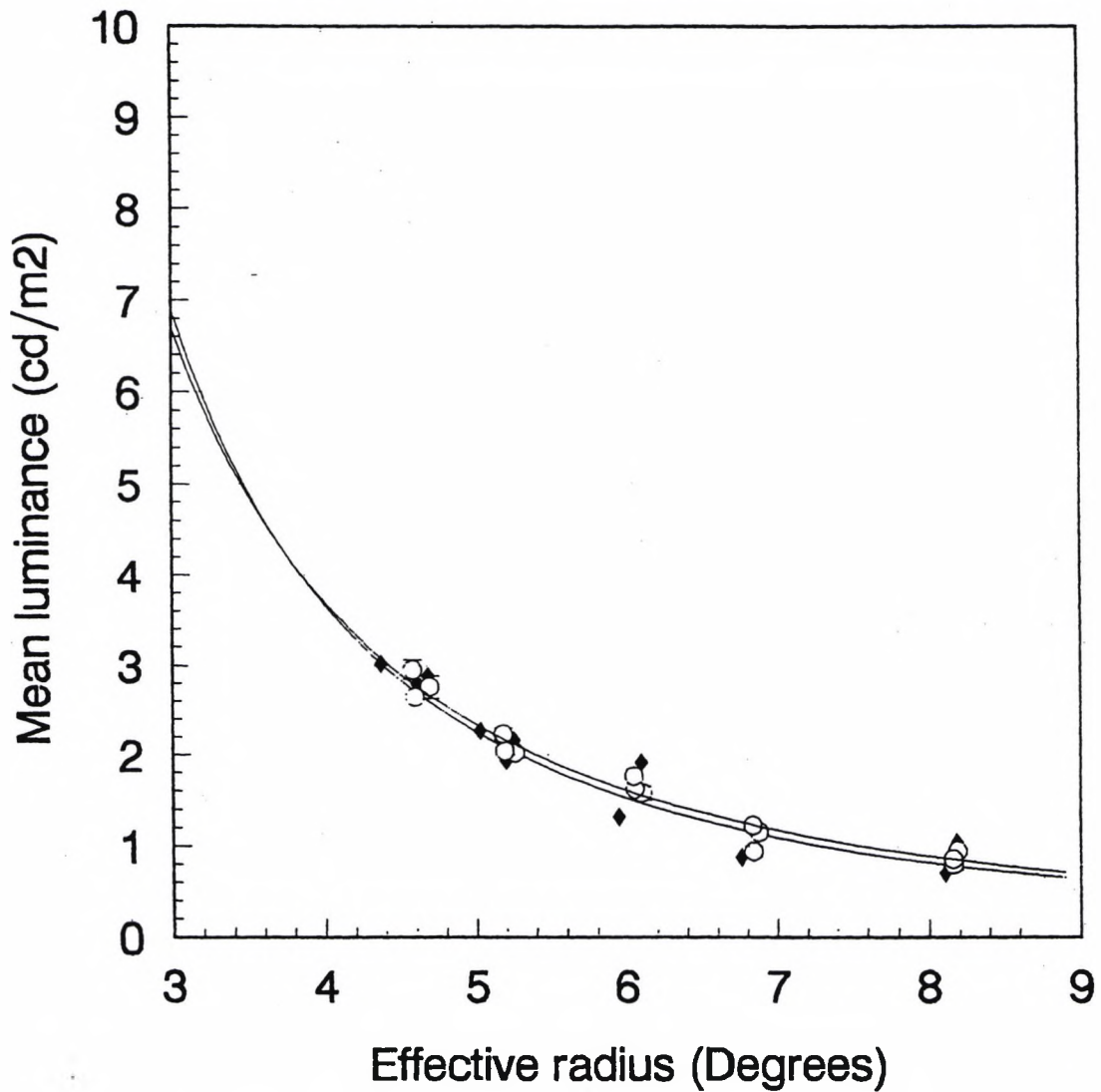
Variation in k' (Fig. 6.13a) and central corneal thickness (Fig. 6.13b) over five hours for Subject 1 following eye patching. Measurements were taken at one hour intervals immediately following removal of the patch, beginning at 08:00. The plotted data points in Fig. 6.13a represent the mean k' obtained over three 'runs'. The plotted data points in Fig. 6.13b represent the mean CT obtained following six measurements. Error bars represent standard errors.

Figure 6.14 (a) scatter results and (b) central corneal thickness following eye patching for Subject 2



Variation in k' (Fig. 6.14a) and central corneal thickness (Fig. 6.14b) over two hours for Subject 2 following eye patching. Measurements were taken at one hour intervals immediately following removal of the patch, beginning at 08:00. The plotted data points in Fig. 6.14a represent the mean k' obtained over three 'runs'. The plotted data points in Fig. 6.14b represent the mean CT obtained following six measurements. Error bars represent standard errors.

Figure 6.15 Scatter results following eye patching for Subject 3



Variation in k' (Fig. 6.15) for subject 3 following eye patching. (◆ Pre-patch, ○ Post-patch). Measurements were taken immediately following removal of the patch beginning at 08:00. The plotted data points represent the mean k' obtained over three 'runs'. Error bars represent standard errors.

6.15.4 Discussion

From the results of Study 3, the amount of light scatter in the eye increased following removal of a patch which had been worn for at least 11 hours. There were considerable inter-individual differences in the effects of patching on k' and central CT. Nevertheless, these results suggest that the immediate post-patching peak in k' and its subsequent reduction may be related to changes in CT. For both Subjects 1 and 2, the CT increased by approximately 8% following patching. This increase in CT is greater than the values reported by Mandell and Fatt (1965) and Gertsman (1972), however, the results are within the range of values more recently reported by Harper et al (1996). The increase in CT observed in these subjects was reflected in the light scatter measurements, as both subjects revealed at least a 50% increase in light scatter following overnight sleep and patching. The increase in CT in Subject 3 was approximately 3% which was associated with a much smaller increase in light scatter compared to the other subjects tested.

The most likely cause of the observed changes in light scatter is corneal oedema induced by sleep and patching, and the results indicate a possible relationship between CT and increased straylight. It was deemed useful to investigate the minimum patching time (and thus the minimum oedema levels) necessary to cause these changes in CT and light scatter in the eye.

6.16 Study 4 - The influence of patching time on light scatter and CT

6.16.1 Aim

To investigate whether eye patching for two and four hours (on non-consecutive days) produces a similar change in CT and intraocular light scatter as that obtained following overnight patching.

6.16.2 Method

Subject 1 (who took part in Study 3) was patched for a two hour and a four hour period, on different days (one week apart). Scatter and CT measurements were recorded before patching so that a baseline value could be recorded. The subject was instructed to tape down the eye and wear the patch for the required period and then to return for testing.

6.16.3 Results

Table 6.11 - Percentage increase in k' and CT for Subject 1 following (i) overnight eye patching, (ii) eye patching for two hours and (iii) eye patching for four hours.

Measurements taken following:-	% increase in k'	% increase in CT
(i) Overnight eye patching	81.7	8.5
(ii) Two hours patching	21.6	3.6
(iii) Four hours patching	46.2	8.3

There was an increase in k' and CT following patching for two and four hours. The greatest increase in scattered light was recorded following overnight patching (81.7%). This was accompanied by the greatest increase in CT (8.5%). Patching for four hours produced a similar increase in CT (8.3%) but produced a lesser increase in k' (46.2%). Patching for two hours revealed the least increase in light scatter (21.6%) and in CT (3.6%).

6.16.4 Discussion

It is apparent that intraocular straylight and CT become noticeably increased following only two hours of eye patching. As discussed in Study 3, the increase in CT is probably attributable to corneal oedema, resulting from lid closure. The effect of lid closure on CT and scatter became more pronounced as the duration of patching was increased to four hours. Corneal oedema increases as the superficial cornea continues to be deprived of oxygen, resulting in an increase in CT, and consequent increases in scattered light. In fact, eye patching for four hours produced a similar increase in CT to patching overnight, despite the fact that the k' values obtained were higher following overnight patching (46.2% compared to 81.7%). One possible factor that may cause such a discrepancy in measures of light scatter is that the testing following four hours of patching was conducted in the afternoon, whereas following overnight patching, the testing was conducted in the early morning. As a result, diurnal increases in CT, which have been shown to be greater than overnight increases (Harper et al 1996), may have caused an additional increase in CT. If the increase in CT in the afternoon was stromal in origin as opposed to epithelial, then it would be unlikely to contribute to increasing light scatter (Feuk and McQueen 1971). Therefore, differing amounts of stromal and epithelial oedema may have been produced following daytime patching compared to overnight patching which resulted in different levels of forward scattered light.

6.17 Study 5 - The variation in scatter when longitudinal measurements are taken at the same time of day

6.17.1 Aim

To investigate the changes in light scatter on a temporal basis (i.e. from day to day). The first subject was female. At this stage there was no reason to suspect that variation in scattered light would be different between males and females. The investigation was initially over a four week period. Following identification of a possible cyclical relationship the study was extended, first to a second menstrual cycle and then to two further cycles, each separated by a non-testing month.

6.17.2 Method

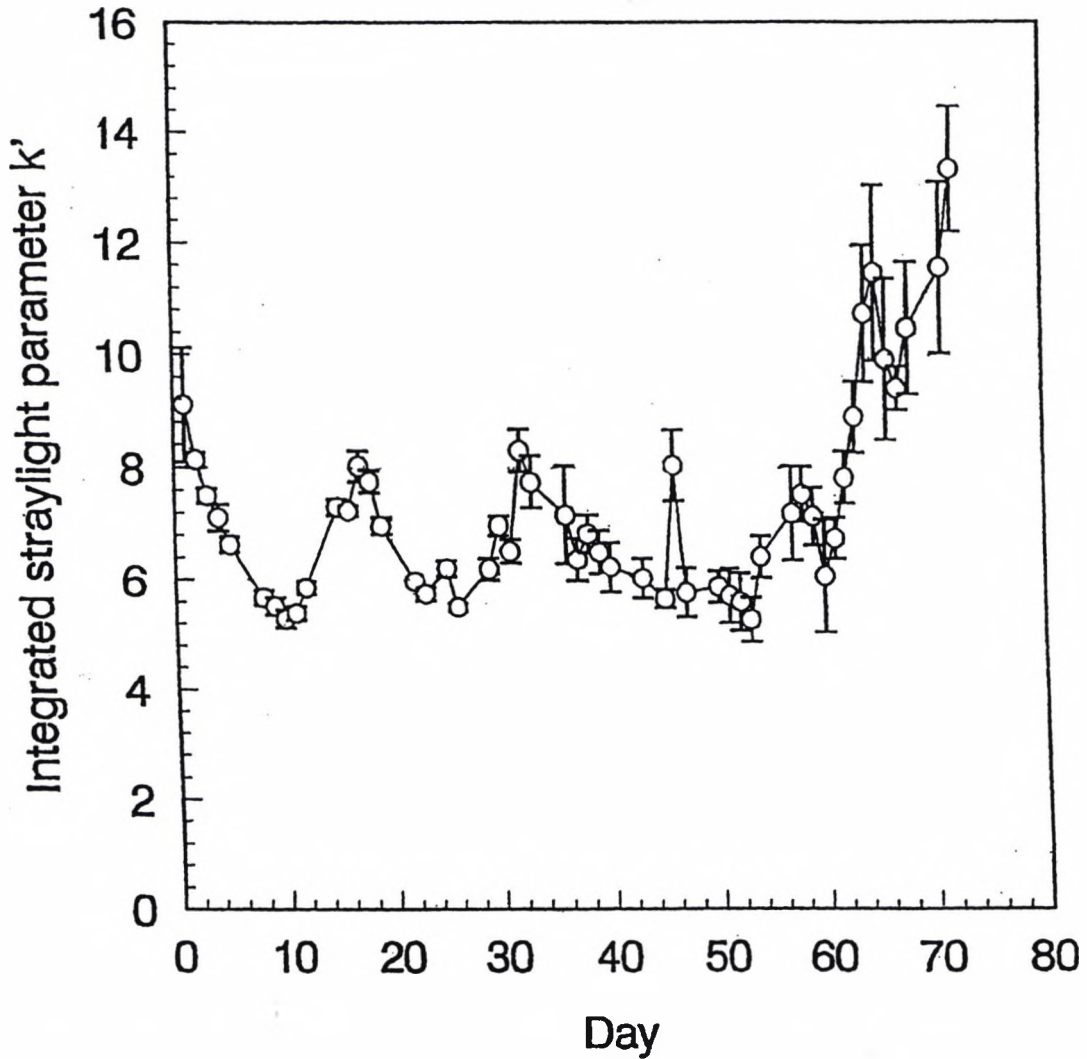
One female subject was recruited and scatter measurements were taken at approximately the same time of day (between 12:00 and 14:00) over the 72 days of the first two menstrual cycles. Before inclusion, a slit lamp examination excluded significant lens opacities using the LOCS II system (Chylack et al 1989) and a fundus examination excluded disease of the posterior segment. The subject had a Snellen VA of at least 6/6, and a refractive error of -3.50/-1.75x180. Spectacles were worn for the duration of testing and the subject did not wear contact lenses. Wherever possible, six scatter measurement were taken each day.

6.17.3 Results

Figure 6.16, shows the variation in k' from day to day over the first 72 day period. The highest k' value was on day 72 (13.33), and the lowest (5.28) was on day 53. Visual inspection of the data indicates that a cyclical trend may exist, with peaks in k' apparent in this cycle on day 1, day 17, day 32, day 46 and days 60 - 72. Subsequent analysis revealed that these peaks may correspond to landmarks in the subject's menstrual cycle. The possible relationship between light scatter and the menstrual cycle can be seen in figures 6.17 and 6.18, where the data is presented from the first day of menstruation.

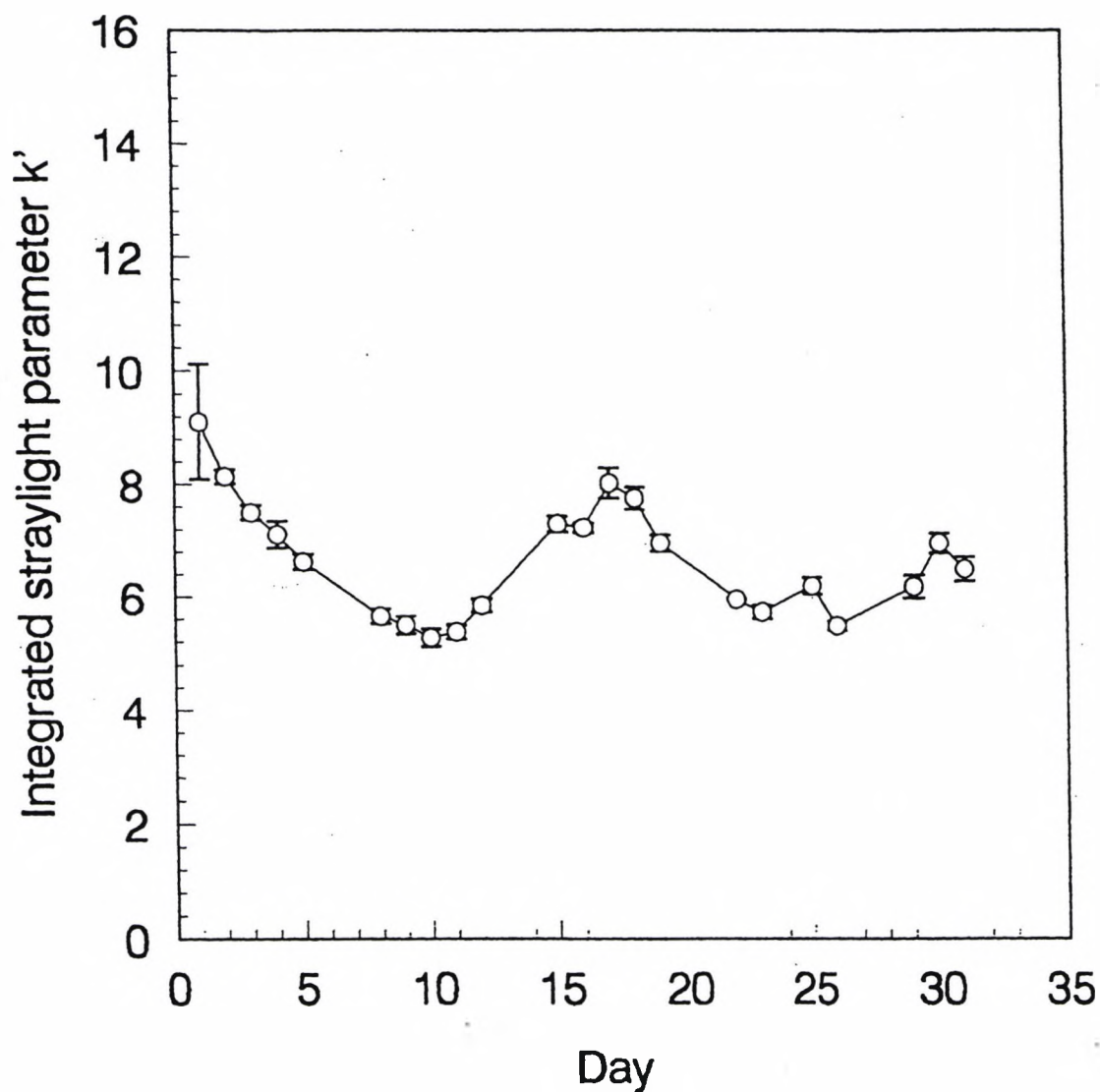
Figure 6.17 (cycle 1), demonstrates that k' is maximal (9.11) on day 1 of the cycle i.e. the first day of menstruation. There is then a decrease in k' from day 1 to day 10, where the minimum value of k' is recorded (5.28). The reduction in the value of k' coincides with the follicular phase of the cycle. The level of k' then increased to day 17 (8.03), whereupon there was a decrease from this second peak towards the end of the cycle. This peak in k'

Figure 6.16 Variation in k' over 72 days for Subject MH



Measurements were taken at approximately the same time of day (between 12:00 and 14:00). The plotted data points represent the mean k' obtained over six 'runs'. Error bars represent standard errors.

Figure 6.17 Variation in k' over 31 days (month 1) for Subject MH



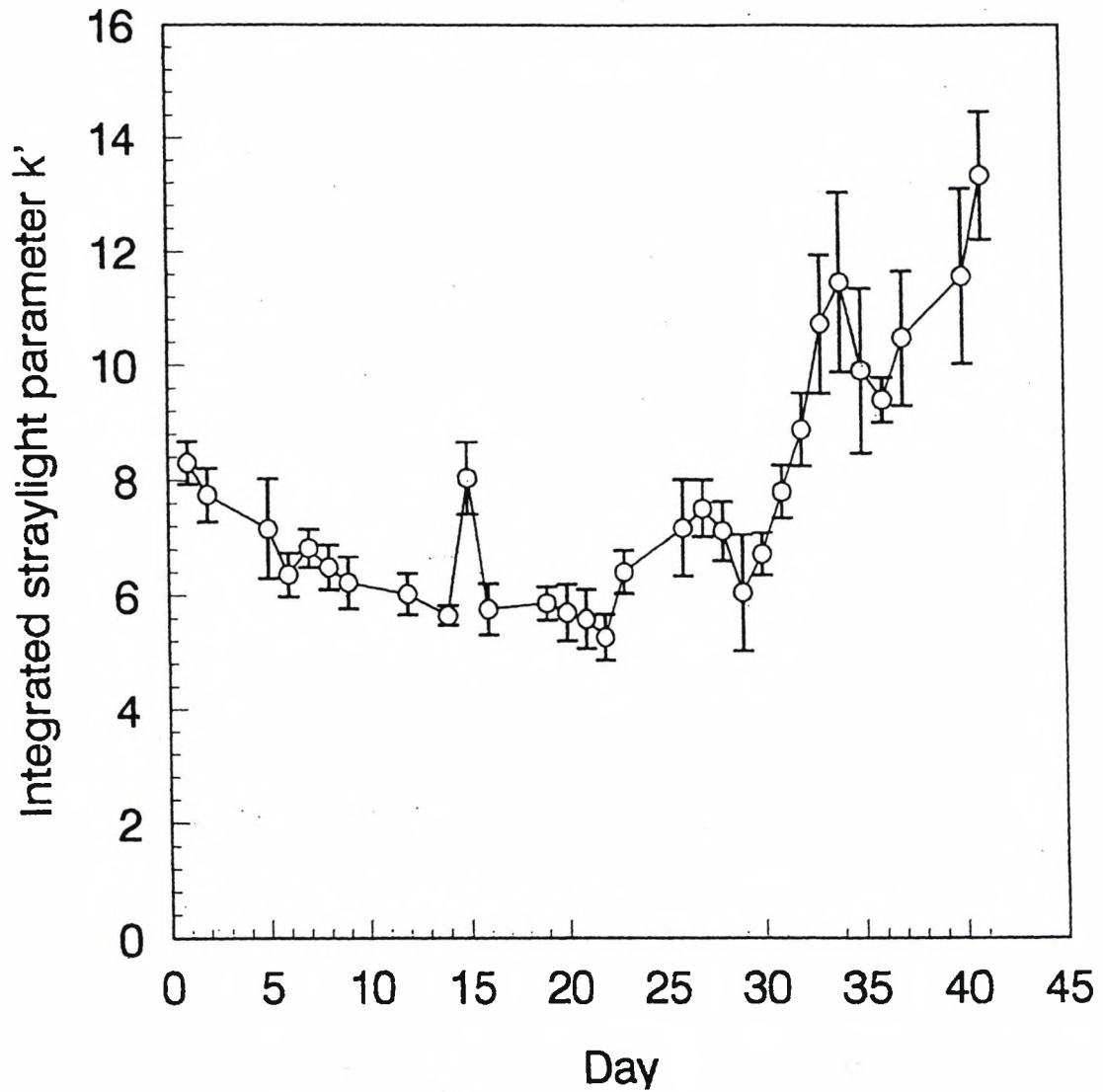
Measurements were taken at approximately the same time of day (between 12:00 and 14:00). The plotted data points represent the mean k' obtained over six 'runs'. Error bars represent standard errors.

may coincide with ovulation. The overall percentage change in k' was 72.5% (CV = 15.7%). Initial statistical analysis revealed a k' mean of 6.66, a within day variability of 0.26 (s.d.) and a between day variability of 0.66 (s.d.).

In cycle 2 (figure 6.18), k' decreased from day 1 (8.30) until day 14 (5.65). There was a marked increase in light scatter on day 15 (8.05). As in cycle 1, light scatter is seen to reduce during the follicular phase, followed by second peak in k' which may be related to ovulation. The value of k' then decreased until a rise on day 23 (6.42). k' decreases to a minimum of 5.28 on day 22 and gradually rises again to day 27 (7.54), whereupon k' decreases until day 29 (6.07). k' increases again to day 34 (11.47) and decreases to day 36 (9.41). k' begins to rise from this point reaching the maximum levels of light scatter on day 41 (13.33). The overall percentage change in k' was 152.5% (CV = 27.2%). Although the possible cyclical fluctuation in k' is still apparent for cycle 2, the variability is greater than recorded for cycle 1. Initial statistical analysis revealed a k' mean of 7.73, a within day variability of 0.66 (s.d.) and a between day variability of 1.04 (s.d.).

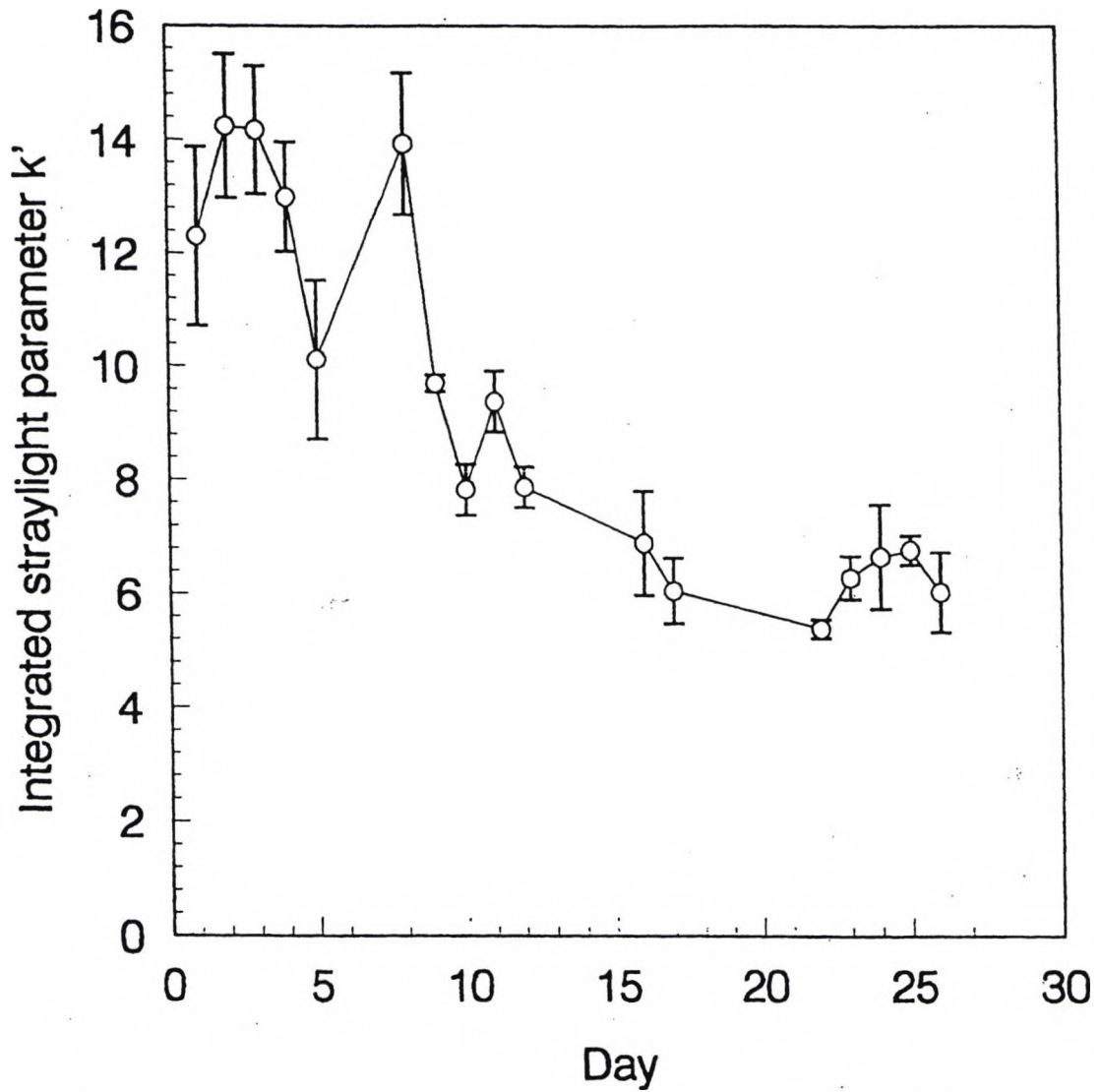
As a result of the differences in the pattern of variation in k' across the two cycles, a third cycle was investigated. During cycle 3 (figure 6.19) the subject was taking oral corticosteroids (Prednisolone 50mg o.d.) due to severe eczema, and this may have altered the previously observed cyclical variation. Despite this, the study was continued through the cycle to take advantage of the opportunity to assess the effects of steroids on scattered light. The maximum k' was on day 2 (14.24), with the minimum value on day 22 (5.39). This represents a 164.2% change in k' over the course of the cycle (CV = 34.4%). Initial statistical analysis revealed a k' mean of 7.98, a within day variability of 0.77 (s.d.) and a between day variability of 1.92 (s.d.). In cycle 4 (following steroid cessation) (figure 6.20) scatter was very variable, with little cyclical relationship evident between scatter and menstruation. The maximum k' was seen on day 15 (10.89), with the minimum k' on day 17 (5.83). This represents a 86.8% change in k' over the course of the cycle (CV = 16.9%). Initial statistical analysis revealed a k' mean of 9.22, a within day variability of 0.46 (s.d.) and a between day variability of 1.73 (s.d.).

Figure 6.18 Variation in k' over 41 days (month 2) for Subject MH



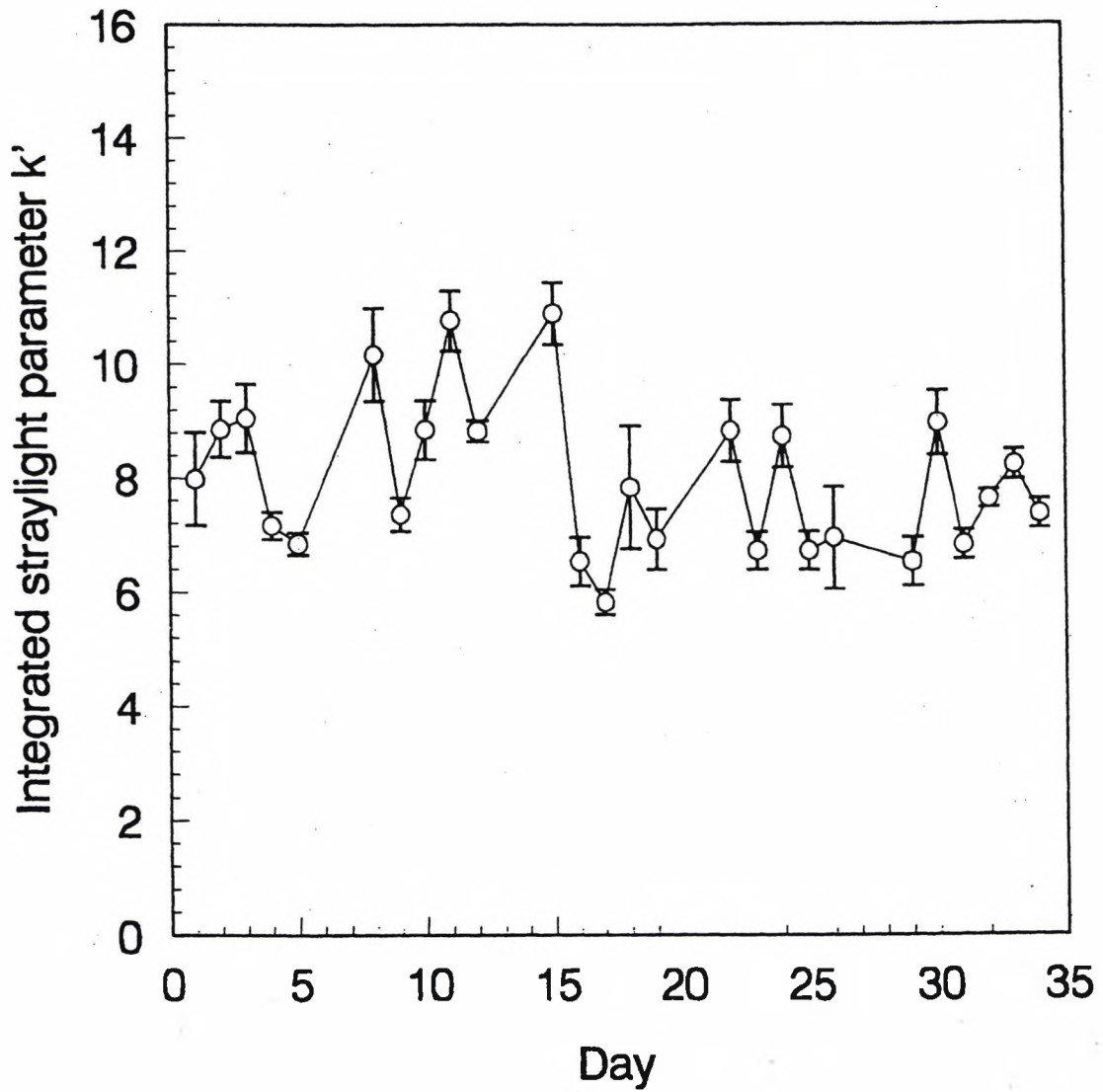
Measurements were taken at approximately the same time of day (between 12:00 and 14:00). The plotted data points represent the mean k' obtained over six 'runs'. Error bars represent standard errors.

Figure 6.19 Variation in k' over 26 days (month 3) for Subject MH



Measurements were taken at approximately the same time of day (between 12:00 and 14:00). The plotted data points represent the mean k' obtained over three 'runs'. Error bars represent standard errors.

Figure 6.20 Variation in k' over 34 days (month 4) for Subject MH



Measurements were taken at approximately the same time of day (between 12:00 and 14:00). The plotted data points represent the mean k' obtained over three 'runs'. Error bars represent standard errors.

6.17.4 Discussion

Testing Subject MH for 72 days revealed a possible cyclical variation in k' . In both cycles, the peak in k' observed on day 1 corresponded to the subject's first day of menstruation. Testing a larger number of subjects (including male control subjects) is required, however, it is possible that light scatter in the eye is affected by the hormonal control of the menstrual cycle.

It was hoped that testing two additional cycles would help to clarify whether a cyclical variation occurred for this subject. However, the subject received a KanalogTM injection (triamcinolone acetonide 49mg/mL) (TA) prior to commencing the tests, and was taking 50 mg oral prednisolone once daily over a period of 4 weeks. Nevertheless, the measurements were continued because this was an opportunity to observe the effects of TA. It is well known that corticosteroids have an effect on the endocrine system and menstrual irregularity is quoted as a possible side-effect. This may explain why cycle 3 is only 26 days long, compared to an average of 36 days found in cycles 1 and 2. In fact, the subject's normal menstrual cycle (i.e. without medication) was 35 days. The effects of TA on the menstrual cycle have been well documented (Hefly et al 1964; Scher 1964; Sherwood et al 1967; Willey et al 1984). Such studies report either temporary menstrual irregularity, menorrhagia, metorrhagia or prolongation of the menstrual period. The mechanism of the effect of TA on the menstrual cycle is not fully understood, however, studies have shown that TA has an inhibitory effect on ovulation (Carson 1977; Cunningham et al 1978).

The results of testing during cycle 4 also show oscillations from day to day across the cycle, with little sign of any pattern. Again, these data may be affected by corticosteroids, as it known that adrenal insufficiency can be observed for a significant time following steroid cessation. This effect, which is dose- and time-dependant, begins with an inhibition of the hypothalamus and culminates in true atrophy of the adrenal cortex (Downie et al 1978; Bondy 1985; Labhart and Martz 1986). Therefore, it is not unreasonable to conclude that following 4 weeks of taking high dose oral prednisolone, the consequences of hypothalamus inhibition will in turn have an effect on the pituitary gland (which controls the menstrual cycle hormones). However, how exactly corticosteroids interfere with the hormonal control of the menstrual cycle is still unknown (Diczfalusy and Landgren 1977).

It is evident that the variability of k' was less during cycle 1 (CV = 15.8%) compared with cycle 2 (CV = 27.2%), cycle 3 (CV = 34.4%) and cycle 4 (CV = 16.9%). The increase in variability in cycle 2 following cycle 1, may have been due to observer fatigue as the scatter measurements were taken consecutively over 72 days. Even though the subject was allowed a 'non-testing' month before commencing cycles 3 and 4, the variability in light scatter during these cycles is still relatively high, particularly so for cycle 3. However, it is possible that measurements of light scatter were influenced by ingested corticosteroids resulting in a larger daily spread of k' values.

6.18 Discussion of Chapter 6

The studies in Chapter 6 reveal that the light scattering characteristics of the eye do not remain constant when measured throughout the day or from day to day. Studies 1 and 2 show that there is an increase in straylight when measured immediately following overnight sleep. The most likely cause of the increase in light scatter is corneal oedema. The results of studies 3 and 4 (in which subjects were patched until testing commenced) confirm that there is an increase in CT as result of prolonged lid closure.

Although increased CT following overnight sleep has been demonstrated by numerous researchers (Mandell and Fatt 1965; Gertsman 1972; Hirji and Larke 1978; Fujita 1980; Mertz 1980; Kiely et al 1982; Harper et al 1996), none have investigated the relationship between intraocular light scatter and increases in CT. Furthermore, no study has investigated the full scatter function as measured by the P_SCAN 100 scatter apparatus. In the present study, large inter-subject variations in the extent of thickening were observed, a finding reported by other authors. The findings of this study are in agreement with Harper et al (1996) who reported a mean overnight swelling of 5.5% (range of 1.9 - 12.6%). In addition, Harper et al (1996) showed that the magnitude of the overnight swelling differed on consecutive days for any particular individual. The wide variety of physiological response levels for any available oxygen tension has been reported by several workers, mainly in relation to contact lens wear (Mandell and Fatt 1965; Holden et al 1983; Holden et al 1984). The high variability in the oedematous response is in line with previous findings, namely, that corneal oxygen distribution is widely distributed between individuals (Larke et al 1981; Quinn and Schoessler 1984).

During sleep, closure of the lids prevents normal levels of atmospheric oxygen from reaching the cornea. As a result, the partial pressure of oxygen falls from 155 mmHg (partial pressure of atmospheric oxygen) to 55 mmHg (partial pressure of the oxygen in tarsal conjunctival capillaries) (Fatt and Beiber 1968). Such changes cause the cornea to be subject to both internal circadian changes, and also changes in the external environment. In the absence of the optimum amount of oxygen, the cornea swells due to tonicity changes in the tears, resulting in hypoxia. Corneal metabolism is compromised, and hence lactic acid accumulates. Glycogen depletion follows, resulting in the inability of the endothelial cell layer to actively transport water out of the cornea at the usual rate (Maurice 1969). As a consequence, less water is removed from the cornea per unit time than is the case when the cornea is exposed to air. The excess water that remains is absorbed by the mucoid ground substance of the cornea. This results in swelling and hence an increase in CT as a result of the increased space between the lamellae of the stroma.

The mechanisms that cause a reduction in corneal swelling following patch removal are less clear. Upon opening of the eyelids there is an increase in oxygen uptake by the corneal endothelial layer, and a change in tonicity of the tear film, from hypotonic to hypertonic. As an osmotic balance between the endothelium and the epithelium no longer exists, water flows passively from the cornea into the tears, causing the cornea to become dehydrated. This results in a thinner cornea. Evaporation is prevented during lid closure, and the tear film remains hypotonic relative to the cornea (Mishima and Maurice 1961). Hence, the osmotic pressure becomes more or less balanced between the adjacent layers, excess water is no longer passively withdrawn from the cornea, and the thinning no longer occurs. The net result is a thinning of the cornea following opening of the eye, and a thickening upon closure. This finding was first noted by Mishima and Maurice (1961) in a study using rabbit corneas. The change in thickness upon opening and closing of the eye amounted to approximately 0.015 mm - about 4% of the total thickness. Mishima (1965) later examined the human cornea and determined that CT reduced by approximately 0.010 - 0.015 mm upon opening of the eye, corresponding to a 2 to 3% change in CT. This finding was later confirmed by Mandell and Fatt (1965), and also by Hirji and Larke (1978), who attributed the corneal thinning following sleep to evaporation of water from the tears.

An additional cause of the changes in CT following sleep is an increase in the rate of corneal metabolism during the waking hours of the day (Gertsman 1972). The net effect of this change in metabolism is to allow the endothelial layer to actively transport water out of the cornea at an increasing rate. As the day progresses, an increasing amount of water is removed from the corneal tissues per unit time and the cornea continues to thin (Gertsman 1972). This theory does not account for the diurnal changes in CT that occur in the mid afternoon reported by certain authors (Peterson 1968; Fujita 1980). Instead, this may be related to fluctuations in endogenous hormone levels during the day (Kikkawa 1974; Fujita 1980).

Tear film evaporation is also thought to be subject to diurnal variations (Tomlinson and Cedarstaff 1992). Tomlinson and Cedarstaff (1992) investigated nine subjects (age range 21-37 years), using resistance hygrometry at two hourly intervals. Each subject slept for two consecutive nights in the laboratory. On the day of measurement, the subjects were awakened and immediately underwent testing. Measurements were repeated at two hourly intervals for a total of fourteen hours. The evaporation rate was found to be low on initial waking, but increased rapidly during the first two hours of eye opening, to a level that was maintained for the rest of the waking day (Tomlinson and Cedarstaff 1992).

The integrated straylight parameter k' , was sensitive to the increases in CT that resulted from prolonged lid closure. The finding that changes in CT affect forward light scatter measurements has previously been reported by Elliott et al (1993a) (section 6.6.3) using the van den Berg straylightmeter. In the latter study, glare test results returned to baseline values approximately 35 minutes after thick hydrogel contact lens removal (following three hours of patching). At this stage, the cornea was still swollen by approximately 8%. This result is similar to the findings of Carney and Jacobs (1984) in a study of the sensitivity of glare tests to hypoxia-induced oedema. The results of Chapter 6 confirm these findings for measures of the full scatter function. i.e the integrated straylight parameter k' . In fact, k' may be more sensitive to CT changes than k (as measured by the van den Berg straylight meter), as increases in k' were evident when CT had increased by 7% (Study 3, Subject 2). In the study conducted by Elliott et al (1993a) the average time for the straylight meter scores to return to baseline was 86 minutes, whereas the pachometry values returned to baseline after 60 minutes. From Study 3, straylight scores seemed to closely follow the CT

decreases following patching, however, measurements were only taken on an hourly basis (due to the time taken for the complete set of measurements), and it is therefore difficult to evaluate the precise time of the return to baseline scores. Linear regression revealed a low r^2 value between CT change and straylight in the study by Elliott et al (1993a), and it was concluded that the straylight meter did not detect increased forward light scatter which resulted from stromal swelling. This confirmed the earlier reports of Lambert and Klyce (1981), Carney and Jacobs (1984) and Cox and Holden (1990). In fact, Cox and Holden (1990) estimated that there was no change in light scatter as a result of stromal oedema until the CT was increased by as much as 10%. The authors suggested that the straylight scores primarily reflected oedema-induced changes in the epithelium caused by the contact lens (Zucker 1966; Carney and Jacobs 1984; Carney 1990; Cox and Holden 1990). Therefore, in the current study, the increase in light scatter observed is most probably due to epithelial oedema in response to hypoxia. Although the corneal stroma is responsible for the majority of backward light scattering from the cornea during oedema, epithelial changes tend to produce increased forward scatter, as opposed to back scattered light (Feuk and McQueen 1971). For light to be scattered, the index of refraction around the epithelial cells must be different from that of the cells themselves. Studies have shown that the epithelial thickness does not change during acute hypoxia, indicating that epithelial oedema occurs without any uptake of water from outside the epithelium (Wilson and Fatt 1980). Hypoxia stimulates lactate production, and leads to an increase in lactate concentration between the basal cells (Lambert and Klyce 1981). Being osmotically active, lactate draws water out of the cells, increasing the extracellular spaces. As this space has little protein relative to the cells, it has a lower RI than the cells and light becomes scattered at its interface (figure 6.21).

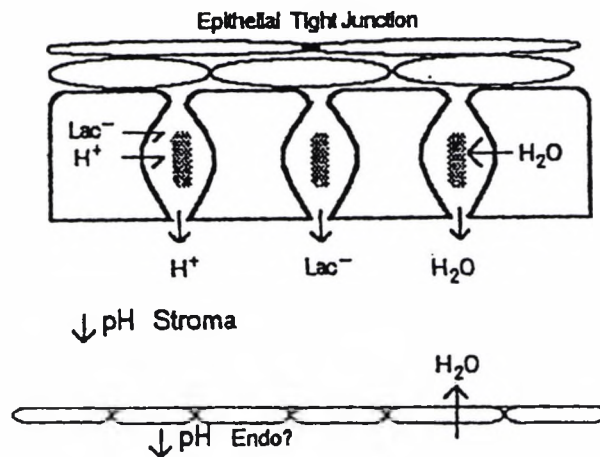


Figure 6.21 - Schematic drawing of the cornea showing the location and progress of lactate and H^+ produced by the epithelium. Lactate and H^+ leave the epithelium via lactate- H^+ cotransporters and diffuse toward the stroma and the aqueous. Accumulation of lactate between the epithelial cells and the stroma osmotically draws fluid into these spaces. In the epithelium, this leads to increased light scatter, and in the stroma, it causes swelling. The pump function of the stroma may also be affected as the metabolic H^+ ions lead to a drop in stromal pH levels (Tomlinson 1992).

Although the presence of epithelial oedema appears to be an adequate explanation of the increased light scatter results of Subjects 1 and 2, it does not appear to fully explain the results from Subject 3 who exhibited little increases in scatter or CT following patching. This is likely to be due to the fact that hypoxia is highly dependant upon the oxygen requirements of the individual. It is thus proposed that certain subjects (in the present study, Subject 3) require lower levels of oxygen tension than other subjects (Subjects 1 and 2), in order to maintain normal corneal conditions. The high variability in the oedematous response observed in this experiment is a feature of the widely distributed population of corneal oxygen consumption in human subjects (Larke et al 1981; Holden et al 1984; Quinn and Schoessler 1984). The low level of corneal oedema evident following eye patching and overnight sleep in the subject that was more resistant to hypoxia did not have a detrimental effect on measures of light scatter. Despite this, it is clear that that in order to

take scatter measurements longitudinally, a certain length of time must elapse after waking before measurements are taken in order to minimise the changes in CT that result from lid closure.

Study 5 shows that the level of scattered light in the eye fluctuates on a day-to-day basis in this female subject. The apparent cyclical nature of the fluctuation seen (particularly in cycle 1 and less so in cycle 2) suggests that a cyclical variation in intraocular light scatter may exist, at least in females. An obvious cause for this cyclical variability is the menstrual cycle. There was a greater day-to-day variation, but without a cyclical trend that was related to landmarks in the menstrual cycle, in cycles 3 and 4. These measurements may have been affected by the high dose oral steroids taken by this subject during cycle 3. This may not contradict the theory that scattered light in the female subject was influenced by her normal menstrual cycle, as it is known that steroids affect the hormonal fluctuation associated with menses. That said, there are numerous other potential causes for the observed fluctuation in light scatter. Further studies are needed to investigate the nature of any cyclical change in straylight. Furthermore, without testing male subjects, it is difficult to ascertain whether the fluctuations in k' differ between gender. The aim of Chapter 7 was to further explore the changes in light scatter that result when measurements are taken longitudinally in female and male subjects.

6.19 Conclusions

The level of light scatter in the eye changes during the course of a day. The changes in scatter that occur in the first hours after waking are the result of normal changes in the eye following prolonged lid closure during sleep. When pachometry measurements are taken, CT is seen to increase following overnight sleep and also following patching. The level of corneal oedema produced by different subjects showed individual variations in corneal hydration control. Increases in CT were accompanied by increases in forward light scatter as measured by the P_SCAN 100 scatter apparatus. The results revealed the importance of the timing of measurements, i.e. in order to obtain an accurate assessment of the changes due to either anterior segment eye disease or contact lens wear, each subject must have been awake for at least four hours before testing. Therefore, in order to minimise the effect of overnight sleep, subsequent investigations were conducted between the hours of 12:00 and 14:00.

Light scatter in the eye was also seen to fluctuate when longitudinal measurements were taken at the same time of day. The results were obtained from one female, and a possible cyclical trend was noted during cycles 1 and 2 which may be related to the subject's menstrual cycle. These results had implications for the recruitment of female subjects in subsequent studies on contact lens wearers. Cycles 3 and 4 revealed a greater variation with little sign of a cyclical trend related to the menstrual cycle. This may have been the result of concomitant corticosteroid administration. The hypothesis that intraocular light scatter is influenced by the female hormonal cycle is tested in Chapter 7.

CHAPTER 7

The effect of the menstrual cycle on the light scattering characteristics of the eye

7.1 Introduction

A possible cyclical variation in light scatter in one female subject was observed in Chapter 6. There was a need to investigate this further because, if confirmed, a cyclical variation has implications for patient inclusion in later studies in this thesis involving contact lens wearers.

The body is exposed to significant changes in the relative concentrations of endogenous circulating hormones. These hormones affect the central nervous system, producing changes in ocular parameters, which in turn may influence visual performance. The most significant hormonal fluctuations affect females during the menstrual cycle. There is widespread agreement concerning the nature of the hormonal changes which occur during the menstrual cycle. However, studies of physical and psychophysical changes (such as those relating to vision) have been few and controversial. What is clear, is that certain women experience pronounced changes in the quality of vision and other ocular symptoms at various times during the menstrual cycle (Bergin 1952).

An understanding of the normal hormonal fluctuations and associated physical changes which occur during the female reproductive cycle is necessary, so that the possible causes for changes in the quality of vision and other ocular variations (including light scatter) during the menstrual cycle may be considered.

7.2 The female reproductive cycle

The normal human reproductive cycle lasts 28 (\pm 4) days (Franz 1988) and may be described by two cycles, namely the ovarian and uterine (Marieb 1989). Figure 7.1 shows a diagrammatic summary of the changes in hormone levels that occur during the menstrual cycle.

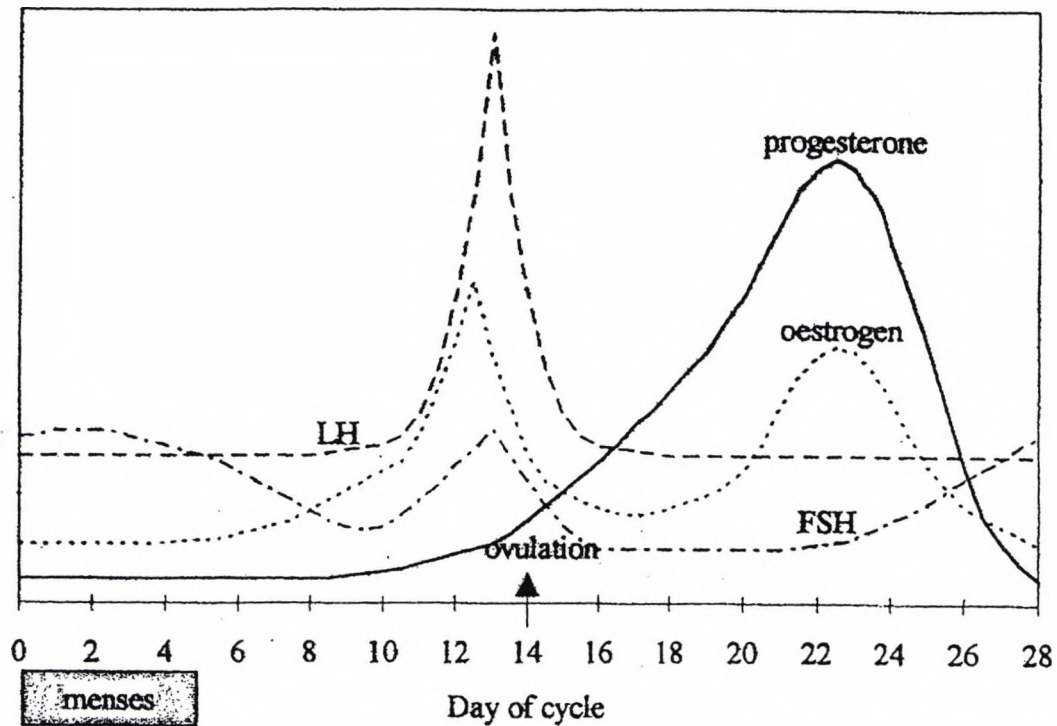


Figure 7.1 - Schematic summary of hormone fluctuations throughout the normal menstrual cycle (Guttridge 1994).

The **ovarian** cycle describes ovulation and its hormonal regulation, and consists of three phases - follicular (days 1 - 10), ovulatory (days 11 - 14) and luteal (days 15 - 28).

During the follicular phase, follicle stimulating hormone (FSH) and luteinizing hormone (LH) become released from the anterior pituitary under the influence of increasing gonadotrophin releasing hormone (GnRH) from the hypothalamus. Increasing levels of these hormones stimulate the development of primordial follicles that are present in the ovary, one of which undergoes complete maturation to become a Graafian follicle. The matured Graafian follicle contains an ovum, which is the female gamete, and the remaining immature follicles degenerate in the ovary.

As the follicle matures it begins to secrete oestrogen into the blood. Initial low levels of oestrogen have a negative feedback effect on the hypothalamus, decreasing the output of FSH and LH, which prevents additional development of follicles. The levels of oestrogen increase still further until a threshold is reached, at which a positive feedback to the hypothalamus is triggered resulting in a sudden burst of LH. LH triggers release of the

ovum into the peritoneal cavity (termed ovulation), where it begins its journey along the fallopian tube. A small quantity of FSH is also released, however, its role at this stage is unclear.

The ruptured follicle that remains collapses to form the corpus luteum, which temporarily acts as an endocrine organ, predominantly secreting progesterone, but also some oestrogen, throughout the early luteal phase. Increasing levels of these hormones exert a powerful negative feedback on the anterior pituitary, inhibiting further release of LH and FSH, and preventing development of follicles. The corpus luteum degenerates after about ten days as the concentration of LH falls in the luteal phase, and with it levels of oestrogen and progesterone fall. This reverses the inhibition of FSH and LH secretion, and the reproductive cycle begins once more.

The **uterine cycle** describes changes occurring in the uterus and the ovary (that is, the reproductive organs), which are broken down into three distinct phases, namely, the menstrual (days 1 - 5), proliferative (days 6 - 15) and secretory (days 16 - 28) phases.

The functional endometrial layer of the uterus wall detaches during the menstrual phase resulting in expulsion of tissue and blood through the vagina (i.e. the "menstrual flow"). Increasing oestrogen levels become released from the ovary, which leads to repair of the endometrium of the uterus wall. At the same time, the spiral arteries become more numerous and tubular glands are repaired. Ovulation occurs at the end of this proliferative phase and increasing levels of progesterone from the corpus luteum cause further elaboration of the uterus wall throughout the secretory phase. Failure to achieve fertilisation of the ovum causes a fall in progesterone levels, depriving the endometrium of its hormonal support, and leading to endometrial cell death. Day 28 of the cycle is characterised by rapid dilation of endometrial arteries causing rupture of the fragile capillary beds, triggering menstrual flow once more.

This two-cycle description deliberately over-simplifies the reproductive cycle, for ease of understanding. In fact, the ovarian and uterine cycles are intimately linked, with changes in the uterus being dependent upon the hormonal fluctuations of the endocrine system. Indeed, most research in this area considers the cycle as being a single cycle, referred to as

the menstrual cycle. A summary of the physiological and physical changes that occur during the various phases of the cycle is shown in table 7.1.

7.3 Ocular physiological changes

As stated, the female body experiences dramatic changes in the levels of circulating hormones during the female cycle. Therefore, it is unsurprising that these hormones cause marked changes in systems that are apparently distant from the reproductive organs. The effects on ocular physiology are less well documented, but are summarised in the sections that follow.

7.3.1 Corneal parameters

It has been suggested that changes in visual performance across the menstrual cycle may be due to increased corneal water retention or corneal oedema (Ward et al 1978). As discussed in section 6.3, such changes in corneal hydration and oedema may be closely monitored by measurements of CT and scatter.

7.3.1.1 Corneal thickness

Studies of the effect of the menstrual cycle upon CT are few and controversial. It has been suggested that both oestrogen and progesterone have an effect on CT, as each are known to influence the retention of salt and water in the body (Ward et al 1978). However, it is generally believed (albeit without experimental support) that oestrogen alone leads to corneal fluid retention and thus to corneal oedema (Soni 1980).

Manchester (1970) observed hydration of the cornea across the menstrual cycle in six normally menstruating women, and one female taking oral contraceptives, using a Haag Streit pachometer. The study concluded that CCT did not vary significantly during the menstrual cycle. In contrast, Leach et al (1971), using the Donaldson pachometer, reported that the time course of CCT changes closely followed the plasma concentrations of oestrogen and progesterone reported in the literature. Hence, it was claimed that the cyclical behaviour of CT is bimodal in nature, increasing during the follicular phase, decreasing at or just following ovulation, and then increasing once more during the luteal phase.

Table 7.1 - Summary of the events of the hormonal human menstrual cycle

Day	Ovarian cycle	Uterine cycle	Hormonal fluctuations	Physical changes
1	follicular	menstrual	Increasing levels of FSH and LH from anterior pituitary.	Menstrual flow
2				Development of primary follicle in ovary.
3				
4				
5	proliferative	Oestrogen secreted from maturing follicles gives negative feedback to hypothalamus preventing the release of FSH and LH, thus preventing further follicle development.	Repair and proliferation of endometrium.	
6				
7				
8				
9	ovulatory	proliferative	High levels of oestrogen lead to positive feedback to anterior pituitary and subsequent surge of LH.	Maturation of Graafian follicle in ovary.
10				
11				
12				Ovulation
13	luteal	secretary	Progesterone and oestrogen secreted by corpus luteum.	Corpus luteum formation in the ovary.
14				
15				
16				Further elaboration and maturation of endometrium.
17	luteal	secretary	Decrease in LH and FSH levels results from negative feedback and further follicle development inhibited.	Breakdown and reabsorption of corpus luteum.
18				
19				
20				
21	luteal	secretary	Decreasing levels of progesterone and oestrogen end the blockade of FSH and LH.	Endometrial wall begins to break down.
22				
23				
24				
25	luteal	secretary	Decreasing levels of progesterone and oestrogen end the blockade of FSH and LH.	Endometrial wall begins to break down.
26				
27				
28				

El-Hage and Beaulne (1973) (using optical pachometry with a millimetre rule and pointer modification) measured the cornea at the centre, 2.5 mm nasal/temporal and at 5 mm nasal/temporal in eight female subjects during the menstrual cycle. Three measurements were taken - (i) at the time of the menstrual flow, (ii) three days after, and (iii) five days before the end of the menstrual cycle. The study noted extensive variation and fluctuation between the different subjects, and no increases or decreases in CT were found centrally or peripherally. It was concluded that no significant variation of CT occurred during menstruation. However, individual subjects demonstrated a trend towards increased CT during the first five days of the menstrual cycle.

Hirji and Larke (1978) using topographic pachometry, enlisted four females in order to investigate CT changes during the menstrual cycle. The thickness of nine corneal positions was recorded for each subject until each had completed one menstrual cycle. Each subject's cycle was divided into nine equal fractions. No statistically significant relationship between CT and the menstrual cycle was evident.

Feldman (1978) investigated CT using the Haag Streit pachometer in eleven normal women between the ages of 19 and 28 years. The subjects were examined once each day for a complete menstrual cycle. CT measurements and blood plasma samples were taken. The blood samples were examined so that the levels of lutinizing hormone, follicle stimulating hormone, esterone, estradiol, progesterone and testosterone could be determined. The author suggested that a thinning of CT occurred prior to ovulation. However, no statistically significant relationship between the levels of circulating sex hormone or the different phases of the menstrual cycle and CT could be found.

Soni (1980) studied twelve females taking combined oral contraceptives, a control group consisting of eight females with normal cycles and also two males. CCT measurements (using optical pachometry) were taken an average of 15 times, at the same time of day, over a period of two months. The measurements were initiated on day one of the menstrual cycle and continued for at least one full cycle. Of the eight women with normal cycles, the thickest cornea was evident on the first or the last day of the menstrual cycle, with minimum CCT recorded between days seven and thirteen. After this period, the cornea steadily increased in thickness, until it reached a maximum on day 28. The thinnest CCT

measurement corresponded to the time of ovulation, a result which is in agreement with Feldman (1978). A day to day variation in CCT was also apparent (mean: approximately 14% for females and 8% for males).

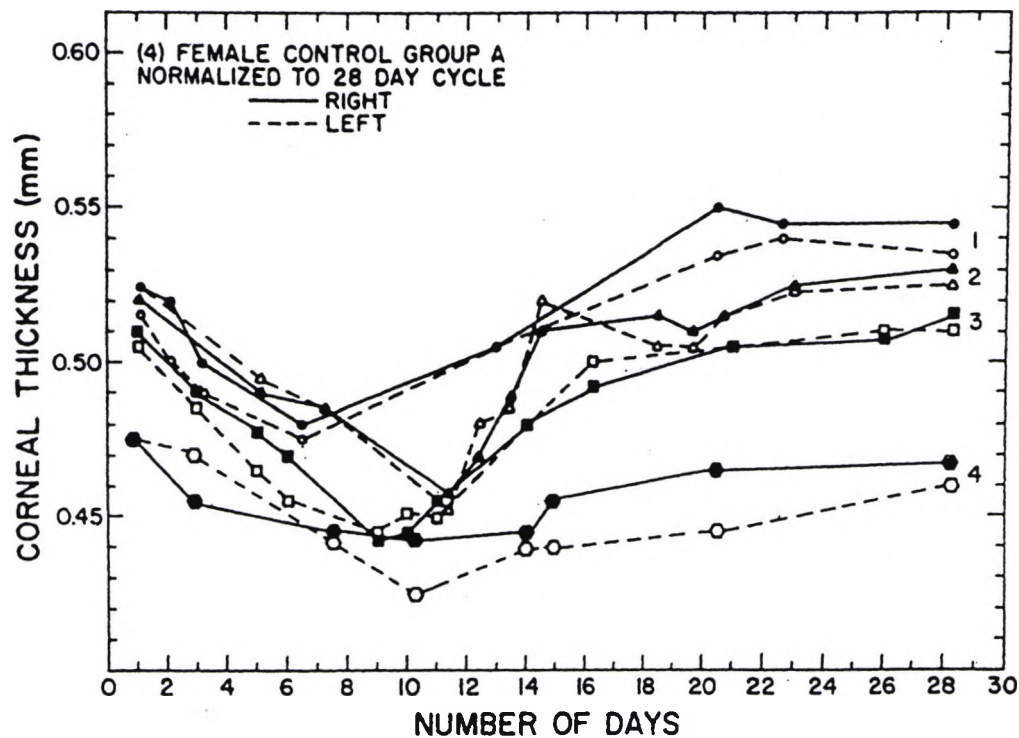


Figure 7.2 - Changes in CCT in the female group during a complete menstrual cycle (Soni 1980).

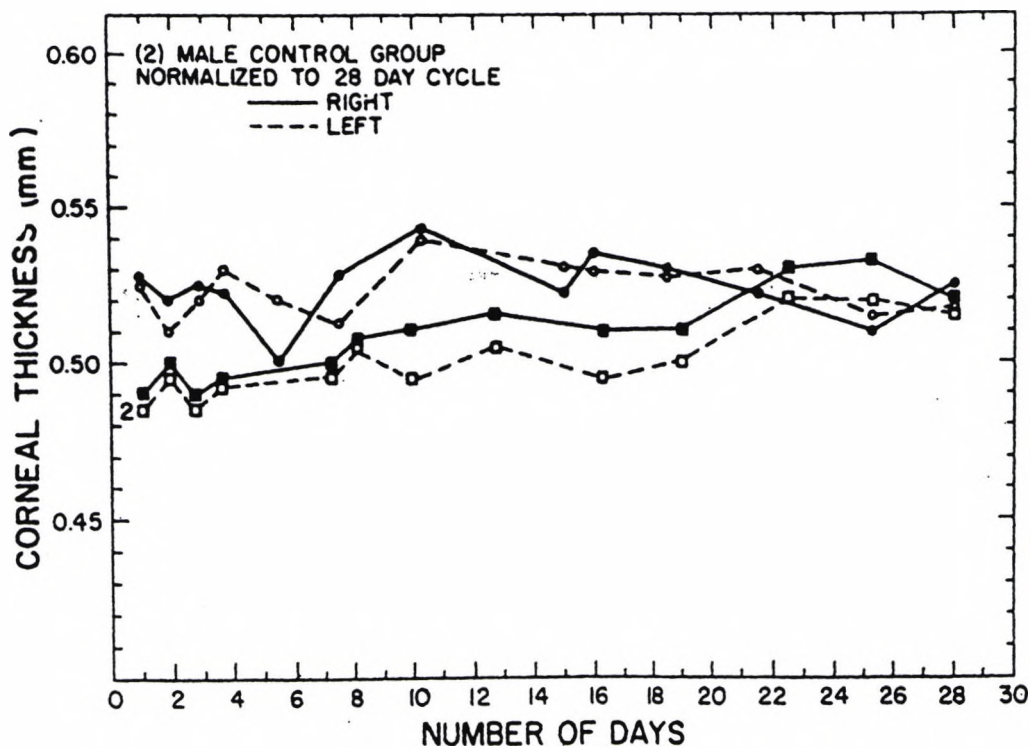


Figure 7.3 - Changes in CCT seen in a male group over a period of 28 days (Soni 1980).

Kiely et al (1983) attempted to study accurately the effect of the menstrual cycle on CT by closely controlling such factors as time of day, and the exact timing of the menstrual cycle. Two study protocols were employed, each using the Haag Streit pachometer. The first involved the study of six women with measurements taken on week days for at least one full menstrual cycle. Pachometry measurements were taken together with urine sampling for endogenous hormones. In the second study, measurements of CT were taken over three consecutive cycles for two subjects. The results showed that corneal thickening occurred at menstruation and at ovulation, followed by corneal thinning. Corneal thickening also occurred during the four days after ovulation. The study concluded that increases in CT accompany rises in endogenous oestrogen levels, suggesting that the cornea is an oestrogen sensitive tissue.

7.3.1.1.1 The effect of the contraceptive Pill on corneal thickness

Interest in the ocular implications of the administration of oral contraceptives was first stimulated by Cogan (1965). The Pill contains varying amounts of oestrogen and progesterone, and when taken daily the resulting elevation in the hormone levels inhibits the production of the gonadotrophic hormones from the pituitary. In particular, the absence of LH prevents ovulation (Toole and Toole 1989). Studies have shown that oral contraceptives may produce corneal intolerance to hypoxia (Feldman et al 1969) and corneal oedema (Davidson 1971). Soni (1980) reported that female subjects taking oral contraceptives failed to show a cyclic variation in CT, and instead yielded similar results to those obtained in male subjects. Measurements were taken prior to and following the administration of both high and low strength progesterone-based contraceptives. CT measurements indicated a 'stabilisation' effect, with less variation in CT being observed, compared to women who were not taking the Pill. The stabilisation of CT measurements took longer to become evident in females taking low dose Pills. The study concluded that there was a correlation between both the gonadotrophin and ovarian hormones, and CT.

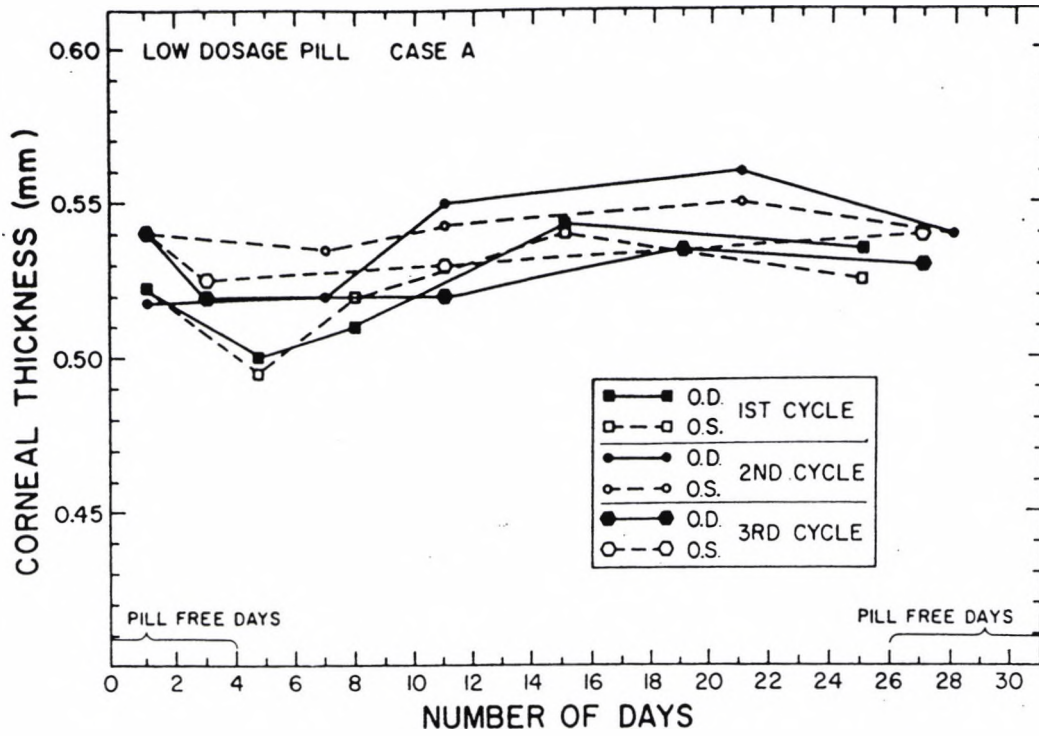


Figure 7.4 - A representative figure of the corneal trends seen in females on low dosage pills (Soni 1980).

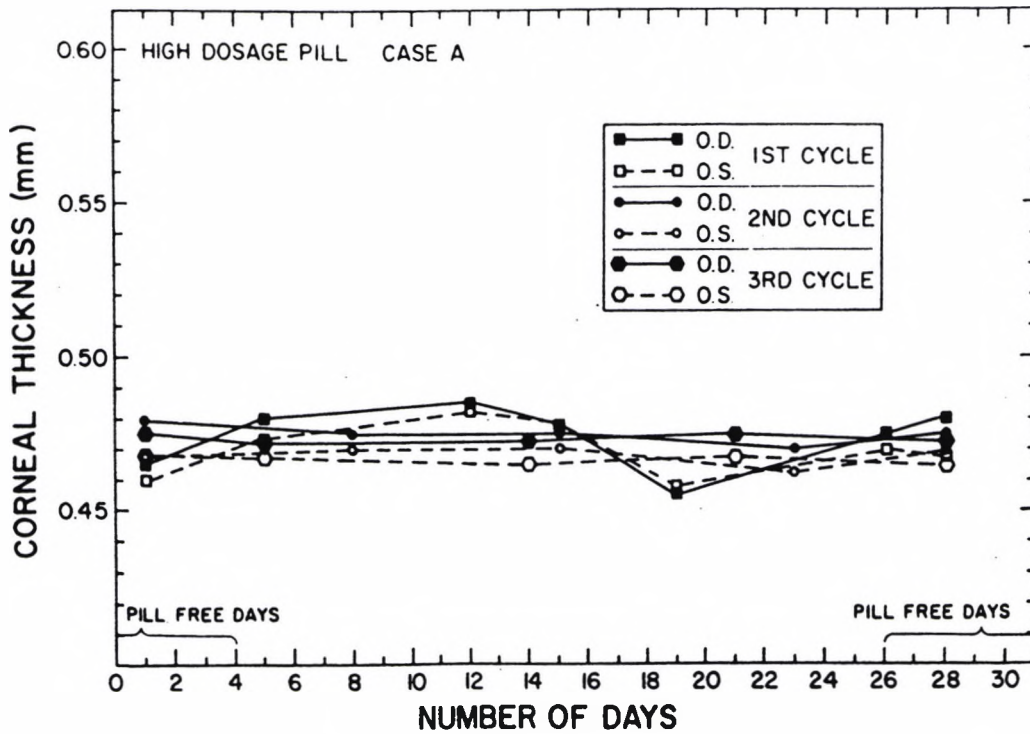


Figure 7.5 - A representative figure of the corneal trends seen in females on high dosage pills (Soni 1980).

Studies of the change in CT across the menstrual cycle are controversial, and it is difficult to compare individual studies, due to differences in methodology and instrumentation. In addition, the drawing of firm conclusions is complicated by the fact that, for quite understandable methodological reasons, small sample sizes are used. In fact, Hirji and Larke (1978) calculated that, for their methods of measurement, at least 122 subjects would need to be examined for the results of such experiments to demonstrate statistical significance.

7.3.1.2 Corneal curvature

Changes in corneal curvature during the menstrual cycle have been documented during studies of CCT in the assessment of corneal hydration. Whilst Manchester (1970) and Leach et al (1971) failed to demonstrate changes in central keratometry, Kiely et al (1983) observed steepened central curvatures in both horizontal and vertical meridians during early stages of the cycle. Using a Bausch and Lomb keratometer, the authors noted a flattening following ovulation. However, a more recent study (using the EyeSys (TM) Corneal Analysis system) showed no detectable temporal effect on corneal curvature measurements with the menstrual cycle (Oliver et al 1996). The authors concluded that the sensitivity of either method was insufficient to detect such small cyclic variations as occurred, or that corneal curvature did not change during the menstrual cycle.

7.3.1.3 Corneal sensitivity

Millodot and Lamont (1974) noted an increase in CTT (corneal touch threshold), representing a fall in corneal sensitivity, during the premenstrual phase of nine normally menstruating females. Such findings were not observed in five females taking the contraceptive pill or male control subjects. As such, the results were indicative of a relationship between corneal sensitivity and the menstrual cycle. Changes in corneal sensitivity during the premenstruum were attributable to either an increase in water retention at this time, or to an increase in IOP. Subsequent studies employed electromagnetic aesthesiometry to determine more accurate and reproducible daily CTT measurements, yet failed to repeat the finding of premenstrual lowering of corneal sensitivity (Riss et al 1982).

7.3.2 Intraocular pressure, aqueous output facility and glaucoma

Fluctuations in IOP and outflow facility have been observed in normally cycling, non-glaucomatous women. For instance, Salvati (1923) noted an increase in IOP during the menstrual phase, using the Schiøtz tonometer in both eyes of nine women, compared with the two days pre- and post-menstrually (Salvati 1923). Subsequent research showed that outflow facility increases occurred, with associated decreases in IOP, during times of elevated oestrogen and/or progesterone (Paterson and Miller 1963).

Feldman et al (1978) attempted to correlate anterior chamber (AC) depth and IOP fluctuations across the menstrual cycle with changes in endogenous hormone levels. No significant change in IOP or AC depth was determined during the cycle, and no statistically significant correlations were observed. Later studies also failed to correlate serum progesterone levels, IOP and aqueous flow rate across the menstrual cycle (Green et al 1984; Gharagozloo and Brubaker 1991).

Changes in IOP during the menstrual cycle may be different in glaucoma patients. For instance, simultaneous rises in IOP (as measured by applanation tonometry), blood pressure and body weight have been recorded in the pre-menstrual or menstrual phase in fourteen women with glaucoma (Dalton 1967).

7.3.3 Tear production and consistency

Discomfort and poor vision have been reported by female contact lens wearers on becoming pregnant, and upon initiation of oral contraceptives. These symptoms have been attributed to excess mucus formation in tears, and a reduction in the sebaceous component, which impairs the lubricant qualities of the tears (Ruben 1966). If such changes are the result of hormonal variations (oestrogen levels are low and progesterone levels are high during pregnancy), then it is likely that similar variations in the quality of the tears may also occur during the menstrual cycle.

The relationship between tear production and the menstrual cycle was investigated by Feldman et al (1978), who attempted to record tear production throughout the menstrual cycle in 10 women, using the Schirmer tear test. Unfortunately, the results were so

variable that the only conclusion drawn was that the test itself was unreliable for assessing tear production.

During pregnancy or oral contraceptive use (Candela et al 1989), the lacrimal secretion, and in particular its mucus components, show particular modifications, which were attributed to the influence of oestrogens and progesterone. A cytological examination of the conjunctiva revealed an increased and modified mucus secretion, but a normal goblet cell number (Candela et al 1989). Therefore, changes in the levels of the female hormones involved in the menstrual cycle may cause ocular discomfort or intolerance to contact lenses. A recent study into conjunctival goblet cells in different hormonal conditions was carried out by Aragona et al (1998). This study investigated four groups of rabbits (males, dioestrous females [low levels of both oestrogen and progesterone], oestrous females [high levels of oestrogen and a concomitant peak of LH and progesterone] and pregnant [mainly high levels of progesterone]) to determine whether gender, and/or different physiological conditions could influence conjunctival goblet cell structure and ultrastructure.

After examination of the external genitalia, each female was paired with a male. The does which showed negative sexual behaviour and had white external genitalia were classified as dioestrous females. The animals which accepted males and showed red hyperaemic and oedematous external genitalia were classified as oestrous females and were submitted to experimental procedure two hours after mating. In all the animals, a biopsy was obtained from the bulbar conjunctiva and light microscopy, transmission electron microscopy and morphometry were performed. In males and oestrous females, the intracytoplasmic goblet cell secretory granules were filled with granular material, whilst in pregnant and dioestrous females the granules were formed by a more homogenous and dense secretory material. The number of goblet cells was not statistically different in the groups studied, however, the goblet cells of pregnant animals had the largest mean diameter. The mean area of the secretory granules was larger in dioestrous females, whilst their optical density was highest in pregnant animals. These observations indicate that the morphology of conjunctival goblet cells varies according to gender and under different physiological conditions (e.g. pregnancy). The study concluded that the qualitative changes in mucin observed in the rabbit during pregnancy could explain the ocular discomfort and intolerance to contact lens

wear (Candela et al 1989) which can occur in humans during pregnancy and with oral contraceptive use.

- The findings of this study may be relevant to the present study of the effect of the menstrual cycle on the light scattering characteristics of the eye, as variations in the amount of mucus production and also changes in its consistency may in turn produce variations in levels of light scatter.

7.3.4 Conjunctiva

The conjunctival epithelium is an important source of mucin in the eye (Srinivasan et al 1978). Electron microscopy of human and rat conjunctiva reveals small granules in the cytoplasm of middle and surface epithelial cells that stain specifically for mucopolysaccharides. Thus, mucus production in the eye, although mainly a goblet cell function, may also be due to the secretory action of epithelial cells. It is thought that this epithelial source may be responsible for the tenacious sticky mucus found in diseases such as keratitis sicca and Stevens Johnson syndrome (Srinivasan et al 1982).

It is well established that mucosa such as the conjunctival epithelium are oestrogen sensitive (Kramer et al 1990; Vavilis et al 1995). Kramer et al (1990) examined the conjunctiva in nine pre-menopausal females, seven post-menopausal females, two oestrogen deficient females and one male subject. Conjunctival smears were taken over 28 days, or over one complete cycle in normally menstruating women. A cyclical variation paralleling the menstrual cycle was reported, with maturational peaks at day 11 or 21 of the menstrual cycle. Mature epithelial surfaces were characterised by a preponderance of superficial cells, representing a hyperestrogenic state. Immature epithelial surfaces were characterised by parabasal and intermediate cells, representing a hypoestrogenic state. The conjunctiva was at its most mature around ovulation, when oestrogen levels were high. In men and post-menopausal women there was no apparent peak in maturity. Kramer and co-workers (1990) suggested that conjunctiva not undergoing maturational change may be more susceptible to aqueous deficiency of the tear film, and thus to subsequent dry eye conditions (such as keratoconjunctivitis sicca (KCS)). In normally menstruating women, aqueous deficiency may also be linked to mucus deficiency. If there is no hydrophilic mucal covering of the cornea, it will be unwettable and therefore there will be no stable aqueous layer to the tear film. Indeed, an unpublished study conducted at City University

which measured the wetting angle of rigid contact lenses during a 28 day period showed that there was a marked increase in the wetting angle at ovulation i.e. a decrease in wettability. This phenomenon was subsequently reversed following ovulation. The results of the study suggest that mucus levels fall as oestrogen levels increase and as maturation of the conjunctival epithelium occurs. This effect is analogous to cervical mucus, which undergoes a similar change at this time, becoming less viscous. In fact, work by Vavilis et al (1995) demonstrated that conjunctival smears of menstruating women revealed cyclical maturation changes which correlated well with the changes of the vaginal epithelium. Conjunctival and vaginal smears were taken on a daily basis in 15 women with ovulatory cycles, 10 post-menopausal women, and 12 pregnant women. Pregnant women and post-menopausal women had no such maturational change in the conjunctival epithelium. Such results show that changes in the nature of the conjunctiva may be directly related to changes in circulating oestrogen and progesterone levels.

7.3.5 Pupil diameter

There have been few investigations of the relationship between pupil diameter and the menstrual cycle. One such study (Barris et al 1980) assessed the dark-adapted pupil across four consecutive days around ovulation during the menstrual cycle of three normally menstruating females. No significant change in pupil diameter was found across these days, a finding that was subsequently corroborated by Guttridge (1994).

7.3.6 Other ocular changes

The menstrual cycle has been implicated as a potential factor in the timing of other ocular conditions and symptoms, e.g. uveitis (Bell 1989) and glaucoma (Dalton 1967). It is also known to produce fluctuations in the symptoms of systemic conditions such as migraine and epilepsy, which are associated with ocular changes (Logothetis et al 1959; Lehtonen et al 1979).

7.4 The effect of the menstrual cycle on visual performance

In the small body of research on visual changes across the menstrual cycle, individual studies are often difficult to compare due to differences in methodology, population sizes, visual modality under examination, menstrual cycle phase designation and the method of statistical analysis method used. Despite this, certain observations can be made, although

Table 7.2 - Summary of visual changes across the menstrual cycle

Key: NC = women with normal cycles, OC = women taking oral contraceptives, M = men, P = pregnant women and BF = breast feeding

Visual task	Results	Author	Subjects	Days/phases examined
Two flash fusion threshold	Decrease in sensitivity premenstrually	Kopell et al (1969)	8NC	Days 3, 14, 26, 28 of 2 cycles averaged into 1 cycle
	“	DeMarchi and Tong (1972)	20NC	3x over 1 cycle, in premenstrual, menstrual and postmenstrual phases
	“	Braier & Asso (1980)	36NC	Between subjects design: 18S premenstrually, 18S intermenstrually
	“	Asso & Braier (1982)	36NC	As above
	Increase in sensitivity in late follicular & ovulatory phase	Wong & Tong (1974)	8NC, 20C	Days 1, 5, 10, 15, 26 of 1 or 2 cycles (only 1 cycle reported)
	“	Friedman & Maeres (1978)	21NC, 70C	3-4x over 2 or more cycles (only 1 cycle reported)
	“	Becker et al (1982)	14NC/OC	Every other day over 1 cycle
	“	Clare et al (1976)	8NC	Days 14 and 27 of 2 cycles (only 1 cycle reported)
Critical flicker fusion threshold	Increase in sensitivity premenstrually	Dye (1989, 1991)	34NC, 11OC	1-3x weekly for 4-7 weeks
Tilt after effect	Increased preovulatory with low contrast (short test duration) & high contrast (long test duration)	Symons et al (1990-91)	17NC	2x over 1 cycle, in preovulatory (days 5-13) & premenstrual (26-28)
Visual detection	Dark adapted: increased mid-cycle (ovulatory)	Diamond et al (1972)	4NC, 4OC, 4M	1x weekly for 5-6 weeks
	“	Barris et al (1980)	5NC	7 consecutive days over ovulation in 1 cycle for 6S, 3 cycles for 1S
	“	Scher et al (1981)	4NC	Days 1, 7, 14, 21, 28 of 1 cycle
	Dark adapted: decrease premenstrually, small menstrual increase	Ward et al (1978)	4NC	4x over 1 cycle, in menstrual (days 2-4), preovulatory (10-14), luteal (19-23) and premenstrual (21-30)
	Light adapted: no significant difference	Scher et al (1981)	4NC	as before
Visual pattern discrimination	Improved premenstrually	Ward et al (1978)	12NC	as before
Visual recognition	No generalised effect, better recognition of sex stimuli around ovulation	Krug et al (1994)	16NC, 16OC	3x – menstrual, preovulatory & midluteal
Letter ID & visual acuity	Dark adapted: worse in ovulatory than menstrual phase	Scher et al (1985)	4NC	2x over 1 cycle, on 1 st day of menses and on day of basal body temperature (BBT) rise
	Landolt rings: acuity better after ovulation	Jordan & Jachinski-Kruza (1986)	5NC	3x weekly for 6 weeks
Contrast sensitivity	Increase in sensitivity in post-ovulatory phase	Dunn & Ross (1985)	10NC, 10OC, 11M	12x over 5 weeks
	Complex relationship with menstrual cycle, with several peaks in sensitivity	Johnson & Petersik (1987)	2NC, 1M, 1BF	Daily for 32 days

Table 7.2 - Summary of visual changes across the menstrual cycle

Key: NC = women with normal cycles, OC = women taking oral contraceptives, M = men, P = pregnant women and BF = breast feeding

Visual task	Results	Author	Subjects	Days/phases examined
Visual fields	Constriction of fields premenstrually and menstrually	Finkelstein (1887)	20NC	not stated
	“	Lanfair & Smith (1974)	3NC, 2OC, 1P	3x weekly for 6 weeks
	Fluctuations in mean sensitivity of the central visual field, with an increase in sensitivity mid-cycle and decrease paramenstrually. Not found to be clinically significant.	Guttridge (1994)	18NC, 8OC, 4M	2-3x weekly for 6-10 weeks
	Constriction of red and green fields premenstrually	Lorenzetti (1926, cited Lanfair & Smith 1974)	unknown	unknown
Colour vision	Perception of yellow & green more difficult premenstrually	Lorenzetti (1926, cited Lanfair & Smith 1974)	unknown	unknown
	Anomaloscope: no reliable results	Mollon (1993)	unknown	unknown
Refraction	No change	Finkelstein (1887)	20NC	not stated
	<0.25DS myopic shift menstrually	Bergin (1952)	7NC	3x weekly over 5 weeks
Tonic accommodation	Variability greatest premenstrually & menstrually, least in ovulatory phase	Hogan (1985)	3NC	Daily over 28 days (different cycles combined)

often no firm conclusions can be drawn. A summary of visual changes across the menstrual cycle is given in table 7.2.

7.5 Aims

The results of experiments in Chapter 6 indicate that there may be a relationship between k' and the menstrual cycle. The experiments described in Chapter 7 investigate:-

- longitudinal light scatter measurements in three female subjects by way of a double blind masked study
- changes in corneal hydration during the menstrual cycle which may be related to measures of light scatter using pachometry
- longitudinal light scatter measurements in three male subjects to further explore whether scattered light is affected by the menstrual cycle.

7.6 Menstrual study design

Menstrual cycle research has been described as 'a methodological minefield with trip-wires set to ensnare the unwary researcher' (Ussher 1991). Several factors must be taken into consideration before research into the menstrual cycle is undertaken. Parlee (1980) demonstrated that prior knowledge of the study focus (i.e. the menstrual cycle), may significantly influence a subject's performance in experiments. For example, if women expect to perform badly in the pre-menstrual phase this may affect their performance as they may change their criterion levels, becoming more careful or apparently less sensitive. The use of masked studies and criterion-free experimental techniques are thus employed in order to reduce this problem.

- The present study was masked to ensure that the subject was unaware of the study focus, and that the examiner had no prior knowledge of the subject's position in their menstrual cycle.

7.6.1 Cycle phase designation

Inter-subject variability in the duration of the menstrual cycle makes statistical analysis of sample data difficult, and comparison between authors problematic. Numerous methods have been used to standardise cycles between subjects, in order to overcome this problem.

- A longitudinal approach to experimentation was selected for the present study. This involved repeated sampling across a number of cycles. Such an approach has been advocated by a number of authors (e.g. Gannon 1981; Parlee 1983; Strauss and Appelt 1983; Rubinow and Roy-Byrne 1984). Disadvantages of this method lie in both the practicalities of data collection and the subsequent analysis of the results. It is a highly time consuming exercise, which requires much greater subject compliance than one or two measurements, and is also very demanding on the researcher's time. Whilst acknowledging these difficulties, the within-subjects longitudinal study design is the most suited to investigations across the menstrual cycle and as such was employed in the present study.

7.7 Subjects

Three 20 year old female subjects (MD, RS and FS) experiencing normal menstrual cycles (as ascertained following a general questionnaire) and three male subjects KJ (aged 30), DE (age 42) and AS (aged 31) were recruited to the study. Before inclusion in the study, a slit lamp examination excluded lens opacities using the LOCS II system (Chylack et al 1989) and a fundus examination excluded disease of the posterior segment. All subjects were non-contact lens wearers, apart from subject DE who had worn contact lenses intermittently for 20 years. This subject was instructed not to wear contact lenses for the duration of the testing period.

The three female subjects were paid volunteers and were first year undergraduate students in the Optometry and Visual Science Department of City University. In order to retrospectively assess the stage of a subject's menstrual cycle a general questionnaire was given to each subject to complete at the end of each week of testing.

7.7.1 Questionnaire

Weekly Questionnaire

All information given will be treated in the strictest of confidence.

On average how many hours of sleep have you had each night this week ?

How many hours of reading have you done this week ?

How many hours of exercise have you done?

Have you used a VDU screen at any point this week? If yes, how many hours did you use it for ?

Have you felt ill at any time this week? If yes, why and when did this happen?

Have you taken any medication this week ?

How many units of alcohol have you consumed in the last week?

How many cigarettes have you smoked this week ?

How many caffeinated drinks have you drank this week?

Please rate the degree to which you have experienced the following symptoms over the last week. (Please use a scale of 0-10, 0 representing no symptoms and 10 representing extremely severe symptoms)

Headache

Depression

Irritability

Lethargy/ tiredness

Skin problems

Abdominal pain

Nausea

Vomiting

Cold sweats

Sneezing

Runny Nose

Dizziness

Coughing

Aches and pains

Small concentration span

Blurred vision

This section is for females only.

*How many days from your last menstrual flow are you today?
(taking day one to be the first day of your menstrual flow)*

How many days did your last menstrual flow last?

Have you had your menstrual flow this week?

If yes,

-has it finished?

-how long did it last?

If no, how many days have you had so far?

7.8 Procedure

7.8.1 Female subjects

The female subjects were examined every day apart from at weekends. In order to minimise the effects of corneal oedema following sleep (section 6.14.4), the subjects were examined between the hours of 12:00 and 14:00 and were advised to refrain from sleeping in the four hours prior to testing. Data were collected from the female subjects over a

period representing between 1 and 3 menstrual cycles (54 days) to ensure capture of a full menstrual cycle. One eye was chosen randomly for each subject and all subsequent measurements were made on this eye alone. The order of the tests remained constant for each session. Five CCT readings were taken using optical pachometry, as described in section 6.12. Three scatter measurements were followed by five pachometry measurements from the chosen eye. The scatter testing protocol described in section 5.7 was employed, which permitted simultaneous measurement of pupil diameter.

The female subjects completed the questionnaire (section 7.7.1) at the end of each week of testing, and the questionnaires were collected by an independent colleague from the University Department immediately following completion. The study was unblinded following completion of the study, so that the subject's menstrual cycle could be ascertained.

7.8.2 Male subjects

The male subjects underwent scatter testing every other day (weekends excluded) in the same manner described for the female subjects. Wherever possible, scatter testing was performed between the hours of 12:00 and 14:00, for a period of five weeks. The subjects were advised to refrain from sleeping in the four hours prior to testing. CCT measurements were also taken from one of the male subjects (subject KJ).

7.9 Results

7.9.1 Female subjects

To facilitate interpretation of results, the measurements were standardised to a cycle length of 28 days, as described by Kendall (1986). The actual specific cycle day is multiplied by 28 and then divided by the total number of days in that cycle, to give a standardised day. Other workers (Dye 1989; Dye and Hindmarsh 1991) have advocated the use of this method of cycle standardisation.

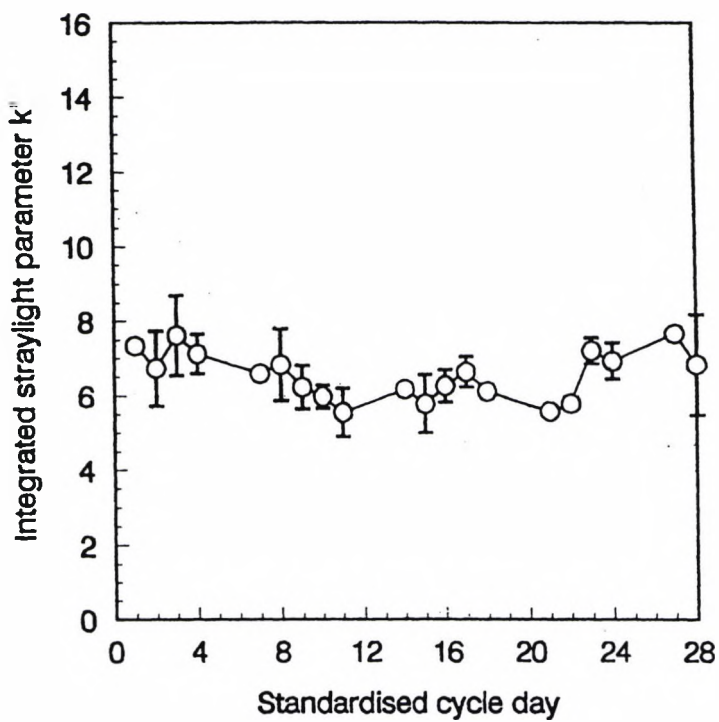
7.9.1.1 Subject MD

7.9.1.1.1 Scatter

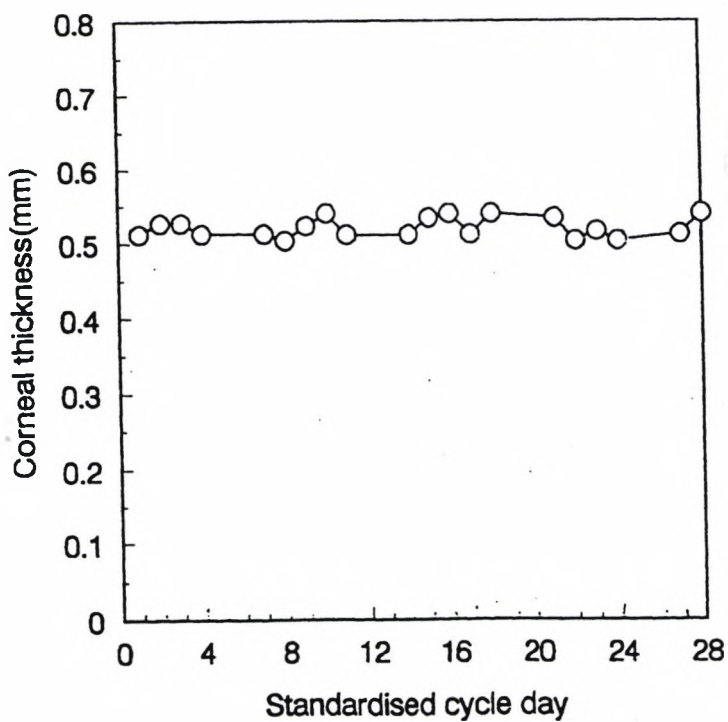
The integrated straylight parameter k' was plotted against the cycle day for subject MD (figure 7.6a). There is a trend towards a reduction in the value of k' from day 1 of the

Figure 7.6

(a) scatter results with s.e.s (3 'runs') and (b) central corneal thickness, as measured during a standardised menstrual cycle for Subject MD

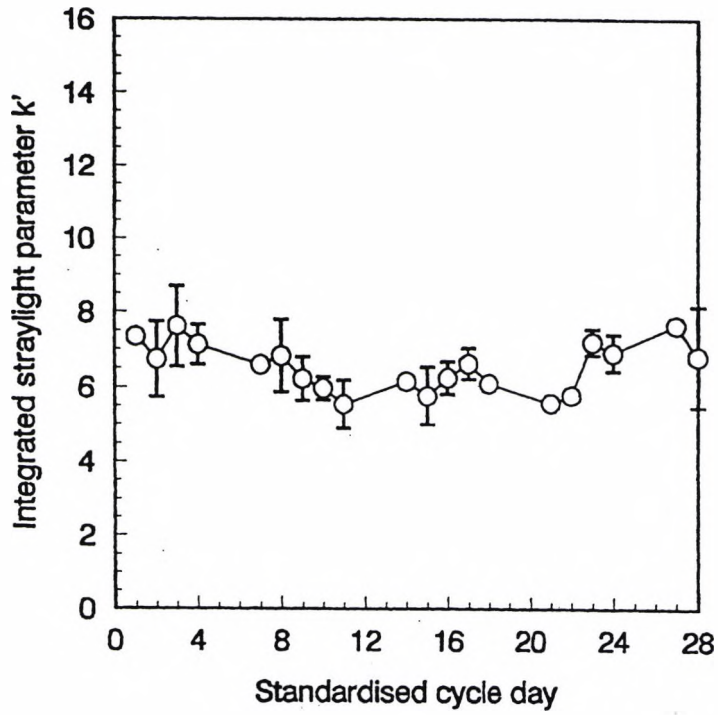


(a)

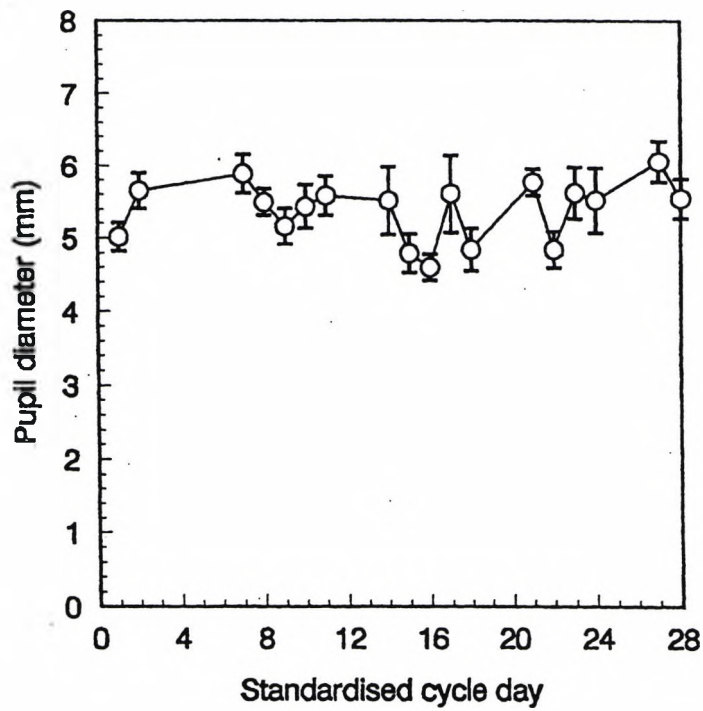


(b)

Figure 7.7 (a) scatter results with s.e.s (3 'runs') and (b) pupil diameter with s.e.s (15 readings), as measured during a standardised menstrual cycle for Subject MD

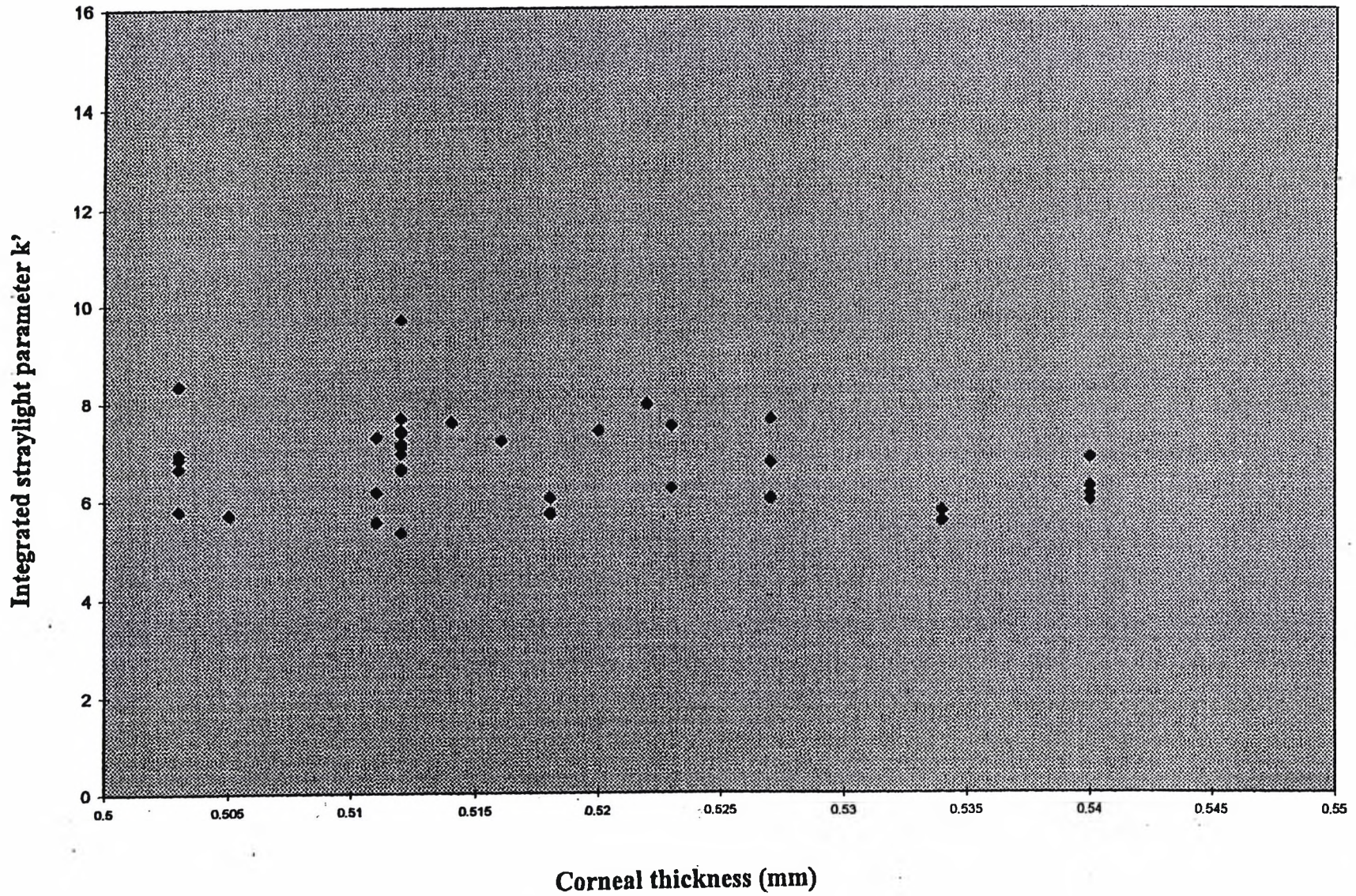


(a)



(b)

Figure 7.8 k' values plotted against central corneal thickness for Subject MD



cycle, through to day 11. From day 11, scatter values increase to day 17 before reducing again until day 21. There is an increase in k' from day 21 to a peak towards the end of the cycle. k' is maximal on day 27 ($k' = 7.66$) and minimal at day 11 ($k' = 5.54$). In order to calculate the percentage change in k' over the course of the cycle, the minimum value was subtracted from the maximum value and divided by the minimum value multiplied by 100. A 38.1% change in k' was recorded for subject MD over the course of the cycle (CV = 10.6%). Initial statistical analysis revealed a mean k' of 6.38, a within day variability of 0.18 (s.d.) and a between day variability of 0.68 (s.d.).

7.9.1.1.2 Pachometry

CCT remains essentially stable across the menstrual cycle (figure 7.6b). The minimum CCT is recorded on day 8 (0.500 mm) and the maximum on days 10, 16, 18, and 28 (0.540 mm). This represents a 7.4% change in CCT over the course of the cycle (CV = 2.4%).

7.9.1.1.3 Pupil diameter

Figure 7.7b shows the pupil diameter data obtained during one full menstrual cycle for subject MD. The pupil diameter varies across the menstrual cycle, with a maximum diameter of 6.06 mm on day 27 and a minimum value of 4.60 mm on day 16. This represents a 31.7% change in pupil diameter over the course of the cycle (CV = 7.3%).

7.9.1.1.4 Correlation analysis

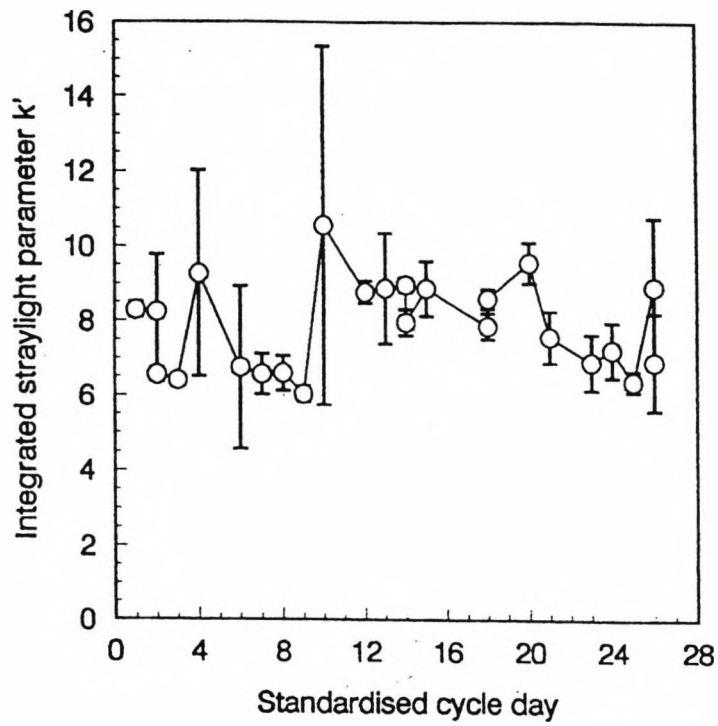
The data confirm that there is little correlation between k' and the pachometry readings ($r = -0.24$) (figure 7.8) or between k' and pupil diameter ($r = 0.19$) (figure 7.9).

7.9.1.2 Subject RS

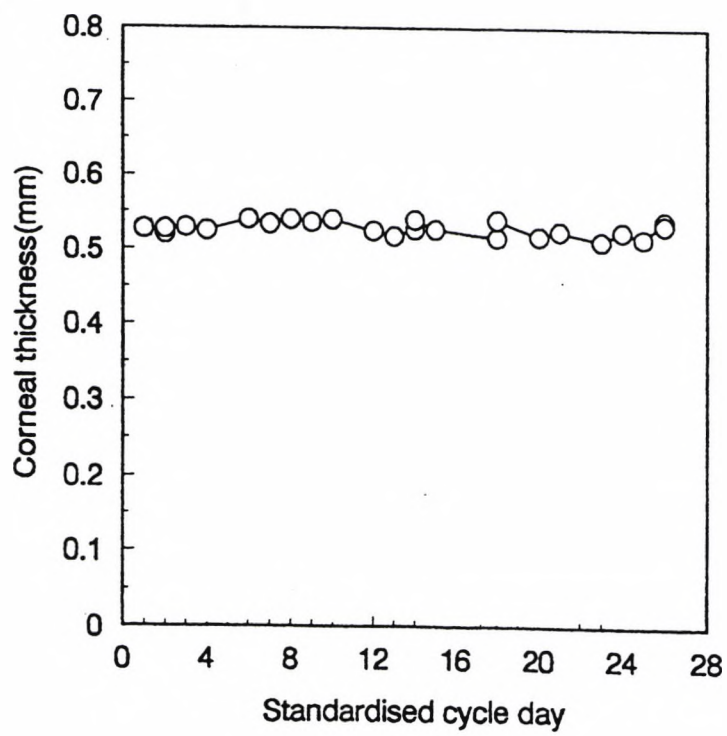
7.9.1.2.1 Scatter

In figure 7.10a, k' is plotted against standardised cycle day for subject RS. k' values are more variable for RS than MD. This variability is apparent from day to day as well as between readings taken on the same day. Visual inspection of the data suggests that there may be a peak in k' in mid cycle with troughs around days 6 to 9 and around day 23. The maximum k' value was 10.55 (day 10) and the minimum k' value was 5.48 (day 6). This represents a 92.5% change in k' over the course of the cycle (CV = 15.6%). Initial

Figure 7.10 (a) scatter results with s.e.s (3 'runs') and (b) central corneal thickness, as measured during a standardised menstrual cycle for Subject RS



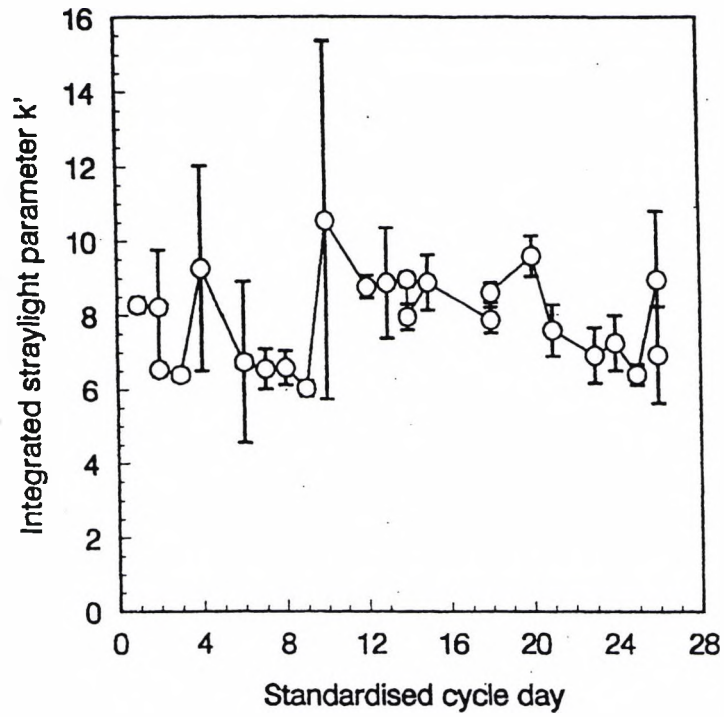
(a)



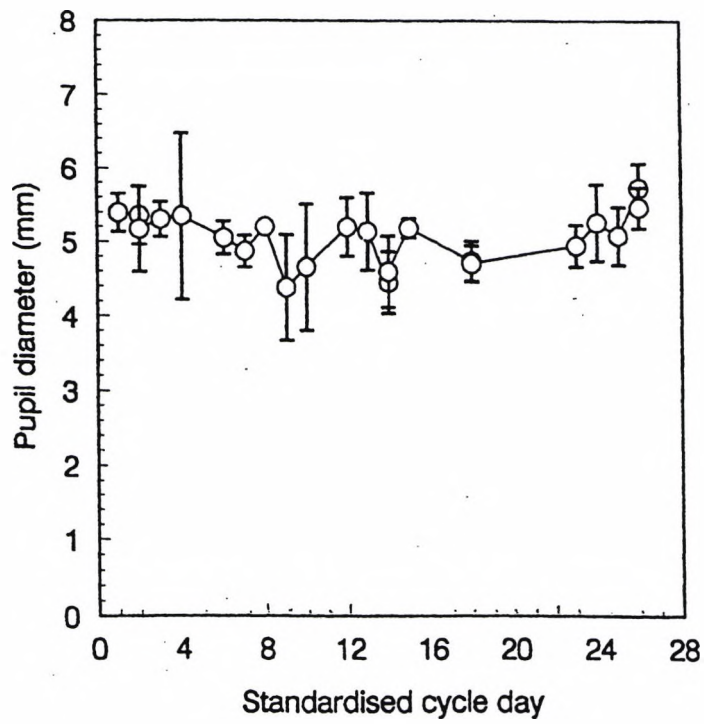
(b)

Figure 7.11

(a) scatter results with s.e.s (3 'runs') and (b) pupil diameter with s.e.s (15 readings), as measured during a standardised menstrual cycle for Subject RS



(a)



(b)

Figure 7.12 k' values plotted against central corneal thickness for Subject RS

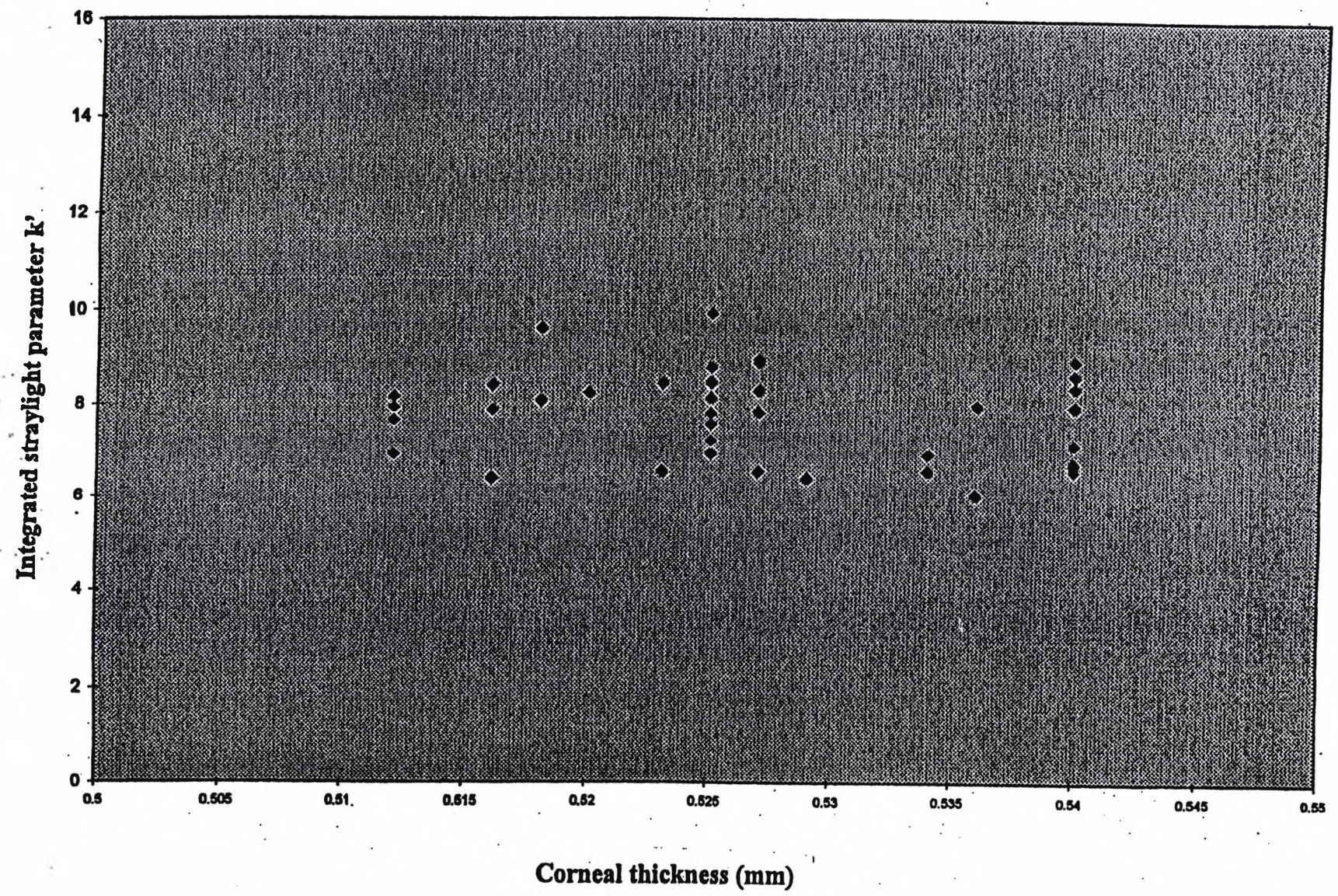
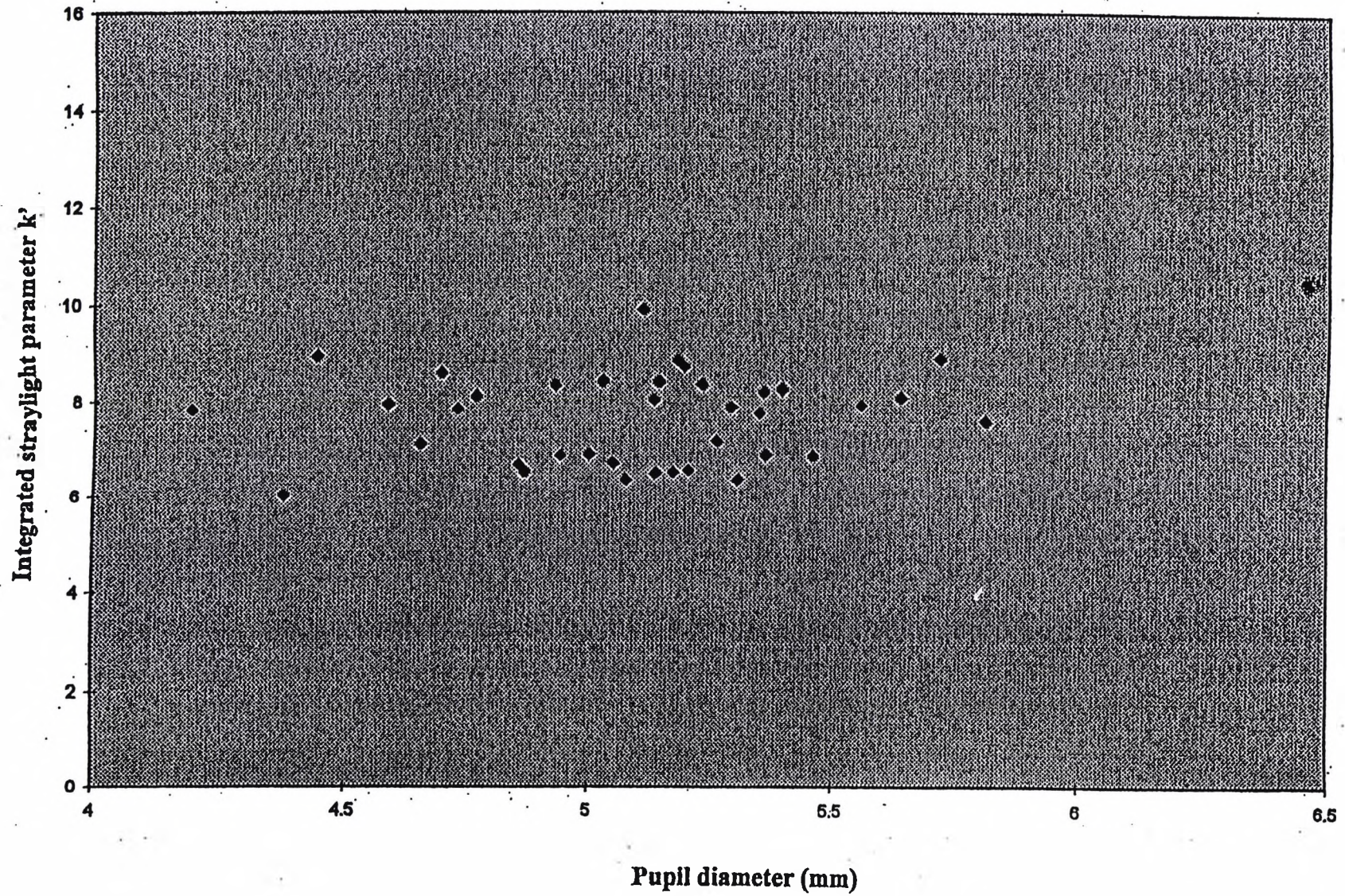


Figure 7.13 k' values plotted against pupil diameter for Subject RS



statistical analysis revealed a mean k' of 7.86, a within day variability of 1.12 (s.d.) and a between day variability of 2.29 (s.d.).

7.9.1.2.2 Pachometry

CCT remains essentially stable across the cycle (7.10b). The minimum CCT was recorded on day 23 (0.512 mm) and the maximum on days 6, 10, 14, 18, and 26 (0.540 mm). This represents an overall change in CCT over the course of the cycle of 5.5% (CV = 1.7%).

7.9.1.2.3 Pupil diameter

Variations in pupil diameter of subject RS with the menstrual cycle are shown in figure 7.11b. The maximum pupil diameter was recorded on day 26 (5.72 mm) and the minimum on day 9 (4.38 mm). This represents a 30.6% change in pupil diameter over the course of the cycle (CV = 7.9%).

7.9.1.2.4 Correlation analysis

The data confirm that there is little correlation between k' and the central pachometry readings ($r = -0.17$) (figure 7.12) or between k' and pupil diameter ($r = 0.12$) (figure 7.13).

7.9.1.3 Subject FS

7.9.1.3.1 Scatter

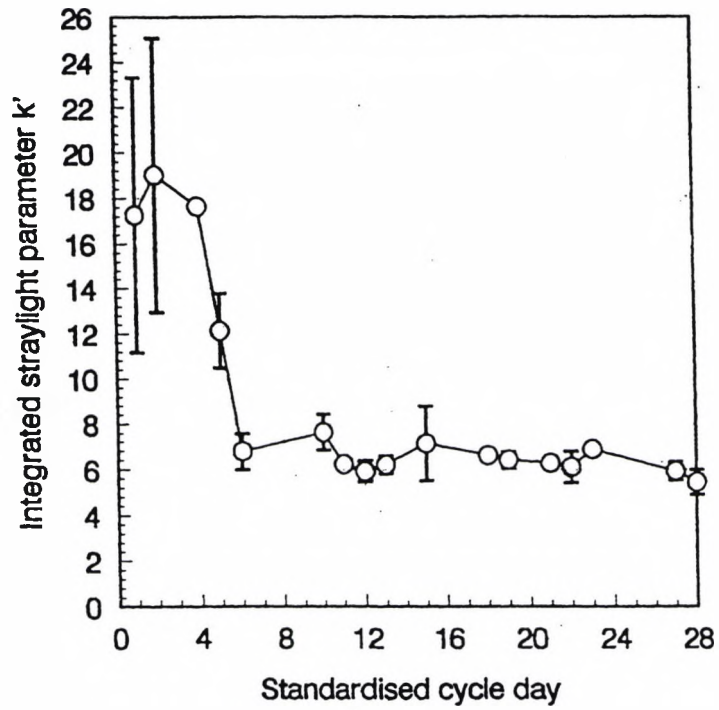
In figure 7.14a, k' is plotted against standardised day of the cycle for subject FS. Highest light scatter is found on days 1 to 3. The level of k' then reduces dramatically from a maximum value of 19.02 on day 2 of the cycle, to day 5. k' remains relatively stable throughout the rest of the cycle with a possible trough around day 12. A minimum value of 5.46 is recorded on day 28. The overall percentage change in k' over the course of the cycle was 248.4% (CV = 43.8%). Initial statistical analysis revealed a mean k' of 8.21, a within day variability of 7.34 (s.d.) and a between day variability of 10.20 (s.d.).

7.9.1.3.2 Pachometry

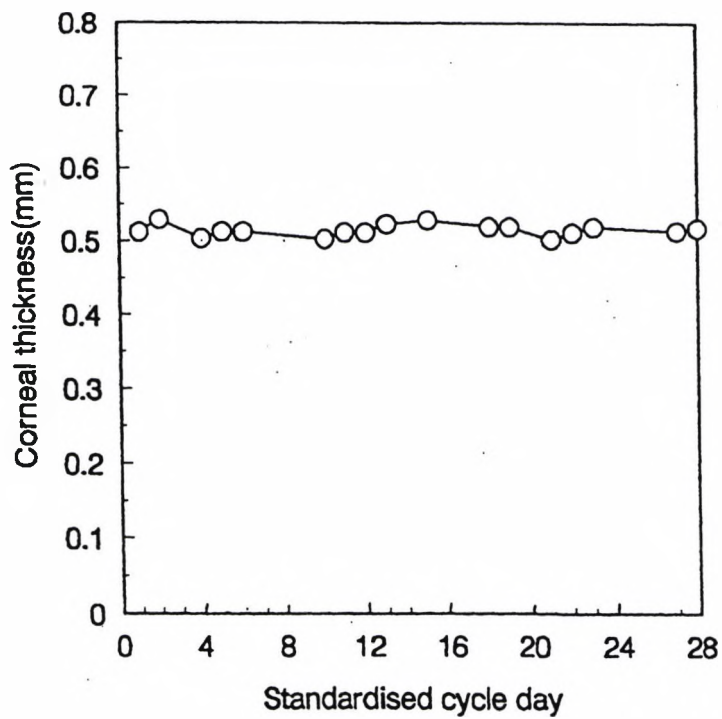
The measurements of CCT can be seen in figure 7.14b. The minimum CCT is seen on days 4, 10 and 21 (0.503 mm) and the maximum on days 2 and 15 (0.529 mm). This represents an overall change of 5.2% over the course of the cycle (CV = 1.6%).

Figure 7.14

(a) scatter results with s.e.s (3 'runs') and (b) central corneal thickness, as measured during a standardised menstrual cycle for Subject FS



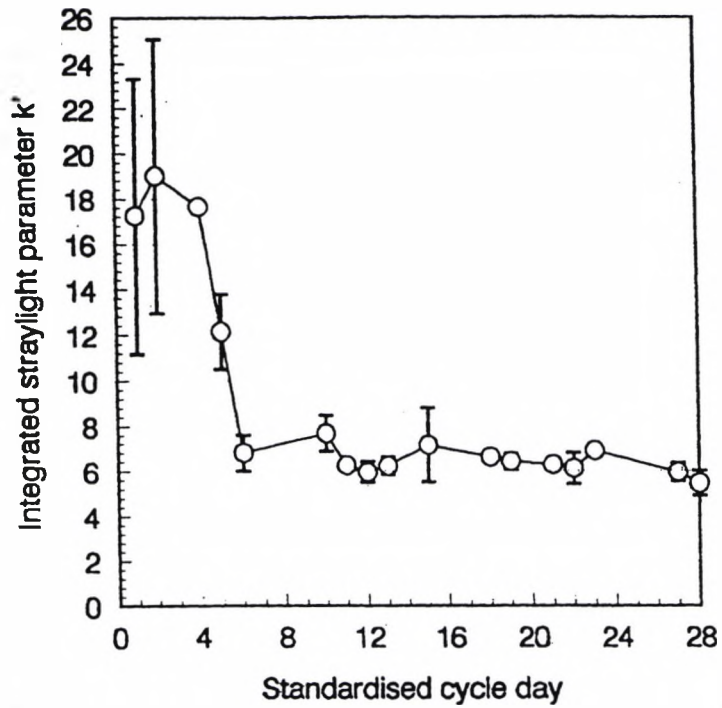
(a)



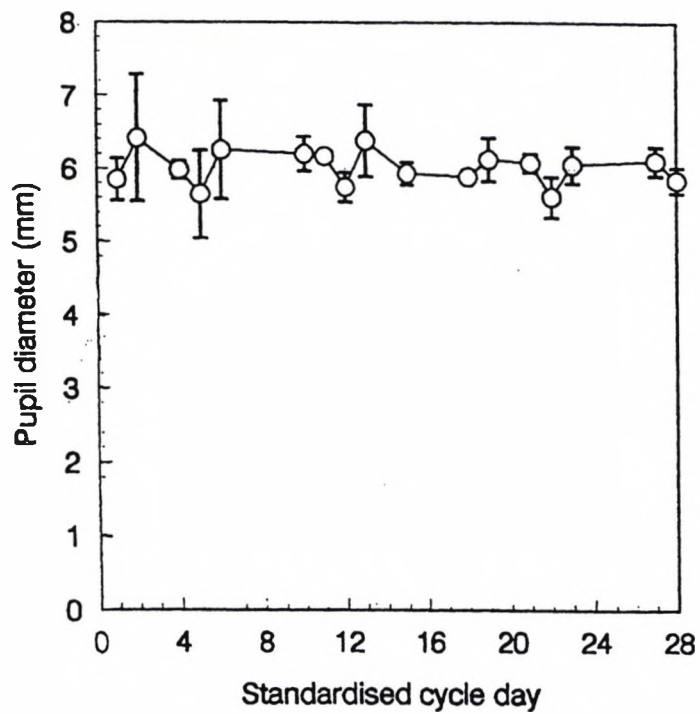
(b)

Figure 7.15

(a) scatter results with s.e.s (3 'runs') and (b) pupil diameter with s.e.s (15 readings), as measured during a standardised menstrual cycle for Subject FS



(a)



(b)

Figure 7.16 k' values plotted against central corneal thickness for Subject FS

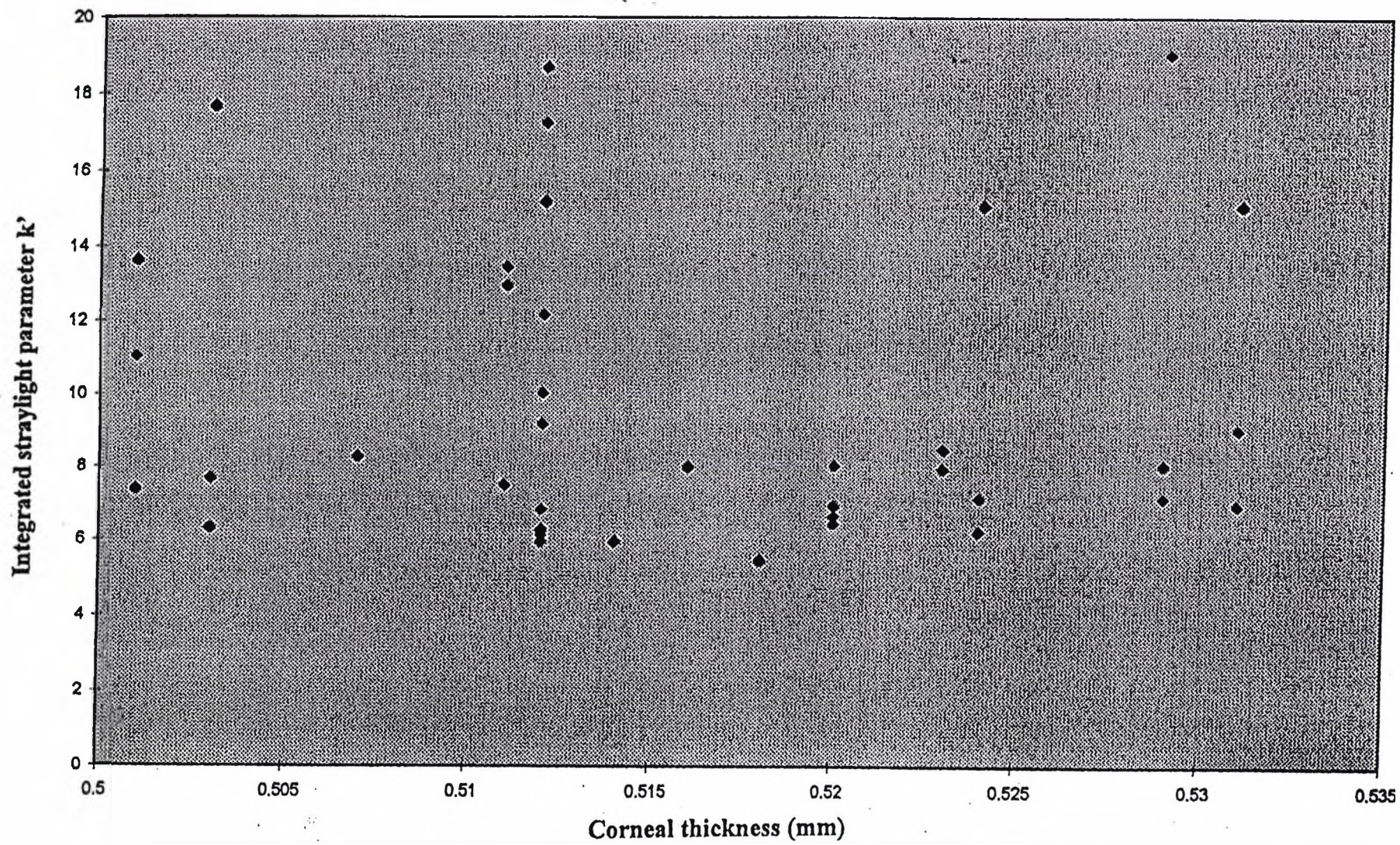
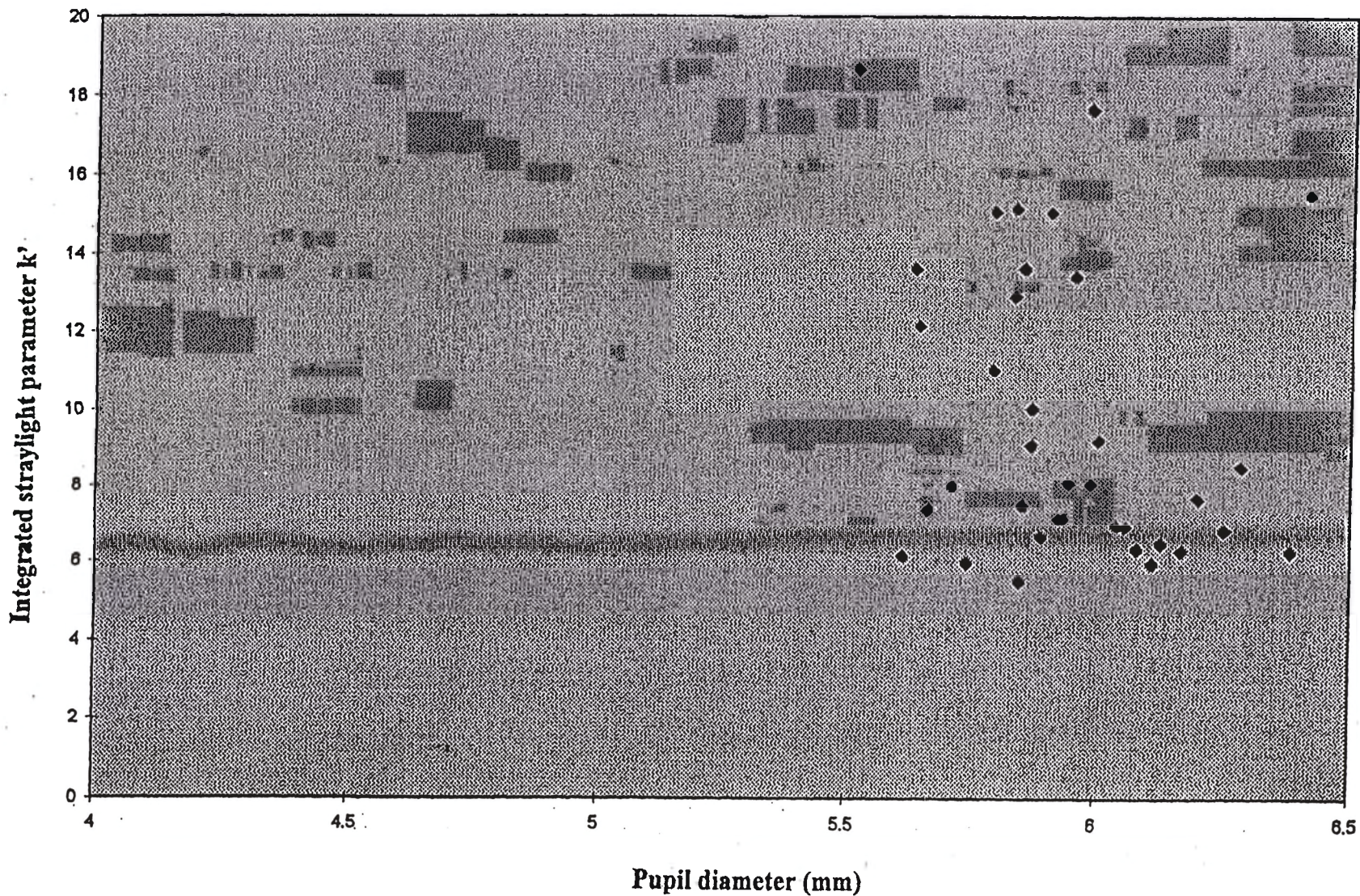


Figure 7.17 k' values plotted against pupil diameter for Subject FS



7.9.1.3.3 Pupil diameter

The pupil diameter of subject FS was at a maximum on day 2 (6.41 mm) and at a minimum on day 22 (5.61 mm). This represents a 14.3% change in pupil diameter over the course of the cycle (figure 7.15b) (CV = 7.3%).

7.9.1.3.4 Correlation analysis

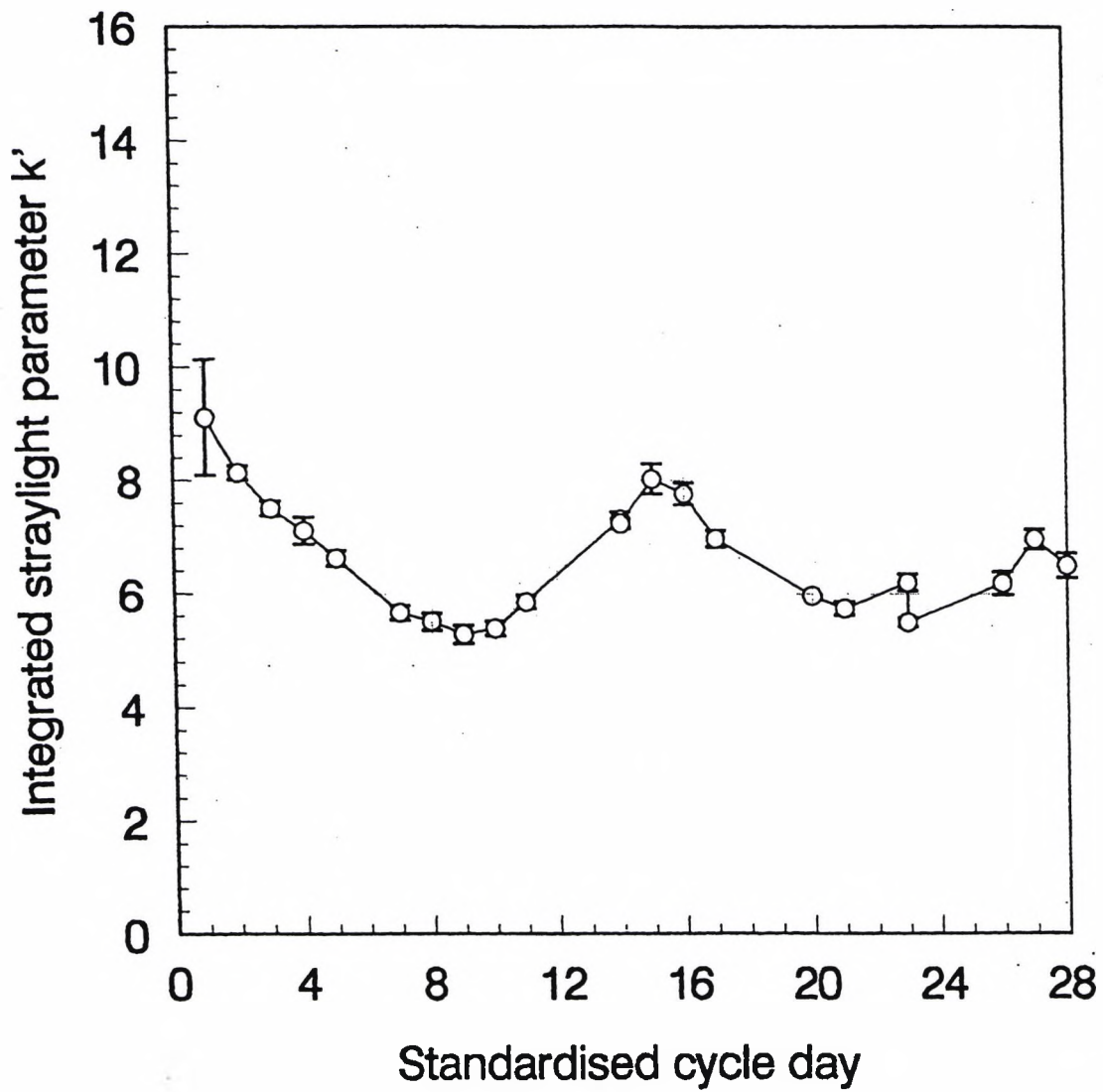
The data confirm that there is little correlation between k' and the central pachometry readings ($r = -0.09$) (figure 7.16) or between k' and pupil diameter ($r = -0.29$) (figure 7.17).

7.9.1.4 Time series analysis

The aim of the time series analysis was to investigate whether the variation in light scatter noted in female subjects has a cyclical nature. Initial statistical analysis revealed that the within day variability inherent in the data from RS and FS (1.12 and 7.34 (s.d.) respectively) was too high to allow meaningful evaluation of the cycle data by time series. Thus, only the more consistent data from subject MD (across 54 days) (0.18 (s.d.)) were included in the analyses. In addition, the data obtained from testing subject MH (cycles 1 and 2) from Chapter 6 were also standardised and used in the analyses (within day variability 0.26 and 0.66 (s.d.) respectively). Cycles 3 and 4 were excluded due to the ingestion of corticosteroids during and prior to testing. The results for subject MH of k' plotted against standardised cycle day are shown in figures 7.18 and 7.19. Thus, three data sets were included in the analysis (namely MD and MH cycles 1 and 2). The data were reduced to day means before plotting k' against cycle day. Cycles 1 and 2 are combined, as the data were taken consecutively from the same subject.

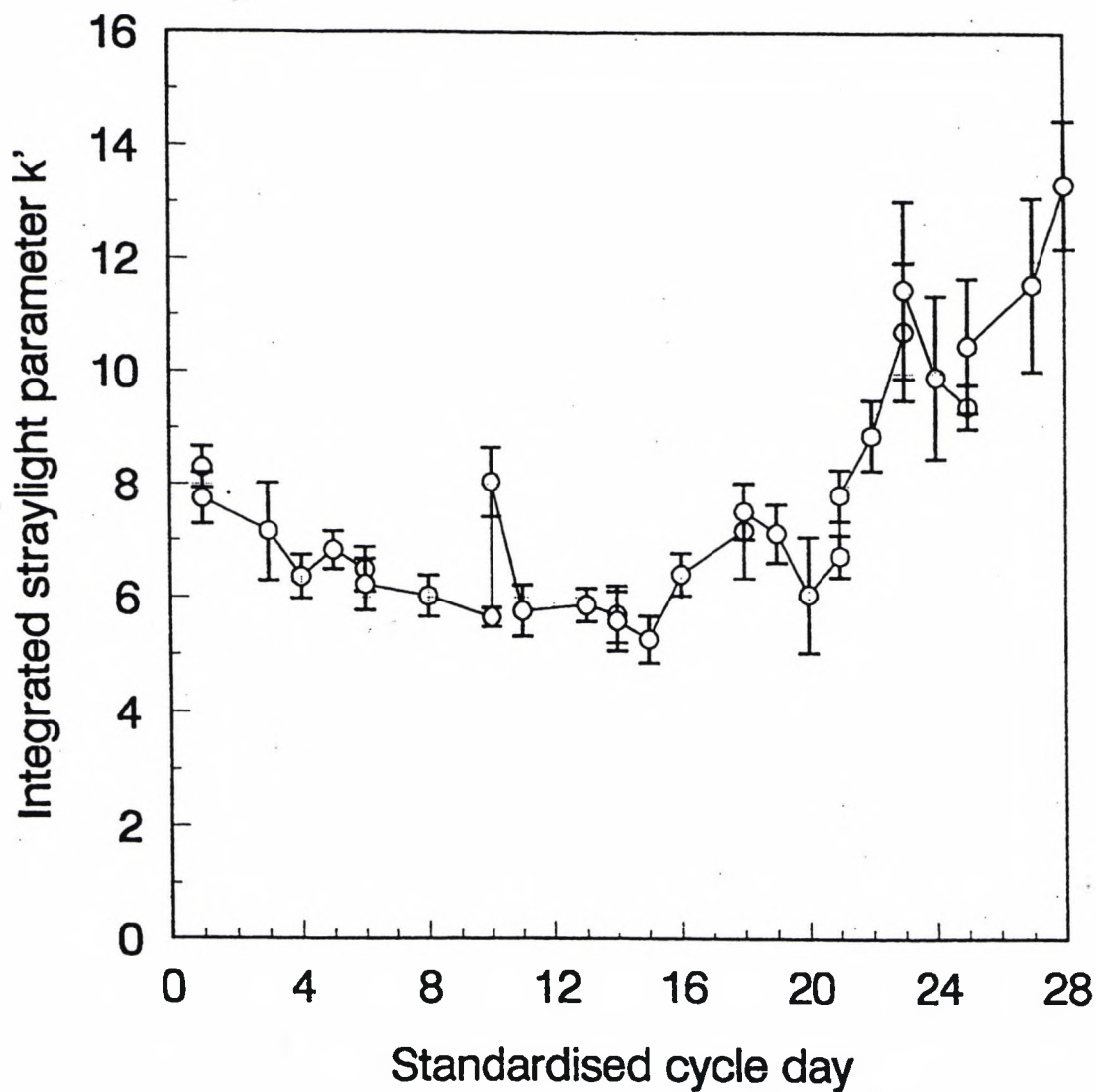
Inspection of figure 7.20 reveals that the only feature common to all cycles is a fall in k' during the first five days of each subject's cycle. The plot shows that whilst the pattern of readings is not consistently related to cycle phase, the variation does have some trends in time rather than each day's value being independent of the previous day. Figure 7.21 reveals that there may exist a peak in k' mid-way through the cycle which may correspond to ovulation. Subjects MD (day 17), MH (cycle 1) (day 15) and MH (cycle 2) (day 10) show a trend towards increased scatter during the ovulatory/luteal phase. However, no obvious mid-way peak is visible from inspection of figures 7.21b, c (RS and FS). This may have been due to the high within day variability in the data obtained from these

Figure 7.18 Variation in k' over a standardised 28 days for Subject MH (cycle 1)



Measurements were taken at approximately the same time of day (between 12:00 and 14:00). The plotted data points represent the mean k' obtained over six 'runs'. Error bars represent standard errors.

Figure 7.19 Variation in k' over a standardised 28 days for Subject MH (cycle 2)



Measurements were taken at approximately the same time of day (between 12:00 and 14:00). The plotted data points represent the mean k' obtained over six 'runs'. Error bars represent standard errors.

Figure 7.20 k' daily means against cycle day for Subject MH (cycles 1 and 2) and Subject MD

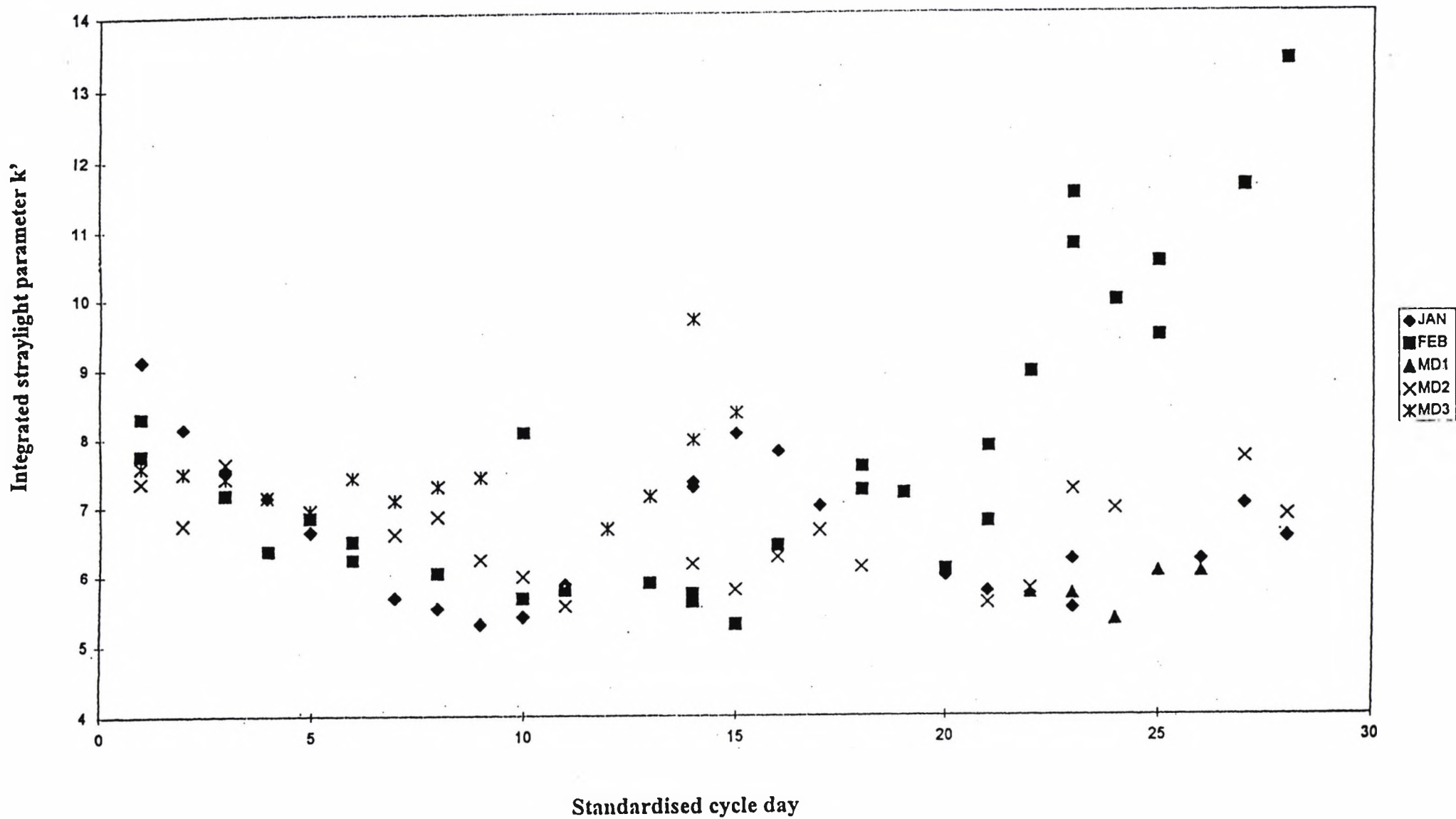
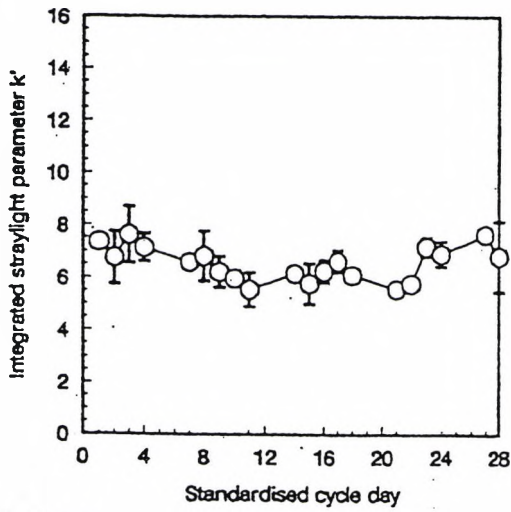
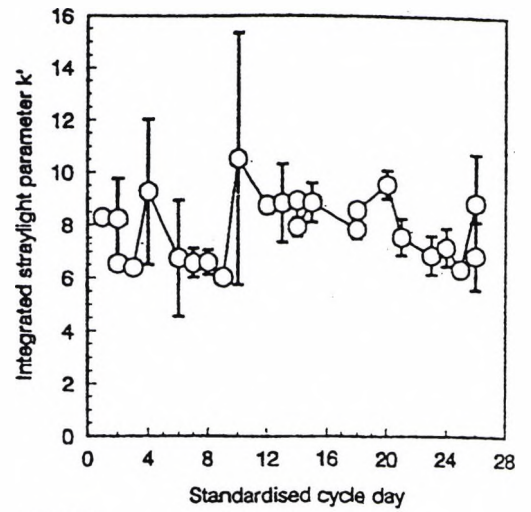


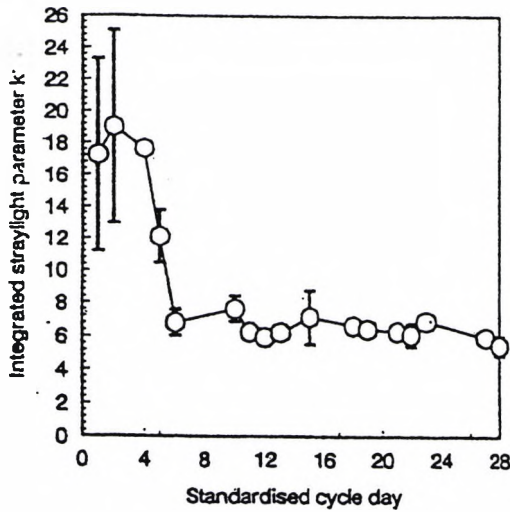
Figure 7.21 Scatter results for female Subjects MN, RS, FS and MH (Cycles 1 and 2)



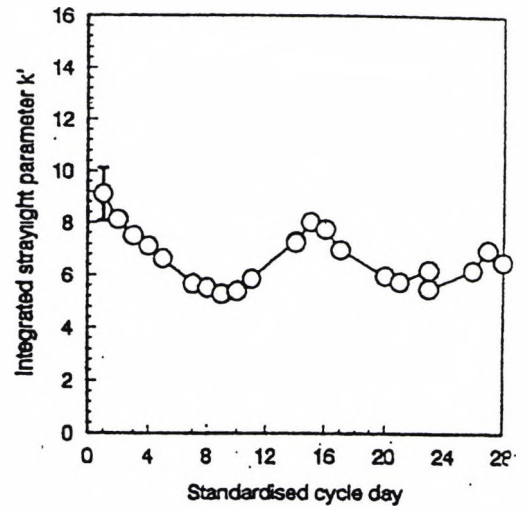
(a) MD



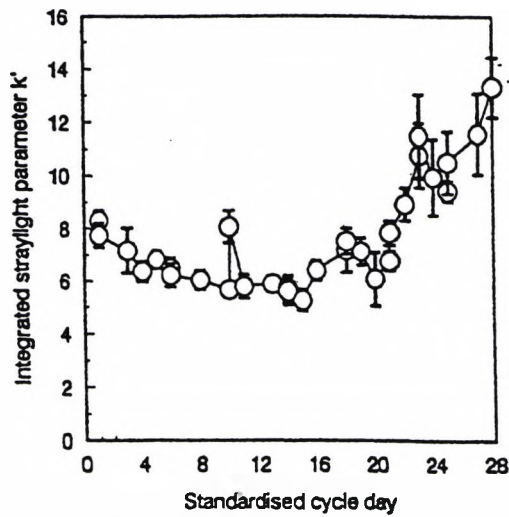
(b) RS



(c) FS



(d) MH (cycle 1)



(e) MH (cycle 2)

subjects. To further investigate the relationship between k' and the menstrual cycle, time series analysis was undertaken. An important guide to the properties of a time series is provided by a series of quantities called sample autocorrelation coefficients, which measure the correlation between observations at different distances in time. These coefficients often provide insight into the probability model which generated the data (see 'The analysis of Time Series An introduction'. 4th Edition C. Chatfield, Chapman and Hall 1994, for a full review). A useful aid in interpreting a set of auto correlation coefficients is a graph called a correlogram in which r_k is plotted against the lag k (where r_k = correlation) between observations a distance k apart. Correlograms for MD and MH (cycles 1 and 2 combined) can be seen in figures 7.22 and 7.23, respectively. These reveal certain characteristic patterns. The gradual fall from very high positive correlations at lag one is an indication of a non-stationary time series, that is, one that has trends. From figures 7.22 and 7.23, there are no clear patterns beyond this initial fall in the early cycle which tends to argue against the presence of cyclic behaviour. There is no significant auto-correlation structure, demonstrating that beyond the simple trends there is no evidence of more complex cyclical variation.

In conclusion, the k' values show non-systematic variation but also show some pattern from day to day. There is strong evidence of trends in the readings at a time scale greater than one day. However, there is only a weak suggestion of a link between this variation and the menstrual cycle.

A correlogram for the pachometry results has not been shown, as the correlation with any lag is virtually zero, indicating the complete absence of a time pattern to the variation. Therefore, it is unlikely that the variation in CCT could explain the time structured variation in k' .

7.9.2 Male subjects

7.9.2.1 Subject KJ

Light scatter and CCT measurements were taken from subject KJ over a five week period. Figure 7.24a demonstrates that there are several points over the course of testing where light scatter was markedly greater than the mean for the five week period (days 10, 15, 17, 24 and 31). Despite having been requested to refrain from sleep prior to testing, on

Figure 7.22 Correlogram for Subject MD

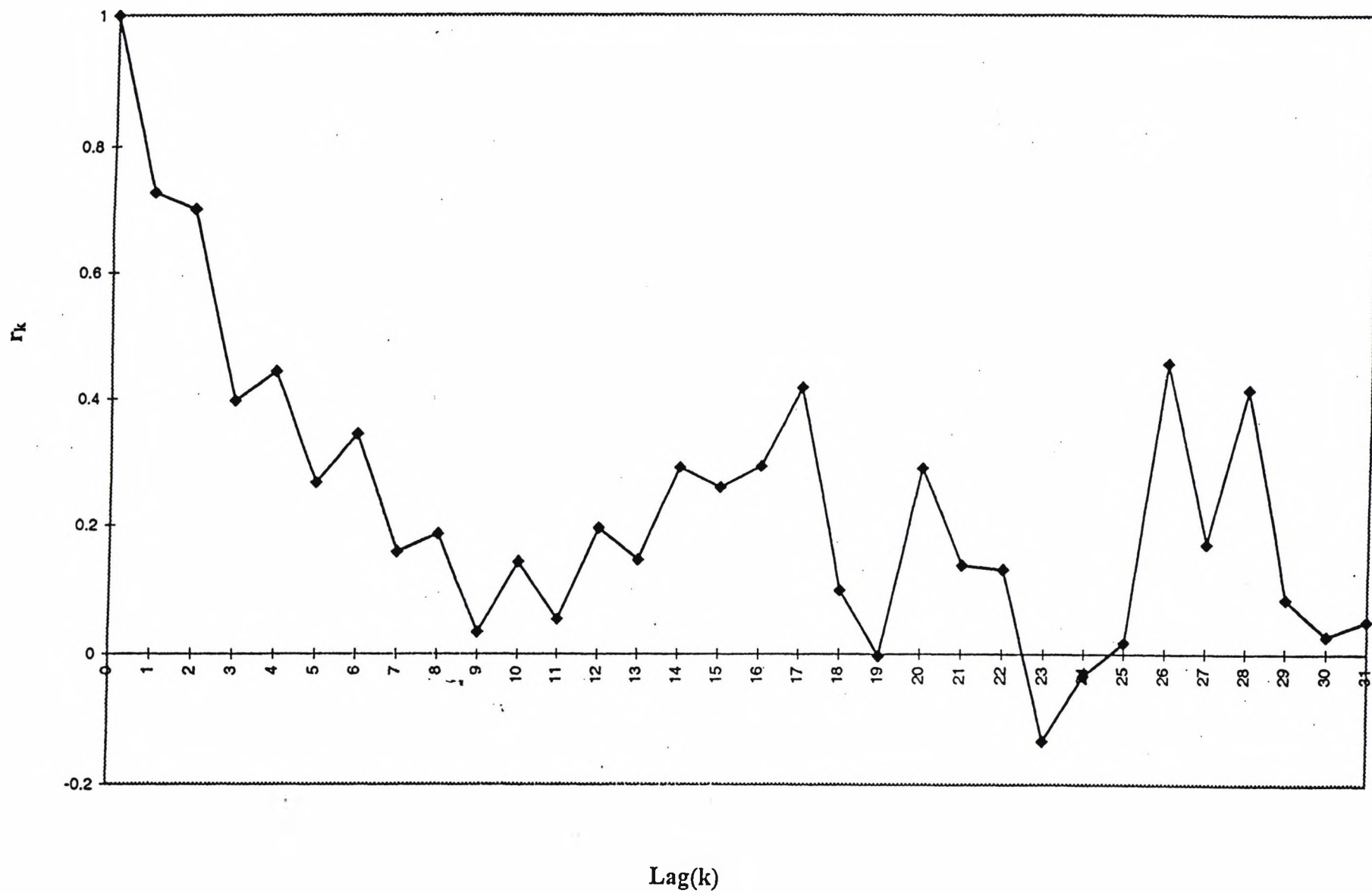


Figure 7.23 Correlogram for Subject MH (cycles 1 and 2 combined)

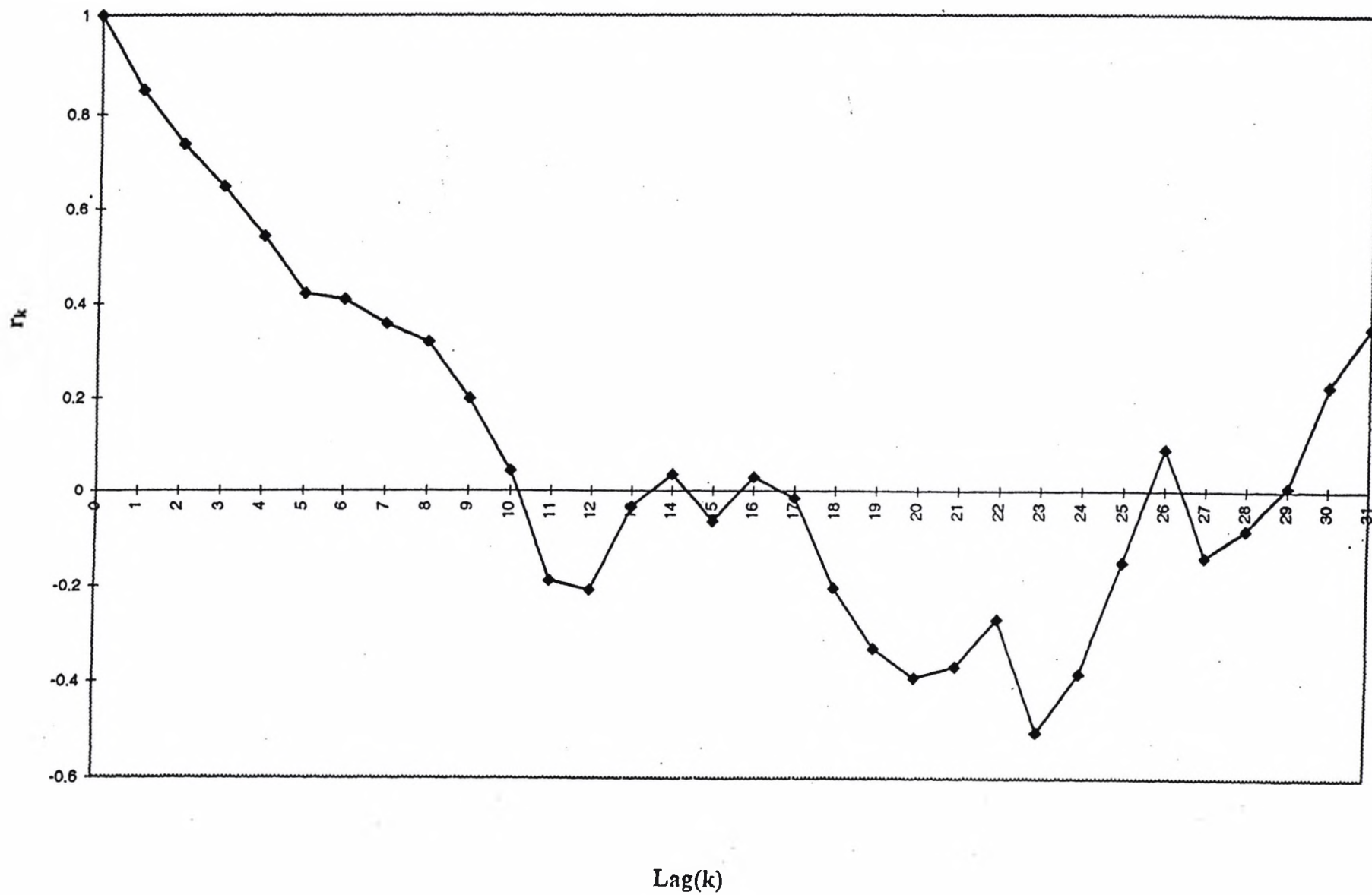
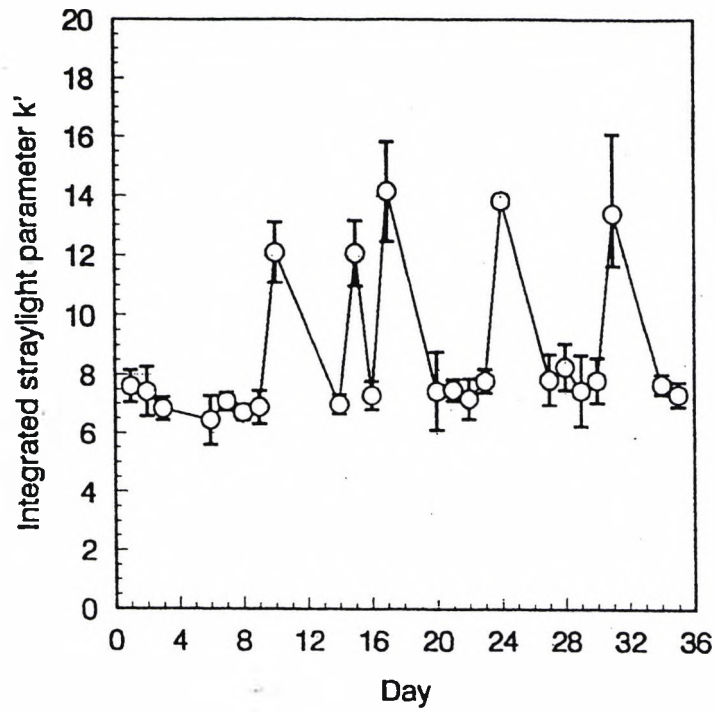
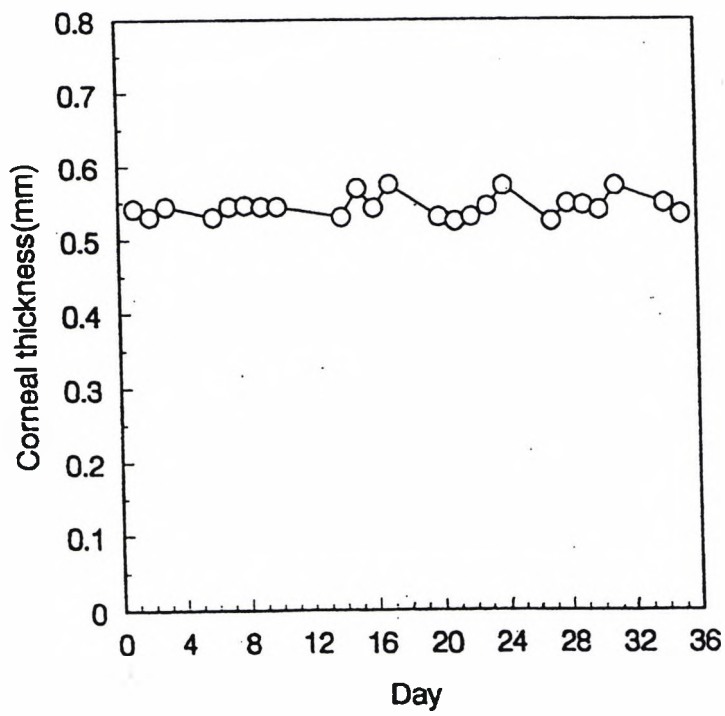


Figure 7.24

(a) scatter results with s.e.s (3 'runs') and (b) central corneal thickness, as measured over 35 days for Subject KJ



(a)



(b)

questioning, the subject revealed that these points in fact coincided with times when measurements were taken shortly after the subject had woken from prolonged "naps". CCT measurements were also elevated for these sampling times (figure 7.24b). These findings are in line with the results of Chapter 6 which showed that CCT, and thus scatter, is elevated immediately following sleep/patching. The aim of the present study was to evaluate changes in light scatter over time when measurements are taken at the same time of day, to investigate day-to-day variability in k' . Therefore, the anomalous outlying results, caused by sleep, were excluded from the data analysis (figure 7.25a, b).

Figure 7.25a demonstrates that k' was relatively constant over the five week period. The maximum k' values were recorded on day 28 (8.28) and the minimum on day 6 (6.44). The overall percentage change in k' was 28.6% (CV = 6.2%). The maximum CCT values were recorded on day 28 (0.549 mm) and the minimum on days 21 and 27 (0.525 mm). This represents an overall CCT change of 4.5% (CV = 1.5%). Initial statistical analysis revealed a mean k' of 7.34, a within day variability of 0.63 (s.d.) and a between day variability of 0.41 (s.d.).

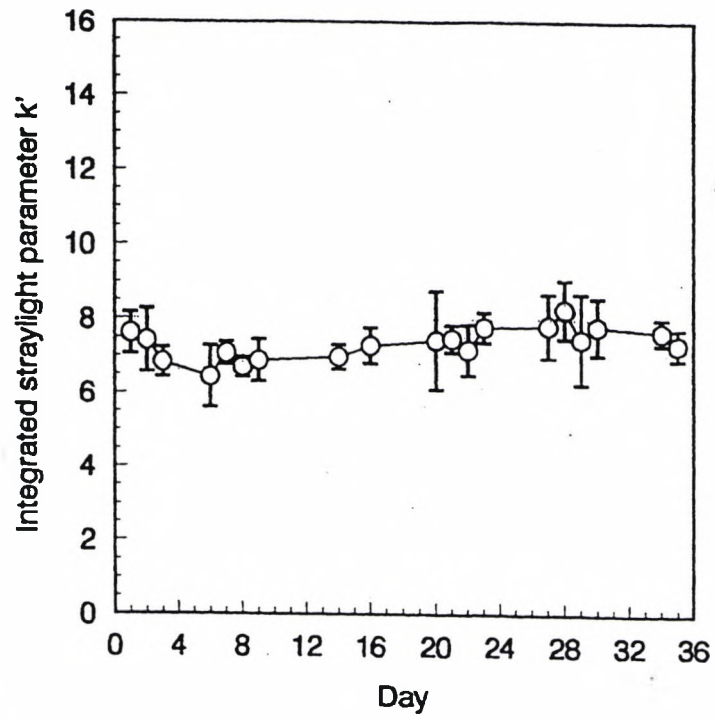
7.9.2.2 Subject DE

Light scatter within the eye of subject DE remained relatively constant from day to day over the 36 day period (figure 7.26). The maximum k' value was recorded on day 5 (6.83) and the minimum on day 36 (5.86). This represents a 16.6% change in k' over the testing period (CV = 4.2%). Initial statistical analysis revealed a mean k' of 6.19, within day variability of 0.42 (s.d.) and a between day variability of 0.38 (s.d.).

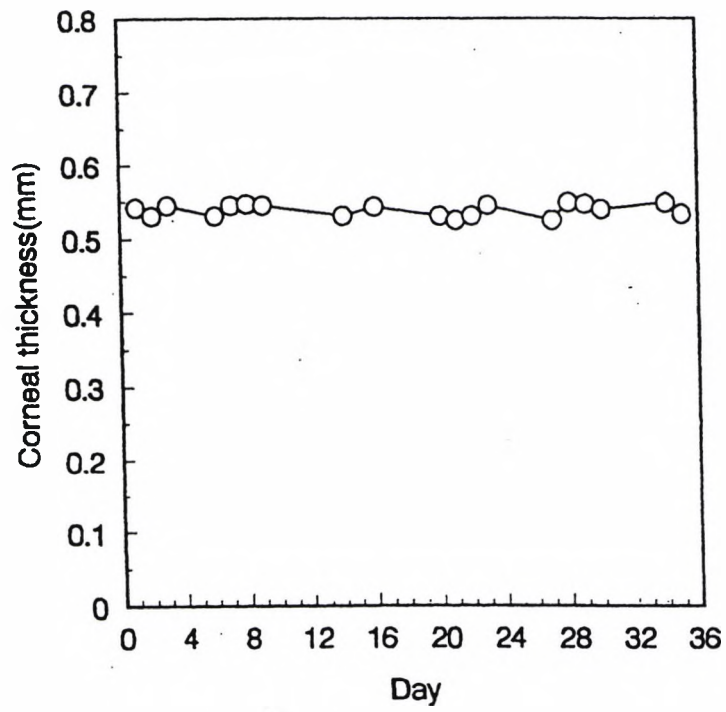
7.9.2.3 Subject AS

Light scatter within the eye of subject AS showed greater variation than subject DE over the 35 day testing period (Figure 7.27). k' values are below 6 from days 1 to 14 but generally above 6 from days 18 to 35. The maximum k' value was recorded on day 24 (6.91) and the minimum value is seen on day 8 (5.26). This represents a 31.3% change in k' over the testing period (CV = 8.7%). Initial statistical analysis revealed a mean k' of 6.10, a within day variability of 0.32 (s.d.) and a between day variability of 0.36 (s.d.).

Figure 7.25 (a) scatter results with s.e.s (3 'runs') and (b) central corneal thickness, as measured over 35 days for Subject KJ (outlying data points excluded)

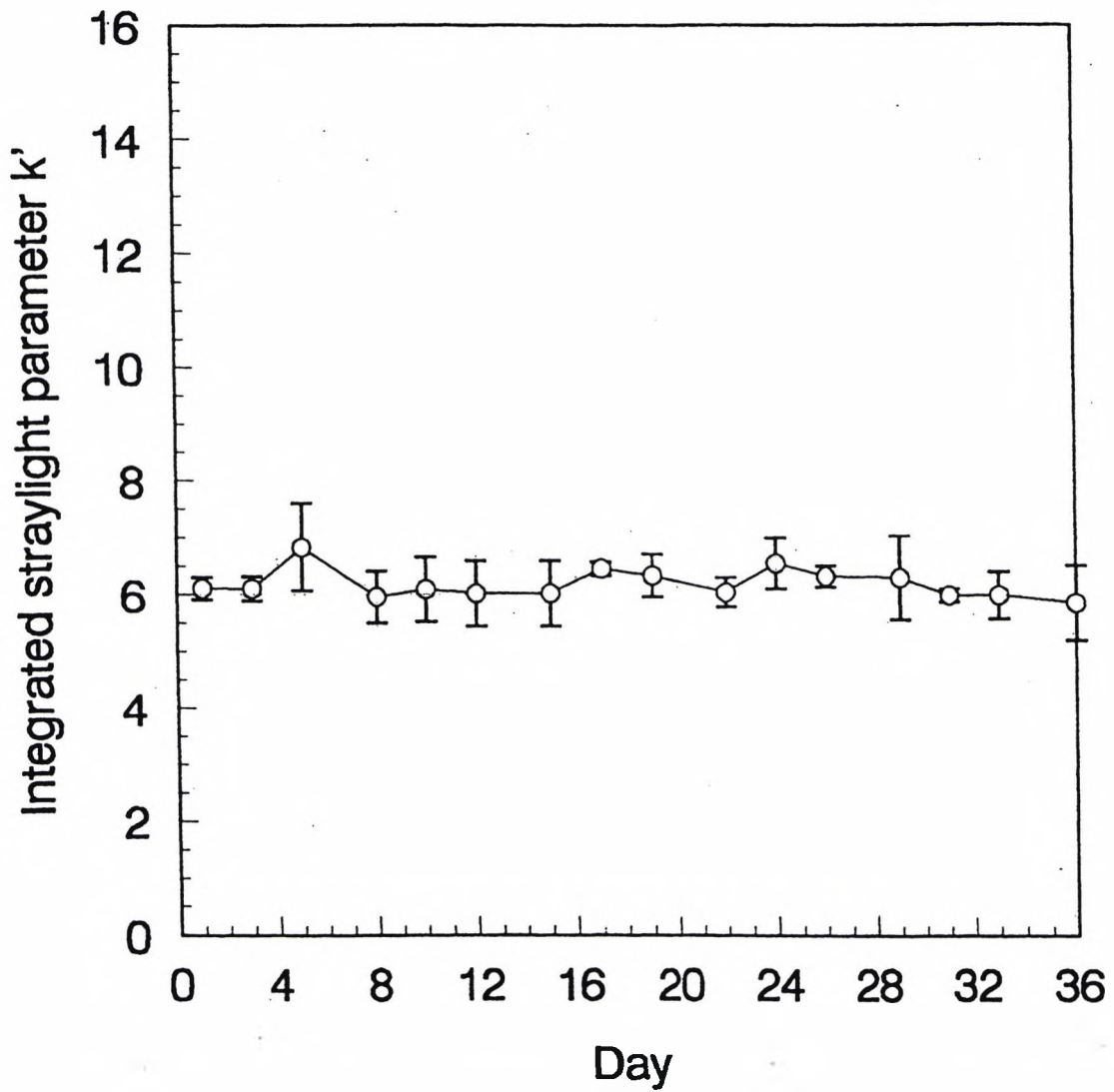


(a)



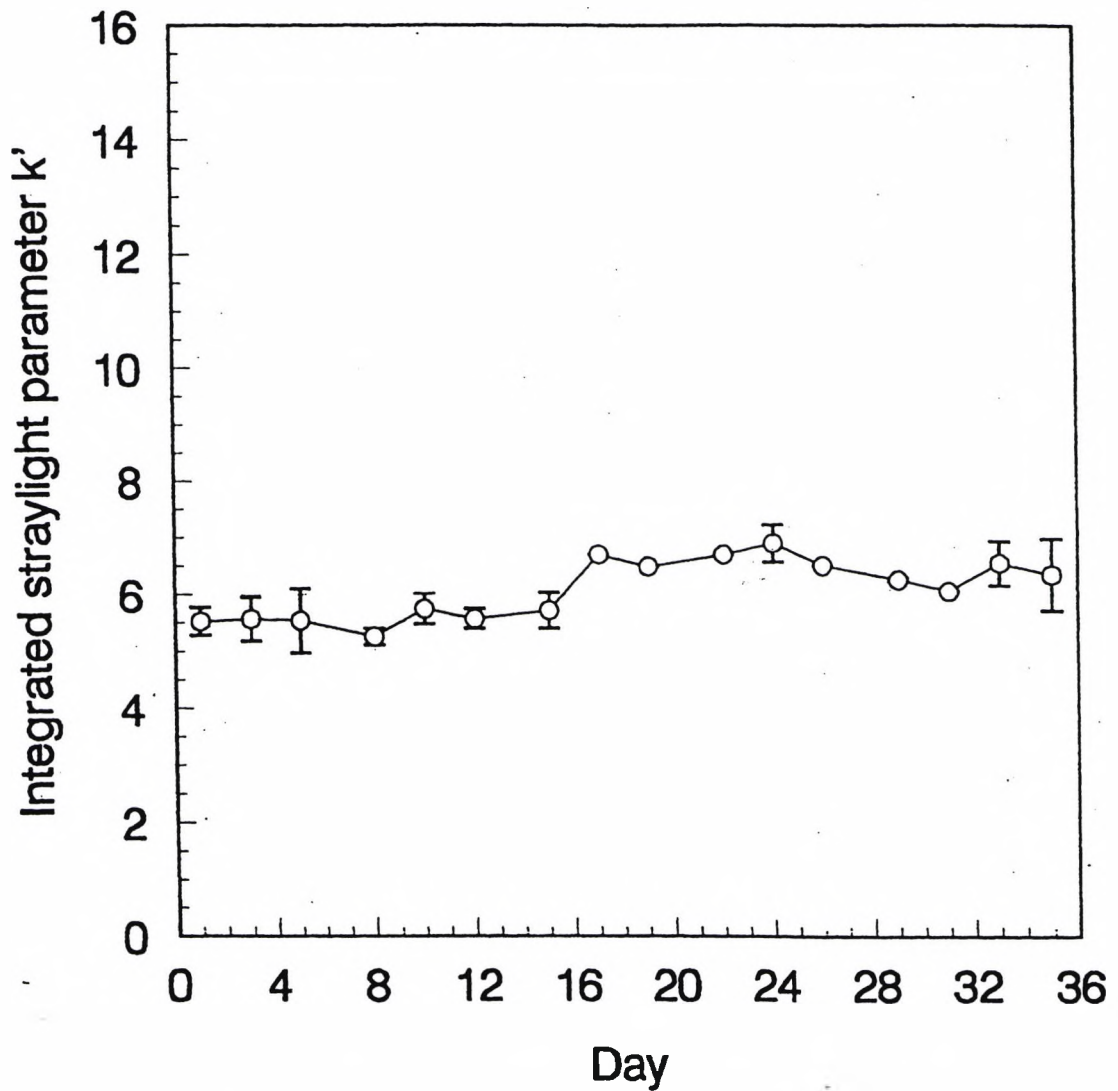
(b)

Figure 7.26 Scatter results for Subject DFE as measured over 36 days



Measurements were taken at approximately the same time of day (between 12:00 and 14:00). The plotted data points represent the mean k' obtained over three 'runs'. Error bars represent standard errors.

Figure 7.27 Scatter results for Subject AS as measured over 35 days



Measurements were taken at approximately the same time of day (between 12:00 and 14:00). The plotted data points represent the mean k' obtained over three 'runs'. Error bars represent standard errors.

7.10 Discussion of male and female results

There are notable differences between the light scatter data generated by the male subjects and those recorded from the females. From figures 7.25a, 7.26 and 7.27, it is apparent that there was an absence of any particular trends or patterns with time in males. A correlogram is shown in figure 7.28 based on the k' daily means for KJ. The gaps in the days on which readings were taken causes the number of data points used in the calculations to fall away sharply, so that little significance can be attached to values for any lags greater than two. However, the lag one correlation is only 0.5, compared with values of 0.73 for subject MD and 0.83 for subject MH (cycles 1 and 2 combined) (figures 7.22 and 7.23). Therefore, females showed a higher correlation with time than male subjects. In addition, the variability in k' was lower, both within a day and between days in males. A histogram of within day variance can be seen in figure 7.29. Figure 7.30 shows the corresponding data recorded in the female subjects, for comparison. Furthermore, the average between day variability for females was 2.97 (s.d.) compared to 0.39 (s.d.) for male subjects.

In conclusion, there is a difference between male and female subjects with regard to light scatter when measurements are taken longitudinally. Other studies measuring visual function have also reported differences between males and female subjects. For example, visual sensitivity (as measured by dark adapted detection of a flash light) has been shown to increase in the mid-cycle or ovulatory phase (Diamond et al 1972; Barris et al 1980; Scher et al 1981), and to decrease in the premenstrual phase. A small increase in visual sensitivity has also been observed during menstruation (Ward et al 1978). No such phase variation was recorded in control groups of men, or in women taking the Pill (Diamond et al 1972).

Studies have demonstrated that a menstrual cycle-related fluctuation in CS is noted in female subjects. Dunn and Ross (1985) measured CS at three spatial frequencies (9, 18 and 26 cpd) and found that there existed both a gender difference, and a relationship with the menstrual cycle. Males were found to have the highest CS, followed by non-cycling women and lastly by women with normal cycles. CS was increased in the post ovulatory phase, compared with the rest of the cycle, in ten women with normal menstrual cycles. Johnson and Petersik (1987) took daily measurements of CS at three different spatial frequencies (2, 4 and 16 cpd) in two normally cycling women and in two control subjects

Figure 7.28 Correlogram for Subject KJ

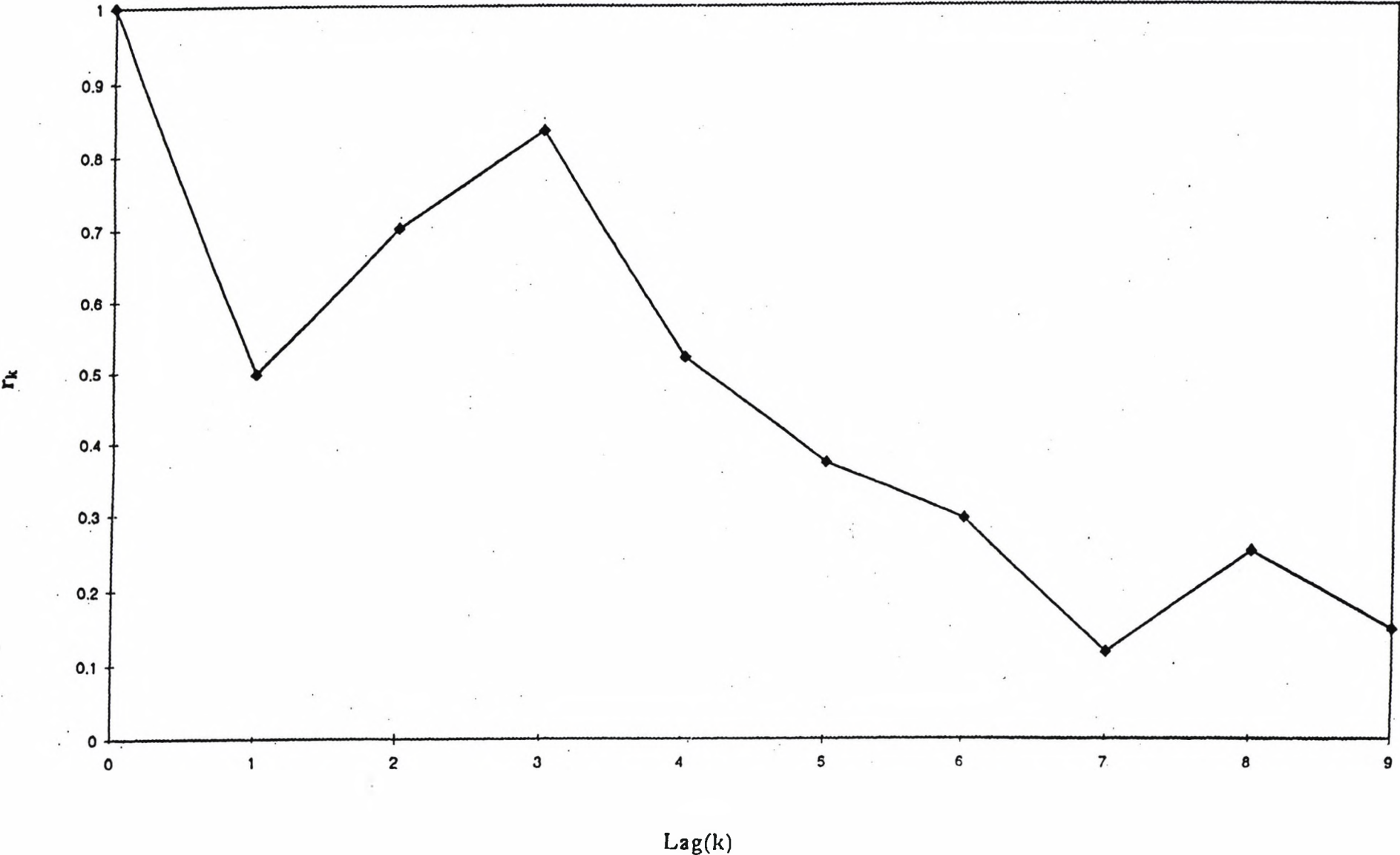


Figure 7.29 Within day variance for male subjects

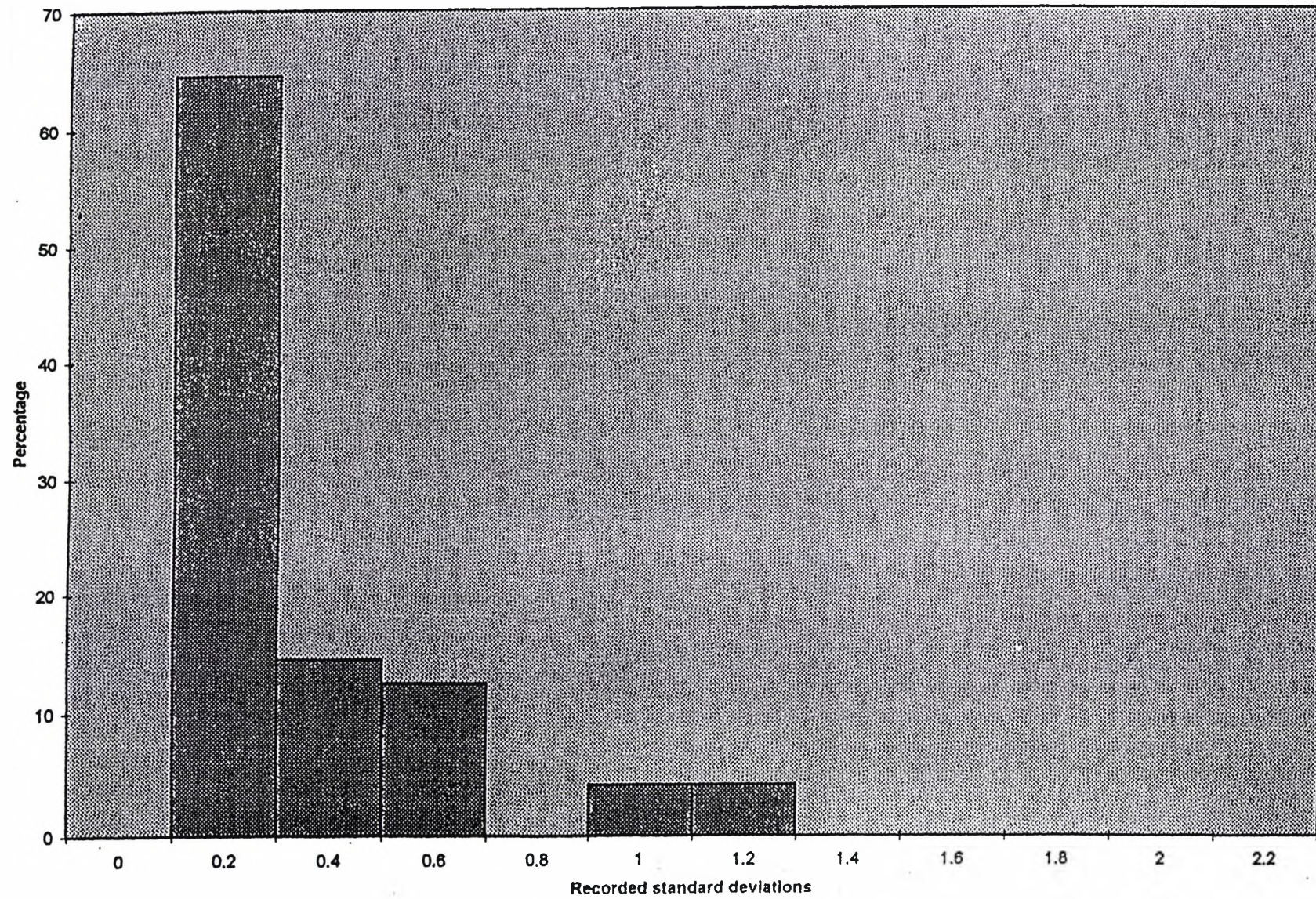
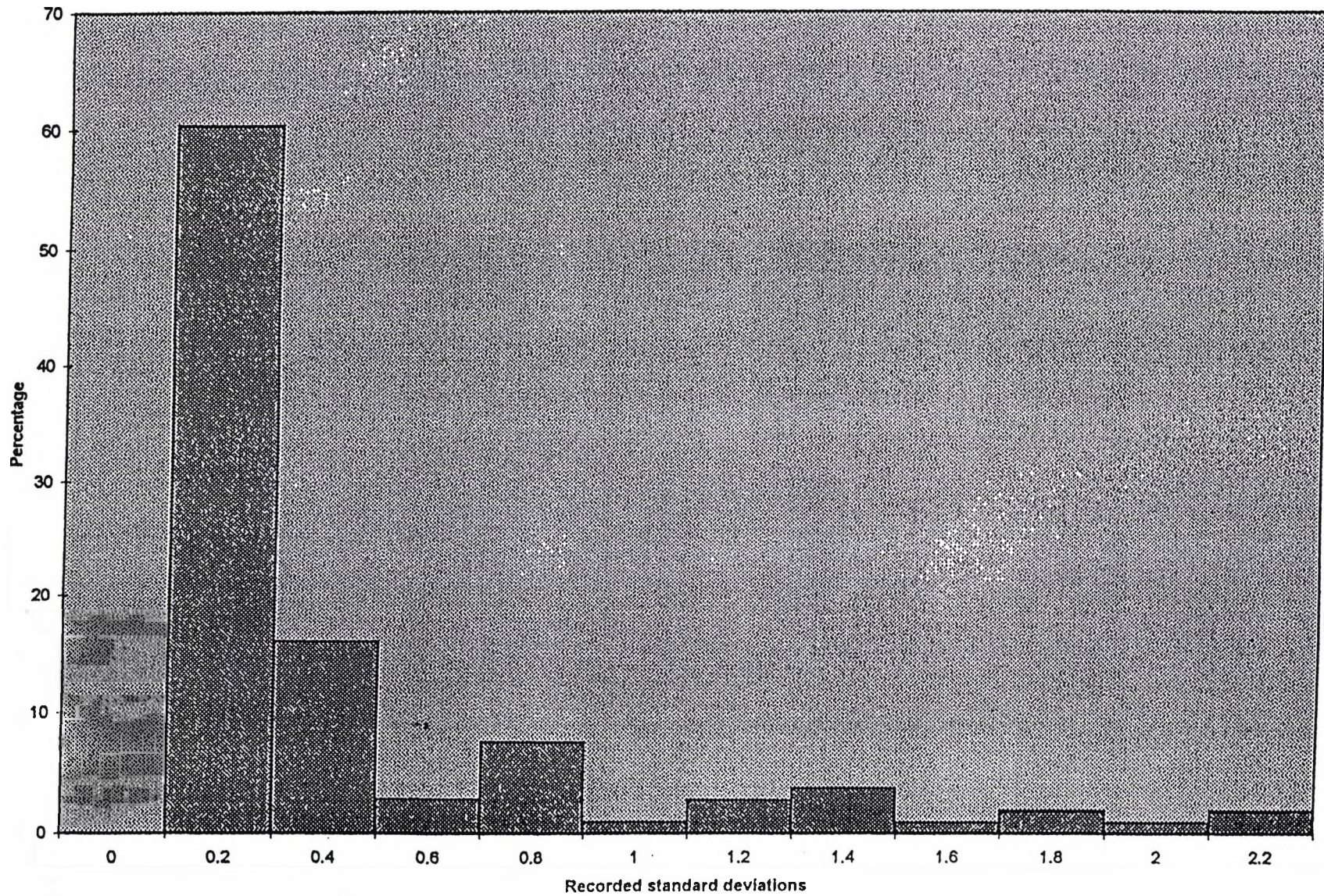


Figure 7.30 Within day variance for female subjects



(one man and one lactating woman). Monitor-based stationary and moving gratings were presented and subjects 'increased' the contrast until they became aware of the grating. Both female subjects with normal cycles underwent cyclical changes that were greatest for the lower spatial frequencies, particularly for a spatial frequency of 4 cpd, (i.e. the closest to the peak of normal CSF). Time series analysis showed several peaks of sensitivity across the menstrual cycles, suggesting a complex relationship between vision and the underlying physiological events in the menstrual cycle. Control subjects did not appear to exhibit such time-dependent fluctuations (Johnson and Petersik 1987).

Guttridge (1994) reported that there was little evidence for a repeatable clinically significant fluctuation in the visual field across the menstrual cycle. In addition to automated perimetry, the study also measured sine-wave grating CS, VA at high and low contrast, and pupil diameter across the menstrual cycle. Again, no clinically significant fluctuations were observed.

It is difficult to draw conclusions from menstrual cycle studies when the number of subjects and controls is small, yet logistic difficulties associated with longitudinal studies inevitably restrict subject numbers. There are a number of possible causes for the variation in light scatter in females found in the present study and other reported variations of visual function with the menstrual cycle. Such cyclical variations may be due to hormonal shifts across the menstrual cycle which are known to alter ocular parameters, (e.g. CCT, pupil diameter, crystalline lens shape). Chapter 6 demonstrated that increases in CCT (e.g. following prolonged lid closure) yield noticeable increases in light scatter values within the eye (as measured by increases in k'). Despite this, there was a conspicuous absence of any relationship between the pachometry measurements and the increase in light scatter recorded during the menstrual cycle of female subjects. This suggests that the marked fluctuations in k' which occur throughout the menstrual cycle of females are not due to changes in CCT. Therefore, the results exclude possible changes in k' resulting from oestrogen-induced corneal oedema. Other ocular changes must be occurring in relation to the menstrual cycle.

Another possible factor that may affect light scatter during the menstrual cycle is a change in pupil diameter. Although there were changes in pupil diameter across the cycle in

females in the current study, there was little correlation with increases in light scatter. Other researchers (Barris et al 1980; Guttridge 1994) have found no significant changes in pupil diameter over the menstrual cycle. Consequently, other possible cycle-related changes in the ocular system must be explored in an attempt to explain the apparent differences between female and male subjects with regard to longitudinal measurements of scatter.

It is well known that both reproductive and buccal mucosae respond to changes in the level of circulating oestrogens. Significant mucosal changes may occur during the ovarian cycle, and also during the female menopause. In particular, this mucosal sensitivity to oestrogens may be observed as cellular maturation in surface epithelia. It is well known that oestrogens cause maturation of the parabasal cells to intermediate and superficial cells, whilst progesterone, during the luteal phase, causes regression of the maturation pattern by opposing the oestrogen proliferative effect. In addition, it has been observed that post-menopausal women suffer more frequently from KCS, compared to women of reproductive age (Holly and Lemp 1977; Judd et al 1981; Gambrell et al 1983). It has been suggested that this is attributable to an oestrogen deficiency (Kramer et al 1990). As oestrogen levels vary significantly throughout the menstrual cycle, it is likely that maturation of the epithelium changes similarly. A number of authors have attempted to quantify changes in the conjunctival epithelium that occur in response to varying levels of oestrogen (Kramer et al 1988; Vavilis et al 1995). Kramer et al (1988) reported cyclical changes in the maturation of conjunctival epithelial cells during the menstrual cycle. No such cyclical changes were found in post menopausal smears, or in smears taken from subjects with endocrine abnormalities. This study did not correlate the changes with vaginal smears. This deficiency was addressed by the work of Vavilis et al (1995) who concluded that the conjunctival smears of menstruating women revealed cyclical maturation changes, and that these changes correlated with changes in the vaginal epithelium. The vaginal epithelial changes in turn reflected the changing levels of circulating oestrogen and progesterone. The conclusion that the corneal epithelium is affected by changes in the levels of circulating hormones was supported by the finding that both pregnant and post menopausal women failed to exhibit similar patterns with regard to the maturational state of the conjunctival epithelium.

A study conducted by Aragona et al (1998) demonstrated that the goblet cells of the conjunctiva are also sensitive to female hormones (section 7.3.3). Elevated progesterone levels and reduced levels of oestrogen were found to produce a thicker mucus in the eyes of rabbits. This indicates that changes in mucus within the eye parallel the morphofunctional modifications of the cervical mucus (Chilton et al 1991). In response to oestrogens, the mucus was abundant, more fluid, filamentous and with low viscosity. In contrast, the mucus was scarce, thicker and with a higher viscosity during the progesterone phase of the menstrual cycle and during pregnancy (when progesterone is high and oestrogen is low) (Gibbons and Mattner 1971; Insler et al 1979; Poon and McCoshen 1985). From this study, it is difficult to determine whether the goblet cells were responding to changing levels of oestrogen or progesterone or perhaps a combination of both hormones. However, it is clear that changes in the levels of oestrogen and progesterone cause distinct changes to mucus within the eye. It is thus likely that there is a change in the viscosity of mucus in the time leading up to the menses, when there are increasing levels of progesterone and/or low levels of oestrogen. A thicker, more viscous secretion may result in increases in light scatter in the eye towards the end of the menstrual cycle (when levels of progesterone are high) and a subsequent decrease once menstruation begins (when levels of progesterone are low). This hypothesis may account for the pattern of scattered light observed in females at these times of the cycle (figure 7.20). Such an hypothesis was tested in a pilot study described in section 7.11.

7.11 Pilot study to investigate the effect of acetylcysteine on light scattering measurements in one female subject

A popular treatment for dry eye resulting from excess mucus production is topical acetylcysteine. Acetylcysteine has a strong mucolytic action, and as such may be used to test the hypothesis that changes in mucus levels within the eye, in response to hormonal changes during the menstrual cycle, lead to changes in recorded light scatter.

Acetylcysteine is a derivative of the amino acid cysteine, and is highly effective in the liquefaction of mucus. The mucolytic action of acetylcysteine is related to its sulfhydryl group, which acts characteristically to open the disulphide bonds which are present within the mucus. It is used in pulmonary and bronchial conditions (e.g. cystic fibrosis) as a 20% solution to clear the airways. For ocular uses, it is administered as a 5% solution, since

higher concentrations cause irritation. The composition of acetylcysteine eye drops is shown in table 7.3.

Table 7.3 - The composition of acetylcysteine 5% drops.

Constituent	Function
Acetylcysteine	Mucolytic action
Sodium Hydroxide	Stabilise pH
Sodium Chloride	Isotonicity
Potassium chloride	Balance salts and act as a buffer
Borax	Buffer
Boric acid	Buffer
Disodium edetate	Chelating agent
Benzalkonium chloride	Preservative
Purified water	Vehicle

The main ocular condition for which a mucolytic is usually recommended is filamentary keratitis associated with KCS. There have been several studies carried out with regard to the efficacy of acetylcysteine in the treatment of various ocular conditions. The results of these studies can be seen in table 7.4.

Table 7.4 - Results of studies reporting an objective improvement in a range of ocular conditions following the use of acetylcysteine drops.

Author	Date	Ocular condition	% improvement
Absolon and Brown	1971	KCS	100
Wright	1972	Superior Limbic Keratoconjunctivitis	65
Williamson et al	1974	KCS	30
Haut et al	1977	'Dry eye'	64
Fraunfelder et al	1977	KCS	Majority

7.11.1 Baseline measurements

In order to study the effect of acetylcysteine on measures of light scatter, it is necessary to establish the baseline levels of scatter, as measured by k' .

7.11.1.1 Subject

One normal female subject who took part in the longitudinal menstrual cycle study was enlisted to investigate whether light scatter varies between eyes, with the aim of

determining the effect of acetylcysteine on the light scattering characteristics of the eye during the menstrual cycle. The menses stage of the menstrual cycle was chosen, as an increase in light scatter was observed at this stage in most subjects tested in section 7.10. This phase of the cycle also corresponds to the time when oestrogen levels are low, resulting in maximal mucus levels and maximal mucus viscosity. The menses also provides a convenient and accurate marker for the precise stage of the menstrual cycle.

7.11.1.2 Method

Measurements were taken from both eyes over the first five days of the menstrual cycle. The subject was examined between the hours of 12:00 and 14:00. Three scatter measurements were taken from each eye.

7.11.1.3 Results

Figure 7.31 reveals little difference between measures of k' when taken from either the right or left eye. Measurements from the right eye reveal that k' is maximal on day 3 (11.78) and minimal on day 5 (7.72). Measurements from the left eye, reveal that k' is maximal on day 1 ($k' = 12.51$) and minimal on day 5 ($k' = 7.69$). The average k' as measured over the five days of menses was 10.46 from the right eye and 10.64 from the left.

Both eyes are subject to similar increases in light scatter when measurements are taken over the first five days of the menstrual cycle. The variation in k' observed over the first five days of the cycle are similar to the patterns observed in figure 7.20, which show a fall in k' over the first five days of the cycle.

7.11.2 Effect of acetylcysteine 5% on measurements of light scatter

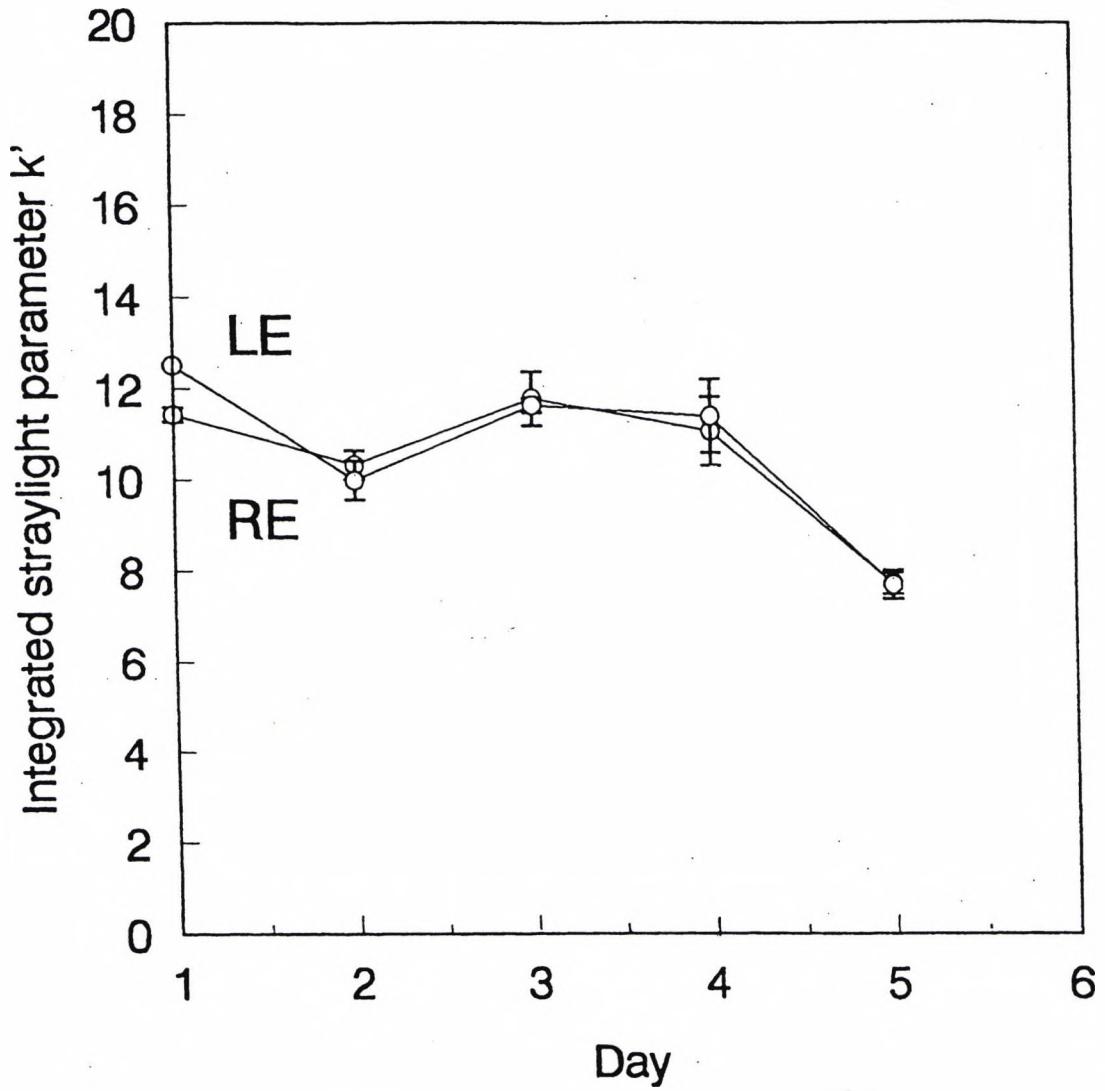
7.11.2.1 Aim

To investigate whether instillation of acetylcysteine 5% at menses affects measures of light scatter.

7.11.2.2 Method

The same subject who took part in section 7.11.1 was enlisted. One drop of acetylcysteine 5% solution was administered four times each day to the right eye, starting three days

Figure 7.31 Baseline scatter results as measured over five days for Subject MH



Changes in k' over the first five days of menses are shown for each eye. Error bars represent standard errors.

before the menses were due. The drops continued to be administered for five days following the onset of menses. Scatter measurements were taken on a daily basis throughout the menses on both the right eye receiving acetylcysteine, and also the left "control eye". The acetylcysteine 5% drop was administered 5 minutes prior to the daily scatter measurement.

7.11.2.3 Results

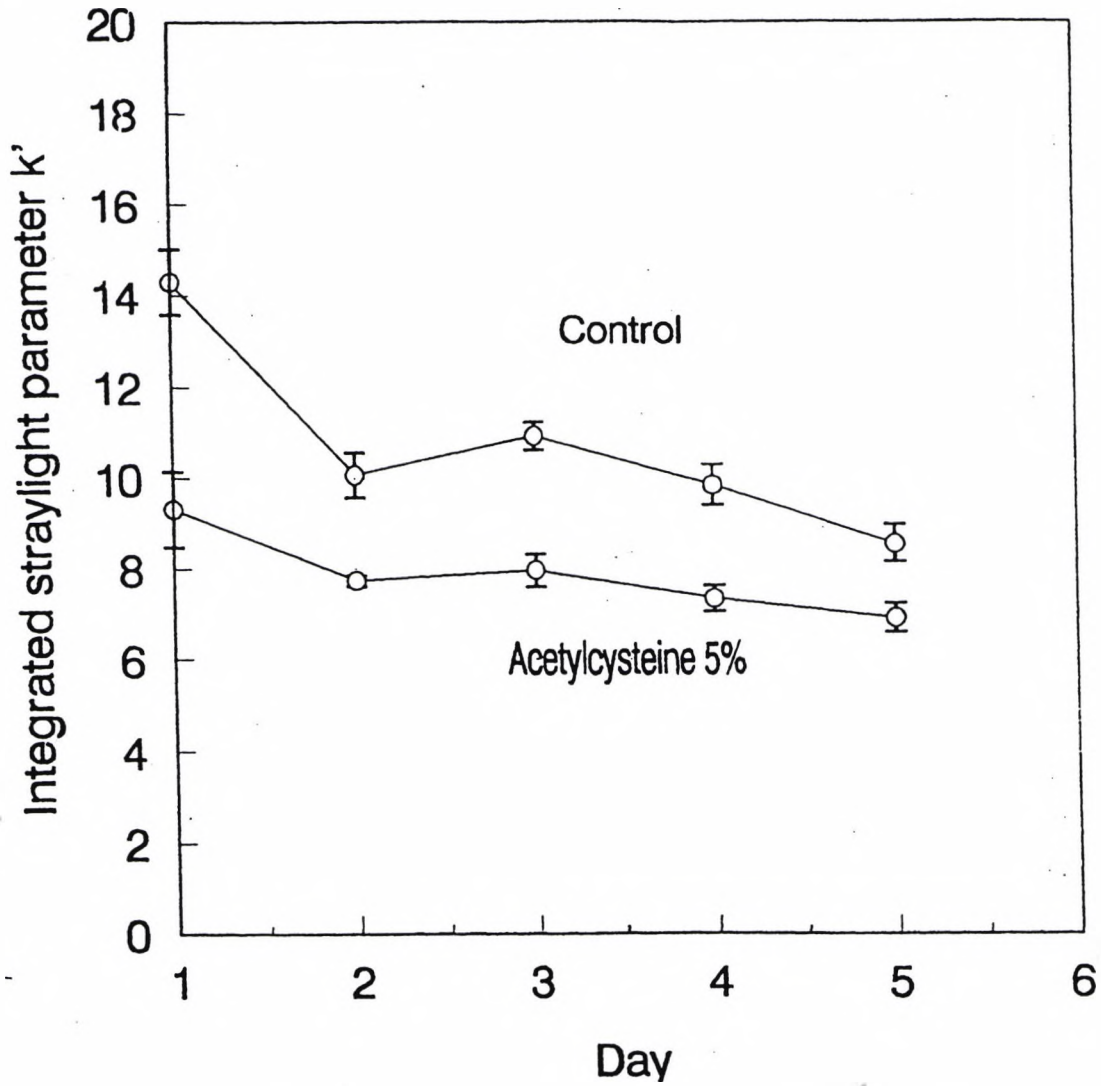
Figure 7.32 shows the light scatter results recorded in the female subject, following the administration of acetylcysteine 5% during the five days of menses. The plot demonstrates that prior administration of acetylcysteine reduced the amount of light scatter in the eye, as measured by k' . Lower levels of scatter were recorded in the eye which had received acetylcysteine 5% on each of the five days. In the treated eye, the maximum level of scatter was again observed on day 1 ($k' = 9.31$) and the minimum on day 5 ($k' = 6.92$). The light scatter in the "control eye" was maximal on day 1 ($k' = 14.3$), reducing to a minimum on day 5 ($k' = 8.56$). The light scatter in the "control eye" maintains a similar pattern to that observed in figure 7.31, although the values obtained on day 1 from the control eye are higher than the baseline values measured on the equivalent day in section 7.11.1.

7.11.2.4 Discussion

Acetylcysteine 5% reduced light scatter in the right eye during the five days of menses. The results indicate that mucus in the tear fluid may indeed influence the light scattering characteristics of the eye. The conjunctival epithelium is known to be oestrogen sensitive, and the goblet cells are thought to parallel the morphofunctional modifications of the cervical mucus during the cycle. Therefore, it is likely that the mucus in the tear film varies in quantity and quality at different times of the menstrual cycle. The levels of mucus are likely to be elevated during the menses, as oestrogen levels are lowest at this time. In addition, the mucus secreted by the goblet cells is thicker and of a higher viscosity at such times when oestrogen levels are low. The mucolytic action of acetylcysteine degrades the mucus in the pre-ocular tear film resulting in reduced levels of scatter. To further test the hypothesis, the same subject was recruited for repeat testing using hypromellose 0.3% in the control eye. Hypromellose 0.3% was chosen because it is a lubricant which does not contain a mucolytic. The constituents of hypromellose are shown in table 7.5.

Figure 7.32

Scatter results following instillation of acetylcysteine 5 % as measured over five days for Subject MH



Acetylcysteine 5 % was instilled into the right eye. The left eye acted as a control. Changes in k' over the first five days of menses are shown for each eye. The plotted data points represent mean k' obtained over three runs. Error bars represent standard errors.

Table 7.5 - The composition of hypromellose drops.

Constituent	Function
Hypromellose 4500	Lubrication
Sodium chloride	Isotonicity
Potassium chloride	Balance salts and act as a buffer
Borax	Buffer
Boric acid	Buffer
Benzalkonium chloride	Preservative
Purified water	Vehicle

7.11.3 The effect of acetylcysteine 5% and hypromellose 0.3% on light scattering measurements

7.11.3.1 Aim

To measure the light scattering characteristics of the eye during the first five days of menses, following administration of a mucolytic and a lubricant.

7.11.3.2 Method

One drop of acetylcysteine 5% eye drops was administered four times each day for eight days, to the right eye of the same subject who took part in the acetylcysteine study. Instillation of drops began three days prior to the menses. At the same time, one drop of hypromellose 0.3% eye drops was administered to the left eye four times each day.

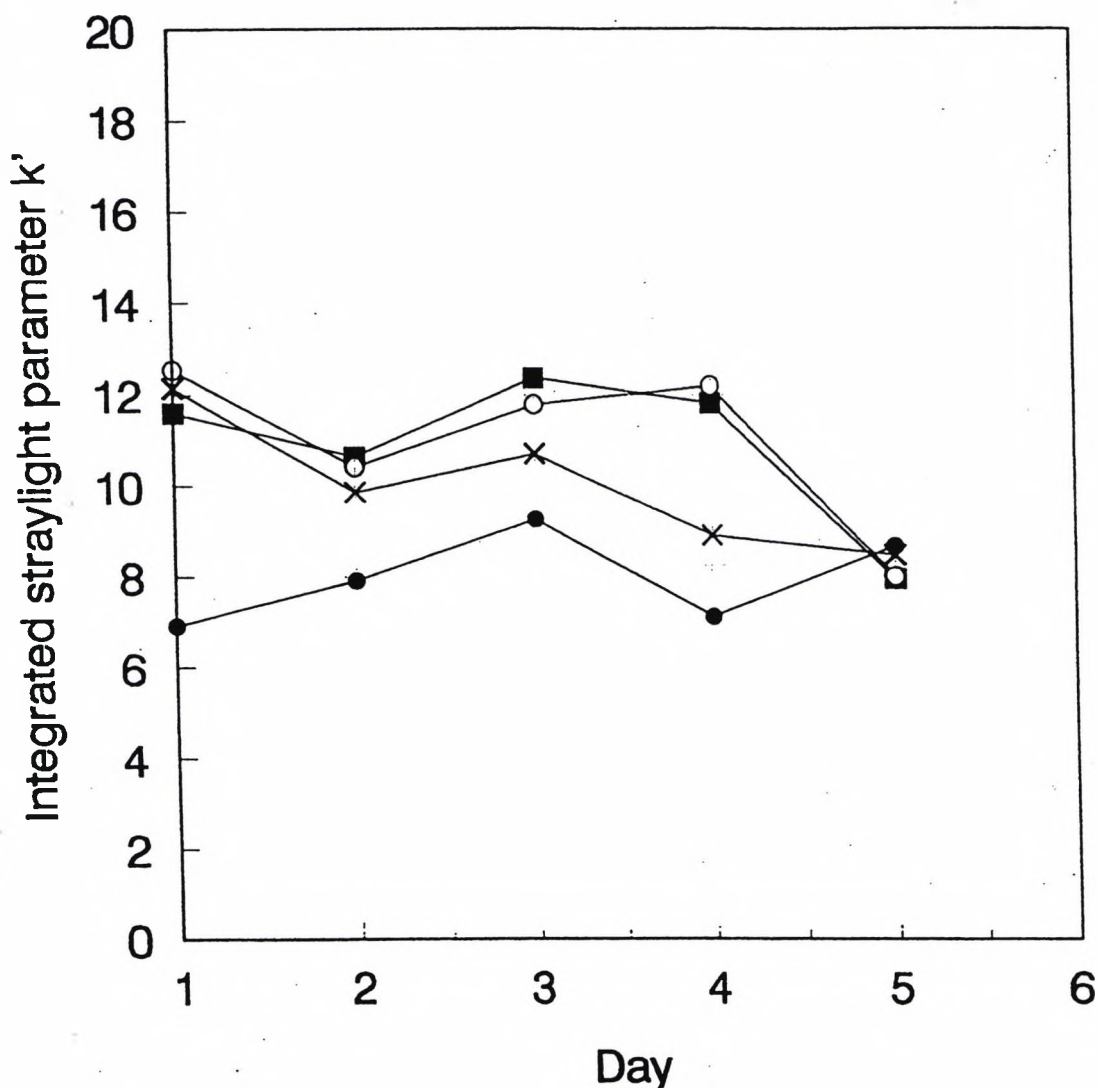
7.11.3.3 Results

From figure 7.33, k' was reduced following administration of acetylcysteine 5%, when compared to the left eye which received hypromellose 0.3%. k' following administration of acetylcysteine 5% was also less than the baseline scatter values (as measured in section 7.11). Hypromellose reduced k' values on days 2, 3 and 4 compared to baseline measurements but it failed to produce the marked reduction in k' seen following instillation of acetylcysteine 5%.

7.11.3.4 Discussion

The results from this single subject indicate that the mucolytic action of acetylcysteine 5% reduced the amount of scattered light in the eye when compared to hypromellose 0.3%.

Figure 7.33 Scatter results following instillation of acetylcysteine 5 % and hypromellose 0.3 % as measured over five days for Subject MH



Acetylcysteine 5 % was instilled into right eye (\bullet), whilst hypromellose 0.3 % was instilled into the left eye (\times). \blacksquare represents the results of the right eye and \circ represents the left eye in Figure 7.31. Changes in k' over the first five days of menses are shown for each eye.

Instillation of hypromellose produced a reduced amount of light scatter on days 2, 3 and 4 compared to the baseline values obtained in section 7.11. There is insufficient data for statistical analysis and these reductions may simply reflect the day to day variation in light scatter. Alternatively, although not acting directly on mucus, the hypromellose may dilute the mucus in the pre-ocular tear film resulting in a slight decrease in k' .

7.12 Discussion of Chapter 7

The results of the masked study into the effects of the menstrual cycle on light scatter indicate that there is marked variability in light scatter in the eye (as measured by k') over the course of the menstrual cycle. Statistical analysis of the results was undertaken, in an attempt to identify trends in the data. Results from subject MD and MH (cycles 1 and 2) suggest that there is a fall in the level of scatter, during the first five days of menses which is accompanied by a mid cycle rise around ovulation. No other cyclical trend beyond this point was evident. Results from subjects RS and FS were inconclusive because the level of variability of light scatter during their cycles was so high. This may have been due to numerous factors, including a change in the individual's criterion level across the menstrual cycle. Such criterion changes have been found across the menstrual cycle (De Marchi and Tong 1970; Wong and Tong 1974), therefore this possibility cannot be excluded. When the results were compared to those obtained from the male subjects, the variability of scatter measurements was lower for males, both within days and between days. Thus, it appears that females have a greater variation in light scatter over time than male subjects. However, the variability in scatter in the female subjects did not appear to follow a clear cyclical trend (other than the possible fall from elevated levels during menses). Pachometry readings did not show an association between scatter and CCT. Nevertheless, a day to day variation in CCT was evident in both male and female subjects, although the timing of these changes did not correlate with changes in light scatter. The absence of menstrual cycle effects on CT is in agreement with Manchester (1970), El-Hage and Beaulne (1973) and Hirji and Larke (1978). The extent of day to day changes in CT (from 5.2% to 7.4% in females, and 4.5% for the male subject (KJ)) were less than those found by Soni (1980), who demonstrated an approximate variation of 14% in females and 8% in males.

Ideally, any study of variability during the menstrual cycle requires knowledge of exactly where each subject is within her cycle on each measurement day. This is difficult to achieve with any accuracy, although several methods have been accepted as being among the more reliable. These include measurements of basal body temperature (BBT) (Billings and Westmore 1980); measurements of cervical mucus (Billings 1972); plasma hormone levels (Rojansky et al 1990), and urine analysis (Rojansky et al 1990). Unfortunately, with the exception of BBT, these methods require operator training, and all the methods would alert the subjects to the true focus of the study. Such monitoring within the menstrual cycle was thus beyond the scope of this study, and for each female the phases of the menstrual cycle were determined solely from the onset and termination of menstruation. This approach is the norm for much menstrual cycle research, however, it makes it difficult to compare the present study with studies that, for example, have been able to identify ovulation by testing plasma concentrations of oestrogen and progesterone (e.g. Leach et al 1971; Kiely et al 1983).

As variations in CT and pupil diameter did not appear to cause the variation in light scatter observed during the menstrual cycle, other causes of light scatter were considered. As the conjunctiva is known to be oestrogen sensitive, and there is a change in the composition of mucus during menses, acetylcysteine 5% was used to investigate the effect of topical administration of a mucolytic agent. The mucolytic agent reduced the level of light scatter in the eye of one female subject during the menses. This suggests that there may be an increase in mucus in the pre-ocular tear film and/or a change in the viscosity of mucus secreted by the goblet cells. These changes may occur in response to changes in the levels of endogenous hormones. However, data was collected from one subject only so no conclusions can be drawn, nevertheless, these data highlight an area that would benefit from further research.

An additional possible explanation for the variation in light scatter observed in female subjects may be the presence of epithelial oedema. Epithelial oedema does not necessarily result in an increase in CT (Wilson et al 1980), but will cause an increase in forward light scatter (Feuk and McQueen 1971; Lambert and Klyce 1981; O' Leary et al 1981). The hormonal sensitivity of the conjunctival epithelium and the goblet cells produce alterations in the level and type of mucus during the menstrual cycle and this may in turn affect the pH

of the tears. If the pH of the tears alters, epithelial oedema may occur. As discussed in section 6.3.3, the tears are normally hypertonic with respect to the cornea, which results in a continuous flow of water across the semi-permeable epithelium and endothelium. If this osmotic balance changes, oedema will result. Therefore, it is possible that epithelial oedema may cause the changes in light scatter observed in females, in addition to alterations in the quantity and quality of the mucus.

Menstrual cycle related changes could occur in any ocular structure. Therefore, other possible causes of increased variability in light scatter in females include changes resulting from variation in the shape of the crystalline lens or from retinal oedema. In fact, retinal oedema has been reported as a consequence of oral contraceptives (Flynn and Esterley 1966; Goran 1967). Crystalline lens oedema or changes in lens shape cannot be excluded as possible causes of increased light scatter during the menstrual cycle, however, no studies investigating such changes have been performed to date.

7.13 Conclusions

Females experience marked variability in intraocular light scatter (as measured by k' , the integrated straylight parameter) when measurements are taken longitudinally. This variation may be related to the menstrual cycle. However, precise cyclical trends were unclear, beyond a fall in scatter levels from initial levels during the menses. Variations in CCT and pupil diameter were also found during the menstrual cycle, however, they appeared to be unrelated to changes in light scatter. The administration of acetylcysteine 5% reduced the amount of light scatter in the eye during menses, suggesting that changes in mucus levels in the tear film (possibly in response to reduced oestrogen levels) may be a contributory factor. Male subjects revealed less day-to-day variability in light scatter, with relatively constant values of k' . This may be due to the absence of hormone-related changes in ocular structures in these subjects. The findings of this chapter will influence subject selection for subsequent studies investigating anterior eye disease and contact lens wearers, resulting in exclusion of pre-menopausal female subjects.